Characterisation of the Role of KLF5 in Normal Haemopoiesis and Acute Myeloid Leukaemia

Sonya Diakiw, B. Sc (Molecular Biology) (Hons.)

A thesis submitted for the degree of Doctor of Philosophy in the School of Molecular & Biomedical Science and the School of Paediatrics & Reproductive Health at the University of Adelaide

April 2011

Contents

Contents **1**
List of figures **6**
List of Tables **8**
Abbreviations **9**
Abstract **13**
Declaration **15**
Acknowledgements **17**

Chapter 1 – Literature review and research proposal **18**
1.1 Acute Myeloid Leukaemia 18
1.1.1 Haemopoiesis and leukaemia *19*
1.1.2 Molecular genetics of myeloid leukaemia *21*
1.1.3 Cooperation of mutations in AML *22*
1.1.4 Epigenetic mechanisms in AML *24*
1.1.4.1 Methylation 24
1.1.4.2 Histone modifications and chromatin remodelling 26
1.1.5 Methods for identification of novel leukaemic lesions and pathways *27*
1.1.5.1 Genome-wide screens 28
1.1.5.2 Functional screens 29
1.2 Identification of novel oncogenes and tumour suppressors using the FDB1 murine myeloid cell line 30
1.2.1 The FDB1 cell line model *30*
1.2.2 Gene expression profiling using the FDB1 cell line system *32*
1.2.3 Identification of Krüppel-like factor 5 as a differentiation-associated gene in the myeloid system *32*
1.2.3.1 *Klf5* expression is associated with the granulocyte lineage 34
1.3 Krüppel-like factor 5 35
1.3.1 The Krüppel-like family of transcription factors *35*
1.3.2 Krüppel-like factor 5 ..... *37*
1.3.3 Gene structure and transcriptional regulation *39*
1.3.4 Protein and post-translational modifications *42*
1.3.5 Target genes *43*

1.3.5.1 Microarray and ChIP studies....45
1.3.6 Interacting proteins....46
1.3.7 Function in cell growth, differentiation and survival....48
1.3.7.1 KLF5 as a positive regulator of proliferation....48
1.3.7.2 Proliferative signalling pathways....50
1.3.7.3 Function in embryonic stem cells and development....52
1.3.7.4 The role of KLF5 in apoptosis....53
1.3.7.5 Growth inhibition and differentiation....54
1.3.8 KLF5 in human tumourigenesis....55
1.3.8.1 KLF5 as an oncogene....55
1.3.8.2 KLF5 as a tumour suppressor....58
1.4 Research proposal....61
1.4.1 Retroviral expression cloning using the FDB1 target cell line....61
1.4.2 Characterisation of the putative tumour suppressor KLF5 in normal myelopoiesis and in AML....62

Chapter 2 - Materials and methods....64
2.1 Materials....64
2.2 Nucleic acid protocols....67
2.2.1 Production, isolation and analysis of DNA samples....67
2.2.2 RNA isolation and analysis, and cDNA production....68
2.2.3 Polymerase chain reactions....69
2.2.4 Plasmids and expression constructs....71
2.3 Cell culture protocols....72
2.3.1 Culture medium and supplements....72
2.3.2 Cell lines....74
2.3.3 Murine bone marrow cells....75
2.3.4 Cell differentiation assays....75
2.3.5 Demethylation of leukaemia cell lines....76
2.3.6 Viral transduction of cells....76
2.3.7 Cellular assays....77
2.3.8 Flow cytometry and Fluorescence-activated cell sorting....79
2.4 Analysis of patient samples....79
2.4.1 AML panel....79
2.4.2 Methylation analysis....81

2.5 General....81
2.5.1 Ethical approval....*81*
2.5.2 Statistical analysis....*83*

Chapter 3 – Retroviral expression cloning for detection of leukaemic oncogenes. 84
3.1 Introduction....84
3.2 Protocols and results....88
3.2.1 M1 library construction....*88*
3.2.1.1 Outline....88
3.2.1.2 cDNA synthesis....91
3.2.1.3 cDNA cloning....92
3.2.2 Composition of the M1 retroviral cDNA library....*92*
3.2.3 Assessment of the FDB1 cell line as a target population for retroviral expression screening....*97*
3.2.4 Utilising the FDC-P1 cell line as a target population for retroviral expression screening....*98*
3.2.4.1 Screening the M1 library for genes which confer factor-independent growth in FDC-P1 cells....101
3.3 Discussion....103
3.3.1 Construction of the M1 retroviral cDNA library....*103*
3.3.2 Screening the M1 retroviral cDNA library....*104*
3.3.3 Retroviral expression screening for the detection of oncogenes in human disease....*105*

Chapter 4 – KLF5 expression and function in myeloid differentiation.....107
4.1 Introduction....107
4.2 Results....109
4.2.1 KLF5 mRNA expression increases during myeloid differentiation and is predominantly associated with granulocyte differentiation....*109*
4.2.1.1 GM-CSF-induced granulocyte-macrophage differentiation of the FDB1 cell line....109
4.2.1.2 G-CSF-induced granulocyte differentiation of the 32D cell line....111
4.2.1.3 M-CSF-induced macrophage differentiation of murine bone marrow progenitors....118
4.2.1.4 mRNA expression of *KLF* family members in primary haemopoietic cell populations....118
4.2.2 Retroviral expression of KLF5 induces macrophage differentiation, cell cycle arrest and cell death....*123*

4.2.2.1 Enforced expression in the FDB1 cell line model....123
4.2.2.2 Enforced expression in primary murine bone marrow progenitors....126
4.2.3 RNAi-mediated knock-down of Klf5 induces effects consistent with reduced granulocyte differentiation 132
4.2.3.1 Knock-down in the 32D cell line model of G-CSF-induced granulocyte differentiation 132
4.3 Discussion....138
4.3.1 Increased expression of KLF5 mRNA is predominantly associated with granulocyte differentiation....138
4.3.2 Enforced expression of KLF5 is sufficient to induce macrophage differentiation of FDB1 cells and primary murine bone marrow progenitors....139
4.3.3 Reduced expression of Klf5 produces functional effects consistent with reduced granulocyte differentiation in the 32D cell line model....141
4.3.4 Evidence for a regulatory pathway involving KLF5 and members of the C/EBP family in G-CSF and GM-CSF-induced differentiation 142
Chapter 5 – Deregulation of KLF5 in human Acute Myeloid Leukaemia. 145
5.1 Introduction....145
5.2 Results....147
5.2.1 KLF5 mRNA expression is reduced in AML....147
5.2.1.1 Expression in a local cohort of primary AML samples and correlation with AML subtype 147
5.2.1.2 Expression in an expanded cohort of primary AML samples and correlation with AML subtype 153
5.2.2 Analysis of the KLF5 5` proximal promoter and intron 1 CpG methylation in AML 155
5.2.2.1 Experimental design....155
5.2.2.2 Identification of regions which are differentially methylated between AML samples and normal controls 157
5.2.2.3 Methylation of *KLF5* DMR-1, DMR-2a and DMR-2b in *de novo* AML 165
5.2.2.4 Correlation of *KLF5* methylation with relative mRNA expression 173
5.2.2.5 Treatment with demethylating agents activates *KLF5* transcription....175
5.2.2.6 Potential significance of differentially-methylated regions for the transcriptional regulation of *KLF5*....177
5.2.3 Enforced expression of KLF5 in the U937 leukaemia cell line enhances differentiation....183

5.2.3.1 KLF5 induces expression of the myeloid marker CD11B in U937 leukaemia cells....183
5.2.3.2 KLF5 enhances the response of the U937 cell line to differentiation-inducing agents185
5.3 Discussion....189
5.3.1 Reduced KLF5 expression potentially contributes to the disease pathogenesis of AML 189
5.3.2 Deregulation of KLF5 expression by common genetic lesions in AML. 190
5.3.3 DNA methylation of KLF5 as a potential mechanism for down-regulation in AML 192
5.3.4 Aberrant methylation of KLF5 is associated with selected cytogenetic subgroups in AML 193
5.3.5 Mechanisms for transcriptional deregulation of KLF5 expression in AML....195
5.3.6 Tumour suppressor function of KLF5 in human leukaemia cells....197
Chapter 6 – Discussion 199
6.1 KLF5 expression and function in normal myelopoiesis 200
6.1.1 Expression of KLF5 during myeloid differentiation....200
6.1.2 KLF5 function....200
6.1.3 KLF family members in the haemopoietic system 203
6.2 Deregulation of KLF5 in AML....205
6.2.1 KLF5 mRNA expression in AML 205
6.2.2 Methylation of KLF5 in AML....207
6.2.3 Transcriptional deregulation of KLF5 by methylation of the 5` proximal promoter in AML and potential relevance to CEBPA activity 208
6.2.4 Transcriptional deregulation of KLF5 by methylation of intron 1 in AML....209
6.2.5 Biological relevance of KLF5 methylation studies in AML....212
6.2.6 Prognostic relevance of methylation studies in AML 213
6.2.7 Other potential mechanisms for KLF5 deregulation in AML....214
6.2.8 Targeting KLF5 for activation in AML....215
6.3 Summary and concluding remarks 217
Appendices....219
References....225

List of figures

Figure 1.1: Haemopoiesis 20
Figure 1.2: FDB1 model system of myeloid differentiation 31
Figure 1.3: *Klf5* expression during FDB1 differentiation 33
Figure 1.4: KLF family proteins (*Homo sapiens*) 38
Figure 1.5: KLF5 gene and protein (*Homo sapiens*) 40
Figure 1.6: The MEK/ERK pathway and KLF5 in proliferation 51
Figure 3.1: Retroviral expression cloning method 85
Figure 3.2: Library construction method 89
Figure 3.3: Vector map of the Sfi1-modified MSCV-IRES-eGFP retroviral expression construct (MIG-Sfi1) 90
Figure 3.4: Analysis of selected clones from each fraction of the M1 library 93
Figure 3.5: Composition of the M1 cDNA library 96
Figure 3.6: PCR recovery of integrated MIG-Sfi1 retroviral construct 100
Figure 3.7: Analysis of retroviral integrations in selected FDC-P1 clones transduced with the M1 library 102
Figure 4.1: Granulocyte-macrophage differentiation of FDB1 cells in GM-CSF 110
Figure 4.2: Expression of *Klf5* and *Cebp* family members during GM-CSF-induced FDB1 cell differentiation 112
Figure 4.3: Granulocyte differentiation of 32D cells in G-CSF 113
Figure 4.4: Expression of *Klf5* and *Cebp* family members during G-CSF-induced 32D cell differentiation 117
Figure 4.5: Macrophage differentiation of primary mouse bone marrow progenitors in M-CSF 119
Figure 4.6: Expression of *KLF* family members in myeloid lineages 121
Figure 4.7: Enforced expression of murine KLF5 in the FDB1 cell line model 124
Figure 4.8: Enforced expression of murine KLF5 in primary mouse bone marrow progenitors 128
Figure 4.9: shRNA knock-down of *Klf5* in the 32D cell line model 134
Figure 5.1: *KLF5* mRNA expression in human AML samples, normal bone marrow controls and human leukaemia cell lines as detected by Q-PCR 151

Figure 5.2: Differences in *KLF5* mRNA expression in human AML samples according to AML subtype 152
Figure 5.3: *KLF5* expression levels in the Valk cohort 154
Figure 5.4: Overview of Sequenom EpiTYPER system for quantitative methylation analysis 156
Figure 5.5: *KLF5* region analysed for methylation status 158
Figure 5.6: Quantitative methylation analysis of *KLF5* from the proximal promoter to the end of exon 2 159
Figure 5.7: Methylation of *KLF5* in normal and leukaemic samples in DMR-1 and DMR-2 161
Figure 5.8: Defining the differentially-methylated regions of *KLF5* 162
Figure 5.9: AML samples with aberrant methylation of *KLF5* DMR-1 166
Figure 5.10: AML characteristics associated with high methylation of *KLF5* DMR-1 167
Figure 5.11: AML samples with aberrant methylation of *KLF5* DMR-2a 169
Figure 5.12: AML characteristics associated with high methylation of *KLF5* DMR-2a 170
Figure 5.13: AML samples with aberrant methylation of *KLF5* DMR-2b 171
Figure 5.14: AML characteristics associated with high methylation of *KLF5* DMR-2b 172
Figure 5.15: Correlation of relative *KLF5* mRNA expression with average methylation of *KLF5* DMR-1, DMR-2a and DMR-2b 174
Figure 5.16: Reactivation of *KLF5* mRNA expression on treatment with demethylating agents 176
Figure 5.17: Methylation and potential mechanisms for deregulation of *KLF5* expression in AML 178
Figure 5.18: *KLF5* EST BG717510 181
Figure 5.19: Enforced expression of KLF5 in the U937 leukaemia cell line model 184
Figure 5.20: ATRA treatment of *KLF5*-transduced U937 cells 186
Figure 5.21: PMA treatment of *KLF5*-transduced U937 cells 188
Figure 6.1: *KLF5* expression levels in AML samples with mutated or hypermethylated *CEBPA* 210

List of Tables

Table 1.1:	Function of KLF family members	36
Table 1.2:	Direct KLF5 target genes and their transcriptional regulation by KLF5 ..	44
Table 1.3:	KLF5 interacting proteins	47
Table 1.4:	Evidence for KLF5 acting as an oncogene	56
Table 1.5:	Evidence for KLF5 acting as a tumour suppressor	59
Table 2.1:	Oligonucleotide sequences	70
Table 2.2:	Details of murine *Klf5* shRNA constructs	73
Table 2.3:	Amplicon details for *KLF5* methylation analysis	82
Table 3.1:	Summary of selected clones from each fraction of the M1 library	95
Table 5.1:	Characteristics of human AML samples	148
Table 5.2:	Characteristics of human leukaemia cell lines	149

Abbreviations

5' RACE	Rapid amplification of 5` cDNA ends
ADP	Adenosine diphosphate
AGRF	Australian Genome Research Facility
ALL	Acute Lymphocytic Leukaemia
AML	Acute Myeloid Leukaemia
AMML	Acute Myelomonocytic Leukaemia
APL	Acute Promyelocytic Leukaemia
ATRA	All-*trans* retinoic acid
Avg	Average
BC	Band cell
BFGF	Basic fibroblast growth factor
BLAST	Basic Local Alignment Search Tool
BMMNC	Bone marrow mononuclear cell
BMU	Bone marrow units
bp	Base pairs
CBF	Core binding factor
cDNA	Complementary DNA
CDP	CDC4 phosphodegron motifs
CFU-G/M/GM	Colony-forming unit-granulocyte/macrophage/granulocyte-macrophage
CGH	Comparative genome hybridisation
ChIP	Chromatin immunoprecipitation
CLL	Chronic Lymphocytic Leukaemia
CLP	Common lymphoid progenitor
CML	Chronic Myeloid Leukaemia
CMP	Common myeloid progenitor
Da	Daulton
DBD	DNA-binding domain
DMEM	Dulbecco’s Modified Eagle’s Medium
DMR	Differentially-methylated region
DNA	Deoxyribonucleic acid

DNAse	Deoxyribonuclease
dNTP	Deoxyribonucleotide triphosphate
DSS	Dextran sulphate sodium
EDTA	Ethylenediaminetetraacetic acid
eGFP	Enhanced green fluorescence protein
EPO	Erythropoietin
ESC	Embryonic stem cell
EST	Expressed sequence tag
FACS	Fluorescence-activated cell sorting
FCS	Foetal calf serum
FISH	Fluorescence *in-situ* hybridisation
G-CSF	Granulocyte colony-stimulating factor
GFP^+	GFP-positive
GM-CSF	Granulocyte-macrophage colony-stimulating factor
GMP	Granulocyte-macrophage progenitor
GMSA	Gel mobility shift assays
Gran	Granulocyte
hβc	Human GM-CSF/IL-3/IL-5 receptor common beta chain
HELP	HpaII tiny fragment enrichment by ligation-mediated PCR
HEPES	4-(2-hydroxyethyl)-1-piperazineethanesulfonic acid
HR	Homology-region
HSC	Haemopoietic stem cell
ID	Identification number
IL-15	Interleukin-15
IL-3	Interleukin-3
IL-6	Interleukin-6
IL-7	Interleukin-7
IMDM	Iscove's Modified Dulbecco's Medium
IMVS	Institute of Medical and Veterinary Science
IRES	Internal ribosome entry site
ITD	Internal tandem duplication
kb	Kilobases
KD	Knock-down

KLF	Krüppel-like factor
LIF	Leukemia inhibitory factor
LOH	Loss of heterozygosity
LPA	Lisophosphatidic acid
LPS	Lipopolysaccharide
LTF	Lactotransferrin
LTR	Long terminal repeat
Mac	Macrophage
MALDI-TOF	Matrix-assisted laser desorption/ionization time-of-flight
Mb	Megabases
M-CSF	Macrophage colony-stimulating factor
MDS	Myelodysplastic syndromes
MEK/ERK	Mitogen activated protein kinase (pathway)
MEM	Eagle's Minimum Essential Medium
MEP	Megakaryocyte-erythrocyte progenitor
MFI	Mean fluorescence intensity
MIG	MSCV-IRES-eGFP
MNC	Mononuclear cell
MOPS	3-(N-morpholino)propanesulfonic acid
MPN	Myeloproliferative neoplasms
MPO	Myeloperoxidase
mRNA	Messenger RNA
MSCV	Mouse stem cell virus
N/A	Not applicable
NCBI	National Center for Biotechnology Information
NES	Nuclear export signal
NK	Normal karyotype
NK cell	Natural killer cell
NLS	Nuclear localisation signal
NT	Non-targeting
NURF	Nucleosome remodelling factor
OACIS	Open Architecture Clinical Information System
PBS	Phosphate buffered saline

PCR	Polymerase chain reaction
PI3K/AKT	Phosphatidylinositol 3-kinase/protein kinase B (pathway)
PMA	Phorbol 12-myristate 13-acetate
pMΔH	pMSCV-ΔLTR-H1
pSM2c	p-SHAG MAGIC 2
PV	Polycythemia Vera
Q-PCR	Quantitative reverse-transcription PCR
RAEB	Refractory anaemia with excessive blasts
RBC	Red blood cell
RMA	Robust Multi-chip average
RNA	Ribonucleic acid
RNAi	RNA interference
RPMI	Roswell Park Memorial Institute medium
RTCGD	Retroviral Tagged Cancer Gene Database
RTK	Receptor tyrosine kinase
S1P	Sphingosine 1-phosphate
SCF	Stem cell factor
SCID	Severe combined immunodeficiency
shRNA	Small hairpin RNA
siRNA	Small interfering RNA
SMART	Switching mechanism at 5’ end of RNA transcript
SNP	Single nucleotide polymorphism
STDEV	Standard deviation
SUMO	Small ubiquitin-like modifier
TAD	Transactivation domain
TAE	Tris-acetate-EDTA
TGFβ	Transforming growth factor beta
TPO	Thrombopoietin
TRIS	Tris(hydroxymethyl)aminomethane
UCSC	University of California, Santa Cruz
VEGF	Vascular endothelial growth factor
VSMC	Vascular smooth muscle cell
ZnF	Zinc finger

Abstract

Krüppel-like factor 5 (*KLF5*) encodes a zinc finger transcription factor involved in growth, differentiation and apoptosis of a number of different tissues, and it has previously been implicated as either a tumour suppressor or oncogene in various solid tumours. Expression of *Klf5* is up-regulated during granulocyte-macrophage differentiation of the murine myeloid cell line FDB1 in response to expression of a constitutively active mutant form of the human GM-CSF/IL-3/IL-5 receptor common β subunit (FIΔ mutant)[1]. The aim of this work was thus to characterise the role of KLF5 in the myeloid lineage and to determine whether deregulation of this gene may contribute to Acute Myeloid Leukaemia (AML). We show that *KLF5* mRNA expression is increased during granulocyte-macrophage differentiation of both cell lines and primary haemopoietic cells. *KLF5* expression levels increase to the greatest extent during granulocyte differentiation, and accordingly we demonstrate that knock-down of *Klf5* in the 32D cell line model attenuates granulocyte differentiation. Enforced expression of KLF5 in the FDB1 cell line model and in primary murine bone marrow progenitors functions to induce terminal myeloid differentiation, coupled with cell cycle arrest and cell death. Consistent with a potential role as a promoter of differentiation and tumour suppressor, we show that mean *KLF5* mRNA expression is significantly reduced in AML samples compared to normal controls (mononuclear cells and bone marrow $CD34^+$ samples). *KLF5* expression is selectively decreased in French-American-British (FAB) subtypes M1, M3 and M4, and in samples positive for the *FLT3-ITD* mutation, relative to primitive bone marrow $CD34^+$ controls. We identify methylation of the *KLF5* 5' proximal promoter and intron 1 as potential mechanisms for down-regulation in AML, and accordingly demonstrate that treatment of leukaemia cell lines with demethylating agents re-activates *KLF5* expression in cells displaying hypermethylation of *KLF5*. Aberrant methylation of the *KLF5* proximal promoter

is associated with samples displaying monosomy 7 or deletions in chromosome 7q, and methylation of *KLF5* intron 1 is significantly higher in samples with normal karyotype than in those displaying abnormal cytogenetics. We demonstrate expression and splicing of an alternative exon within *KLF5* intron 1, which is encompassed by the region shown to be hypermethylated in a subset of AML samples. It is likely that this exon represents an alternative transcription start site which is regulated by an alternative promoter associated with a high level of interspecies conservation. Translation of this alternative *KLF5* isoform is predicted to code for an N-terminal-truncated KLF5 protein, and further research is now required to determine the regulation and functional significance of this isoform in normal haemopoiesis and in AML. Finally, we demonstrate that enforced expression of *KLF5* in the leukaemia cell line U937 induces changes associated with myeloid differentiation, and enhances differentiation in response to differentiation-inducing reagents. Collectively, these data are consistent with *KLF5* acting as a tumour suppressor in the myeloid lineage.

Declaration

This work contains no material which has been accepted for the award of any other degree or diploma in any university or other tertiary institution to Sonya Diakiw and, to the best of my knowledge and belief, contains no material previously published or written by another person, except where due reference has been made in the text. With respect to my relative contribution in each of the experimental Chapters, I certify that I carried out all of the experimentation described except where duly noted in the text. A list of publications and abstracts presenting the work described in this thesis is included on Page 16.

I give consent to this copy of my thesis, when deposited in the University Library, being made available for loan and photocopying, subject to the provisions of the Copyright Act 1968.

I also give permission for the digital version of my thesis to be made available on the web, via the University's digital research repository, the Library catalogue, the Australasian Digital Theses Program (ADTP) and also through web search engines, unless permission has been granted by the University to restrict access for a period of time.

Sonya Diakiw

April 2011

Publications and Abstracts

Published abstracts:

- **DIAKIW, S.M**., Brown, A.L., Kok, C.H., D'Andrea, R.J. (2010). The role of KLF5 in normal haemopoiesis and in Acute Myeloid Leukaemia. *Experimental Hematology*, 38 (9) S1.
- **DIAKIW, S.M**., Brown, A.L., Salerno, D.G., Gonda, T.J., Murphy, K., Bardy, P.G., Revesz, T., Lewis, I., Gonda, T.J., D'Andrea, R.J. (2007). Identification of oncogenes from myeloid leukaemias by retroviral expression cloning. *Experimental Hematology*, 35 (9) S2.
- Brown, A.L., Wilkinson, C., Waterman, S.R., Salerno, D.G., **DIAKIW, S.M**., Tsykin, A., Goodall, G.J., Solomon, P.J., Gonda, T.J., D'Andrea, R.J. (2005). Analysis of gene expression changes induced by leukaemogenic mutants of the GM-CSF receptor reveals genes important for self-renewal versus differentiation of myeloid cells. *Experimental Hematology*, 33 (7).

Oral presentations:

- **DIAKIW, S.M**., Brown, A.L., Kok, C.H., D'Andrea, R.J. The role of KLF5 in normal haemopoiesis and in Acute Myeloid Leukaemia. *International Society for Experimental Hematology Conference, 2010.*
- **DIAKIW, S.M**., Brown, A.L., Kok, C.H., D'Andrea, R.J. A role for Klf5 as a tumour suppressor in AML. *HAA-HSANZ Conference, 2009.*

Poster presentations:

- **DIAKIW, S.M**., Brown, A.L., Kok, C.H., D'Andrea, R.J. The role of KLF5 in normal haemopoiesis and in Acute Myeloid Leukaemia. *International Society for Experimental Hematology Conference, 2010.*
- **DIAKIW, S.M**., Brown, A.L., Salerno, D.G., Gonda, T.J., Murphy, K., Bardy, P.G., Revesz, T., Lewis, I., Gonda, T.J., D'Andrea, R.J. Identification of oncogenes from myeloid leukaemias by retroviral expression cloning. *University of Adelaide Inaugural Postgraduate Research Expo, Faculty of Health Sciences, 2007.*
- Brown, A.L., Wilkinson, C., **DIAKIW, S.M**., Das, S., Salerno, D.G., Kok, C.H., Waterman, S.R., Goodall, G.J., Solomon, P.J., Lewis, I., Young, S., Gonda, T.J., D'Andrea, R.J. Potential C/EBP targets and AML tumour suppressor genes identified by microarray gene expression analysis. *New Directions in Leukaemia Research Conference, 2008.*
- **DIAKIW, S.M**., Brown, A.L., Kok, C.H., D'Andrea, R.J. A role for Klf5 as a tumour suppressor in AML. *Lorne Cancer Conference, 2009*.
- **DIAKIW, S.M**., Brown, A.L., Kok, C.H., D'Andrea, R.J. Klf5 as a potential novel tumour suppressor in AML. *New Directions in Leukaemia Research Conference, 2010.*

Acknowledgements

I would like to thank all the staff and students at the Institute of Medical and Veterinary Science, and in particular my colleagues and friends in the Acute Leukaemia Laboratory for their help and support, both scientific and non-scientific, during my undertaking of this program. I would especially like to thank my supervisors, Richard D'Andrea and Anna Brown, for their support and guidance throughout my PhD. Thank you also to the staff and students at the University of Adelaide and the Discipline of Genetics. Lastly, I would like to say thank you to my parents, family, and close friends for all their encouragement and support over these years – I dearly appreciate the continuing motivation you have given me.

Chapter 1 – Literature review and research proposal

1.1 Acute Myeloid Leukaemia

Leukaemia is a malignancy of the blood system characterised by the continued proliferation and suppressed differentiation of haemopoietic progenitor cells. Pathologically, leukaemias result in a high proportion of progenitor cells in the blood system, causing a variety of clinical symptoms such as fatigue, weakness and recurrent infections. Approximately 2500 Australians are diagnosed with leukaemia each year, and myeloid leukaemia in particular accounts for more than half of these cases (Australian Institute of Health and Welfare and Australian Associated Cancer Registry, 2005). Although therapy for myeloid leukaemia is available the success rates are usually low and the treatment involved is associated with significant morbidity and mortality[2]. Current treatment regimes for Acute Myeloid Leukaemia (AML) have an average of 40-50% 5 year survival, although this can be as low as 10-20% in some subtypes[2,3]. A significant proportion of patients experience relapse of disease following induction chemotherapy (33-78% depending on subtype[4-6]), and approximately 1000 deaths result from AML per year in Australia alone (Australian Bureau of Statistics, 2008). Conventional chemotherapy is not specific for targeting haemopoietic cells, and can result in life-threatening toxic side-effects by destroying healthy tissue. Consequently there is a need for improved treatments, and in order to develop these a clear understanding of the molecular mechanisms involved in normal haemopoiesis and leukaemia is essential.

1.1.1 Haemopoiesis and leukaemia

During haemopoiesis, multipotent haemopoietic stem cells (HSCs) maintain the adult blood system through reciprocal processes of self-renewal and progressive cell maturation. These stem cells respond to a variety of intrinsic and extrinsic factors which control the formation of lymphoid, myeloid, erythroid and megakaryocytic cell types. In particular, a complex interplay of growth factors and transcriptional regulators is required for directing haemopoietic cell fate (Figure 1.1)[7-14]. The early stages of haemopoiesis require transcription factors such as TAL1 and RUNX1 (also known as AML1), which are necessary for the derivation of adult HSCs[15]. HSCs are transcriptionally primed for multi-lineage differentiation, expressing low levels of lineage-specific genes and transcription factors which fluctuate in response to external cues[7,16]. Developmental morphogens such as the WNT proteins or members of the BMP family can influence the decision for HSC to either maintain self-renewal or to differentiate to more committed progenitor types[17,18]. In response to such extrinsic signals the balance of transcription factor expression is shifted and lineage commitment initiated. Progression through subsequent developmental stages in which committed progenitor cells differentiate to mature cell types is coordinated by a range of haemopoietic cytokines, for example EPO, GM-CSF, and IL-7[19,20], and through cooperation of a number of lineage-specific transcription factors, for example KLF1 (erythroid), C/EBPε (granulocytic), and PAX5 (B-cell lineage)[21-23] (see Figure 1.1). Differentiation is coupled with reduced lineage potential and proliferative capacity, with mature haemopoietic cells retaining only a very limited ability for proliferation and self-renewal. These highly-coordinated mechanisms sustain the adult blood and immune system, however genetic disturbances which interfere with these processes can contribute to the development of haemopoietic disorders

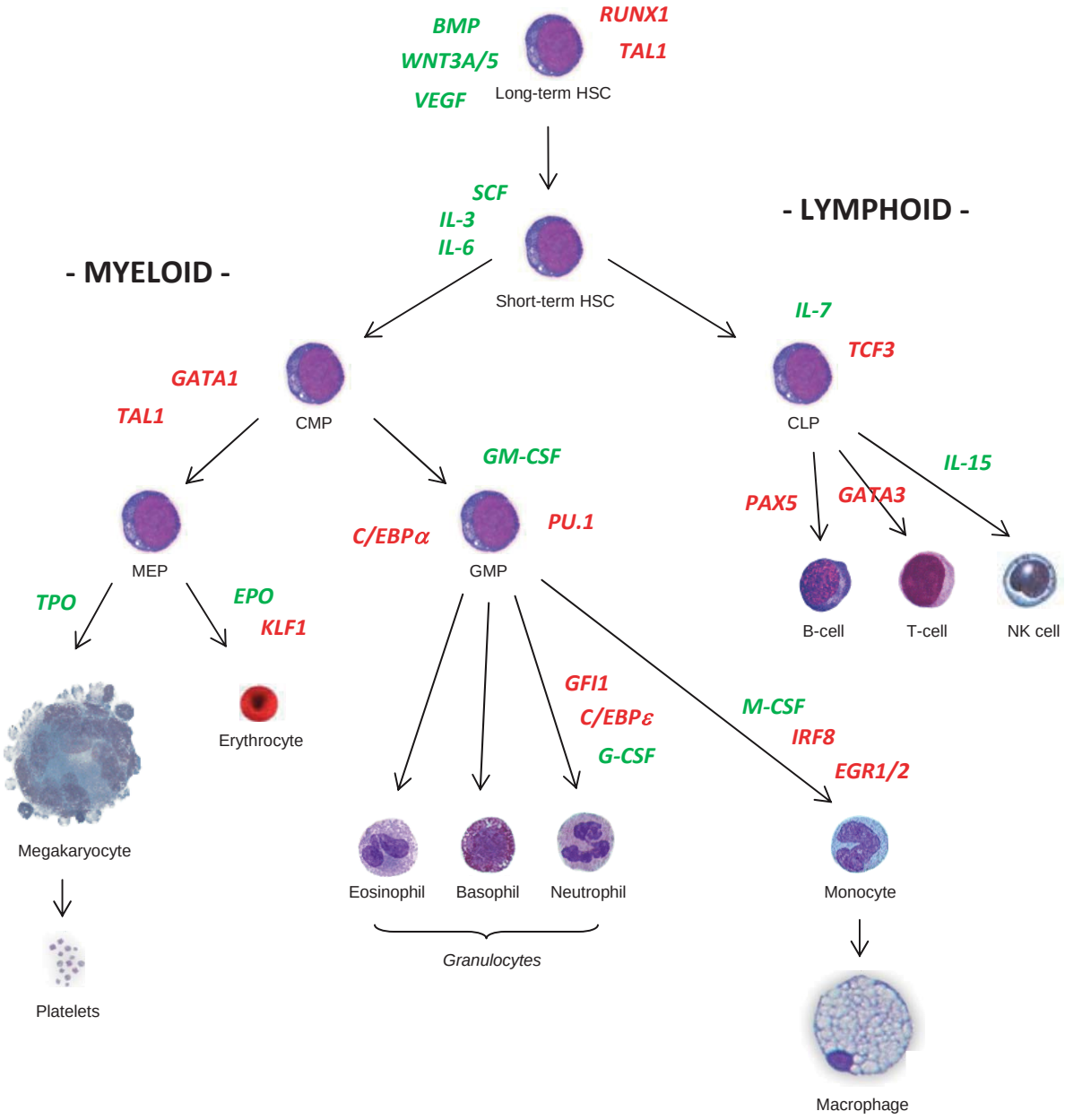

Figure 1.1: Haemopoiesis. Multipotent haemopoietic stem cells (HSC) maintain a balance of self-renewal and differentiation to a series of committed progenitor types then to mature cell types of myeloid and lymphoid lineages. Examples of growth factors influencing this process at various stages of development are shown in green text, whereas transcription factors are shown in red. CMP = common myeloid progenitor, CLP = common lymphoid progenitor, MEP = megakaryocyte-erythrocyte progenitor, GMP = granulocyte-macrophage progenitor, NK cell = natural killer cell.

such as myeloproliferative neoplasms (MPN), myelodysplatic syndromes (MDS), and leukaemia.

1.1.2 Molecular genetics of myeloid leukaemia

Myeloid leukaemias are a group of diseases displaying heterogeneity in clinical presentation, cellular morphology, and causative genetic lesions. Despite this variability, each case is characterised by acquired mutations conferring deregulated proliferation, survival advantages, and impaired differentiation of haemopoietic cells. It has been proposed that mutational events in AML can be broadly separated into two complementation groups or classes[24,25]. The first class of mutations result in enhanced proliferation and/or increased survival capacity of haemopoietic cells. These primarily include activating mutations in signalling molecules such as *FLT3*, *RAS*, and *KIT*, which give rise to autonomous cell proliferation[26,27]. However, a number of other lesions may also be categorised as Class I mutations, such as inactivating mutations in, or deletion of, key regulators of the cell cycle (e.g. *TP53* and *RB1*[28-31]), or genetic lesions which promote cell survival through inhibition of apoptosis (e.g. over-expression of BCL2[32-35]).

The second class of lesions are those which primarily impair differentiation of haemopoietic cells. These mutations often involve deregulation of transcription factors important for the control of myeloid differentiation; for example, point mutations have been described which alter the activity of the myeloid regulators PU.1 and C/EBPα[36,37]. Haemopoietic transcription factors are frequently disturbed in AML by chromosomal translocations or inversions, giving rise to chimeric transcription factors with altered properties. For example, common chromosomal abnormalities involving *RUNX1* (*AML1*), such as the t(8;21) translocation, or

RARA, such as the t(15;17) translocation, result in expression of the fusion proteins AML1-ETO and PML-RARα respectively, which act as dominant negative forms of the original transcription factor and contribute to the leukaemic differentiation block[38]. Abnormal activation of key haemopoietic transcription factors involved in the self-renewal and maintenance of progenitor populations may also be categorised as Class II lesions. For example, members of the HOX family are commonly over-expressed or activated by translocation in AML, where they contribute to aberrant differentiation and enhanced self-renewal[39-42].

Identification of lesions contributing to the pathogenesis of myeloid leukaemia has led to the development of targeted therapies which have significantly improved survival in selected subtypes. For example, the tyrosine kinase inhibitor Imatinib (Gleevec) inhibits the constitutively active BCR-ABL fusion protein in treatment of Chronic Myeloid Leukaemia (CML)[43], and All-*trans* retinoic acid (ATRA) acts to restore expression of differentiation-inducing genes blocked by the PML-RARα fusion protein in treatment of Acute Promyelocytic Leukaemia (APL)[44]. Therefore, it is clear that a more thorough understanding of the particular pathways and genetic lesions involved in AML will be necessary to aid in the development of more effective and less toxic targeted therapies for this disease.

1.1.3 Cooperation of mutations in AML

Like other cancers, AML requires the accumulation of multiple genetic lesions. This has been demonstrated in a number of murine models where expression of a single aberrant gene or fusion protein is not sufficient to induce leukaemia. For example, expression of the Class I-acting ETV6-ABL fusion protein (complex t(9;12) translocation), or the FLT3 internal

tandem duplication (FLT3-ITD) activated receptor, induces a hyperproliferative response in mouse bone marrow transplantation studies, resulting in a phenotype similar to that of human MPN[45,46]. Accordingly, Class I mutations are commonly found in patients with MPN, for example the BCR-ABL fusion protein generated by the t(9;22) translocation in CML[47], or the *JAK2 V617F* mutation prevalent in Polycythemia Vera (PV)[48]. Alternatively, over-expression of Class II-acting fusion proteins involving components of the Core binding factor (CBF) complex, such as AML1-ETO (t(8;21)) or CBFβ-MYH11 (inv(16)), impairs haemopoietic differentiation in mice and results in a myelodysplastic-like phenotype[49,50]. However, transplantation of haemopoietic progenitor cells expressing both FLT3-ITD and CBFβ-MYH11 induces an aggressive AML phenotype in mice[51], demonstrating the importance of cooperation between these two classes of lesions in the biology of AML. Class II mutations contribute to the transformation of MPN to AML in human disease, for example, individuals displaying chronic phase CML associated with the BCR-ABL translocation may develop blast crisis with subsequent acquisition of the NUP98-HOXA9 t(7;11) translocation[52]. Recent studies have demonstrated that point mutations in *RUNX1*, which inhibit differentiation of haematopoietic stem cells, are often acquired in the transformation of MPN to leukaemia[53,54].

The observation that more than one genetic abnormality is detected in most individuals with AML further supports the idea of cooperating mutations in the pathogenesis of this disease. For example, studies have shown a strong association of Class I mutations in *FLT3*, *RAS*, or *KIT* with translocations involving elements of the CBF complex[25,55,56]. Mutations in *FLT3* can also occur in conjunction with Class II acting mutations in *NPM1* and *CEBPA*[55,56]. Further insights have been obtained from studies of familial myeloid disorders, where it has been noted that germline mutations in *RUNX1* and *CEBPA* predispose individuals to AML[57].

1.1.4 Epigenetic mechanisms in AML

1.1.4.1 Methylation

Although genetic events such as mutation or chromosomal translocation play an important role in the development of AML, an expanding number of studies have also implicated epigenetic regulation in leukaemogenic processes[58,59]. Chromatin state is affected by a combination of DNA methylation, histone modification and nucleosome remodelling, which lead to large-scale, heritable gene silencing[60,61]. DNA methylation involves the addition of a methyl group to the 5 position of a cytosine pyrimidine ring within a DNA sequence, typically in a CpG dinucleotide context. Methylation of CpG dinucleotides within gene promoter sequences can repress expression by disrupting the ability of transcription factors to bind to their target sites[62,63], or by enhancing the ability of methylation-dependent transcriptional repressors to bind to these regions[64,65]. A hallmark of cancer is aberrant methylation of CpG islands in gene promoter regions, particularly those associated with tumour suppressor genes, which are normally hypomethylated in healthy tissues[66].

The importance of aberrant DNA methylation as an initiating event in the development of leukaemia has not yet been fully elucidated. In some tumour types, such as colon cancer, it has been suggested that epigenetic changes are accumulated subsequent to primary mutations which initiate the cancerous phenotype[67]. However, large-scale methylation profiling studies such as that conducted by Figueroa, et al., have demonstrated that hypermethylation is a wide-spread phenomenom in AML[68]. A number of tumour suppressors are frequently found to be silenced by methylation in AML, such as the cell cycle regulators *CDKN2B* (*p15*) and *TP73*, and the growth suppressors *HIC1* and *RARB*[69-74]. Methylation-induced silencing of the

differentiation-associated myeloid transcription factor *CEBPA* may be critical in a particular subgroup of AML[75]. Studies have shown that overall CpG methylation increases during progression of MDS to AML, suggesting that methylation may be a key event in the early stages of acute transformation[76,77].

The mechanisms associated with aberrant methylation in AML have not yet been comprehensively determined. Studies have shown that the *de novo* DNA methyltransferases DNMT3A and DNMT3B are over-expressed in AML, and in the case of DNMT3B this correlated with hypermethylation of the tumour suppressor gene *CDKN2B*[78]. A recent study by Ley, et al., identified mutations predicted to affect translation of *DNMT3A* in 22% of AML patients[79]. Although it is not yet clear how these mutations may contribute to aberrant methylation in leukaemia, it was observed that mutations in *DNMT3A* were associated with poor patient outcome. Gain-of-function mutations in the metabolic proteins IDH1 and IDH2 have been recently linked to specific hypermethylated epigenetic subgroups in AML[80]. Functional studies demonstrated that these mutant IDH proteins interfere with the activity of the hydroxymethylase enzyme TET2, which normally plays a role in DNA demethylation. Interestingly, mutations in *TET2* are also found in AML, and the authors demonstrated that patients with *TET2* mutations display a similar hypermethylated epigenetic profile to patients with *IDH1/2* mutations[80]. Aberrant methylation in AML can also be induced through the actions of common leukaemic fusion proteins such as AML1-ETO and PML-RARα via recruitment of DNA methyltransferases[81,82]. It is likely that tumour suppressor gene silencing by DNA methylation cooperates with other genetic mechanisms in the development of AML.

1.1.4.2 Histone modifications and chromatin remodelling

Histone proteins are the core component of nucleosomes, which act as a scaffold to package DNA into a higher order chromatin structure. Post-translational modification of key amino acids in histone proteins can effect structural changes in chromatin, either remodelling the chromatin structure to allow transcriptional activation (euchromatin), or resulting in a condensed chromatin formation associated with transcriptional repression (heterochromatin)[83,84]. Histone modifications also act to recruit protein complexes which further modify chromatin state, such as the Nucleosome remodelling factor (NURF) complex[85-88], or which can influence methylation of DNA, such as complexes involving the CBX family of heterochromatin proteins (HP1 proteins) and DNA methyltransferases[89-91]. Most histone modifications occur on the N-terminal tails of Histones H3 and H4, generating a complex pattern of modifications referred to as the Histone Code[92].

The most extensively studied histone modification is acetylation of lysine residues, which is associated with an open chromatin state and gene activation[93,94]. Lysine methylation can be a mark of open or condensed chromatin depending on the amino acid position being modified and the extent of methylation, for example, di- or tri-methylation of lysines 9 and 27 in Histone H3 are associated with transcriptional repression, whereas mono-methylation of lysine 4 in Histone H3 is associated with transcriptional activation[95]. A number of other modifications have also been reported such as phosphorylation, glycosylation, SUMOylation (addition of Small ubiquitin-like modifier (SUMO) proteins), Adenosine diphosphate (ADP) ribosylation, and ubiquitination, and the specific contribution of these to the chromatin state is the subject of ongoing investigation[84].

It is clear that aberrant histone modification plays a role in a number of subtypes of AML. The common fusion proteins PML-RARα and AML1-ETO directly recruit histone deacetylases (HDACs) which result in inactivation of genes important for haemopoietic differentiation[96-98]. The *MLL* gene is translocated to a number of different partners in AML, such as *AF4*/*AF9*/*AF10* which contain intrinsic histone methyltransferase activity, and *CBP*, a known histone acetyltransferase, which results in deregulated modification of histones and aberrant target gene activation or repression in AML[99,100]. An increasing number of point mutations have been recently discovered in members of the Polycomb-group protein family, such as *UTX*, *ASXL1*, and *EZH2*[101-103]. The Polycomb-group of proteins are involved in methylation of histone residues, and are key regulators of Homeobox gene expression[104]. Although the mechanisms involved have not yet been fully elucidated, it is clear that histone modifications and DNA methylation cooperate to induce stable silencing of tumour suppressor genes in cancer pathogenesis[61,105].

1.1.5 Methods for identification of novel leukaemic lesions and pathways

Many genetic lesions contributing to AML have been identified by cytogenetic techniques. Genes located at chromosomal breakpoints are often involved in the leukaemic process, and can be involved in the creation of fusion proteins with altered activity as discussed previously in Section 1.1.2. However in up to 50% of myeloid leukaemias the key aberrations involved cannot be identified from chromosomal abnormalities as these are lacking or apparently random[2,106,107].

1.1.5.1 Genome-wide screens

Advances in genomics-based methods have allowed development of large-scale screening techniques for identification of genes with roles in leukaemogenesis. Comprehensive microarray analyses to study gene expression changes in primary AML patient samples have been used to identify biologically relevant pathways in specific subtypes of leukaemias. For example, Wouters, et al. demonstrated that the subgroup of AML samples with silenced *CEBPA* were associated with aberrant NOTCH1 signalling[108]. A gene expression profiling study of APL patients with a t(11;17) translocation identified the retinoic acid binding protein *CRABP1* as a downstream target of the RARα-PLZF fusion protein, which was subsequently shown to contribute to retinoid-resistance in these patients[109,110].

Large-scale analyses of methylation patterns have been successfully used to identify potential tumour suppressor candidates in AML. For example, Gebhard, et al. developed a novel approach for genome-wide assessment of methylation using a methyl-binding protein chromatin immunoprecipitation (ChIP) technique[111]. They identified a number of transcription factors whose promoters were hypermethylated in leukaemia cell lines and in primary patient samples, which correlated with reduced gene expression (e.g. *MAFB, KLF11*). Methylation profiling of 344 AML patients using the HpaII tiny fragment enrichment by ligation-mediated PCR (HELP) approach identified a set of 45 genes which were consistently methylated in the majority of AML samples assessed, suggesting that down-regulation of these genes may be a common factor necessary for leukaemic transformation[68,112].

Genome-wide approaches have also been utilised to identify novel mutations contributing to the development of AML. Screening for copy number alteration in patient samples using

single nucelotide polymorphism (SNP) arrays has identified previously undetected deletions, amplifications, and mutations, providing a host of candidate genes to be further investigated in the pathogenesis of AML[113,114]. The application of this technology has led to identification of novel mutations in genes such as *CBL* and *TET2* in a range of myeloid disorders[115-117]. Whole-genome sequencing of AML patient samples has been utilised to detect mutations in genes previously not associated with AML, for example, recurrent heterozygous mutations were identified in the gene encoding the metabolic protein *IDH1*, and further screening revealed that these mutations occur in approximately 9% of *de novo* French-American-British (FAB) M1 subtype AMLs, as well as in other myeloid neoplasms[118-120].

1.1.5.2 Functional screens

Genomics-based screens have provided valuable insight into potential mechanisms underlying leukaemogenesis, especially in recent years with improved capacity and sensitivity of screening methods such as next-generation sequencing[121]. For any changes identified by these approaches, further research is required to validate the functional role of candidate genes and to determine the biological consequences of their deregulation. Functional screens are an alternative approach to identify novel genes involved in haemopoiesis and in AML. One example is gene dysregulation by retroviral insertion mutagenesis giving rise to leukaemia in animal models. This approach has revealed oncogenes such as *MYB* and *REL*[122,123]. The Retroviral Tagged Cancer Gene Database (RTCGD) is an extensive compilation of genes associated with these insertions, allowing scientists to rapidly screen potential oncogenes for association with a leukaemic phenotype[124]. Functional expression cloning screens have identified genes involved in leukaemic processes based on their ability to confer a specific phenotype in a target cell system. This approach has been successfully used to isolate both

novel oncogenes, such as *SOCS1*and the RAS-related protein *RASGRP4*, and putative tumour suppressors such as the protein phosphatase *PP4*[125-127].

1.2 Identification of novel oncogenes and tumour suppressors using the FDB1 murine myeloid cell line

1.2.1 The FDB1 cell line model

In order to study the regulation of growth and differentiation in the granulocyte-macrophage lineage and the mechanisms underlying the pathogenesis of AML, our laboratory has made use of the unique murine myeloid cell line FDB1. The FDB1 cell line arose spontaneously in murine foetal liver cell cultures following retroviral infection with the human *GM-CSF/IL-3/IL-5 receptor common beta chain* (*hβc*)[128]. FDB1 cells are completely growth factor-dependent; when maintained in IL-3 they proliferate continuously with an immature promyelocytic morphology, whereas in GM-CSF they differentiate to produce approximately equal proportions of granulocytes and macrophages over 5 days (Figure 1.2). Interestingly, factor-independent growth of FDB1 cells can be achieved with enforced expression of activated mutants of hβc. Expression of the leukaemogenic V449E mutant allows cells to proliferate with a similar morphological appearance to cells in IL-3 in media without factor, whereas with expression of the FIΔ extracellular mutant cells differentiate to granulocytes and macrophages (see Figure 1.2)[128]. These properties make the FDB1 cell line a useful model for studying aspects of normal and malignant myelopoiesis, as the growth, survival and differentiation of these cells can be manipulated through the use of cytokines or by expression of constitutively activated cytokine receptors.

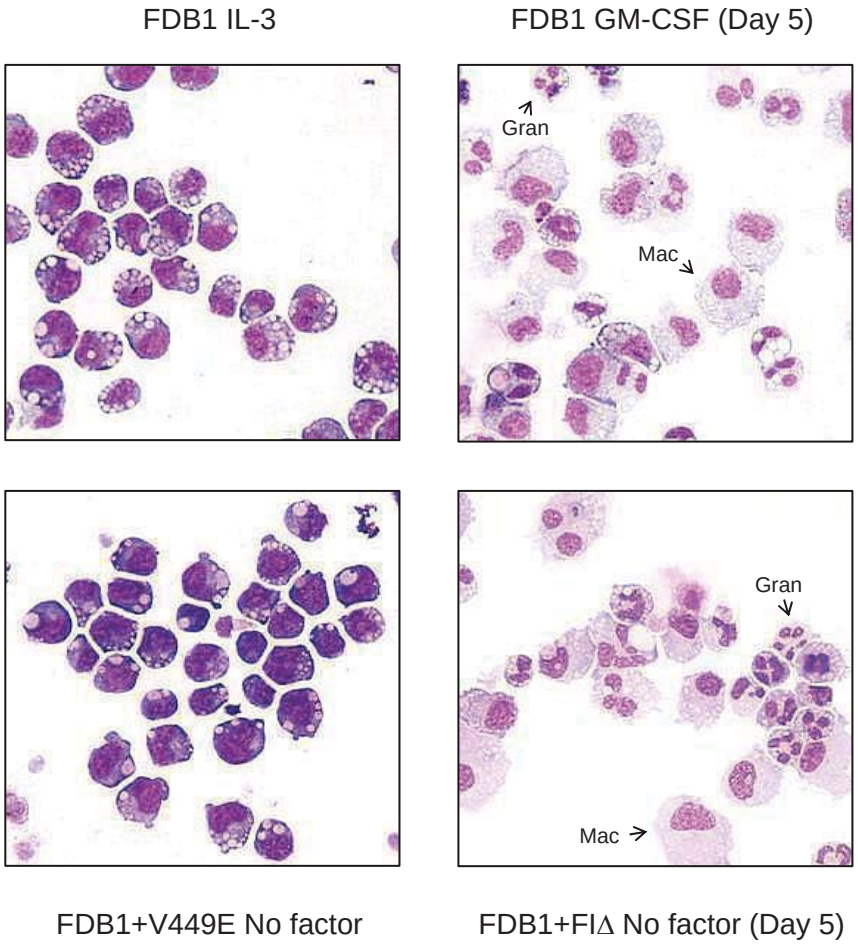

Figure 1.2: FDB1 model system of myeloid differentiation. FDB1 parental cells cultured in IL-3 proliferate continuously and display an immature myeloblastic morphology. When cultured in GM-CSF for 5 days they differentiate to produce approximately equal proportions of granulocytes and macrophages[128]. FDB1 cells expressing activated mutants of hβc display factor-independent growth. Expression of the V449E mutant leads to continuous proliferation with a morphology similar to that of parental cells in IL-3, whereas expression of the FIΔ mutant results in differentiation to macrophages and granulocytes similar to parental cells in GM-CSF[129]. Gran = granulocyte, Mac = macrophage. No factor = media not supplemented with growth factors.

1.2.2 Gene expression profiling using the FDB1 cell line system

To identify potential myeloid tumour suppressors or oncogenes, an extensive series of microarray analyses were previously performed using FDB1 cell populations to detect gene expression signatures associated with the switch from continuous cell proliferation to granulocyte-macrophage differentiation. Gene expression profiles were generated using FDB1 cells undergoing continuous proliferation (either with addition of IL-3 or expression of the hβc mutant V449E) or granulocyte-macrophage differentiation (either with addition of GM-CSF or expression of the hβc mutant FIΔ)[1]. Although expression of the hβc mutants produces similar cellular outcomes to cytokine stimulation, the signalling redundancy is greatly reduced allowing for better dissection of the pathways and genes involved in these processes[130]. We hypothesised that gene expression signatures associated with continued proliferation of FDB1 cells, particularly those activated by the leukaemogenic V449E mutant, would be consistent with a potential oncogenic role for these genes in the development of leukaemia. Alternatively, gene expression signatures associated with differentiation of FDB1 cells (i.e. repressed by V449E and/or activated by FIΔ/GM-CSF) would represent potential tumour suppressor function. These studies highlighted a number of transcription factors with potential for playing a critical role in governing the process of myeloid differentiation[1].

1.2.3 Identification of Krüppel-like factor 5 as a differentiation-associated gene in the myeloid system

Krüppel-like factor 5 (*Klf5*) was identified as a transcription factor whose messenger RNA (mRNA) expression increased in FDB1 cells undergoing granulocyte-macrophage differentiation induced by expression of FIΔ (Figure 1.3A)[1]. In contrast, proliferating cells

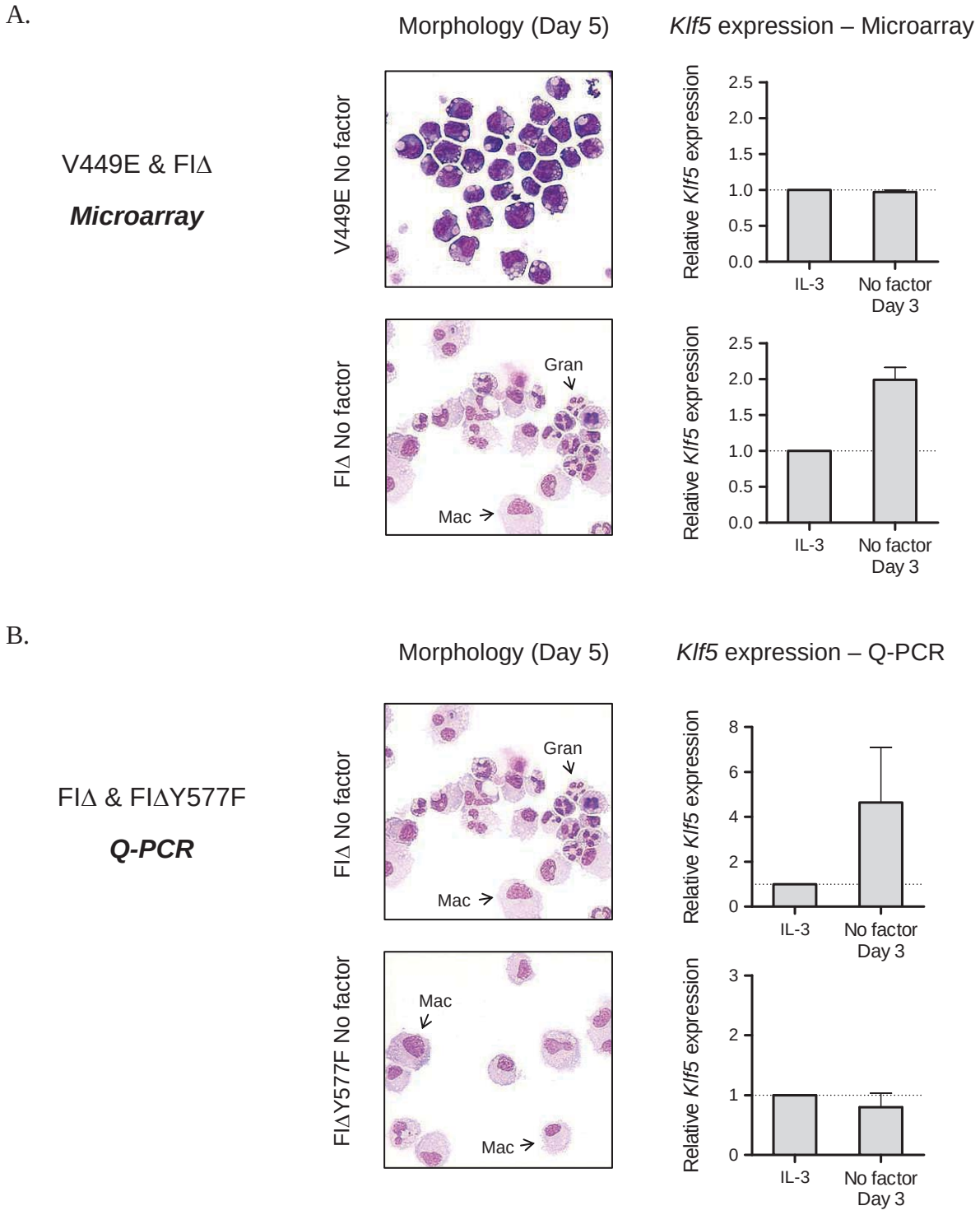

Figure 1.3: *Klf5* expression during FDB1 differentiation. A. *Klf5* mRNA expression increases during factor-independent granulocyte-macrophage differentiation of FDB1 cells expressing the hβc FIΔ mutant, but not during factor-independent culture of cells expressing the V449E mutant (continuous proliferation). Data was extracted from microarray analyses performed by Brown, et al.[1], and *Klf5* fluorescence plotted relative to Day 0 (cells in IL-3). The morphology of cells on Day 5 of culture is shown. n=4. **B.** *Klf5* mRNA expression increases during factor-independent granulocyte-macrophage differentiation of FDB1 cells expressing the hβc FIΔ mutant, but not during factor-independent macrophage-only differentiation of cells expressing the FIΔY577F mutant. Data was extracted from Q-PCR analyses performed by D. Salerno (unpublished data), and *Klf5* fluorescence plotted relative to Day 0 (cells in IL-3). The morphology of cells on Day 5 of culture is shown. n=3. Gran = granulocyte, Mac = macrophage. No factor = media not supplemented with growth factors.

expressing V449E showed no change in *Klf5* expression under similar conditions. Unsupervised hierarchical cluster analysis performed using the gene expression profiling data grouped *Klf5* with a number of genes known to induce growth arrest and/or terminal myeloid differentiation, such as *Egr1* and *Egr3*, and the homeobox-related *Hlx* gene[1], suggesting that KLF5 may have a similar functional role in the haemopoietic system.

1.2.3.1 *Klf5* expression is associated with the granulocyte lineage

Further microarray analyses were utilised to identify gene expression signatures associated specifically with granulocyte or macrophage differentiation (A. Brown and C. Wilkinson, unpublished data). Lineage-specific manipulation of the FDB1 cell line was achieved using enforced expression of additional mutant forms of hβc. As described above, expression of the FIΔ mutant drives factor-independent differentiation of FDB1 cells to both granulocytes and macrophages. A second-site tyrosine to phenylalanine mutation in FIΔ (Y577F) reduces granulocyte differentiation, thus driving factor-independent differentiation of FDB1 cells predominantly to macrophages[129]. By comparing gene expression profiles from cells expressing the FIΔ or FIΔ Y577F mutant, we were able to identify gene-sets associated with macrophage or granulocyte differentiation (A. Brown, unpublished data). In particular, *Klf5* expression increased significantly during FIΔ-induced granulocyte-macrophage differentiation, but not during FIΔ Y577F-induced macrophage differentiation, consistent with selective increased expression in the granulocyte lineage. These results were validated using quantitative reverse-transcription PCR (Q-PCR) analysis, as shown in Figure 1.3B (D. Salerno, unpublished data).

Significant regulation of a number of C/EBPα target genes was identified within the granulocyte-specific gene-set (A. Brown, unpublished data). *CEBPA* encodes a transcription factor expressed early during myeloid differentiation, and *in vivo* studies have demonstrated an essential role for this protein in development of the granulocyte lineage[131]. Within the granulocyte-specific gene-set, the expression profile of *Klf5* was associated with that of a number of C/EBPα target genes, suggesting that it too may be regulated downstream of C/EBPα during FDB1 myeloid differentiation. This is consistent with a study by Cammenga, et al., who identified *KLF5* as a target of C/EBPα in human $CD34^+$ haemopoietic progenitor cells[132]. Regulation of *KLF5* by C/EBPα further supports a role for KLF5 in granulocyte differentiation. From these observations we have hypothesised that KLF5 may function as a transcription factor regulating differentiation in the myeloid lineage, particularly along the granulocytic pathway. This function would also be consistent with a potential role for KLF5 as a tumour suppressor in the myeloid system.

1.3 Krüppel-like factor 5

1.3.1 The Krüppel-like family of transcription factors

KLF5 belongs to the family of Krüppel-like transcription factors. Members of this family have been implicated in an extensive array of biological processes including embryonic development, control of cellular proliferation and differentiation, stress response, and many others (Table 1.1)[133,134]. The KLF family of proteins all share a common zinc finger motif displaying homology to the *Drosophila melanogaster* '*Krüppel'* gene, deletion of which results in the loss of central segments to give the 'crippled' phenotype[135,136]. KLF family members are closely related to the Sp family of transcription factors but are distinguished by a

NOTE:
This table is included on page 36
of the print copy of the thesis held in
the University of Adelaide Library.

Table 1.1: Function of KLF family members.
‘-/-’ indicates homozygous knock-out, ‘+/-’ indicates heterozygous knock-out model. Adapted from McConnell and Yang[134].

unique pattern of three cysteine-2/histidine-2 zinc finger motifs separated by 7 conserved amino acids at the carboxy terminal of the proteins[195,196]. These zinc fingers comprise the DNA-binding domain of the KLF transcription factors, which all bind to similar elements within GC-rich promoter sequences of target genes. Outside of the DNA-binding domain, the KLF family members display relatively low conservation, although phylogenetic analysis has identified distinct subgroups within the KLF family (Figure 1.4). Members of these subgroups share similar features such as specific activation or repression domains, or domains used for protein interaction with other transcriptional coregulators. Specificity of action for members of the KLF family is determined in part by differences in the amino-terminal transactivation domains of these proteins and also by their tissue-specific expression[195].

1.3.2 Krüppel-like factor 5

KLF5 was originally cloned as the *Basic transcription element binding protein 2* (*BTEB2*) gene[197]. It was independently identified as a member of the KLF family of transcription factors by its homology with KLF2[198]. Prior to the reclassification of KLF family nomenclature KLF5 was known as Intestinal krüppel-like factor (IKLF) due to high levels of protein expression in intestinal epithelial cells[198]. Interest in this gene has greatly expanded in recent years as studies have revealed emerging functions in a variety of cell types and biological systems, with homologues identified in numerous vertebrate species. KLF5 has known functions in different aspects of cellular regulation (proliferation, self-renewal, survival and differentiation), as well as in embryonic development, cardiovascular remodelling, stress and immune response, and many other systems[199]. KLF5 plays a number of diverse roles, and has been reported to act as a transcriptional activator or repressor, a

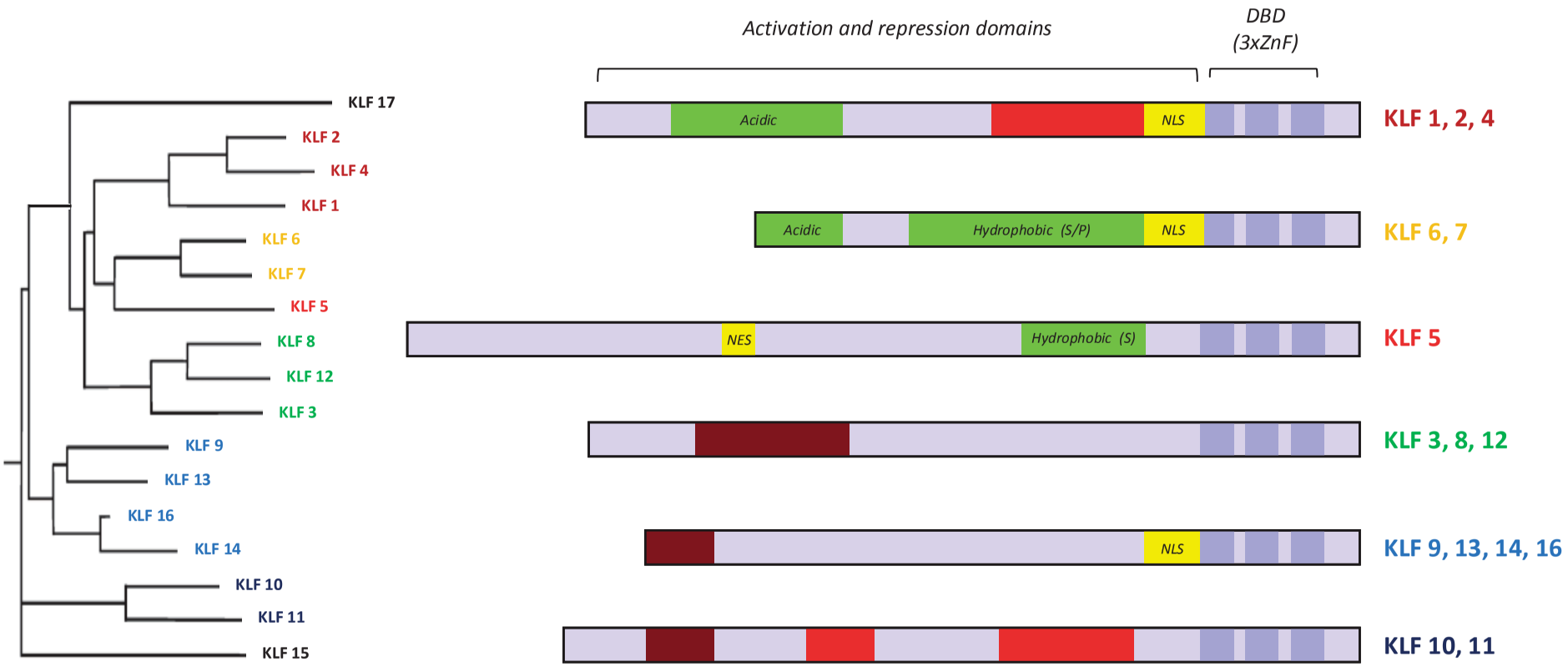

Figure 1.4: KLF family proteins (*Homo sapiens*). Clustering of KLF family members based on amino acid sequence (LEFT) separates them into evolutionarily conserved sub-groups with defined structural domains (RIGHT). All KLF members have a conserved C-terminal DNA-binding domain (DBD) consisting of 3 zinc finger (ZnF) sequences, however subgroups show variation in the N-terminal protein region with distinct activation or repression domains and cellular localisation sequences. Green boxes represent activation domains (S = serine rich, P = proline rich), red boxes represent repression domains (dark red boxes represent repression domains necessary for protein interaction with common corepressors), and yellow boxes represent nuclear localisation signals (NLS) or nuclear export signals (NES). Adapted from van Vliet, et al.[193], Kaczynski, et al.[195], and Moore, et al.[200].

promoter or inhibitor of cell growth, and has been implicated as either a tumour promoter or suppressor depending on the cellular and genetic context in which it is being studied[199].

1.3.3 Gene structure and transcriptional regulation

The *KLF5* gene is located on human chromosome 13q21-22 (Figure 1.5A). The primary transcript comprises 4 exons generating a 3350 nt mRNA, however a smaller 1.5 kb transcript has been detected in the testes[201]. KLF5 is expressed in a variety of epithelial cell types as well as vascular smooth muscle cells (VSMCs), neural cells and lymphoid cells[202-204]. It is highly expressed in the digestive system, with lower levels found in the reproductive organs, pancreas, prostate, skeletal muscle, lung and bladder[197,198,201,202].

The *KLF5* promoter is high in GC content and does not have a canonical TATA box consensus sequence[205]. A number of functional regulatory elements have been identified for transcription factors activating *KLF5* gene expression (see Figure 1.5A). These include the common transcription factors Sp1, EGR1 and EVI1, all of which bind to the *KLF5* promoter to up-regulate transcription[205-207]. *Klf5* expression is also directly activated by the embryonic stem cell (ESC) transcription factor Nanog in mouse cells, and by two members of the C/EBP family in a murine pre-adipocyte cell line (C/EBPβ/δ)[156,208]. Deletion mapping of the *KLF5* promoter region has identified a 6 bp element (nucleotides -454 to -448 where +1 denotes the first nucleotide of the ATG start codon) which is necessary for transcriptional activity in human epithelial cells[206]. In the rat *Klf5* promoter this element corresponds to a functional CCAAT box, which binds the RUNX family of transcriptional regulators as shown by gel mobility shift assays (GMSA)[209]. In addition, the rat *Klf5* promoter contains a functional NF1 binding element[209]. Deletion of a 1.5 kb region of the human *KLF5* promoter (nucleotides

A.

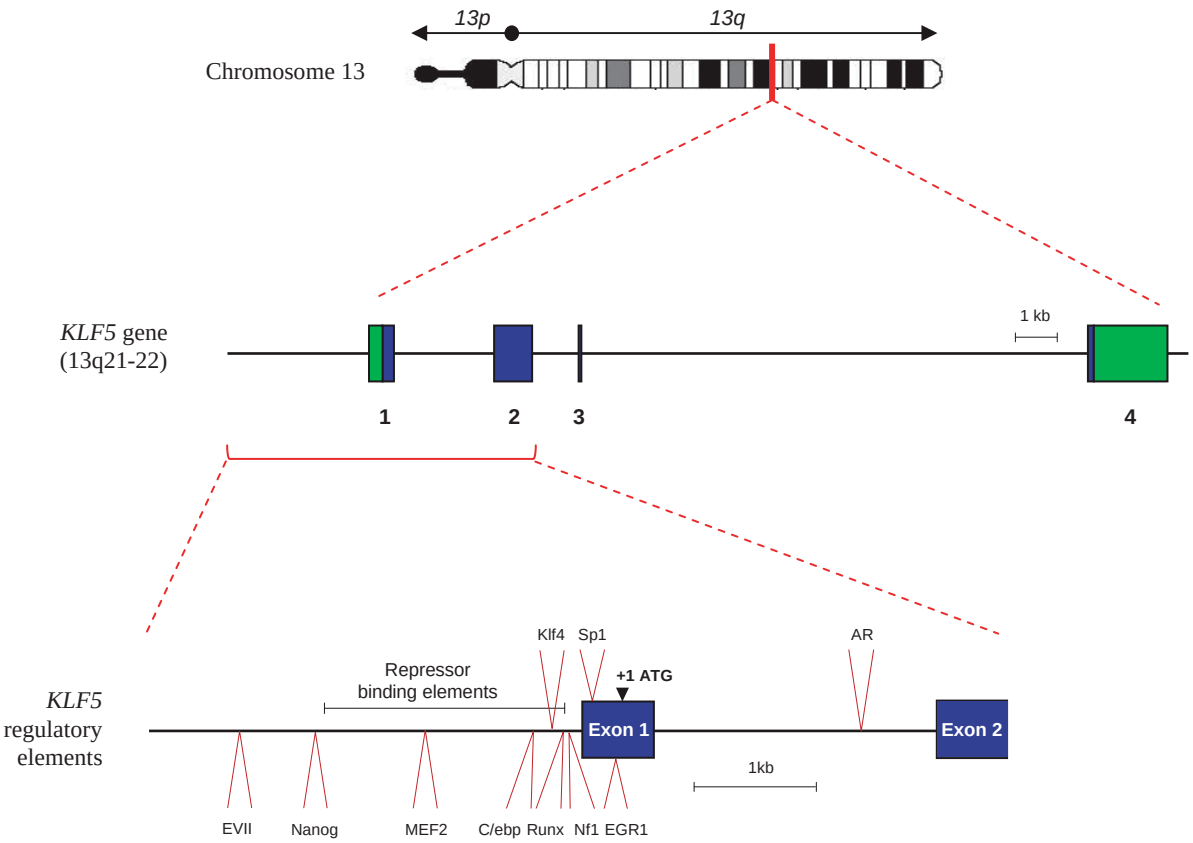

B.

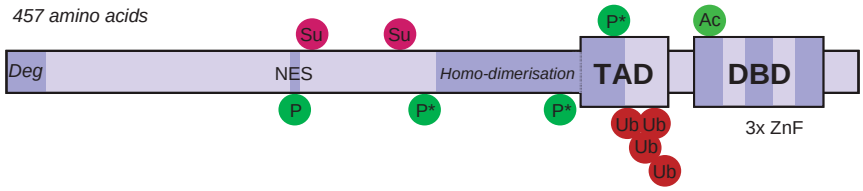

Figure 1.5: KLF5 gene and protein (*Homo sapiens*). A. The human *KLF5* gene contains four exons spanning approximately 18.5 kb on chromosome 13q21-22 (exon 1 - 585 bp, exon 2 - 874 bp, exon 3 - 60 bp, and exon 4 - 1831 bp). 5`- and 3`- untranslated regions are indicated in green. The *KLF5* promoter region and regulatory transcription factor binding elements spanning the proximal promoter and exons 1-2 are shown. Note that lower case transcription factor names indicate that regulation by these transcription factors has been shown in rat or mouse and remains to be validated for the human promoter. **B.** The human KLF5 protein is 457 amino acids in length and contains two main functional domains – a transactivation domain (TAD) and a DNA-binding domain (DBD) consisting of 3 zinc finger motifs (ZnF). Other regions or motifs shown are: The region required for ubiquitin-independent degradation (Deg), a nuclear export signal (NES), and the region required for KLF5 homo-dimerisation. KLF5 can be modified post-translationally by phosphorylation on S153, S303, T234 and T323 (P), SUMOylation on K162 and K209 (Su), acetylation on K369 (Ac) and ubiquitination on residues 323-348 (Ub). Note that P* indicates phosphorylation at these residues targets the KLF5 protein for ubiquitin-mediated degradation.

-1959 to -454) results in increased promoter activity suggesting that this sequence may contain elements for binding repressor proteins[206], and in fact a recent study performed by Tetreault and colleagues in mouse primary esophageal keratinocytes demonstrated that another member of the KLF family, KLF4, can bind to the *Klf5* promoter within this region (at approximately -600 bp) to repress transcription[210]. KLF5 in turn can bind to the *Klf4* promoter and repress expression, which highlights the antagonistic activities of these two related transcription factors[211]. The muscle-specific MEF2 protein can also bind to the *KLF5* promoter to activate transcription[212]. Interestingly, a single nucleotide polymorphism (rs3812852) within the MEF2 binding site can alter the binding affinity of MEF2 and subsequent *KLF5* expression[212]. The G>A polymorphism at -1606 from the ATG codon (positive strand) enhances MEF2 binding and *KLF5* expression, and is associated with increased risk of hypertension in human disease[212]. An A>G change at this position has been linked to decreased *KLF5* expression associated with schizophrenia[203]. Transcription of *KLF5* can also be directly modulated by enhancer elements located outside of the proximal promoter. ChIP analysis and deletion mapping demonstrated binding of the Androgen receptor (AR) protein to intron 1 of the *KLF5* gene which up-regulates expression in prostate cancer cells[213].

Recent studies have shown that *KLF5* mRNA expression may also be regulated through the action of selected microRNAs. In rat VSMCs, *Klf5* is targeted by microRNA-145 which plays a functional role in phenotypic modulation of vascular development[214]. *Klf5* mRNA is also regulated through the actions of microRNAs 143 and 448, which have important roles in adipogenesis[215,216].

1.3.4 Protein and post-translational modifications

The human KLF5 protein (Figure 1.5B) is 457 amino acids in length and consists of the common Krüppel-like factor DNA-binding domain (three zinc finger motifs), a transactivation domain (TAD), and a nuclear export signal (NES). As a transcription factor it is primarily present in the nucleus[201]. However an active NES domain can promote cytoplasmic localisation of KLF5 which effectively inhibits function[217].

It has been shown that various post-translational modifications are crucial in determining the transactivation function of KLF5. Phosphorylation of KLF5 can lead to activation or repression of downstream target genes, through recruitment of various cofactor proteins such as CBP or JUN[218-220]. Acetylation can also switch the transactivation function of KLF5 with respect to regulation of selected target genes. For example, it has been shown that the non-acetylated KLF5 protein acts as a repressor of *CDKN2B* transcription via recruitment of MYC and other transcriptional coregulators. However, upon TGFβ signalling KLF5 is acetylated by the coactivator p300 and instead becomes an activator of expression through altered binding to the promoter and subsequent recruitment of coactivators including SMADS2/3/4 and FOXO3[221,222].

SUMOylation of KLF5 near the NES domain promotes nuclear localisation, where it can act as a repressor of genes (e.g. for the lipid oxidation genes *CPT1B* and *UCP2/3*) [217,223]. This occurs through formation of a corepressor complex which involves the nuclear receptor corepressors NCoR1 and NCoR2 together with the unliganded metabolic protein PPARδ. Treatment with a PPARδ agonist deSUMOylates KLF5 which binds liganded PPARδ together with the coactivator CBP and results in transcriptional activation of lipid oxidation

genes[223]. Thus SUMOylation can act as a switch for KLF5 activity from activator to repressor, and the levels of this modification may explain the different functional roles seen in various sytems.

Finally, KLF5 can also be ubiquitinated and targeted for proteasomal degradation via protein-protein interaction with the E3 ubiquitin ligases WWP1 and FBW7[224-226]. FBW7 regulates ubiquitination of the KLF5 protein through binding to phosphorylated CDC4 phosphodegron (CPD) motifs[225]. Interestingly, it appears that KLF5 can also be degraded by the proteasome in a ubiquitin-independent manner via its N-terminal 19 amino acids; Chen, et al. generated a lysine-less mutant which could still be degraded without ubiquitination, however deletion of the N-terminal 19 amino acids protected against this degradation[227]. While such a mechanism does not affect the transactivation function of KLF5, it serves to control the level of KLF5 protein and may be important in modulating activity in many systems.

1.3.5 Target genes

KLF5 preferentially binds to GC-boxes and CAAT/GT-boxes within promoters of target genes[197,201]. These elements mainly lie in GC-rich areas of proximal promoter regions. A number of direct target genes of KLF5 have been identified with roles in cell proliferation, renewal, survival, and differentiation (Table 1.2). Although in most cases KLF5 has been shown to increase expression of target genes, there have been a growing number of examples where it acts to repress transcription[199]. As discussed above, the transactivation function of KLF5 can be reversed in different conditions via post-translational modification and alternate recruitment of coactivators or corepressors (see Section 1.3.4).

GENE SYMBOL	GENE NAME	REGULATION BY KLF5	GENE FUNCTION	REFERENCES
ABCG2	ATP-binding cassette, sub-family G (WHITE), member 2	Repressed	Membrane transporter	228
CCNB1	Cyclin B1	Activated	Cell cycle progression	229-231
CCND1	Cyclin D1	Activated	Cell cycle progression	219, 229-231
CDK1 (CDC2)	Cyclin-dependent kinase 1	Activated	Cell cycle progression	229-231
CDKN1A (p21)	Cyclin-dependent kinase inhibitor 1A	Repressed	Cell cycle control	220
CDKN2B (p15)	Cyclin-dependent kinase inhibitor 2B	Both	Cell cycle progression	229-231
CPT1B	Carnitine palmitoyltransferase 1B	Both	Lipid synthesis	156
DAF	Decay accelerating factor	Activated	Survival (complement system protection)	232
EGFR	Epidermal growth factor receptor	Activated	Proliferation	233
EGR1	Early growth response 1	Activated	Proliferation/migration/prevents differentiation	234
FASN	Fatty acid synthase	Activated	Lipid metabolism	156, 223
FGFBP1	Fibroblast growth factor binding protein 1	Activated	Proliferation/survival	235, 236
HBG1	Hemoglobin, gamma A	Activated	Haemoglobin protein	237
IGF1	Insulin-like growth factor 1	Activated	Growth factor	158
ILK	Integrin-linked kinase	Activated	Migration	238
KLF4	Krüppel-like factor 4	Repressed	Differentiation	211
LAMA1	Laminin alpha 1	Activated	Differentiation/tumour cell proliferation	239
LTF	Lactotransferrin	Activated	Differentiation marker	201
MAOB	Monoamine oxidase B	Repressed	Amine degradation	240
MIR146A	MicroRNA-146a	Activated	Proliferation	241
MMP9	Matrix metalloprotease 9	Activated	Migration	242
MYC	V-myc myelocytomatosis viral oncogene	Both	Proliferation	243
MYH10	MYH10 myosin, heavy chain 10, non-muscle	Activated	Proliferation/migration/prevents differentiation	202, 244
NANOG	Nanog homeobox	Activated	Self-renewal	208, 245
OCT3	Octamer 3	Activated	Self-renewal	208, 245
OCT4	Octamer 4	Activated	Self-renewal	208, 245
SERPINE1	Serpin peptidase inhibitor, clade E, member 1	Activated	Proliferation/migration/prevents differentiation	234
PDGFA	Platelet-derived growth factor A	Activated	Proliferation/migration	157, 246
PDGFB	Platelet-derived growth factor B	Activated	Proliferation/migration	247
PIM1	Pim-1 oncogene	Activated	Survival	248
PPARG	Peroxisome proliferator-activated receptor gamma	Activated	Differentiation	156
TAGLN	Transgelin	Activated	Proliferation/migration/prevents differentiation	249
SURVIVIN	Survivin	Activated	Survival	250
TCL1	T-cell leukemia/lymphoma 1	Activated	Self-renewal	208, 245
TRB	T cell receptor beta chain locus	Activated	T-cell receptor component	204
UCP2	Uncoupling protein 2	Both	Lipid synthesis	156
UCP3	Uncoupling protein 3	Both	Lipid synthesis	156
VEGFA	Vascular endothelial growth factor A	Activated	Proliferation/migration	159

Table 1.2: Direct KLF5 target genes and their transcriptional regulation by KLF5.
Adapted from Dong and Chen[199].

1.3.5.1 Microarray and ChIP studies

There have been several microarray studies performed to date to study gene expression changes associated with KLF5 activity. Chen et al. showed that over-expression of KLF5 in the TSU-Pr1 bladder cancer cell line induces proliferation, and in this system they used microarray analysis to identify 58 genes which were differentially regulated in KLF5-expressing clones versus controls[251]. Putative target genes were known to have roles in proliferation, cell cycle, differentiation and apoptosis, as well as in cell migration/angiogenesis and metabolic pathways. Genes involved in the MEK/ERK and retinoic acid pathways were also affected by KLF5 expression. Interestingly, almost three quarters of the regulated genes were activated on KLF5 over-expression, and only one quarter were repressed. Wan, et al. developed a mouse model with conditional ablation of *Klf5* in the lung[159]. Deletion of *Klf5* inhibited lung maturation, and genome-wide microarray analyses were utilised to identify genes which were differentially expressed in this system compared to wild-type littermates. These included genes involved with lung morphogenesis (vasculogenesis, smooth muscle cell differentiation, paracrine interactions) and those with roles in cancer and the cell cycle. Many members of the TGFβ, BMP and MEK/ERK signalling pathways were also regulated by KLF5 expression. Although the microarray studies performed by Chen, et al. and Wan, et al. have identified many putative target genes of KLF5, the authors did not attempt to confirm that these are directly regulated by KLF5 using ChIP analysis. Two independent studies have utilised microarray gene expression profiling combined with ChIP analyses to identify direct targets of KLF5 in murine ESCs[208,245]. Reduced *Klf5* expression by siRNA knock-down or gene targeting induces ESC differentiation, and accordingly these studies have demonstrated that KLF5 activates expression of genes involved in the maintenance of ESC self-renewal, such as *Oct4*, *Nanog*,

Tcl1, and *BMP4*, and represses expression of lineage-specific markers of differentiation[160,208,252]. Interestingly, Parisi and colleagues demonstrated that a subset of KLF5 target genes were oppositely regulated in ESCs and keratinocytes on *Klf5* knock-down, which is consistent with KLF5 having different target gene specificity in distinct tissue types[208].

1.3.6 Interacting proteins

KLF5 has been shown to homo-dimerise when binding to a KLF5 target sequence probe *in vitro*, with deletion assays identifying amino acids 251-353 as the region necessary for homo-dimerisation (see Figure 1.5B)[253]. Whether KLF5 forms complexes with other KLF proteins is not yet known.

Direct interaction of KLF5 with other proteins has been shown by coimmunoprecipitation, yeast two-hybrid screening and mass spectrometry. These interacting proteins include post-translational modifiers and coactivators or corepressors (Table 1.3). KLF5 has been shown to recruit various coactivators or repressors to target gene promoters through direct interaction, as discussed in Section 1.3.4. Interaction of KLF5 with histone modifiers such as HDAC1 and the histone chaperone ANP32B can directly inhibit KLF5 binding to target gene promoters[254,255]. KLF5 has been shown to recruit ANP32B to the promoter of the *PDGFA* target gene where it inhibits histone acetylation and down-regulates transactivation of the promoter[255]. These observations suggest that KLF5 may have an important role in modulating histone modification.

PROTEIN SYMBOL	PROTEIN NAME	FUNCTION	REFERENCES
Effectors of KLF5 function			
ANP32B	Acidic (leucine-rich) nuclear phosphoprotein 32 family B	Inhibition of KLF5 binding to target genes	255
CBP	CREB binding protein	Transactivation of KLF5	218
FBW7	F-box and WD repeat domain containing 7	Ubiquitin-dependent KLF5 protein degradation	225
HDAC1	Histone deacetylase 1	Deacetylation and inhibition of KLF5	254, 257
p300	E1A binding protein p300	Acetylation of KLF5 and transactivation	221, 257
PIAS1	Protein inhibitor of activated STAT 1	Transactivation of KLF5 (SUMOylation?)	258
PKC	Protein kinase C	Phosphorylation and transactivation of KLF5	218
SET	SET nuclear oncogene	Deacetylation and inhibition of KLF5	257
WWP1	WW domain containing E3 ubiquitin protein ligase 1	Ubiquitin-dependent KLF5 protein degradation	224
Transcriptional coregulators			
C/EBPβ	CCAAT/enhancer binding protein beta	Coactivator	156
C/EBPδ	CCAAT/enhancer binding protein delta	Coactivator	156
JUN	Jun oncogene	Coactivator/Corepressor	219, 220
NCoR1	Nuclear receptor corepressor 1	Corepressor	223
NCoR2	Nuclear receptor corepressor 2	Corepressor	223
NF-κB	Nuclear factor kappa-light-chain-enhancer of activated B cells	Coactivator	246, 253
p53	Tumour protein p53	Coactivator	250
PPARδ	Peroxisome proliferator-activated receptor delta	Coactivator/Corepressor	223
RAR/RXR	Retinoic acid receptor/Retinoid X receptor	Coactivator	157
SREBP1	Sterol regulatory element binding protein-1	Coactivator	259
Other			
β-catenin	Beta-catenin	Transcription factor	260
ERα	Estrogen receptor alpha	Transcription factor	261
HIF1α	Hypoxia inducible factor 1 alpha	Transcription factor	262
TFIIB	General transcription factor 2B	Basal transcriptional component	256
TFIIEβ	General transcription factor IIE 2	Basal transcriptional component	256
TFIIFβ	General transcription factor IIF 2	Basal transcriptional component	256
KLF5	Krüppel-like factor 5		253
PARP1	Poly (ADP-ribose) polymerase 1	Activator of apoptosis	263
TBP	TATA box binding protein	Basal transcriptional component	256

Table 1.3: KLF5 interacting proteins.
Adapted from Dong and Chen[199].

Studies have demonstrated that KLF5 can interact with basal transcriptional components such as the transcription factors TFIIβ, TFIIEβ, TFIIFβ, and the TATA box-binding protein TBP)[256]. It has also been reported to interact with a variety of other transcriptional coregulators to control expression of downstream targets. For example, the KLF5 protein forms a heterodimer with unliganded RAR to activate expression of *PDGFA*[264], and interacts with NF-κB p65 to synergistically activate a NF-κB reporter construct[253]. It associates with C/EBPβ and C/EBPδ, p53 and SREBP1 to activate gene expression[156,250,259].

KLF5 binding can also directly inhibit protein function, for example binding to the ERα protein inhibits ERα transcriptional activity in the presence of estrogen, thereby preventing induction of downstream ERα target genes[261]. KLF5 interacts with the pro-apoptotic PARP1 protein, which results in inhibition of apoptosis[263].

1.3.7 Function in cell growth, differentiation and survival

1.3.7.1 KLF5 as a positive regulator of proliferation

Spatial and temporal expression patterns of KLF5 suggest a role in proliferation in many systems. Expression levels of KLF5 are high in actively dividing cell types such as ESCs or proliferating cells of the intestinal epithelium, and expression decreases on differentiation to terminally mature cells[152,245]. In murine tooth development KLF5 is expressed early in proliferating cells but expression is decreased on differentiation into mature tooth structures[265]. KLF5 is also highly expressed in rapidly proliferating keratinocytes of the hair matrix, and expression is further increased on treatment with the pro-proliferative agent phorbol 12-myristate 13-acetate (PMA)[253]. Serum stimulation of fibroblasts and smooth

muscle cells induces proliferation with a concordant increase in KLF5 expression[198,266]. KLF5 expression is induced in rodent models of biological stress caused by physical injury, irradiation or bacterial pathogens, which may suggest a proliferative role in the body's inflammatory or immune response systems[202,205,267-269].

Ectopic expression of KLF5 in a variety of cell types also provides supporting evidence for the role of KLF5 as a positive regulator of cell proliferation. Over-expression of KLF5 increases growth rates of intestinal and esophageal epithelial cells, keratinocytes and NIH-3T3 fibroblasts[229,270-273]. RNA interference (RNAi) knock-down of *Klf5* shows the expected opposite effect with reduced cellular proliferation of keratinocytes, VSMCs, and normal mammary epithelial cell lines[233,236,266]. *In vivo* studies support a growth-promoting role for KLF5 in the intestine, with heterozygous knock-out mice displaying shorter intestinal crypts and villi and decreased thickening of arterial walls, consistent with a reduction in cell growth[157]. A number of rat and mouse models have shown that KLF5 contributes to vasculogenesis and angiogenesis through modulating smooth muscle cell phenoytpe. KLF5 up-regulates expression of genes which increase VSMC proliferation and migration, and prevent differentiation, such as *Vegfa*, *Myh10*, *Tagln*, *Serpine1*, and *Egr1*[159,202,234,244,249]. A rat model of cardiovascular injury has shown that over-expression of KLF5 leads to a higher frequency of neointima formation due to increased proliferation and migration of VSMCs[274], and heterozygous ablation of *Klf5* in a mouse model of colitis results in significantly increased disease severity due to reduced epithelial proliferation and migration in the colon[275]. A key role in promoting proliferation is consistent with studies indicating an oncogenic role for KLF5 in some tissues such as intestinal epithelium (discussed further in Section 1.3.8.1).

1.3.7.2 Proliferative signalling pathways

There is considerable evidence that the function of KLF5 as a positive regulator of cell growth is intimately linked with activation of the pro-proliferative MEK/ERK pathway (Figure 1.6). The MEK/ERK pathway can be stimulated by a variety of mitogenic factors such as growth factors and small molecule agonists. A number of studies have shown that treatment of epithelial cells with various stimuli (e.g. Lipopolysaccharide, PMA, Basic fibroblast growth factor, Angiotensin II, Sphingosine 1-phosphate, dextran sulphate sodium) activates the MEK/ERK pathway which in turn stimulates *KLF5* expression primarily through the transcription factor EGR1[205,246,247,269,275,276]. The MEK/ERK pathway can be activated to promote expression of *KLF5* via the RAS pathway (e.g. downstream of the EGF receptor) and also via up-regulation of PKC (downstream of Lisophosphatidic acid and non-canonical WNT signalling) in epithelial cell types[233,277-279]. The functional activity of KLF5 may also be altered through MEK/ERK induced serine phosphorylation downstream of Angiotensin II signalling[219,220] (see Figure 1.5B). Following induction via the MEK/ERK pathway, KLF5 can bind to proteins such as NF-κB or RARα to form complexes which directly activate expression of *PDGFA* and *PDGFB*, which contribute to increased proliferation and cell migration[157,246,264,266]. KLF5 also promotes proliferation via up-regulation of the cell cycle-promoting proteins *CCND1*, *CCNB1* and *CDK1* (*CDC2*), and down-regulation of the cell cycle regulator *CDKN1A* (*p21*), which act to increase the G1-S phase transition of cells[219,220,229,230,277]. Although in many systems *KLF5* is activated by the MEK/ERK pathway, there is evidence to suggest that *KLF5* expression and function may also be mediated by additional signalling pathways. For example, the p38 MAPK pathway has been shown to influence *KLF5* expression in both pancreatic cancer cells and in VSMCs[212,219,262], and in ESCs *Klf5* transcription is induced by the STAT3 pathway[252]. The KLF5 protein is

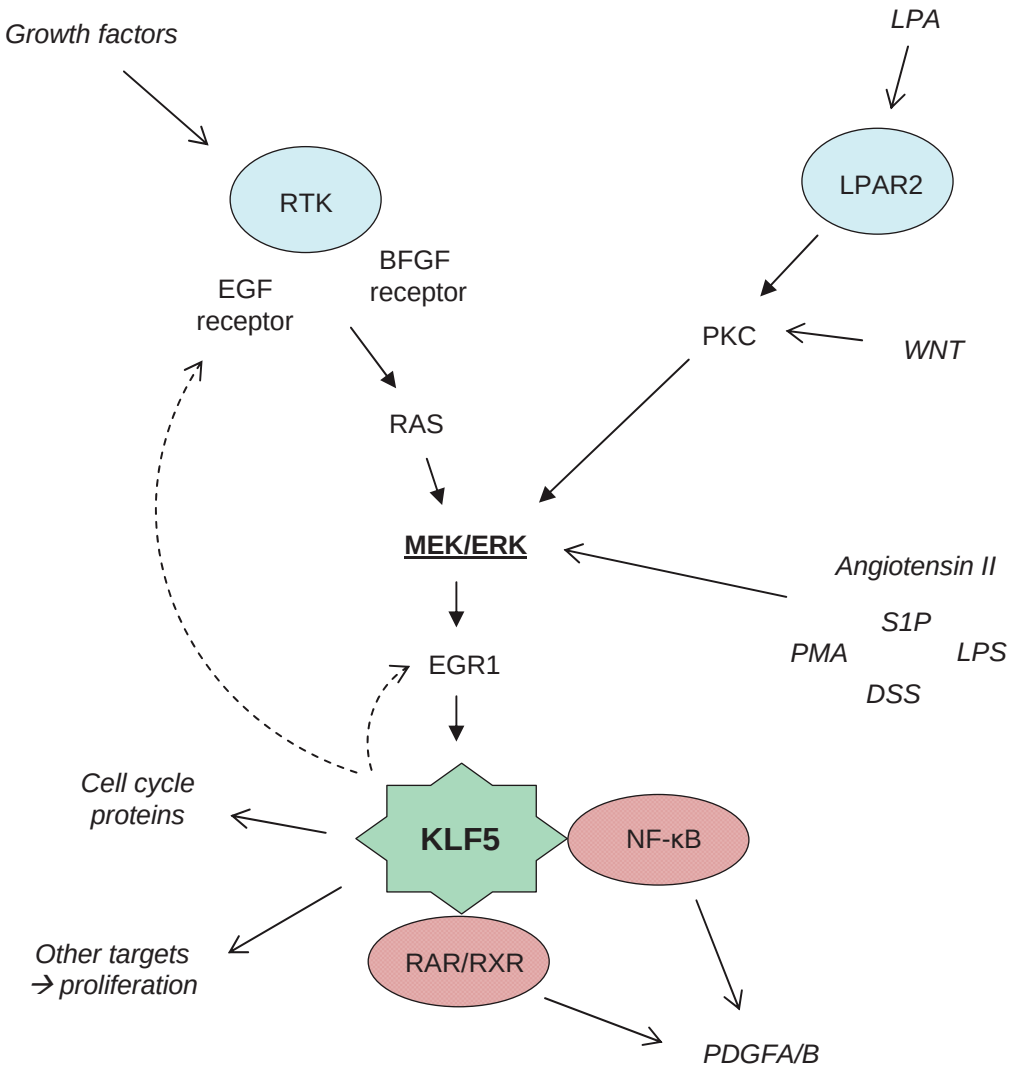

Figure 1.6: The MEK/ERK pathway and KLF5 in proliferation. The MEK/ERK pathway is a central component for activation of KLF5 in proliferative signalling pathways. MEK/ERK components can be stimulated by a variety of growth factors and other mitogens, via RAS or PKC signalling, or other pathways which are yet to be identified. *KLF5* is up-regulated downstream of MEK/ERK via EGR1, where it then activates genes to promote cellular proliferation. In particular, KLF5 up-regulates expression of *PDGFA/B* (through formation of complexes with NF-κB and RAR/RXR), and various cell cycle proteins. RTK = receptor tyrosine kinases, LPA = Lisophosphatidic acid, S1P = Sphingosine 1-phosphate, DSS = Dextran sulfate sodium, PMA = Phorbol 12-myristate 13-acetate, LPS = Lipopolysaccharide. Dotted arrows represent feedback loops within this pathway.

phosphorylated downstream of the PI3K/AKT and GSK3β signalling pathways, which can alter protein function or stability[225,280].

1.3.7.3 Function in embryonic stem cells and development

In the mouse embryo, *Klf5* expression is increased during development and gastrulation, reaching maximum levels at e8.5-10.5[281]. Accordingly, a homozygous null mutation in *Klf5* results in early embryonic lethality (before e8.5) in mice[160]. Studies have demonstrated that ablation of *Klf5* results in a developmental block at the blastocyst stage, as KLF5 is required for differentiation of the inner cell mass and trophectoderm, and for suppression of the primitive endoderm lineage[160,161]. KLF5 also contributes to the proliferation and self-renewal of ESCs. Knock-down of *Klf5* by RNAi or complete knock-out by gene targeting have shown that loss of KLF5 expression leads to an increase in expression of differentiation markers, particularly in the mesoderm/trophoblast lineages[160,208,252]. *Klf5* knock-out ESCs also show reduced proliferation due to G1 cell cycle arrest. Correspondingly, over-expression of KLF5 increases proliferation of ESCs and prevents their differentiation in response to removal of LIF[160]. KLF5 promotes these effects in ESCs by directly regulating expression of a number of genes which are necessary for maintenance of the ESC pluripotent state[162,163,208,245]. The key ESC transcription factors, *Oct4* and *Nanog*, are activated by KLF5 and two other members of the KLF family, KLF2 and KLF4[162,163,208,245]. Concurrent knock-down of these three *Klf* members induces differentiation of ESC to a greater extent than that of *Klf2*, *Klf4*, or *Klf5* alone, suggesting that cooperation of these transcription factors is essential for complete maintenance of ESC self-renewal[162,208,245]. An independent study demonstrated that *Klf5* expression is repressed in ESCs by the homeobox transcription factor HOXA1, which inhibits proliferation during retinoic acid-mediated differentiation of ESCs[231]. Together these studies

strongly support a role for KLF5 in ESC self-renewal and proliferation, as well as in maintenance of blocked differentiation.

1.3.7.4 The role of KLF5 in apoptosis

As well as promoting proliferation and self-renewal in certain cell types, some studies suggest that KLF5 also contributes to cell survival through inhibition of apoptotic pathways. In VSMCs and Acute Lymphocytic Leukaemia (ALL) cell lines, KLF5 up-regulates expression of the anti-apoptotic *Survivin* gene[250,282]. This process forms a positive regulatory loop as Survivin subsequently increases *KLF5* expression[282]. Correspondingly, small interfering RNA (siRNA) knockdown of *KLF5* in ALL cell lines with high KLF5 expression sensitises the cells to apoptosis induced by chemotherapeutic drugs[250]. *In vivo* studies have shown that *Klf5*$^{+/-}$ mice have increased apoptosis in vascular lesions, and this may be due to reduced KLF5 interaction with the PARP1 protein in VSMCs to inhibit its pro-apoptotic effect[263]. A recent study utilising a rat model has shown that VSMCs over-expressing KLF5 have decreased apoptosis on cardiovascular injury associated with reduced cleavage of Caspase-3[274]. In intestinal epithelial cell lines, RNAi knock-down of *KLF5* increases sensitivity to Fluorouracil (5-FU) induced apoptosis[248]. Interestingly, it was found that this effect is independent of p53. Knock-down of *KLF5* in this system reduces expression of PIM1 kinase which usually acts to phosphorylate the pro-apoptotic protein BAD. Non-phosphorylated BAD sequesters inhibitors of apoptosis, and hence reduced phosphorylation promotes apoptosis. In breast cancer cell lines siRNA knock-down of *KLF5* induces apoptosis through reduced expression of the FGF binding protein and subsequent inhibition of the pro-survival protein MKP1[235,236].

In other examples, evidence has suggested that KLF5 may alternatively act as a pro-apoptotic protein. *KLF5* expression increases in cardiac myocytes treated with Endothelin-1, a peptide which causes cells to undergo apoptosis through cardiac hypertrophy[283]. Over-expression of KLF5 in the TE2 esophageal cancer cell line induces apoptosis through activation of the pro-apoptotic protein BAX[284].

1.3.7.5 Growth inhibition and differentiation

In contrast to the growth-promoting and pro-survival role KLF5 plays in a number of different cell types, there are relatively few examples where KLF5 acts to decrease cell proliferation and induce differentiation. A well-characterised example of this is in differentiation of adipose tissue. *Klf5* expression is induced in the early stages of differentiation of pre-adipocyte cell lines. In the 3T3-L1 cell line, over-expression of KLF5 stimulates differentiation to adipocytes even without the addition of relevant hormones, whereas expression of a dominant-negative form of KLF5 inhibits insulin-induced differentiation[156]. *In vivo* studies support this observation, with heterozygous knock-out mice exhibiting decreased formation of mature adipose tissue due to reduced differentiation[156]. In 3T3-L1 cells it has been shown that members of the C/EBP family are key factors in inducing adipocyte differentiation. C/EBPβ and C/EBPδ up-regulate expression of KLF5, and these three proteins then form complexes to activate expression of *Pparg* which promotes differentiation. *Cebpa* expression is also induced downstream of KLF5 during differentiation of adipose tissue[156].

Although most evidence supports a growth-promoting role for KLF5 in keratinocytes (see Section 1.3.7.1 above), epidermal-specific KLF5 over-expression in a transgenic mouse model resulted in loss of the epidermal stem cell population and consequently a reduction of

keratinocyte regeneration potential[285]. Mechanistic studies have shown that KLF5 normally promotes proliferation in the HaCaT keratinocyte cell line by repressing *CDKN2B* and activating *MYC*[221,222,243]. However, on TGFβ treatment KLF5 is acetylated and its function reversed, resulting in activation of *CDKN2B* and repression of *MYC* to inhibit cell growth. These studies highlight that the function of KLF5 will depend not only on tissue type, but also on the presence of various stimuli which may lead to modifications that alter activity.

1.3.8 KLF5 in human tumourigenesis

1.3.8.1 KLF5 as an oncogene

Consistent with a role for KLF5 as a promoter of proliferation and survival, a number of studies have suggested that KLF5 may act as an oncogene in various epithelial tumours (Table 1.4). For example, in human cancers of the salivary gland, comparative genome hybridisation (CGH) analysis identified amplification of the *KLF5* chromosomal region in 45% of tumours examined[271], and in bladder cancer, enforced expression of KLF5 was shown to enhance tumour formation of Tsu-Pr1 bladder cancer cells when injected into severe combined immunodeficiency (SCID) mice[251]. However, the strongest evidence for KLF5 acting as an oncogene is in transformation of intestinal epithelial cells leading to colon cancer. In primary intestinal cancers with *KRAS* mutations, *KLF5* expression was found to be elevated in comparison to normal tissues[286]. In support of this observation, functional studies showed that knock-down of KLF5 in a KRAS-transformed intestinal epithelial cell line reduced cell growth. Enhanced nuclear localisation of KLF5 due to SUMOylation was shown to increase anchorage-independent growth of the HCT116 (*KRAS D13*$^{+/-}$) colon cancer cell line[217]. Interestingly, although KLF5 has a pro-proliferative role in KRAS-transformed

TUMOUR TYPE	EXPERIMENTAL SYSTEM	EVIDENCE	REFERENCE
Colon	Human tumour	Expression elevated in KRAS-positive tumours compared to normal tissue	287
	In vivo models	Reduced expression associated with lower tumour incidence (*Lpar2*$^{-/-}$ mice)	287
		Haploinsufficiency decreases tumour incidence (*Apc*$^{min/+}$ mice)	260
		Haploinsufficiency decreases tumour incidence (*Apc*$^{min/+}$ *Kras-V12*-positive mice)	288
	Tumourigenic cell lines	Expression decreased in response to ATRA-induced differentiation	272
		Elevated expression detected in colony-forming cells compared to those in a monolayer	289
		Ablation reduces cell proliferation (*KRAS*-positive cell lines)	286
		Increased nuclear localisation enhances anchorage-independent growth	217
Breast	Human tumour	Elevated expression associated with more aggressive cancer and poorer survival	290
	In vivo models	Enforced expression enhances tumour formation (xenograft model)	236
	Tumourigenic cell lines	Ablation reduces cell proliferation	
Salivary gland	Human tumour	Amplification of the *KLF5* chromosomal region reported	271
Bladder	*In vivo* models	Enforced expression enhances tumour formation (bone marrow transplantation model)	251
Prostate	Tumourigenic cell lines	Increased expression enhances migration (role in metastasis)	213
Lung	Tumourigenic cell lines	Ablation reduces anchorage-independent growth	228
Esophageal	Tumourigenic cell lines	High expression in cancer stem-like cells	291

Table 1.4: Evidence for KLF5 acting as an oncogene.

tumours, over-expression of KLF5 in a HRAS-transformed epithelial cell line was reported to inhibit colony formation[229]. These observations suggest that the status of RAS may alter the function of KLF5 in intestinal tumourigenesis, and is consistent with studies which have identified KLF5 as a downstream effector of the RAS pathway[233,277,292].

In vivo murine models have provided further evidence supporting an oncogenic role for KLF5 in intestinal epithelium. Reduced KLF5 levels were detected in a mouse model of colitis-associated colon cancer; *Lysophosphatidic acid receptor 2* (*Lpar2*) knock-out mice displayed lower tumour incidence due to inhibition of intestinal epithelial cell proliferation[287,293]. Although one study by Bateman, et al., showed that Klf5 expression is decreased in $Apc^{min/+}$ mice[229], McConnell, et al., demonstrated that haploinsufficiency of *Klf5* can rescue the intestinal adenoma phenotype seen in these mice[260]. Interestingly, it was shown that this effect is even greater in mice harbouring combined $Apc^{min/+}$ and *Kras-V12* mutations, as *Klf5* haploinsufficiency reduced tumour formation by 92% in these mice compared with 75% in mice transgenic for $Apc^{min/+}$ alone[288]. Evidence from these mouse models suggests that reduced KLF5 expression acts to decrease tumour formation through down-regulation of *Ccnd1*, *Mki67*, and also by reducing nuclear Beta-catenin levels[260,288].

In order to target the proliferative effects of KLF5 in colon cancer, studies have been aimed at identification of chemical inhibitors of *KLF5* expression. ATRA was shown to decrease *KLF5* expression in selected colon cancer cell lines and subsequently reduce proliferation[272]. More recently a screen of almost 1300 small molecule compounds identified 8 inhibitors of *KLF5* expression using a reporter construct containing approximately 2 kb of the *KLF5* promoter upstream of the ATG[294]. These included selected PI3K inhibitors and receptor tyrosine kinase

inhibitors, and application of 3 of these (Wortmannin, AG17 and AG879) to colorectal cancer cell lines decreased *KLF5* expression and inhibited proliferation.

1.3.8.2 KLF5 as a tumour suppressor

Although in most tissues KLF5 is thought to have a pro-proliferative function consistent with the evidence for an oncogenic role in colorectal cancer (see Sections 1.3.7.1 and 1.3.8.1), there is increasing evidence to suggest that KLF5 may alternatively act as a tumour suppressor in selected epithelial malignancies (Table 1.5). The strongest evidence for KLF5 acting as a tumour suppressor gene is in epithelial tumours from prostate cancer patients and in prostate cancer cell lines. *KLF5* is commonly deleted or down-regulated in prostate cancer, consistent with tumour suppressor function in this tissue[295,296]. Deletion mapping using primary tumour samples identified a 3 Mb common region of deletion on chromosome 13q21[296]. This region was further narrowed to a 142 kb region using human tumour samples (xenografts) and prostate cancer cell lines, with *KLF5* being the only complete gene to lie within this region[295]. Approximately 90% of total samples tested showed decreased *KLF5* expression, with hemi- or homozygous deletions in 13q accounting for one third of these[295]. No mutations were found in the coding region of the *KLF5* gene. Other studies have shown down-regulation of KLF5 expression or activity by excess protein ubiquitination and degradation, increased cytoplasmic localisation, and possibly methylation, as global demethylation of prostate cancer cell lines led to increased expression of *KLF5*[206,224,297,298]. Enforced expression of KLF5 in the PC3 prostate cancer cell line, where the KLF5 protein is actively degraded, overcame the differentiation block in response to TGFβ signalling[221]. Duhagon and colleagues recently demonstrated that *KLF5* mRNA expression was further reduced in cancer-stem cells of prostate cell lines and primary prostate tumour samples when

TUMOUR TYPE	EXPERIMENTAL SYSTEM	EVIDENCE	REFERENCE
Prostate	Human tumour	Reduced expression compared to normal tissues	295
		Deletion of *KLF5* chromosomal region reported (common region of deletion contains *KLF5* only)	295, 296
		Reduced expression in cancer-stem cells compared to the remaining blast population	299
	Tumourigenic cell lines	Excessive degradation compared to normal tissues	224, 297
		Inhibition of function due to increased cytoplasmic localisation	298
		Enforced expression induces differentiation	221
Breast	Human tumour	Deletion of *KLF5* chromosomal region reported (linked to *BRCA1/2*-negative breast cancer)	300
	Tumourigenic cell lines	Reduced expression compared to normal tissues	301
		Excessive degradation compared to normal tissues	224, 297
		Hemizygous deletion, loss of heterozygosity, coding-sequence mutation reported	301
		Enforced expression inhibits colony formation	301
Colon	Human tumour	Reduced expression compared to non-tumourous tissue (Familial Adenomatous Polyposis)	229
	In vivo models	Reduced expression compared to non-tumourous tissue ($Apc^{min/+}$ mice)	229
	Tumourigenic cell lines	Enforced expression inhibits proliferation and colony formation	229
Gastrointestinal stromal	Human tumour	Loss of *KLF5* chromosomal region reported (associated with high-risk patients)	302
Nasopharyngeal	Human tumour	Reduced expression compared to normal tissue	303
Gastric	Human tumour	High expression associated with less aggressive tumours and improved survival rate	304
Lung	Human tumour	High expression associated with improved survival rate	228
	Tumourigenic cell lines	Ablation increases expression of ABCG2 (increased resistance to chemotherapy)	228
Leukaemia	Human tumour	Loss of *KLF5* chromosomal region reported	305, 306
		Loss of heterozygosity of *KLF5* chromosomal region reported	307, 308
		Loss of heterozygosity of *KLF5* chromosomal region reported	307, 308
		Methylation of *KLF5* genomic locus reported	111, 309

Table 1.5: Evidence for KLF5 acting as a tumour suppressor.

compared with the remaining blast population, suggesting that decreased *KLF5* expression is an important event in the initiation of prostate cancer[299].

Although these studies collectively point to tumour suppressor function in the prostate epithelium, an independent study has suggested that KLF5 may alternatively have a role in promoting metastasis[213]. KLF5 was shown to up-regulate expression of the cell-surface chemokine receptor *CXCR4*, enabling migration of cancer cells to areas with high levels of the chemoattractant CXCL12 such as that found in the bone microenvironment. KLF5 may also play a pro-migratory role in other epithelial tissues such as in esophageal keratinocyte cells, where it stimulates expression of the pro-migratory protein *ILK*[238], or in skeletal muscle cells, where it up-regulates expression of *MMP9*, resulting in degradation of gelatine in skeletal muscle cell systems and enhanced migratory activity[242]. These conflicting observations suggest that KLF5 may have alternate functions in different stages of tumour formation, potentially acting as a tumour suppressor which is down-regulated in initiation of tumourigenesis but later acting as an oncogene in metastatic transformation.

There is also substantial evidence for KLF5 acting as a tumour suppressor in breast cancer, with 70% of breast cancer cell lines tested showing reduced *KLF5* mRNA levels compared to the BRF-97T non-neoplastic breast epithelial cell line[301]. Mechanisms for this down-regulation included hemizygous deletion in 43% of cell lines and frequent copy number neutral loss of heterozygosity (LOH), but did not include homozygous deletion or promoter methylation. One cell line tested also showed a point mutation in the coding sequence of *KLF5* (resulting in a methionine to valine amino acid change at codon 294) in addition to hemizygous deletion. An independent study demonstrated that KLF5 may also be down-regulated in breast cancer cell lines by excessive protein degradation due to amplification of

the ubiquitin ligase *WWP1* gene[297]. Loss of the 13q21-q22 genomic region, which includes *KLF5* and 7 other known genes, has been linked to hereditary breast cancer in families with *BRCA1* and *BRCA2*-negative breast cancer[300]. Functional evidence for KLF5 acting as a tumour suppressor in breast cancer was initially provided by Chen, at. al., who demonstrated that re-expression of KLF5 in the T47d breast cancer cell line significantly inhibited colony formation of these cells[301]. More recently, it has been reported that KLF5 can inhibit proliferation of ERα-positive breast cancer cell lines in response to Estrogen. KLF5 binds to ERα and reduces its transcriptional activity, providing a potential mechanism for the tumour suppressor activity of KLF5 in ERα-positive breast cancer[261]. Although the majority of evidence supports a tumour suppressor role for KLF5 in breast cancer, recent studies have demonstrated that it may also have oncogenic potential in this tissue (see Table 1.4). The reason for these conflicting observations has not yet been fully elucidated, although it is interesting to speculate that expression of ERα may influence the function of KLF5 in breast cancer, as KLF5 was not able to inhibit proliferation of an ERα-negative breast cancer cell line in the study mentioned above[261].

1.4 Research proposal

1.4.1 Retroviral expression cloning using the FDB1 target cell line

We propose to use retroviral expression cloning to identify novel oncogenes which confer factor-independent growth or a block in differentiation of myeloid progenitor cells. The properties of the FDB1 cell line make it an ideal target to screen for oncogenes which confer the two major types of abnormalities found in myeloid leukaemias, i.e. (i) improved proliferation and/or survival (through reduced dependence on growth factors) and (ii) suppression of differentiation (see Section 1.2.1). Specific aims are as follows:

1. Optimise construction of high quality retroviral complementary DNA (cDNA) libraries.
2. Construct and screen a library from a leukaemic source to identify genes which effectively suppress differentiation or improve proliferation/survival of the FDB1 cell line.

The identification of putative oncogenes based on function will provide valuable insights into the normal process of haemopoiesis, and how this may be deregulated in the development of AML.

1.4.2 Characterisation of the putative tumour suppressor KLF5 in normal myelopoiesis and in AML

We previously identified *Klf5* as a gene whose expression is associated with granulocyte-macrophage differentiation of the FDB1 cell line model (see Section 1.2). The expression profile of *Klf5* in this system was similar to that of other genes known to regulate myeloid differentiation, and our hypothesis is thus that KLF5 may have a related role as an inducer of granulocyte-macrophage differentiation. As a potential novel regulator of myelopoiesis, we also hypothesised that *KLF5* may be deregulated in AML and hence contribute to disease pathogenesis. Thus we propose to characterise the role of KLF5 in normal haemopoiesis and in the development of AML. Specific aims are as follows:

1. Determine *KLF5* expression profiles during myeloid differentiation in selected cell lines and primary cell systems.

    a. Characterise *KLF5* mRNA expression during granulocyte-macrophage differentiation.
    b. Assess whether *KLF5* expression is associated specifically with the granulocyte or monocyte lineages.

2. Analyse KLF5 function in normal haemopoiesis. This will be achieved by:
    a. Retroviral over-expression of KLF5 in haemopoietic systems.
    b. Knock-down of KLF5 in systems where its expression is shown to increase during differentiation.

3. Assess *KLF5* expression in leukaemia cell lines and in primary AML patient samples.
    a. Compare *KLF5* mRNA expression in a panel of leukaemia cell lines, primary AML samples, and normal bone marrow controls.
    b. Compare these findings with results of bioinformatic analysis of published microarray data using larger patient cohorts.

4. Examine methylation of the *KLF5* gene as a mechanism for deregulation in AML.
    a. Perform quantitative methylation analysis of the *KLF5* gene using samples described in *3a* above.
    b. Determine whether demethylation of the *KLF5* gene is associated with reactivation of expression.

5. Determine if re-expression of KLF5 in selected leukaemia cell lines is sufficient to overcome the leukaemic differentiation block.

Collectively these studies will define KLF5 as a regulator of myeloid growth and differentiation and will establish the potential for KLF5 to act as a tumour suppressor in AML.

Chapter 2 - Materials and methods

2.1 Materials

Supplier	***Reagent***
American Tissue Culture Collection - USA	32D cell line FDC-P1 cell line HEK-293T cell line HL-60 cell line K562 cell line M1 cell line MCF7 cell line MOLM-13 cell line MV4;11 cell line U937 cell line
Applied Biosystems - USA	BigDye Terminator v3.1 sequencing reagent
BDH Chemicals - USA	DEPEX mounting medium Formaldehyde 40% solution
Beckman Coulter - USA	Anti-CD14-PE antibody (human) Matched isotype control antibody
Biolegend - USA	Anti-CD15-PE antibody (human) Anti-CD34-PE antibody (human) Matched isotype control antibodies
Biotium - USA	EvaGreen fluorescent nucleic acid dye
eBioscience - USA	1x RBC lysis buffer (red blood cell lysis buffer) Anti-CD11b(Mac-1)-PE antibody (human/murine) Anti-CD115(c-Fms)-PE antibody (murine) Anti-CD117(c-Kit)-PE antibody (murine) Anti-Ly6G(Gr-1)-PE antibody (murine) Matched isotype control antibodies
GE Healthcare Life Sciences - USA	Ficoll-Paque PLUS

Geneworks - Australia	Oligonucleotide primers
German Collection of Microorganisms and Cell Cultures - Germany	KG-1 cell line THP-1 cell line
Invitrogen - USA	0.5-10 Kb RNA ladder 1 Kb Plus DNA ladder Opti-MEM T4 DNA Ligase kit Trizol solution Trypan Blue solution
Kirin Pharmaceuticals - Japan	SCF (human)
Merck Australia - Australia	Ethanol, absolute Isopropanol
Miltenyi Biotec - Germany	MACS Human CD34 MicroBead kit
New England Biolabs - USA	EcoRI restriction endonuclease Sfi1 restriction endonuclease XhoI restriction endonuclease Restriction endonuclease buffers
Open Biosystems - USA	I.M.A.G.E. Consortium clones pSM2c shRNAmir constructs
Peprotech	G-CSF (human) IL-6 (human) M-CSF (human)
Qiagen - USA	HiSpeed Plasmid Midi kit QIAamp DNA Blood and Cell Culture Mini kit QIAprep Spin Miniprep kit QIAquick Gel Extraction kit QIAquick PCR Purification kit QuantiTect Rev. Transcription kit RNeasy Micro kit
Roche - Australia	FastStart Taq reagents
SAFC Biosciences - USA	1x Trypsin-EDTA solution (0.25% Trypsin, 0.2% EDTA)
Sigma-Aldrich - USA	1x Phosphate buffered saline (PBS) 1x TAE buffer (tris-acetate-EDTA) 5-aza-2-deoxycytidine 5-azacytidine

	Agar Agarose Amphotericin B (Fungizone) Ampicillin ATRA (All-*trans* retinoic acid) Bovine serum albumin Chloramphenicol Dimethyl sulfoxide DMEM (Dulbecco's Modified Eagle's Medium with L-glutamine, $NaHCO_3$, 1000 mg/L glucose and pyridoxine) Ethidium bromide Foetal calf serum (FCS) lot #3A0561 Fluorouracil Glucose IMDM (Iscove's Modified Dulbecco's Medium with L-glutamine and 25 mM HEPES) L-glutamine-penicillin-streptomycin solution for cell culture Leukocyte peroxidase (Myeloperoxidase) kit Luria Broth MEM (Eagle's Minimum Essential Medium with L-glutamine and $NaHCO_3$) MOPS buffer (3-(N-morpholino)propanesulfonic acid) PMA (12-O-Tetradecanoylphorbol-13-acetate) Polybrene Propidium iodide Puromycin Ribonuclease A RPMI (Roswell Park Memorial Institute medium with L-glutamine and $NaHCO_3$) Sodium acetate Sodium azide Triton X-100
StemCell Technologies - Canada	Methocult incomplete medium for murine cells (M3231)
Veterinary Services of Australia - Australia	Isofluorane inhalation anaesthetic

2.2 Nucleic acid protocols

2.2.1 Production, isolation and analysis of DNA samples

Plasmid DNA - Chemically competent JM109 *Escherichia coli* cells were prepared by D. Salerno according to the method described by Hanahan, et al.[310]. For transformation, 5 μl of ligation product or 10 ng of plasmid was added to 200 μl of cells and mixed gently. The cells were incubated on ice for 30 mins then heat shocked at 42°C for 1 min and returned to ice briefly. Transformed cells were then plated onto Luria Broth/agar plates containing appropriate antibiotics and left at 37°C overnight[311]. Potential clones were selected using ampicillin resistance (100 μg/ml) or chloramphenicol resistance (25 μg/ml). Overnight bacterial cultures of 2 mls and 50 mls Luria Broth (with appropriate antibiotics) were prepared from single colonies and DNA isolated according to the Qiagen Miniprep and Midiprep protocols respectively. Gel extraction and DNA purification were performed according to protocols contained in the Qiagen QIAquick Gel Extraction or PCR Purification kits. Where necessary, ethanol precipitation of DNA was undertaken following addition of sodium acetate (adapted from Sambrook, et al.[311]). Plasmid DNA was stored at -20°C.

Genomic DNA - Genomic DNA was isolated using either the Qiagen Blood and Cell Culture Mini kit or the Invitrogen Trizol protocol according to the manufacturer's instructions and stored at 4°C.

DNA Analysis - DNA samples were analysed by electrophoresis using 0.5-2% agarose in 1x TAE buffer according to the protocol outlined by Sambrook, et al.[311]. The Invitrogen 1 Kb Plus DNA ladder was used in determining DNA size. Agarose gels were stained for 1 min in 2.5 μg/ml ethidium bromide solution, then destained for 1 min in reverse osmosis quality water. Stained gels were visualised and photographed using an Integrated Sciences UVItec gel documentation system and UVIPhotoMW1 software. An Integrated Sciences UVP transilluminator was utilised for gel excision. Quantitation of DNA was performed using a NanoDrop Spectrophotometer. Sequencing of DNA was performed by the Institute of Medical and Veterinary Sciences (IMVS) Molecular Pathology Sequencing Division (SA Pathology). Sequencing reactions were set up according to protocols specified by the Sequencing Division using BigDye Terminator v3.1 sequencing reagents.

2.2.2 RNA isolation and analysis, and cDNA production

Total RNA was isolated using either the Qiagen RNEasy Micro kit or the Invitrogen Trizol protocol according to the manufacturer's instructions. Quantitation of RNA was performed using a NanoDrop Spectrophotometer. RNA was analysed by electrophoresis on a denaturing agarose-formaldehyde gel according to the protocol outlined in Fritsch, et al. (MOPS buffer method)[312]. The Invitrogen 0.5-10 Kb RNA ladder was used for RNA size determination. RNA gels were visualised on a gel documentation system as described above for DNA. RNA was stored in aliquots at -80°C. For production of cDNA, between 200-1000 ng of RNA was DNAse treated and reverse-transcribed using the Qiagen QuantiTect Rev. Transcription kit as per the manufacturer's protocol. cDNA samples were stored at -20°C.

2.2.3 Polymerase chain reactions

Polymerase chain reaction (PCR) detection of KLF5 isoforms from cDNA - PCR was performed using the Roche FastStart Taq PCR kit according the manufacturer's protocols with the following parameters: 2.5 μl cDNA template, primer annealing temperature of 50°C, and 40 amplification cycles. PCR was performed on a Corbett Gradient Palm-Cycler. 5 μl of each PCR reaction was separated and visualised using gel electrophoresis. Oligonucleotide primer sequences are shown in Table 2.1.

Quantitative reverse transcription PCR (Q-PCR) - Q-PCR reactions were carried out using the following conditions per reaction: 1.25 U/μl Roche FastStart Taq, 1x Taq Buffer (without magnesium), 2.5 mM magnesium chloride, 200 μM each dNTP, 1x EvaGreen fluorescent nucleic acid dye, 450 nM each forward and reverse PCR primers, and 1 μl cDNA template. Q-PCR was performed on a Corbett RotorGene 6000 instrument with the following cycling conditions: 95°C for 10 mins (1 cycle), 95°C for 25 secs - 60°C for 25 secs - 72°C for 30 secs (40 cycles – acquiring to green), 72°C for 1 min (1 cycle). Products of Q-PCR were analysed by melt curve analysis as follows: Increments of 1°C for 5 secs each from 72°C-99°C, acquiring to green. For each sample duplicate reactions were performed for detection of the gene of interest and a control gene (*Beta-actin, ACTB*). QGene software was used for analysis of relative mRNA expression levels[313]. Oligonucleotide primer sequences are shown in Table 2.1.

DETECTS	USE	SPECIES	FORWARD PRIMER (5`-3`)	REVERSE PRIMER (5`-3`)	DESIGN
Actb	Q-PCR (control)	*Mus musculus*	AGTGTGACGTTGACATCCGTA	GCCAGAGCAGTAATCTCCTTCT	Common
ACTB	Q-PCR (control)	*Homo sapiens*	AAGAGCTACGAGCTGCCTGAC	GTAGTTTCGTGGATGCCACAG	Common
BG717510	Detection from cDNA	*Homo sapiens*	TCA TGT CTA TCC GGG AAA CC	ACT CTG GTG GCT GAA AAT GG	Primer 3
Cebpa	Q-PCR	*Mus musculus*	CAAGAACAGCAACGAGTACCG	GTCACTGGTCAACTCCAGCAC	Common
Cebpe	Q-PCR	*Mus musculus*	TGCGACGTGAACGTAACAAC	CTAGCAGCCTCAGGGATCTG	Primer 3
KLF5	Q-PCR & detection from cDNA	*Mus musculus* & *Homo sapiens*	AGCTCAGAGCCTGGAAGT	TGAGTCCTCAGGTGAGCTTT	Common
Ltf	Q-PCR	*Mus musculus*	TGAGGCCCTTGGACTCTGT	ACCCACTTTTCTCATCTCGTTC	PB ID: 31560677a1
Csf3	Q-PCR	*Mus musculus*	ACAAAGCAGGGACCTCTTCA	ATGGTGTTAAGGTCTTGGGC	Sasmono, et al.[314]
pBluescriptR	Sequencing	N/A	(T3) GCAATTAACCCTCACTAAAGG	(T7) TAATACGACTCACTATAGGG	Logel, et al.[315]
pMSCV-IRES-eGFP	Sequencing	N/A	GAACCTCCTCGTTCGAC	GCCTTATTCCAAGCGGC	Common

Table 2.1: Oligonucleotide sequences. "Design" column indicates how primers were designed or obtained. Common = Common primers designed and utilised by the Acute Leukaemia Laboratory, IMVS (SA Pathology), Adelaide, AUSTRALIA. Primer 3 = Primer3 WWW Primer tool, web-based primer design program[316]. PB ID: PrimerBank ID, web-based database of human and mouse PCR primer sets[317-319]. N/A = Not applicable.

2.2.4 Plasmids and expression constructs

Constitutive retroviral expression constructs - cDNAs were cloned into the bicistronic MSCV-IRES-eGFP (MIG) vector[320] (kind gift of Dr. Elio Vanin, St Jude Childrens Research Hopsital, Memphis USA). Murine *Klf5* had previously been cloned into this vector. Human *KLF5* cDNA was purchased as an I.M.A.G.E. Consortium clone in the pOTB7 vector (clone ID 5454169). Both the MIG vector and pOTB7-*KLF5* plasmid were digested using EcoRI and XhoI restriction endonucleases according to the manufacturer's instructions. The products of digestion were separated on a 1% agarose gel, then MIG and *KLF5* DNA bands were excised and isolated using the Qiagen QIAquick Gel Extraction kit. Ligations were undertaken in accordance with the Invitrogen T4 DNA Ligase protocol and products were transformed into chemically competent JM109 *Escherichia coli* cells. A selection of ampicillin-resistant clones were amplified and sequenced to ensure correct generation of the MIG-*KLF5* construct. Sequencing oligonucleotide primers for the MIG construct are shown in Table 2.1. cDNA sequences for the MIG-*Klf5* (murine) and MIG-*KLF5* (human) constructs aligned with the nucleotide sequences NM_009769 and NM_001730 respectively (National Center for Biotechnology Information (NCBI) database[321]).

RNAi knock-down – Small hairpin RNA (shRNA) cassettes were expressed constitutively using the retroviral constructs pMSCV-ΔLTR-H1 (pMΔH) or p-SHAG MAGIC 2 (pSM2c). pMΔH is based on the pRETRO-SUPER vector[322], and shRNA cassettes had previously been designed and cloned into this plasmid. These included 6 sequences predicted to target murine *Klf5* (pMΔH K1-K6) and 2 control shRNAs (1 non-targeting (NT) sequence and 1 targeting eGFP). pSM2c constructs were purchased from Open Biosystems' shRNAmir library collection (microRNA-based shRNA design)[323]. These included 3 sequences predicted to

target murine *Klf5* (pSM2c K1-K3) and 2 control shRNAs (1 non-targeting (NT) sequence and 1 eGFP-targeting sequence). Details of all shRNA constructs are shown in Table 2.2. Both pMΔH and pSM2c constructs contained the *Pac* gene sequence for selection using puromycin.

Retroviral cDNA expression libraries - The construction of retroviral cDNA expression libraries is described in Chapter 3, Section 3.2.1. cDNA for human *CD4* had previously been cloned into the MIG-Sfi1 vector (MIG-Sfi1-*CD4*).

Other constructs – The BG717510 expressed sequence tage (EST) clone was purchased as an I.M.A.G.E. consortium clone in the pBluescriptR vector (clone ID 4821765). T3 and T7 oligonucleotide primers were used for sequencing (see Table 2.1).

2.3 Cell culture protocols

2.3.1 Culture medium and supplements

All cells were cultured in medium supplemented with 2 mM L-glutamine, 100 U/ml penicillin and 100 μg/ml streptomycin. Cultures were maintained in a Sanyo humidified incubator with 5% CO_2 at 37°C. Recombinant murine IL-3 and murine GM-CSF were produced from baculoviral vectors supplied by Dr Andrew Hapel (John Curtin School of Medical Research, Canberra, Australia). Recombinant human SCF was a kind gift of Dr Ian Lewis. All other recombinant cytokines were purchased in lyophilised form and stocks prepared using 0.2 μM sterile filtered 0.5% bovine serum albumin solution. Cytokines were aliquoted and stored at -80°C.

CONSTRUCT	shRNA	*Klf5* NUCLEOTIDES	TARGET SEQUENCE (5`-3`)	DESIGN
pMΔH-NT	Non-targeting	N/A	GCACGACTTCTTCAAGTCCTT	Leirdal, et al.[324]
pMΔH-GFP	eGFP-targeting	N/A	GGAGCGCACCATCTTCTTCTT	Leirdal, et al.[324]
pMΔH-K1	*Klf5*-targeting #1	572-590	GAACTGGCCTCTACAAATC	Wistar Institute siRNA design program
pMΔH-K2	*Klf5*-targeting #2	599-617	CATGCGTAACACAGATCAA	Wistar Institute siRNA design program
pMΔH-K3	*Klf5*-targeting #3	743-761	CACAGGAGGTGAACAATAT	Wistar Institute siRNA design program
pMΔH-K4	*Klf5*-targeting #4	824-842	ACCTGTACCAGCTGTTGAA	Wistar Institute siRNA design program
pMΔH-K5	*Klf5*-targeting #5	1014-1034	AACCAGACGGCAGTAATGGAC	Nandan, et al.[277]
pMΔH-K6	*Klf5*-targeting #6	1119-1137	CGCTACAATTGCTTCCAAA	Wistar Institute siRNA design program
pSM2c-NT	Non-targeting	N/A	Not provided	Open Biosystems catalogue number RHS1706
pSM2c-GFP	eGFP-targeting	N/A	Not provided	Open Biosystems catalogue number RHS1707
pSM2c-K1	*Klf5*-targeting #1	1382-1402	CCGTATCCACTTCTGCGATTAT	Open Biosystems clone ID V2MM_73715
pSM2c-K2	*Klf5*-targeting #2	1280-1300	AGCGATTCACAACCCAAATTTA	Open Biosystems clone ID V2MM_67484
pSM2c-K3	*Klf5*-targeting #3	1301-1321	CCCTGCCACTCTGCCAGTTAAT	Open Biosystems clone ID V2MM_72281

Table 2.2: Details of murine *Klf5* shRNA constructs. shRNA sequences in pMSCV-ΔLTR-H1 (pMΔH) or p-SHAG MAGIC 2 (pSM2c) vectors. Details for control non-targeting or eGFP-targeting constructs in pSM2c were not provided by Open Biosystems. All *Klf5*-targeting sequences are for murine *Klf5*, and nucleotide numbers listed are relevant to NM_009769 (NCBI database). "Design" column indicates how sequences were designed or obtained. Wistar Institute siRNA design program = web-based siRNA design program[325]. N/A = not applicable.

2.3.2 Cell lines

Murine cell lines - FDB1 cells[128] and FDB1-ITD cells[326] were maintained in IMDM supplemented with 10% foetal calf serum (FCS) and 500 bone marrow units (BMU)/ml murine IL-3. FDC-P1 cells were culture in DMEM supplemented with 7.5% FCS and 80 BMU/ml murine GM-CSF. 32D cells were maintained in RPMI medium with 10% FCS and 500 BMU/ml murine IL-3, and cells were passaged using sterile cell scrapers. Leukaemic M1 cells were maintained in RPMI supplemented with 10% FCS.

Human cell lines - The leukaemia cell lines HL-60, KG-1, MOLM-13, MV4;11, THP-1 and U937 were cultured in RPMI supplemented with 10% FCS. The CML cell line K562 was maintained in IMDM supplemented with 10% FCS. The breast cancer cell line MCF7 was cultured in MEM supplemented with 10% FCS, and was passaged using a 1x Trypsin-EDTA solution. Fibroblastic HEK-293T cells were cultured in DMEM supplemented with 7.5% FCS, and were passaged as for MCF7 cells above.

Cell line methods - For centrifugation, cells were spun at 1200 rpm for 5 mins in an Eppindorf 5810R Centrifuge. Cells were frozen at densities of up to $5x10^6$/ml in FCS supplemented with 10% dimethyl sulfoxide using an isopropanol cycler. Cell line stocks were stored in liquid nitrogen. Aliquots of cells were thawed in a 37°C water bath then added to complete medium in a 1 in 10 dilution. Cells were centrifuged then resuspended in complete medium for culture. For selection and maintenance of cells expressing the *Pac* gene, puromycin was added to culture medium at 1 μg/ml.

2.3.3 Murine bone marrow cells

C57BL/6 female mice (8-12 weeks) were purchased through and housed in the IMVS Veterinary Services Division (SA Pathology) in a conventional holding type. Mice were treated with 150 mg/kg fluorouracil by intraperitoneal injection to enrich for haemopoietic progenitors. After 4 days mice were humanely killed using a lethal dose of isofluorane inhalation anaesthetic followed by cervical dislocation. Bone marrow cells were harvested then cultured in IMDM supplemented with 15% FCS and 50 ng/ml human SCF, 10 ng/ml human IL-6 and 500 BMU/ml murine IL-3 unless otherwise stated. For centrifugation, cells were spun at 1500 rpm for 10 mins in an Eppindorf 5810R Centrifuge.

2.3.4 Cell differentiation assays

FDB1 - Cells were washed 3 times in 1x phosphate buffered saline (PBS) to remove IL-3, then seeded at $1x10^5$/ml in culture medium containing 500 BMU/ml murine GM-CSF for differentiation to granulocytes and macrophages over 5 days.

32D - Cells were washed 3 times in 1x PBS to remove IL-3, then seeded at $1x10^5$/ml in culture medium containing 50 ng/ml human G-CSF for differentiation to granulocytes over 7 days.

U937 - Cells were seeded at $1x10^5$/ml in complete culture medium. For differentiation to neutrophils, cultures were treated with 0.3 μM ATRA for 4 days; and for differentiation to monocytes, cultures were treated with 5 nM PMA for 4 days. ATRA was dissolved in ethanol

to form a stock solution of 10 mM which was stored at -80°C for up to 1 month. PMA was dissolved in ethanol to form a stock solution of 150 μM which was stored at -20°C.

Mouse bone marrow - Bone marrow was harvested from fluorouracil treated C57BL/6 female mice then treated with 1x RBC lysis buffer according to manufacturer's instructions. Cells were seeded at $3x10^5$/ml in medium containing 100 ng/ml human M-CSF for differentiation to macrophages over 7 days.

2.3.5 Demethylation of leukaemia cell lines

Selected human leukaemia cell lines were seeded at $5x10^5$ cells/ml in complete culture medium and treated with 4 μM 5-azacytidine or 5 μM 5-aza-2-deoxycytidine for 48 hrs. Cells were then harvested for isolation of RNA and production of cDNA. Q-PCR was performed for detection of *KLF5* reactivation. Solutions of 5-azacytidine and 5-aza-2-deoxycytidine were made up fresh on the day of use in 1x PBS and were 0.2 μm sterile filtered prior to use in assays.

2.3.6 Viral transduction of cells

Production of viral supernatant - The pEQ-Eco packaging vector was used for production of murine retrovirus, and the pEQ-PAM3 vector was used for production of human retrovirus[327] (kind gift of Dr. Elio Vanin, St Jude Childrens Research Hopsital, Memphis USA). Viral supernatant was generated using HEK-293T cells. Cells were seeded at $1x10^6$ cells total in 5 mls of medium in a $25cm^2$ flask. 24 hrs after seeding cells were transfected with constructs of interest using Invitrogen's Lipofectamine 2000 according to the manufacturer's protocol.

Briefly, 4 μg of the retroviral construct of interest and 4 μg of packaging construct were added to 500 μl of Opti-MEM medium. 20 μl of Lipofectamine 2000 reagent was added to 500 μl of Opti-MEM medium and the mixtures were incubated separately for 10-15 mins at room temperature. The mixtures were combined and incubated for a further 1 hr at room temperature before adding to cells. 24 hrs post-transfection the medium was replaced with 5 mls complete culture medium for the intended target cells. Viral supernatant was collected after 24 hrs, and 5 mls of fresh culture medium was added for collection of a second volume of viral supernatant at 48 hrs. The supernatants were combined and stored at -80°C.

Transduction - Viral supernatant was thawed in a water bath at 37°C prior to use. Cells were transduced at a maximum cell density of $1x10^6$/ml of supernatant for cell lines and $1x10^8$/ml for mouse bone marrow. Cells were suspended in neat viral supernatant supplemented with 1 μg/ml polybrene and 2.5 μg/ml amphotericin B (Fungizone) then aliquoted into 6-well plates (2-5 mls total per well). Plates were spun at 1800 rpm for 1 hr at 37°C in an Eppindorf 5810R Centrifuge then transferred to an incubator for 5 hrs. Following transduction fresh culture medium was added to the wells as needed and cells were incubated for at least a further 18 hrs prior to use in assays.

2.3.7 Cellular assays

Cell and viability counts - Cells were mixed with Trypan Blue solution in a 1:1 ratio then counted using a haemocytometer (at least 100 total live and dead cells per sample).

Morphology - Up to 30,000 cells were centrifuged onto slides using a Thermo Shandon Cytospin 4 cytocentrifuge at 500 rpm for 5 mins. Slides were air-dried then Wright-Giemsa

stained courtesy of the IMVS Core Laboratory (SA Pathology). Slides were mounted using DEPEX mounting medium and cover-slipped for analysis. Photographs were taken using an Olympus BX51 microscope and DP70 camera system at 200x or 400x original magnifications. Morphology was scored by counting a minimum of 200 cells per slide.

Surface marker expression analysis - For staining, at least 5,000 cells per sample were suspended in 50 µl Fluorescence-activated cell sorting (FACS) wash solution (5% FCS and 0.1% sodium azide in 1x PBS) containing antibody (at the manufacturer's recommended concentration) then incubated for 30 mins on ice without exposure to light. Cells were washed once in FACS wash then fixed in FACS fix solution (2% glucose, 1% formaldehyde and 0.02% sodium azide in 1x PBS) and stored at 4°C prior to flow cytometric analysis.

Myeloperoxidase enzyme activity - Up to 30,000 cells were centrifuged onto slides using a Thermo Shandon Cytospin 4 cytocentrifuge at 500 rpm for 5 mins. Slides were treated using the Sigma-Aldrich Leukocyte peroxidase (Myeloperoxidase) kit according to the manufacturer's instructions (Hanker-Yates method[328]). Slides were mounted using DEPEX mounting medium and cover-slipped for analysis. Photographs were taken using an Olympus BX51 microscope and DP70 camera system at 200x original magnifications. Myeloperoxidase activity was scored by counting a minimum of 200 cells per slide.

Cell cycle analysis - A minimum of 10,000 cells were suspended in 300 µl cold 1x PBS. Ice cold ethanol was then added drop-wise while vortexing. Cells were fixed overnight at 4°C. For staining, cells were suspended in 500 µl propidium iodide staining solution (40 µg/ml propidium iodide, 100 µg/ml Ribonuclease A and 0.1% Triton X-100 in 1x PBS) and

incubated for 30 mins at 37°C away from light. Cells were analysed by flow cytometry within 4 hrs of staining for propidium iodide fluorescence.

Colony formation - Methylcellulose colony forming assays were performed using Methocult incomplete medium for murine cells according to the manufacturer's protocol. Cells were seeded at densities as stated in results chapters in triplicate plates for each condition. Colonies greater than 40 cells in size were counted at Day 7 post-seeding. Representative photographs for colony morphology were taken using an Olympus CK2 microscope and DP11 camera system at an original magnification of 100x.

2.3.8 Flow cytometry and Fluorescence-activated cell sorting

Flow cytometric analyses were performed using the Beckman Coulter analysers FC500 and XL-MCS. For FACS, cells expressing the construct of interest were centrifuged then resuspended in complete medium diluted 1 in 4 with medium containing no supplements. FACS was performed by the IMVS Flow Cytometry Division using a Beckman Coulter ALTRA or Becton-Dickinson ARIA cell sorter. Cells were resuspended in complete medium immediately following sorting.

2.4 Analysis of patient samples

2.4.1 AML panel

AML samples - A panel of 30 *de novo* AML patient samples was assembled using bone marrow mononuclear cell (BMMNC) samples taken at diagnosis from the Queen Elizabeth

Hospital, Adelaide AUSTRALIA and the IMVS, Adelaide AUSTRALIA. Samples were thawed at 37°C then diluted 1 in 10 with IMDM + 10% FCS (drop-wise addition with regular mixing). Previous studies have shown that this freeze-thaw process results in AML samples containing 80-100% blasts regardless of initial blast count at diagnosis[329]. Following dilution, thawed samples were left at room temperature for 10-15 mins before resuspension in IMDM + 10% FCS. Samples were then analysed using various cellular assays or lysed in Trizol for production of genomic DNA and total RNA. Genomic DNA was stored at 4°C, RNA was stored in aliquots at -80°C, and excess vials of cells were stored in liquid nitrogen. Clinical information relevant to the AML cohort was compiled through the use of the South Australian Open Architecture Clinical Information System (OACIS). Samples were screened for mutations in *CEBPA*, *FLT3*, and *NPM1* by the Therapeutic Product Facility, IMVS, Adelaide AUSTRALIA.

Normal controls - Normal bone marrow samples were obtained using an approved collection process through the Royal Adelaide Hospital, Adelaide AUSTRALIA. Samples were processed on the day of collection. Bone marrow was diluted 1 in 2 with 1x PBS then mononuclear cells were extracted using Ficoll density gradient centrifugation (according to manufacturer's instructions). For total BMMNC samples, cells were lysed in Trizol at this stage for collection of RNA and DNA. Excess cells were frozen and stored in liquid nitrogen. For isolation of $CD34^+$ progenitor cells, BMMNC were sorted using the Miltenyi Biotec MACS Human CD34 MicroBead kit according to the manufacturer's protocol. Isolated cells were stained for purity using anti-CD34-PE and matched isotype control antibodies, and $CD34^+$ and $CD34^-$ fractions were then lysed in Trizol for RNA and DNA extraction. A total of 4 normal BMMNC and 5 normal bone marrow $CD34^+$ samples were collected for use as controls.

2.4.2 Methylation analysis

Genomic DNA samples were analysed for methylation by the Australian Genome Research Facility (AGRF), Brisbane AUSTRALIA. The genomic region investigated encompassed the *KLF5* proximal promoter, exon 1, intron 1 and exon 2 (genomic coordinates chr13:72521648-72526071 of the Mar.2006 (NCBI36/hg18) assembly – International Human Genome Sequencing Consortium). The design of amplicons for methylation analysis (and relevant oligonucleotide primer pairs) was accomplished with the aid of Sequenom EpiDesigner Software (see Table 2.3 for details). Between 0.2-1.0 μg of genomic DNA was sent to the AGRF for quantitative methylation analysis using a matrix-assisted laser desorption/ionization time-of-flight (MALDI-TOF) mass spectrometry-based system (Sequenom EpiTYPER using the MassARRAY system)[330]. The standard deviation of quantitation using EpiTYPER is 5%[331]. MultiExperiment Viewer v4.5.1 was utilised for generation of heat maps and hierarchical cluster analysis[332]. The University of California, Santa Cruz (UCSC) Genome Browser was utilised for bioinformatic analysis of the KLF5 region assessed for methylation[333,334].

2.5 General

2.5.1 Ethical approval

All laboratory work was carried out in PC2 approved facilities with approval from the Office of the Gene Technology Regulator, AUSTRALIA (certificate numbers PC2NLRD30/2007 and NLRD1144/2003). Studies involving mice were conducted using existing ethical

AMPLICON	LOCATION (BP)	FORWARD PRIMER (5`-3`)	REVERSE PRIMER (5`-3`)	INFORMATIVE CpG RESIDUES
1	1-470	TTTTGAAGGAGTGGGAAAAATTTAG	ACACAACTTCTCTAACAAATTAAACTAAC	3, 5-10
2	443-552	GTTAGTTTAATTTGTTAGAGAAGTTGTGT	AAAAAAACAACCAAAACCCC	20-24
3	541-782	GGGGTTTTGGTTGTTTTTTT	CCCACCRTACTCTCAAACTCTC	27, 31-42, 49-54
4	754-1035	GGTTTYGGAGAGTTTGAGAGTA	CTCAACACCCTTATAACCATAAACA	55-62, 67-68, 71-82
5	1011-1285	TGTTTATGGTTATAAGGGTGTTGAG	TCTTCCTACCTAAACCAAATCCTCT	83-89, 91-100, 110-121
6	1669-1252	GGTTTTAATGTTTTGGTATTGGAGA	ACTACCTCCAAAAAACCTAATCCAA	122-133, 135-143, 146-151, 153-155
7	1644-1953	TTTTTTAATGTTAAGGTATTGGAGTTTT	AAACAAATATAAACCAACTACCACT	156-157, 159, 161-164, 169-171
8	2254-1935	TGTTTTTTTATAGTAAGATTTTGGTAGATT	TTAACTTTTACACTTACCCAACAACC	172-181, 184
9	2117-2550	GTYGYGGGAGYGTAGTGT	AATCRCCTCAAACCTTTTCCAA	182-186, 188-190, 193
10	2261-2638	TTTGTTAGAGATGTGATTTATATGATGAGA	CCTCCAAAACAAAAAATTAACAAAC	189-190, 193, 196
11	2394-2655	TGATTGTTTTATTTATTTGTTAAGGTG	CCCTTATCTTCTTAATACCTCCAAAA	193, 195
12	2695-3170	TGGTTTATTGAGAAGGATATGATAAATG	AAAATATTACCAAACTACCTCAATTCTA	-
13	3217-3537	ATTTTGTTTGTATAGGGGTGATGGT	AAAATATAAAATACATAATCCACCTAATTC	201, 203-206
14	4134-3782	GGGGTATGTTTTGGAATTGTTTTAT	TATTACCATTTTCAACCACCAAAAT	212-214, 217
15	4100-4424	GTAGATTGTAGTGAAATAATTTTAGGGT	TCAACCAAATAAAAACACATACCAA	218-219

Table 2.3: Amplicon details for *KLF5* methylation analysis. "Location" column indicates the genomic location of each amplicon, with BP #1 representing nucleotide 72521648 (chr13) of the Mar.2006 (NCBI36/hg18) genomic assembly. 15 amplicons were designed to cover a total of 4424 bp containing 222 CpG residues, and informative CpG residues for each amplicon are noted. Amplicons were designed with the aid of the Sequenom EpiDesigner program (available at http://www.epidesigner.com/index.html).

approval from the Central Northern Adelaide Health Service Animal Ethics Committee, Adelaide AUSTRALIA (approval number 103/07). For compilation and use of the panel of human AML tissue samples, ethical approval was sought and obtained from the following institutes and committees in Adelaide AUSTRALIA: Central Northern Adelaide Health Service Human Ethics Committee (approval number 2007072), Royal Adelaide Hospital Research Ethics Committee (approval number 070604), and the Children, Women's and Youth Health Service Women's and Children's Hospital Human Research Ethics Committee (approval number REC1927/2/2010). Approval was granted for use of archived AML samples, freshly collected AML samples with appropriate consent, and for use of normal bone marrow samples obtained with consent. Approval to access clinical information for patient samples through the OACIS Healthcare System was obtained for each of the institutes listed above.

2.5.2 Statistical analysis

Unless otherwise stated, all error bars in figures indicate standard error of the mean of independent experiments. Probability and statistical significance were analysed using the two-tailed student *t*-test.

Chapter 3 – Retroviral expression cloning for detection of leukaemic oncogenes.

3.1 Introduction

Retroviral expression cloning is a powerful strategy developed in the mid-1990s for the identification of genes based on their ability to confer a specific phenotype in a target cell line[335-338]. The approach is similar to other plasmid-based expression cloning methods as it involves the cloning of expressed cDNAs in an experimental cell-based system of interest and subsequent selection of clones displaying a specific phenotype. Briefly, the retroviral expression cloning approach (Figure 3.1) involves cloning of expressed cDNAs from a source cell population (e.g. a leukaemia cell line) into retroviral expression vectors. These vectors produce viruses which are unable to replicate themselves due to deletion of the *Gag-Pol* and *Env* gene sequences. The library is introduced into packaging cell lines, which provide the required retroviral proteins to generate infections retroviruses[339,340]. The viral stock generated is used to transduce a target cell population, where the cDNA of interest is integrated into the host genome and expressed from retroviral promoter sequences. Infected target cells are subsequently selected for a specific phenotype, and the integrated gene is recovered for analysis. Retroviral expression cloning displays several advantages over conventional plasmid-based functional screening methods. The most important is delivery of cDNA constucts into a wide variety of biologically relevant target cell lines (e.g. haemopoietic cells). The limited number of proviral integrations per cell facilitates identification of the causative gene of interest, and stable expression of cDNAs following viral integration enables the use of a wide variety of functional assays for detection of relevant genes[341].

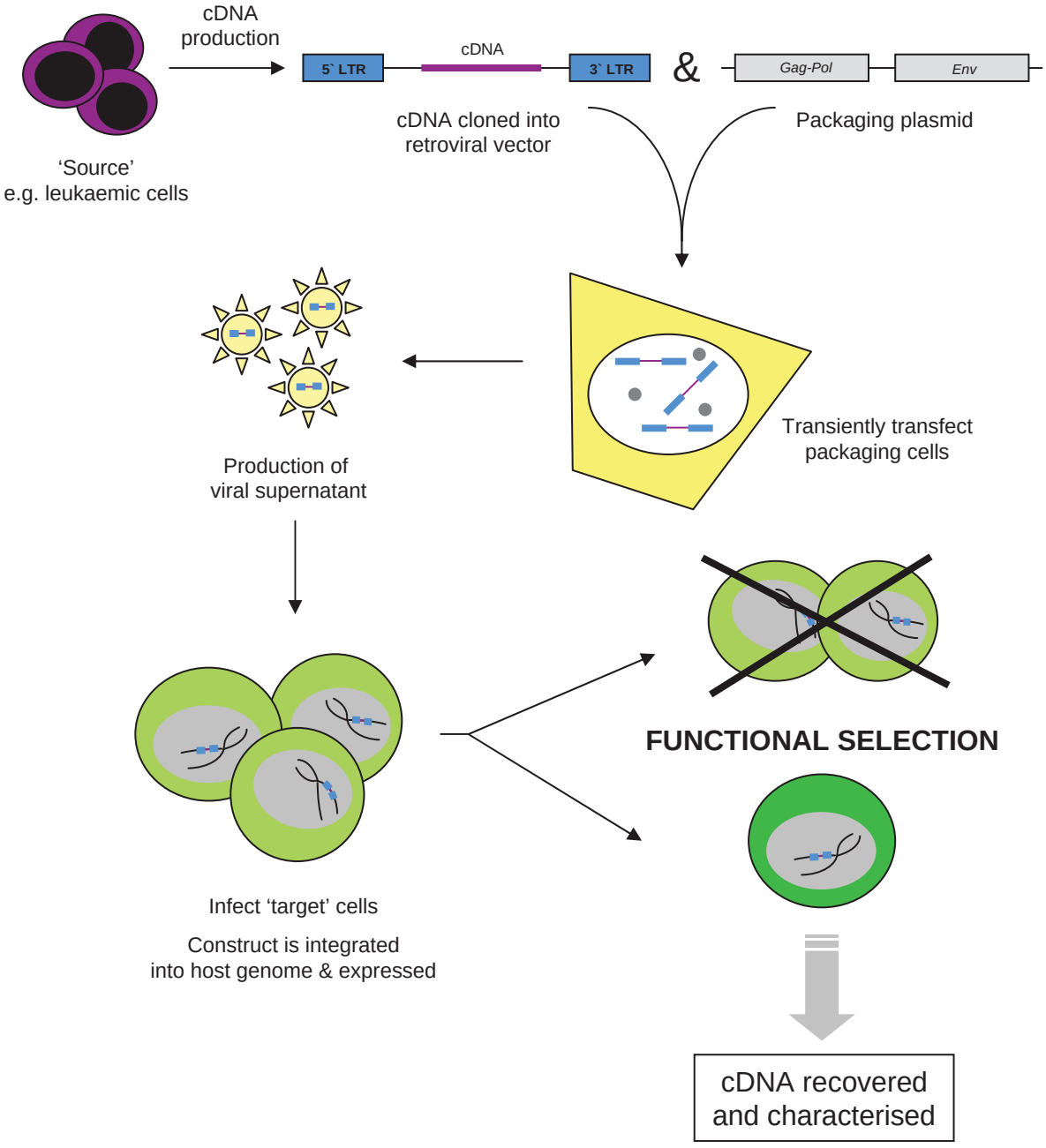

Figure 3.1: Retroviral expression cloning method. cDNA is produced from a 'source' population then cloned into retroviral vectors which lack the necessary *Gag-Pol* and *Env* viral protein sequences for replication. The resulting plasmids are cotransfected with a packaging plasmid into an intermediate cell line which is used to create live retroviruses. The viral supernatant is then used to infect the 'target' cell population, and the construct is integrated into the host genome and expressed. Infected cells are selected for the desired functional phenotype, and the cDNA expressed in the particular clonal population of interest is recovered for further characteristion. LTR = long terminal repeat (for retroviral integration and expression).

Early studies in which libraries generated from haemopoietic cell lines were screened demonstrated the feasibility of the retroviral expression cloning method, with isolation of both known oncogenes (*RAF1*, *ETS2*, and *LCK*), as well as novel genes with oncogenic potential (*Rho-related guanine nucleotide exchange factors*), based on their ability to transform fibroblastic NIH-3T3 cells[337]. More relevant haemopoietic target cell lines have also been successfully used for detection of genes involved in leukaemogenesis. For example, the murine haemopoietic cell line, FDC-P1, has been utilised to detect genes conferring factor independent growth[335], and the leukaemic M1 cell line has been utilised to detect genes which suppress differentiation in response to IL-6[125,342]. Mourtada-Maarabouni, et al. performed a screen utilising mouse thymoma W7.2 cells treated with dexamethasone and γ-irradiation, which allowed identification of genes involved in apoptosis[127,343].

Over the last two decades, cDNA library construction methods have advanced considerably, allowing for the generation of high-quality, normalised libraries containing a high proportion of full-length cDNAs[344]. These newer methods may now aid in the discovery of novel oncogenes which were previously difficult to detect using expression cloning approaches due to low transcript frequency or long transcript length. We sought to utilise improved methods for cDNA library construction to generate high-quality retroviral cDNA libraries from leukaemic sources.

In previous studies, oncogenes have been successfully isolated by screening cDNA libraries from both non-tumourigenic haemopoietic cell lines such as the murine B6SUta and FDC-P1 cell lines[125,337,343], and also from leukaemia cell lines such as the T-cell leukaemia Jurkat and the myeloid leukaemia HL-60 cell lines[345,346]. We selected the M1 murine leukaemia cell line

for retroviral cDNA library construction to identify novel putative oncogenes. M1 is a factor-independent cell line with an immature myeloblast-like morphology. It was established *in vitro* from a spontaneous myeloid leukaemia of SL strain mice[347], and can be induced to undergo terminal macrophage differentiation through addition of cytokines such as LIF, IL-6 and Oncostatin M[348-350]. Interestingly, these particular properties of M1 have led to its use as a target cell line in the identification of oncogenes such as the differentiation suppressor *SOCS1*[125], although thus far there have been no reports of its use as a source of library material. The karyotype of M1 is atypical, with the majority of clones examined exhibiting a hypodiploid karyotype[351]. However the particular genetic lesions responsible for either the factor-independence or suppressed differentiation of the cell line remain unknown. In selecting a target cell line in which to screen the M1 library we considered that a cell line which is normally factor-dependent, and also capable of differentiation, would be required. The properties of the FDB1 cell line (see Chapter 1, Section 1.2.1) make it an ideal target cell population for detection of oncogenes present in the M1 leukaemia library which confer factor-independence or a block in differentiation.

This chapter describes the construction of a retroviral cDNA library from murine M1 leukaemia cells, assessment of the FDB1 cell line system as a target population for detection of oncogenes using expression cloning methods, and functional screening of the M1 library for genes which confer factor-independent growth of myeloid cells.

3.2 Protocols and results

3.2.1 M1 library construction

3.2.1.1 Outline

For cDNA library construction, we chose to utilise the Clontech SMART Library Construction kit in combination with a size fractionation protocol (Figure 3.2). The SMART protocol optimises production of full-length cDNA at the 3` end using a modified oligo(dT) primer (CDSIII) for first strand reverse transcription. Powerscript reverse transcriptase adds several additional 'C' nucleotides when reaching the end of a transcript. A modified oligonucleotide (SMART IV) is designed to hybridise to the poly-C tail for second strand cDNA extension, thereby enhancing the production of full-length cDNA at the 5` end of mRNA transcripts[352,353]. We have incorporated a size fractionation protocol following this step to prevent bias towards amplification and cloning of small cDNA[354]. Double-stranded cDNA is separated into different size fractions using gel electrophoresis, and these fractions are handled independently in subsequent steps. Each cDNA fraction is amplified by PCR using the SMART oligonucleotide primers, which produce non-identical Sfi1A and Sfi1B sites on either end of the resulting cDNA for directional cloning. We used a modified form of the bicistronic MSCV-IRES-eGFP retroviral expression construct[320] adapted to incorporate two non-identical Sfi1 restriction sequences in the multiple cloning site (MIG-Sfi1, D. Salerno, Figure 3.3). Following Sfi1 digestion, cDNA from each size fraction is ligated to the Sfi1-modified vector then transformed into bacteria for production of the cDNA library.

NOTE:
This figure is included on page 89 of the print copy of the thesis held in the University of Adelaide Library.

Figure 3.2: Library construction method. cDNAs are produced using the SMART SfiI-modified oligonucleotide primers. Reverse transcription of messenger RNAs produces a poly-C tail at the 3` end of the first strand. The second strand primer is specific to this poly-C tail enabling production of full-length cDNAs. This is followed with size fractionation using gel electrophoresis, then amplification of each fraction using PCR. cDNA products are digested with Sfi1 and ligated to an appropriate SfiI-modified vector prior to bacterial transformation for production of the cDNA library. The aim is for a library complexity of $>1x10^6$ independent clones. Figure is modified from the Clontech SMART cDNA Library Construction kit manual.

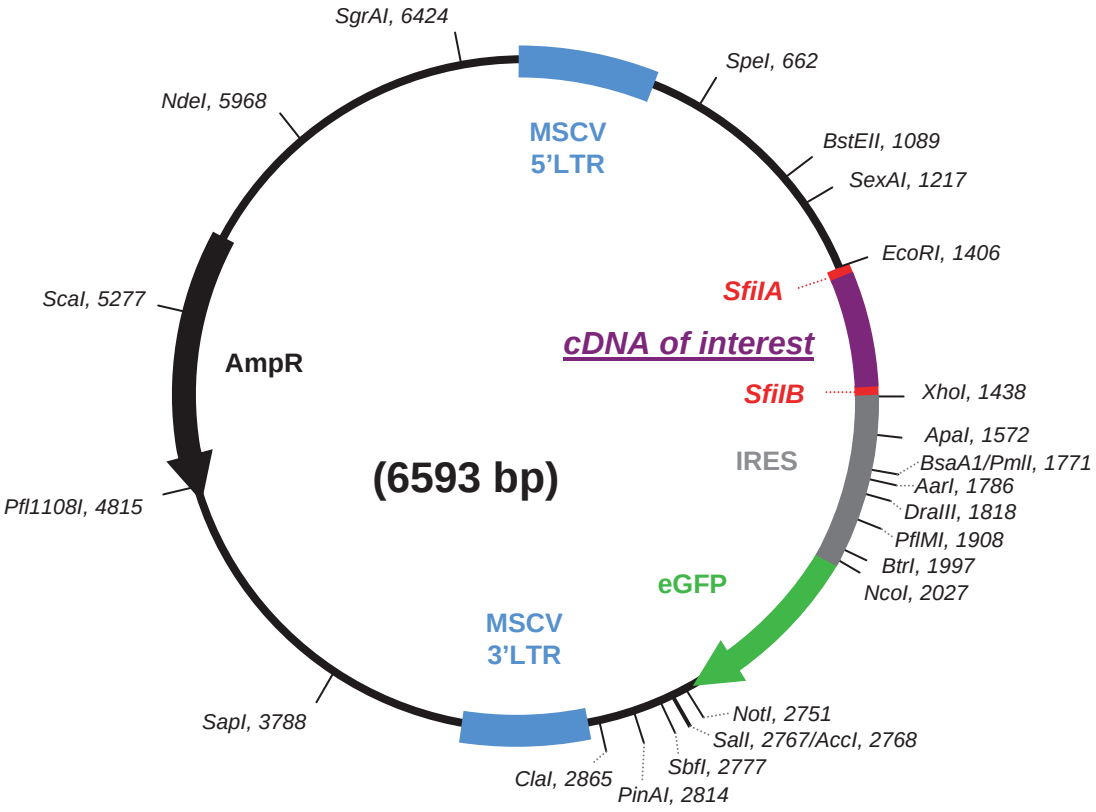

Figure 3.3: Vector map of the Sfi1-modified MSCV-IRES-eGFP retroviral expression construct (MIG-Sfi1). The cDNA of interest is cloned using non-identical Sfi1 restriction sites. Mouse stem cell virus (MSCV) long terminal repeat (LTR) sequences promote integration into the host genome and expression of the transcript. Enhanced green fluorescence protein (eGFP) is coexpressed with the cDNA of interest from a single transcript via an internal ribosome entry site (IRES) allowing selection of transduced cells. Unique restriction sites are shown. Note that the MIG-Sfi1 construct was initially cloned to contain an eGFP cassette sequence between the Sfi1 restriction sites. AmpR = ampicillin resistance for plasmid production in bacteria. Note that sizes and positions given are for the vector backbone only (not including cDNA cloned into the Sfi1 sites).

3.2.1.2 cDNA synthesis

For construction of the M1 library, first strand cDNA synthesis was performed on 1 μg of M1 total RNA using Powerscript reverse transcriptase as described in the SMART Library kit protocol. Double-stranded cDNA synthesis by primer extension was also performed as described using Advantage 2 DNA polymerase. cDNA was separated on a 1% agarose gel, and different sized fractions were excised and isolated using the Qiagen QIAquick Gel Extraction kit.

The cDNA fractions were subsequently amplified by PCR using the Clontech Advantage 2 Polymerase kit according to the manufacturer's protocols. For this amplification step the SMART Library kit 5` PCR primer and CDSIII primer were utilised. The Advantage 2 polymerase mix is designed for efficient amplification of PCR products up to 18 kb in length and contains a proof-reading polymerase for high-fidelity amplification. This PCR step was required to produce a sufficient quantity of cDNA in each size fraction for subsequent digestion and ligation to the MIG-Sfi1 vector, however it was necessary to optimise the number of cycles as excessive amplification can bias towards a greater representation of smaller or more abundant transcripts. We observed that the smaller sized fractions contained a larger amount of cDNA and hence required fewer PCR amplification cycles, whereas the opposite was true of larger sized fractions. The optimum number of PCR cycles was as follows: Fraction 1 (0.2-1.7 kb) = 5 cycles, Fraction 2 (1.7-3 kb) = 15 cycles, Fractions 3 (3-5 kb) and 4 (>5 kb) = 20 cycles. Following amplification, PCR products were separated on an agarose gel and isolated with the Qiagen QIAquick Gel Extraction kit.

3.2.1.3 cDNA cloning

The four amplified cDNA fractions were digested with Sfi1 restriction endonuclease according to the manufacturer's protocol. These were purified using the Qiagen QIAquick PCR Purification kit then precipitated overnight. The MIG-Sfi1 retroviral expression construct was prepared for cloning by Sfi1 digestion according to the manufacturer's protocol. The digested MIG-Sfi1 vector was isolated by gel electrophoresis and purified using the Qiagen QIAquick Gel Extraction kit. This isolation step was performed twice to ensure purity of the digested construct. Ligations of Sfi1-digested MIG-Sfi1 vector with each of the four M1 cDNA fractions were undertaken in accordance with the Invitrogen T4 DNA Ligase protocol. Each ligation was transformed into Lucigen's electrocompetent *E. Cloni* 10G cells using the manufacturer's recommended protocol, and plated on Luria Broth/Agar plates containing 100 μg/ml ampicillin. A small proportion of transformed cells were plated separately at a known dilution for estimation of the number of colonies formed in each fraction. Plates were incubated overnight then scraped twice following addition of 10 ml Luria Broth for collection of transformed clones. DNA from each fraction was isolated using the Qiagen HiSpeed Maxiprep kit, and retroviral cDNA library fractions were stored at -20°C until further use.

3.2.2 Composition of the M1 retroviral cDNA library

The composition of the M1 library was assessed using a selection of clones from each of the four size fractions. Twelve bacterial colonies were selected from each fraction and plasmid DNA prepared for analysis. DNA was digested using Sfi1 according to the manufacturer's protocol then separated by gel electrophoresis to visualise cloned cDNA inserts (Figure 3.4).

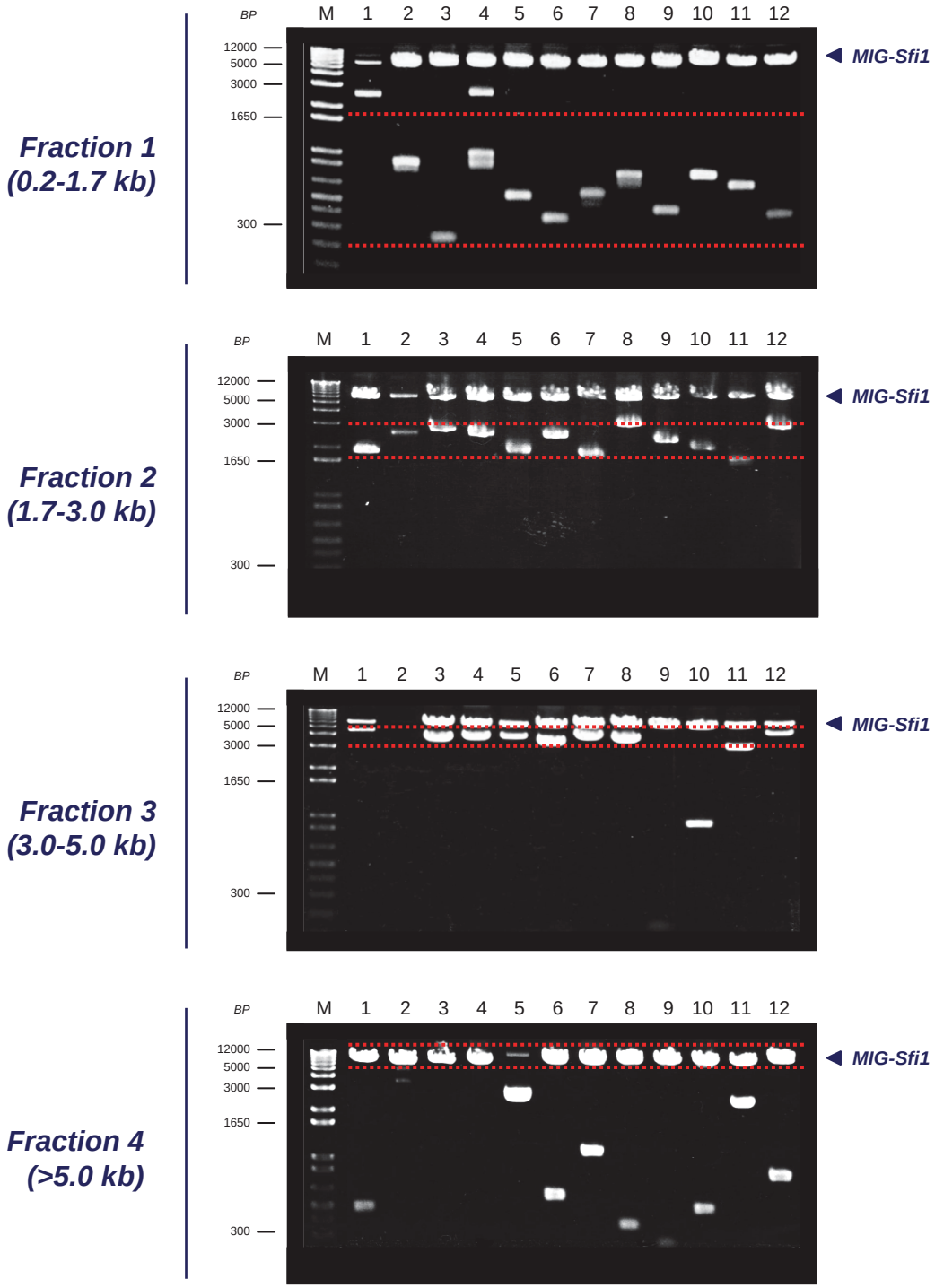

Figure 3.4: Analysis of selected clones from each fraction of the M1 library. 12 representative clones from each fraction of the M1 cDNA library were cultured overnight and plasmid DNA extracted. Clones were then digested using Sfi1and separated on a 1% agarose gel. Note that one clone in Fraction 3 (#2) did not grow when cultured overnight. M = DNA size marker (1 Kb Plus ladder). The size of selected marker bands is indicated to the left of each agarose gel photograph, and the expected size for inserts in each fraction is indicated with red dotted lines on each gel photograph. The band showing linearised MIG-Sfi1 vector backbone is indicated with a blue arrow for each photograph (MIG-Sfi1 = 6.5 kb). Note that clones #3 and #4 in Fraction 4 contain large inserts which are not visible as they are a similar size to the vector backbone (determined by sequencing, see Appendix A).

Clones were also sequenced using MIG sequencing oligonucleotides. The properties of clones in each fraction of the M1 cDNA library are summarised in Table 3.1.

Between 75% and 92% of clones in each fraction contained a single cDNA insert in the MIG-Sfi1 vector. The remaining clones consisted of the original MIG-Sfi1 vector which had not taken up a cDNA insert, clones which had taken up multiple cDNA inserts, or clones containing genomic DNA sequence. For Fractions 1 (0.2-1.7 kb), 2 (1.7-3 kb) and 3 (3-5 kb), 82-92% of clones contained inserts of the anticipated size for each fraction. For Fraction 4, only 17% of clones contained inserts of the anticipated size (>5 kb). Sequencing revealed that Fractions 2 and 3 contained the highest proportions of full-length cDNA clones (50% and 64% respectively), whereas Fractions 1 and 4 contained relatively few full-length clones (17% and 25% respectively). The majority of clones which did not contain full-length cDNA were truncated at the 5` end (up to 67% 5`-truncated clones – Fraction 1), with relatively few truncated at the 3` end (up to 17% 3`-truncated clones – Fraction 1).

The data obtained from digestion and sequencing of selected clones was extrapolated to estimate the composition of the M1 library (Figure 3.5A). A total number of $3.4x10^6$ clones were obtained, 41% of which are estimated to be full-length cDNA ($1.4x10^6$), over a size range of 0.2 to >5 kb. To assess the overall composition of each fraction of the library, an aliquot of plasmid DNA from each fraction was digested with Sfi1 and analysed by gel electrophoresis (Figure 3.5B). This confirmed the predicted size range of cDNA inserts as 0.2-1.7 kb (Fraction 1), 1.7-3 kb (Fraction 2) and 3-5 kb (Fraction 3). A smear of the anticipated size was not visible for Fraction 4 due to the linearised MIG-Sfi1 vector being a similar size (6.5 kb). However, sequencing revealed approximately 17% of clones in Fraction 4 contained inserts of >5 kb. The total number of clones in each fraction ranged from $5x10^5$

	FRACTION 1	FRACTION 2	FRACTION 3*	FRACTION 4
Number of clones assessed	12	12	11	12
Clones with 1 cDNA insert	10 (83%)	11 (92%)	10 (91%)	9 (75%)
Other	2 (17%)	1 (8%)	1 (9%)	3 (25%)
Predicted size range (kb)	0.2-1.7	1.7-3	3-5	>5
Actual insert size range (kb)	0.25-0.85	1.8-3.0	0.15-4.5	0.2->5**
Clones within predicted size range	10 (83%)	11 (92%)	9 (82%)	2 (17%)
Full-length clones†	2 (17%)	6 (50%)	7 (64%)	3 (25%)
5`-truncated clones††	8 (67%)	4 (33%)	3 (27%)	6 (50%)
3`-truncated clones††	2 (17%)	1 (8%)	1 (9%)	0 (0%)

Table 3.1: Summary of selected clones from each fraction of the M1 library. 12 representative clones (see Figure 3.4) were sequenced from each fraction of the M1 cDNA library. *One clone in Fraction 3 did not grow when cultured overnight. The approximate insert size range of selected clones following Sfi1 digestion is indicated for each fraction. **Fraction 4 contains 17% (2/12 clones) with inserts >5 kb in length. †Sequences were interrogated using the NCBI Basic Local Alignment Search Tool (BLAST)[355] and relative completeness of each clone was assessed by alignment with the accession numbers shown in Appendix A. ††Note that some clones were truncated at both 5` and 3` ends. 'Other' indicates vector alone (uncut vector, linearized vector, original vector with eGFP stuffer), clones with multiple inserts, clones with genomic DNA inserts, or clones for which sequence was not able to be obtained.

A.

COMPOSITION OF THE M1 LIBRARY	
Size range	0.2 to >5 kb
Total clones	$3.4x10^6$
Clones with 1 cDNA insert	$2.9x10^6$ (86%)
Full-length clones	$1.4x10^6$ (41%)
5`-truncated clones	$1.5x10^6$ (44%)
3`-truncated clones	$3.3x10^5$ (10%)
Other	$4.6x10^5$ (14%)

B.

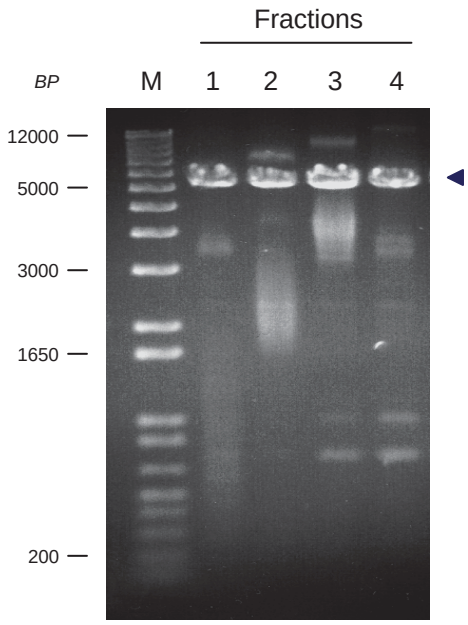

FRACTIONS	SIZE RANGE	TOTAL CLONES	FULL-LENGTH CLONES
FRACTION 1	0.2-1.7 kb	$1x10^6$	$1.7x10^5$
FRACTION 2	1.7-3 kb	$1x10^6$	$5.0x10^5$
FRACTION 3	3-5 kb	$9x10^5$	$5.8x10^5$
FRACTION 4	>5 kb	$5x10^5$	$1.3x10^5$

Figure 3.5: Composition of the M1 cDNA library. A. Overall composition of the M1 library. Estimates were based on total clone numbers in each fraction and data shown in Figure 3.4 and Table 3.1. **B.** The four fractions of the M1 library. Plasmid DNA from individual fractions was digested with Sfi1 and separated by gel electorphoresis. Filled arrow indicates the linearised vector backbone (MIG-Sfi1 = 6.5kb). M = DNA size marker (1 Kb Plus). The size of selected bands is indicated to the left of the gel photograph. Characteristics of each fraction are summarised in the adjacent table. 'Size range' indicates the size of cDNA inserts in each fraction estimated using gel electrophoresis (except for Fraction 4 which contains 17% large inserts (>5 kb) as determined by sequencing selected clones). The number of full-length clones in each fraction was estimated by sequencing a selection of clones (see Figure 3.4 and Table 3.1 for details).

(Fraction 4) to $1x10^6$ (Fractions 1 and 2), and the number of full-length clones in each fraction ranged from $1.3x10^5$ (Fraction 4) to $5.8x10^5$ (Fraction 3).

3.2.3 Assessment of the FDB1 cell line as a target population for retroviral expression screening

We wished to establish the suitability of the FDB1 cell line for use as a target population in functional screening for oncogenes which confer factor-independent growth or a block in differentiation. It has been previously shown that FDB1 cells display factor-independent proliferation in response to expression of oncogenes such as the V449E mutant form of hβc[128], or the ITD mutant form of the FLT3 receptor (FLT3-ITD)[326]. However identification of such oncogenes using a functional expression cloning screen requires clonal outgrowth from a single cell in conditions without growth factor, and on a background of dead or dying untransformed cells. To test the efficiency of clonal FDB1 outgrowth in these conditions, we used FACS to seed one FDB1 cell expressing FLT3-ITD (FDB1-ITD) on a background of $1x10^4$ parental FDB1 cells per well in medium without growth factor (100 μl /well, one 96-well plate). Both parental FDB1 cells and FDB1-ITD cells were washed three times in 1x PBS to remove growth factor prior to sorting. Following one week of culture, we observed factor-independent outgrowth in 9/96 (approximately 10%) of wells seeded with a single FDB1-ITD cell. FDB1-ITD cells lose approximately 10-20% viability overnight following removal from growth factor, which may account for some wells seeded with a single FDB1-ITD cell not displaying any growth (M. Perugini and D. Salerno, personal communication). The observation that we detected growth in approximately 10% of wells seeded suggests that FDB1 cells are not adept at clonal growth from single cells, but rather, they may require

seeding at a minimum density for survival and proliferation. Hence, the FDB1 cell line is not a suitable system for screening of genes conferring factor-independent growth.

We were also interested to utilise the FDB1 cell line system to screen for genes which would block differentiation in GM-CSF. Preliminary studies have shown that this system is suitable for detection of such oncogenes, with suppression of FDB1 differentiation achieved through expression of oncogenic MYB[1]. We hypothesised that as parental cells remain viable in GM-CSF, this would support the outgrowth of a single cell with a blocked-differentiation phenotype. To this end, we carried out a negative control test screen to assess background outgrowth of parental FDB1 cells in GM-CSF. FDB1 cells were washed three times in 1x PBS to remove IL-3, then seeded at $1x10^4$ cells per well in medium containing 500 BMU/ml GM-CSF (100 μl per well, one 96-well plate). Wells were scored weekly for possible outgrowth, and at week 4 we observed growth in 13/96 wells (13.5%). Of these, 4 wells gave rise to continuous culture in GM-CSF (4.2%). To completely screen the M1 library in duplicate, this would require seeding $6.8x10^6$ cells in GM-CSF in a total of 680 wells. This would be predicted to give a high rate of background growth, making FDB1 system an unsuitable cell line for identification of genes conferring a differentiation block in GM-CSF.

3.2.4 Utilising the FDC-P1 cell line as a target population for retroviral expression screening

As the FDB1 cell line proved unsuitable for the proposed functional screening experiments, we instead turned to the FDC-P1 cell line to screen the M1 library. Similarly to FDB1 cells, the FDC-P1 cell line is an immature myeloid cell line, although it was initially derived from murine bone marrow cultures as opposed to foetal liver cells[356]. FDC-P1 cells can be

maintained in culture supplemented with IL-3 or GM-CSF for growth. However, unlike FDB1 cells, FDC-P1 cells cannot be induced to differentiate with the addition of cytokines. The FDC-P1 cell line has successfully been used in a previous study to identify genes conferring factor-independent growth from a haemopoietic retroviral cDNA library[335]. In addition, we have previously observed clonal outgrowth of FDC-P1 cells expressing the FIΔ mutant form of hβc in conditions without growth factor, making this a suitable cell line for screening of oncogenes which confer factor-independent growth in the M1 library[357].

Before screening we wished to optimise recovery of integrated retroviral sequences from transduced FDC-P1 clones using PCR. Primers for recovery of the integrated MIG-Sfi1 retroviral construct were designed as shown in Figure 3.6A. To test these primers on genomic DNA, FDC-P1 cells were transduced with the MIG-Sfi1 construct containing human *CD4* cDNA cloned into the Sfi1 restriction sites (*CD4* = 1.3 kb). FACS was utilised to obtain a stable population expressing GFP. Genomic DNA was prepared from FDC-P1 cells transduced with MIG-Sfi1-*CD4* and also from untransduced FDC-P1 cells as a negative control. PCR was performed using the Qiagen LongRange PCR kit according to the manufacturer's protocols with the following parameters: 2 μl genomic DNA template, primer annealing temperature of 60°C, and 30 amplification cycles. 4 μl of each PCR reaction was separated and visualised using gel electrophoresis. Using these conditions, the recovery primers efficiently amplified a product of 1.4 kb in length from FDC-P1 cells transduced with MIG-Sfi1-*CD4* but not from untransduced cells, as shown in Figure 3.6B.

A.

GTCAAGCCCTTTGTACACCCTAAGCCTCCGCCTCCTCTTCCTCCATCCGCCCCGTCTCTCCCCCTT

MIG-Sfi1-forward

GAACCTCCTCGTTCGACCCCGCCTCGATCCTCCCTTTATCCAGCCCTCACTCCTTCTCTAGGCGCC

EcoR1 Sfi1A *Cloned insert* Sfi1B Xho1

G**GAATTC**GGCCATTATGGCC ——— **GGCCGCCTCGGCC**CTCGAGGATCAATTCC

MIG-Sfi1-reverse

GCCCCTCTCCCTCCCCCC**CCCCTAACGTTACTGGCCGA**AGCCGCTTGGAATAAGGCCGGTGTGCGT

TTGTCTATATGTTATTTTCCACCATATTGCCGTCTTTTGGCAATGTGAGGGCCCG

B.

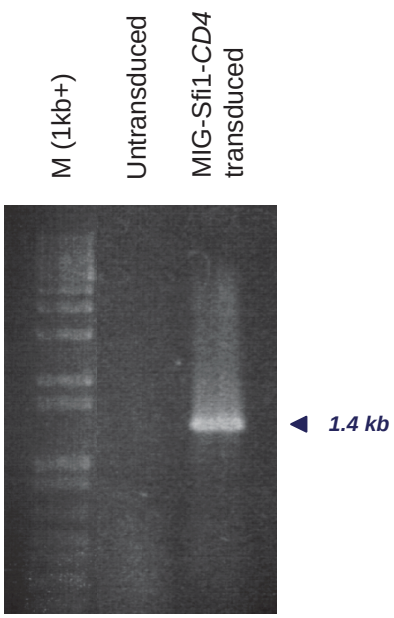

Figure 3.6: PCR recovery of integrated MIG-Sfi1 retroviral construct. A. Location of primers for PCR recovery of integrated MIG-Sfi1 retroviral construct. The DNA sequence of the MIG-Sfi1 multiple cloning site is shown. Restriction sites for EcoRI and Xho1 are indicated in blue text, and for Sfi1A/B are indicated in red text. The position of recovery primers is highlighted in green. **B.** Optimisation of PCR recovery of the integrated MIG-Sfi1 construct from genomic DNA. Genomic DNA was harvest from untransduced FDC-P1 cells or FDC-P1 cells transduced with MIG-Sfi1-*CD4*, and PCR performed using recovery primers shown in part 'A'. A PCR product of 1.4 kb was detected indicating the presence of integrated MIG-Sfi1-*CD4* in transduced FDC-P1 cells.

3.2.4.1 Screening the M1 library for genes which confer factor-independent growth in FDC-P1 cells

We initially sought to assess the number of retroviral integrations per FDC-P1 clone following transduction with the M1 library. FDC-P1 cells were transduced with DNA from each of the four fractions of the M1 library. 24 hrs post-infection, FACS was utilised to sort a single GFP positive (GFP^+) FDC-P1 cell per well in medium containing 80 BMU/ml GM-CSF (100μl per well, one 96-well plate per fraction). After 1 week of culture, we selected 12 wells from each fraction which showed clonal outgrowth and removed half of the cells in each well for production of genomic DNA. PCR was performed as described above using 2 μl of genomic DNA template per reaction and 30 amplification cycles. Extension was carried out for 10 mins in each cycle to ensure amplification of long cDNA inserts (sufficient for amplification of products up to 10 kb). 4 μl of each PCR reaction was then separated and visualised using gel electrophoresis as shown in Figure 3.7. Under these reaction conditions, we obtained a PCR product indicating integrated retroviral constructs in 83% of clones assessed. For the remaining 17% of clones, it is possible that an untransduced clone had been seeded using FACS for single-cell sorting. Alternatively, it is possible that the PCR reaction was not successful using these parameters due to the location of the integration or the length/composition of the cDNA insert. We observed that 53% of clones showed one integration as judged by the presence of a single dominant band in the gel photograph. 25% showed two integrations, and the remaining 22% showed three or more integration products detected by PCR (see Figure 3.7).

For functional screening of the M1 library, DNA from each of the four size fractions of the M1 library was used to transduce FDC-P1 cells. 24 hrs post-infection, cells positive for the

A.

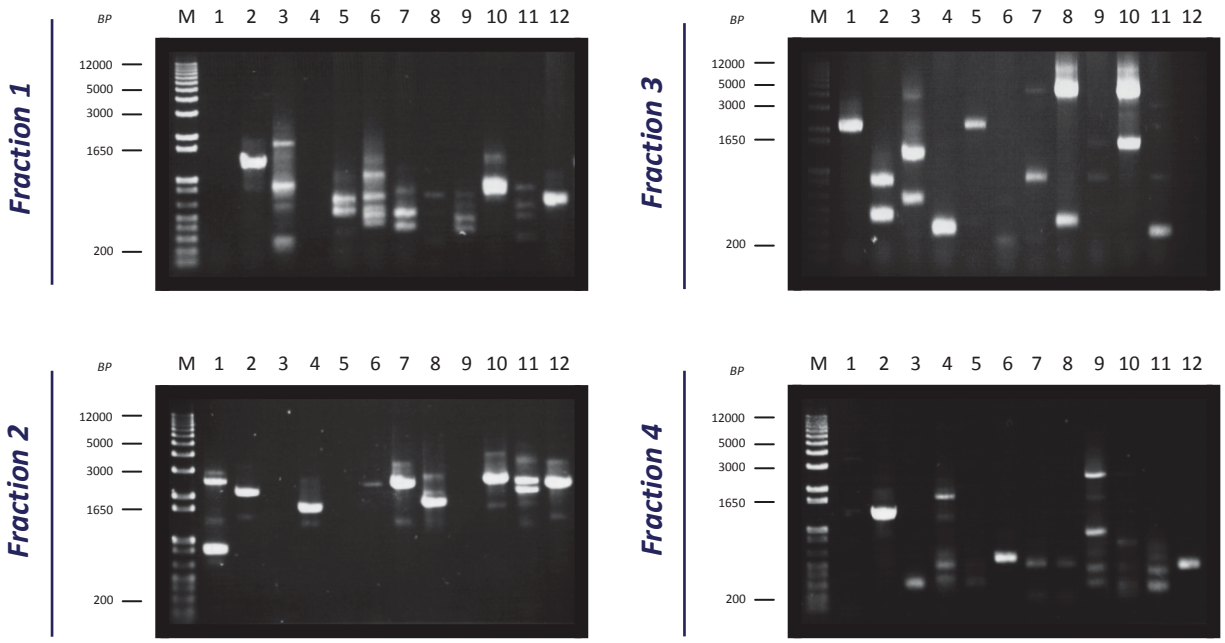

B.

	1 INTEGRATION	2 INTEGRATIONS	≥3 INTEGRATIONS	NO PCR PRODUCT
FRACTION 1	4 (40%)	1 (10%)	5 (50%)	2 (17%)
FRACTION 2	7 (78%)	2 (22%)	0 (0%)	3 (25%)
FRACTION 3	5 (50%)	5 (50%)	0 (0%)	2 (17%)
FRACTION 4	5 (46%)	2 (18%)	4 (36%)	1 (8%)
TOTAL	21 (53%)	10 (25%)	9 (22%)	8 (17%)

Figure 3.7: Analysis of retroviral integrations in selected FDC-P1 clones transduced with the M1 library. FDC-P1 cells were transduced with each fraction of the M1 library then FACS was utilised to seed one GFP^+ cell per well the following day. These were cultured for 1 week in the presence of GM-CSF then 12 representative FDC-P1 clonal populations from each fraction were lysed and genomic DNA extracted. PCR was performed to amplify the retroviral integrations in each clonal population. **A.** PCR products from amplification of retroviral integrations in FDC-P1 clonal populations were separated on an agarose gel. M = DNA size marker (1Kb plus). The size of selected bands is indicated to the left of each agarose gel photograph. **B.** Summary of the number of retroviral integrations in FDC-P1 clones transduced with the M1 library. Note that the PCR reaction did not generate a product in all clones under these reaction conditions. For the clones from which a PCR product was obtained, the percentage of clones containing 1, 2 or ≥3 integrations (detected as dominant bands in gel photographs in part 'A') per clone is indicated.

GFP marker were sorted using FACS. We obtained cells representing two-fold the number of clones in each fraction to ensure adequate representation of the library in our screens. Sorted cells were recovered overnight, then washed three times in 1x PBS to remove growth factor. Cells were resuspended at $1x10^4$ cells per well in medium without growth factor (100 μl per well, 96-well plates). Note that untransduced FDC-P1 cells were also seeded in medium without growth factor at $1x10^4$ cells per well as a negative control (100 μl per well, one 96-well plate). Cells were cultured for a total of 5 weeks, however we saw no outgrowth in wells containing M1 library-transduced cells.

3.3 Discussion

3.3.1 Construction of the M1 retroviral cDNA library

This chapter describes the successful modification of existing methods for generation of full-length cDNA libraries. We utilised a combination of the SMART system and size fractionation to generate a retroviral cDNA library in the MIG-Sfi1 vector. This library was cloned from expressed sequences in the murine leukaemia cell line M1, which has not previously been utilised as a source in retroviral expression cloning studies. The M1 library contained a total of $1.4x10^6$ full-length cDNA clones ranging in size from approximately 200 bp to over 5 kb. Although studies have estimated that the mammalian transcriptome contains approximately 20,000 protein coding genes, the full complexity of the transcriptome has not yet been wholly elucidated[358]. Traditionally, a cDNA library complexity of $>1x10^6$ individual clones is considered an adequate representation of the mouse or human transcriptome[359], and hence the M1 library contained sufficient full-length cDNAs to represent the mouse transcriptome. Despite the use of the SMART (Switching mechanism at 5` end of RNA

transcript[352,353]) protocol for enrichment of full-length transcripts at the 5` end, we found that 44% of clones contained cDNA which was truncated at the 5` terminus. This is likely due to hybridisation of the poly-G-modified 5` SMART IV primer at C-rich sequences within cDNA transcripts during second strand cDNA production. It is possible that other methods may be employed to improve cloning of the 5` end of transcripts, such as the CAP-trapper or oligo-capping methods which involve modification of the 5` cap structure as part of the library construction protocol[360,361].

3.3.2 Screening the M1 retroviral cDNA library

Assessment of the FDB1 cell line showed that these cells do not represent a suitable experimental system for the identification of genes conferring factor-independent growth or blocking differentiation in functional screening assays, due to inefficient clonal growth in growth factor-free conditions, and a high background of clonal growth in GM-CSF. The M1 library was subsequently screened for genes conferring factor-independent growth in the FDC-P1 cell line. However no factor-independent growth was observed, suggesting that the M1 library may not contain an oncogene which, on its own, is sufficient to transform FDC-P1 cells to factor-independent growth. It may be possible to modify the screen to identify genes that confer growth of FDC-P1 cells in sub-optimal concentrations of growth-factor. Alternatively, it is possible that oncogenes conferring factor-independent growth may be under-represented in the M1 library. It may therefore be of benefit to employ a cDNA normalisation method such as duplex-specific normalisation to remove abundant cDNAs in the M1 library[362].

Other target cell systems could potentially be utilised to continue screening the M1 library,

such as the myeloid cell line HF6 or non-myeloid cell lines such as NIH-3T3. However, these cell lines have previously been used in a number of retroviral expression screening studies[126,335,337,345]. It is important to consider also that our experimental approach will only detect single oncogenes which are sufficient to induce the particular leukaemic properties of interest, however it is now generally accepted that cooperation of multiple genetic lesions is required for the development of AML[24,55]. Thus it may be useful to consider modifying our screens to look for genes which might cooperate with known leukaemia oncogenes. This approach has been successfully used to identify genes cooperating with the RAS pathway in leukaemia, for example, Passioura, et al. detected *IRF2* as a putative oncogene which overcomes NRAS-induced growth suppression of U937 leukaemia cells[363]. Scholl, et al. used a similar approach to screen an RNAi library to identify genes which are necessary for the oncogenic properties of KRAS[364]. This 'synthetic lethality' screen identified the serine/threonine kinase *STK33* as one such gene, and the authors demonstrated that suppression of STK33 in KRAS-positive cells inhibited proliferation and induced cell death.

3.3.3 Retroviral expression screening for the detection of oncogenes in human disease

Although most of the studies mentioned previously have utilised various haemopoietic cell lines for library construction, there are fewer examples of screens where libraries have been constructed using primary samples from patients with haemopoietic disorders. The two homeobox genes *PRH* and *HLX*, although previously known to be involved in embryonic development, were isolated from a retroviral cDNA library screen of patients with MPD, suggesting a hitherto unknown role for these genes in haemopoiesis with potential involvement in HSC development[365]. A study utilising a retroviral cDNA library from an

AML patient revealed a deletion mutation in a nerve growth factor-receptor gene previously suspected to play a role in glioma formation[366]. In theory, with appropriate screening methods it should be possible to identify disease-causing genes or mutations for almost any disorder, which makes retroviral expression cloning an attractive application once optimised. As we have successfully optimised methods for construction of cDNA libraries, it will be interesting to apply these methods further to screening libraries constructed from primary AML samples. The PCR step in the Clontech SMART Library Construction kit allows construction from limited amounts of starting material, which is particularly relevant to the construction of libraries from patient samples.

The primary advantage of expression cloning over other methods of oncogene identification is that genes are identified based directly on their function[341]. However, a number of groups have now performed expression cloning screens to identify leukaemia-associated genes, and thus it is likely that subsequent screens may identify oncogenes which are already known. One such example is the oncogenic RAS activator, *RASGRP4*, which was isolated in two independent studies screening libraries from patients with MDS or cytogenetically normal AML[126,367]. It is likely that oncogenic lesions could potentially be more readily detected using genome-wide approaches such as exon capture and whole genome sequencing. However, these approaches are not based on functional screening and a high level of validation is required to show a causal association of any change with disease. Continued research utilising a combination of these technologies will be essential in elucidating oncogenes and related pathways contributing to the development of AML. Due to technical limitations and time constraints, these retroviral expression cloning studies were discontinued and characterisation of the putative AML tumour suppressor KLF5 was alternatively undertaken.

Chapter 4 – KLF5 expression and function in myeloid differentiation.

4.1 Introduction

The expression patterns of transcription factors often reflect their function in determining cell fate or promoting differentiation, whether it be a role in proliferation and self-renewal, or induction of growth arrest and activation of cell-type-specific gene expression programs[368]. KLF5 is highly expressed in proliferating cells of a number of different tissues, for example, in proliferating intestinal epithelial cells, VSMCs, and ESCs (see Chapter 1, Section 1.3.7.1). Accordingly it has been demonstrated that KLF5 has a pro-proliferative function in these tissues with additional effects on suppression of differentiation. Conversely, KLF5 expression is increased during hormone-induced adipogenesis, and it has been demonstrated that over-expression of KLF5 in this tissue is sufficient to induce adipocyte differentiation, whereas haploinsufficiency of *Klf5* in mouse models impairs adipogenesis[156]. In an extensive series of microarrays performed to elucidate mechanisms of myeloid differentiation, *Klf5* was identified as a gene for which mRNA expression increased during granulocyte-macrophage differentiation of the murine myeloid cell line FDB1 in response to expression of a constitutively activated cytokine receptor, FIΔ hβc[1] (see Chapter 1, Section 1.2.3). We have thus hypothesised that KLF5 plays a key role in induction of myeloid differentiation.

In the myeloid system, there are a number of transcription factors which have been identified as important for determination of granulocyte-macrophage lineage differentiation[369]. For

example, the interferon regulatory factor IRF8 is highly expressed in the monocyte lineage but not in the granulocyte lineage. Consistent with this observation, functional studies have shown that over-expression of IRF8 directs macrophage differentiation of bipotential myeloid progenitors[370,371], and that *Irf8* knock-out mouse models develop myeloproliferative-like disorders characterised by an increased proportion of granulocytes in the peripheral blood[372]. In contrast, C/EBPε expression is restricted to the granulocyte lineage[373], and functional studies have confirmed that it acts in determination of granulocyte commitment[374,375]. Previous unpublished microarray studies performed by our research group demonstrated that *Klf5* expression was specifically associated with the granulocyte lineage in the FDB1 cell system (see Chapter 1, Section 1.2.3.1). In particular, *Klf5* expression was associated with that of a number of C/EBPα target genes[1]. C/EBPα is a transcription factor known to have an essential regulatory role in granulocyte development[131]. Interestingly, KLF5 has been shown to directly activate expression of the neutrophil-specific secondary granule gene *Lactotransferrin* (*LTF*) in endometrial carcinoma cells[201], which is up-regulated by both C/EBPα and C/EBPε in granulocyte differentiation[376,377]. Given these observations, we predicted that KLF5 may have a function in differentiation of the granulocyte lineage.

In this Chapter we wished to characterise *Klf5* expression during granulocyte-macrophage differentiation of the FDB1 cell line in response to GM-CSF. We also sought to characterise *KLF5* expression specifically in granulocyte and monocyte lineages using an alternative cell line model and primary haemopoietic cell systems, and to compare expression of *KLF5* with expression profiles of the granulocytic transcription factors *CEBPA* and *CEBPE*. To gain insights into the function of KLF5 in haemopoiesis, we utilised both retroviral over-expression and gene knock-down approaches to modulate KLF5 expression in murine cell

lines and primary haemopoietic cells, and have analysed the effects of KLF5 on myeloid differentiation.

4.2 Results

4.2.1 KLF5 mRNA expression increases during myeloid differentiation and is predominantly associated with granulocyte differentiation

4.2.1.1 GM-CSF-induced granulocyte-macrophage differentiation of the FDB1 cell line

Klf5 expression increases during granulocyte-macrophage differentiation of the FDB1 cell line in response to enforced expression of the activated receptor FIΔ hβc, and we hence sought to determine if expression similarly increases in this system during granulocyte-macrophage differentiation in response to cytokine induction. FDB1 cells were cultured in GM-CSF (500 BMU/ml) for a period of 5 Days. On Day 0 (cells in IL-3 (500 BMU/ml)), FDB1 cells displayed an immature myeloblastic cell morphology, with the majority of cells exhibiting rounded nuclei, dark-staining cytoplasms, and a low cytosplam-to-nucleus volume ratio (Figure 4.1A). By Day 5 in GM-CSF, the majority of cells underwent morphological differentiation to granulocytes and macrophages. Mature granulocytes were characterised by polylobular nuclei (often presenting in a ring shape), diminished size, and light-staining, granular cytoplasms. Mature macrophages displayed a large cytoplasm-to-nucleus volume ratio, light-staining granular cytoplasms, small rounded nuclei, and ruffled cellular edges. Analysis of cell surface marker expression correlated with the observed morphological appearance of differentiated FDB1 cells, with an increase in expression of both the

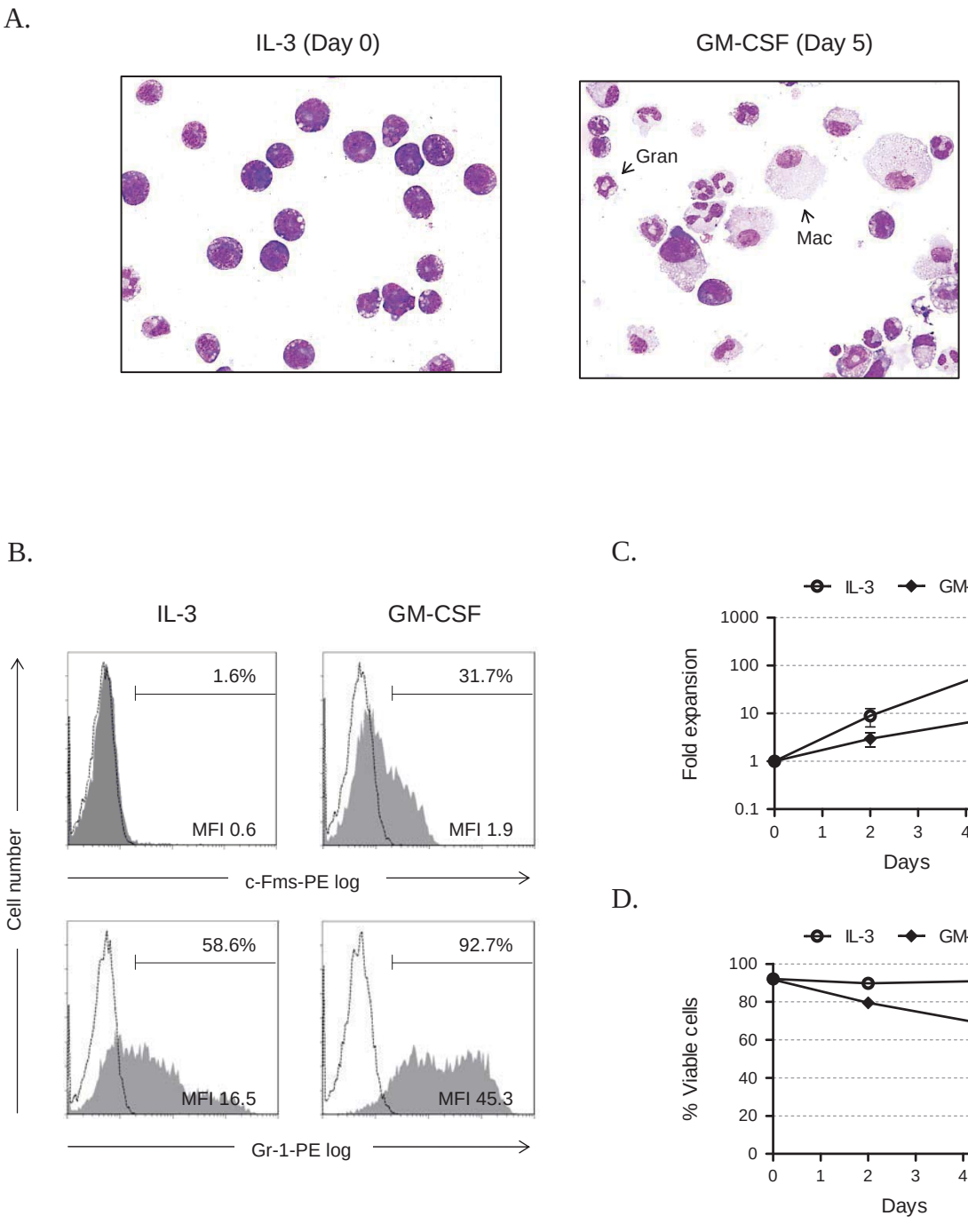

Figure 4.1: Granulocyte-macrophage differentiation of FDB1 cells in GM-CSF. A. Representative photomicrographs showing Wright-Giemsa stained cytospin preparation of FDB1 cells cultured in IL-3 (Day 0) or GM-CSF (Day 5). Gran = granulocyte, Mac = macrophage. Original magnification = 200x **B.** Flow cytometric detection of c-Fms and Gr-1 expression on FDB1 cells in IL-3 (Day 0) or in GM-CSF (Day 5). Representative results from a typical experiment are shown. Empty peak = isotype control, grey peak = marker expression. MFI = mean fluorescence intensity. **C.** Expansion of FDB1 cells in IL-3 or GM-CSF relative to Day 0. Live cell numbers were determined at each time-point using Trypan Blue staining and cell counts. n=2, *p<0.05. **D.** Viability of FDB1 cells in IL-3 or GM-CSF. Percentage of live cells were determined at each time-point using Trypan Blue exclusion. n=2, *p<0.05.

macrophage-specific marker c-Fms, and the granulocyte-associated marker Gr-1 by Day 5 in GM-CSF (Figure 4.1B). Differentiation of FDB1 cells was accompanied by a 10-fold reduction in cell expansion compared to cells cultured in IL-3 (Figure 4.1C), and cell viability was reduced from 91% in IL-3 to 66% by Day 5 in GM-CSF (Figure 4.1D).

RNA was prepared from cells harvested at Days 1, 2, 3 and 5 post-induction with GM-CSF, as well as on Day 0. Q-PCR analysis demonstrated that *Klf5* expression increased over the first two days following addition of GM-CSF (Figure 4.2A), which is consistent with the increased *Klf5* expression observed during granulocyte-macrophage differentiation of FDB1 cells in response to the activated receptor FIΔ hβc (see Chapter 1, Figure 1.3). Interestingly, we found that *Klf5* expression reached a maximum level at Day 2 in GM-CSF then by Day 5 had decreased to levels below that found in IL-3. Thus *Klf5* expression peaks early before morphological differentiation of FDB1 cells, consistent with a potential role in granulocyte or macrophage differentiation. Q-PCR was also performed to detect expression of *Cebpa* and *Cebpe* during FDB1 cell differentiation. The pattern of *Cebpe* expression showed a similar trend to that of *Klf5*, with a peak occurring at Day 2 in GM-CSF (Figure 4.2B). In contrast, *Cebpa* expression decreased rapidly during differentiation (Figure 4.2C).

4.2.1.2 G-CSF-induced granulocyte differentiation of the 32D cell line

The 32D murine myeloid cell line was selected as a model of granulocytic differentiation in response to G-CSF stimulus[378]. 32D cells were maintained in IL-3 (500 BMU/ml), where they showed continuous proliferation with a myeloblastic morphology (Figure 4.3A). Cells were induced to differentiate using G-CSF (50 ng/ml), and by Day 7 in G-CSF the majority of cells showed morphologic differentiation along the granulocyte lineage. Mature granulocytes were

A.

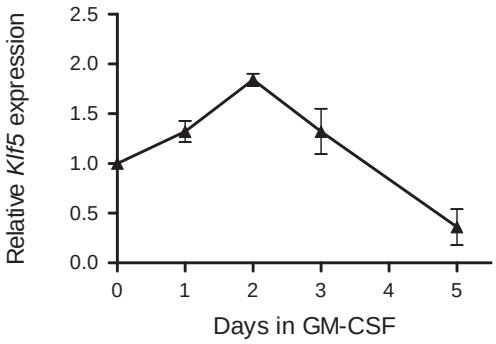

B.

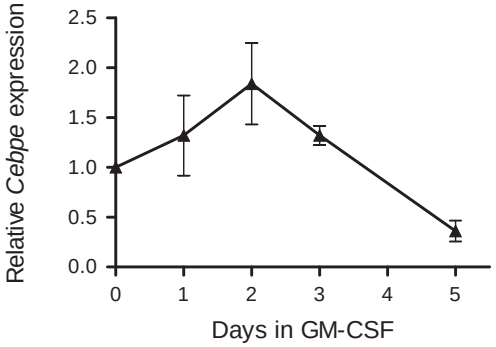

C.

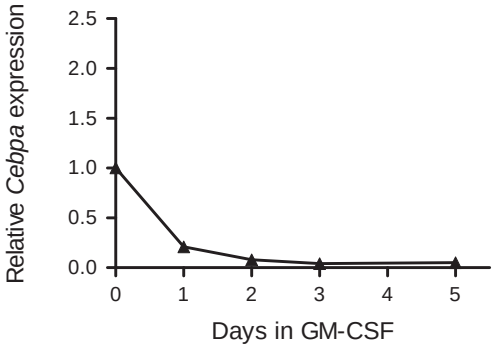

Figure 4.2: Expression of *Klf5* and *Cebp* family members during GM-CSF-induced FDB1 cell differentiation. FDB1 cells were induced to differentiate over 5 days in GM-CSF. Q-PCR was performed to determine: **A.** *Klf5* mRNA expression, **B.** *Cebpe* mRNA expression, and **C.** *Cebpa* mRNA expression. Expression is plotted relative to Day 0 (IL-3). n=3.

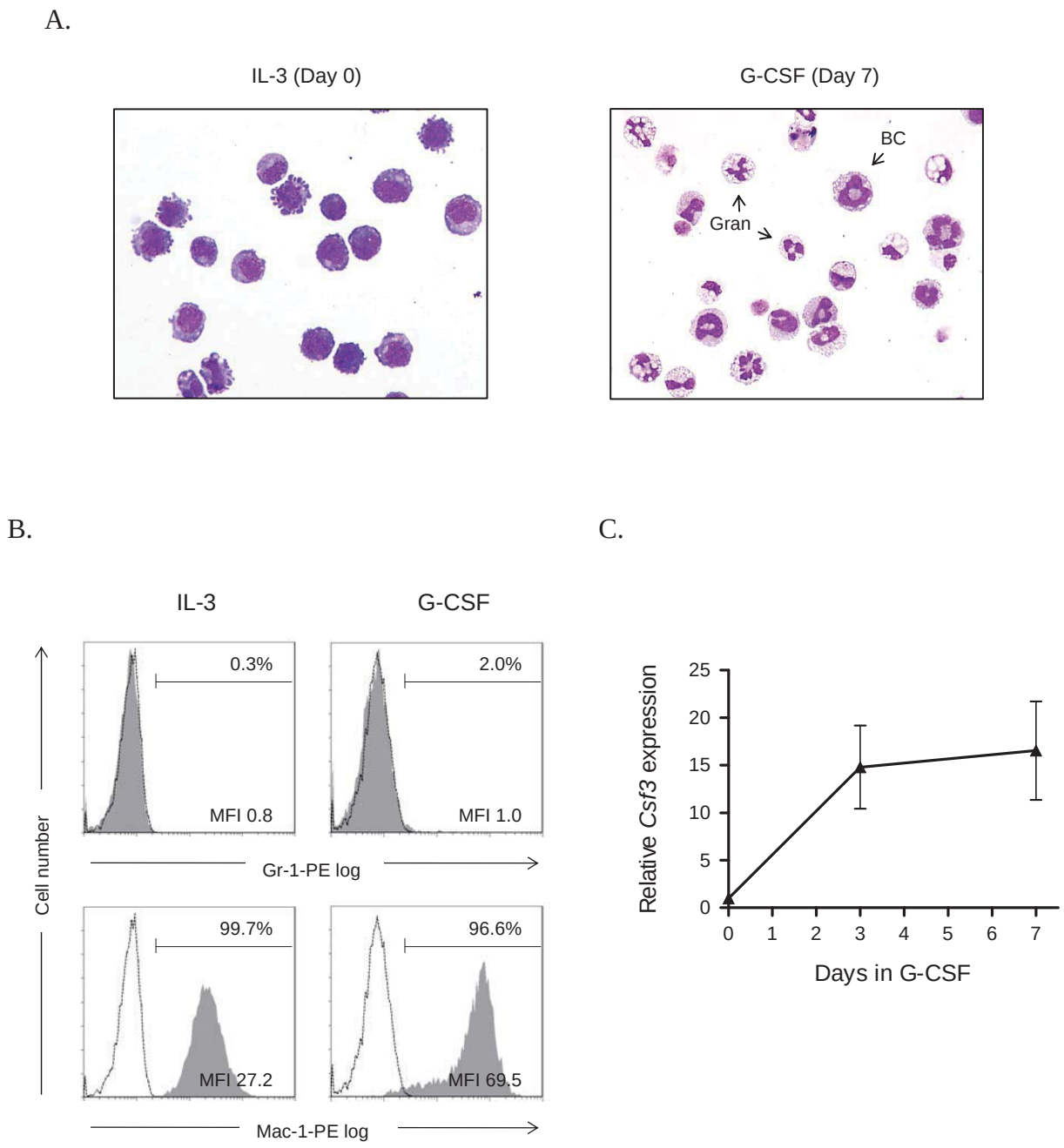

Figure 4.3 (A-C): Granulocyte differentiation of 32D cells in G-CSF. A. Representative photomicrograph showing Wright-Giemsa stained cytospin preparation of 32D cells in IL-3 (Day 0) or in G-CSF (Day 7). Original magnification = 200x. Gran = granulocyte, BC = band cell. **B.** Flow cytometric detection of Gr-1 and Mac-1expression on 32D cells in IL-3 (Day 0) or in G-CSF (Day 7). Representative results from a typical experiment are shown. Empty peak = isotype control, grey peak = cell surface marker expression. MFI = mean fluorescence intensity. **C.** Q-PCR detection of *Csf3* mRNA expression in 32D cells differentiated over 7 days in G-CSF. Expression was plotted relative to Day 0 (cells in IL-3). n=3.

D.

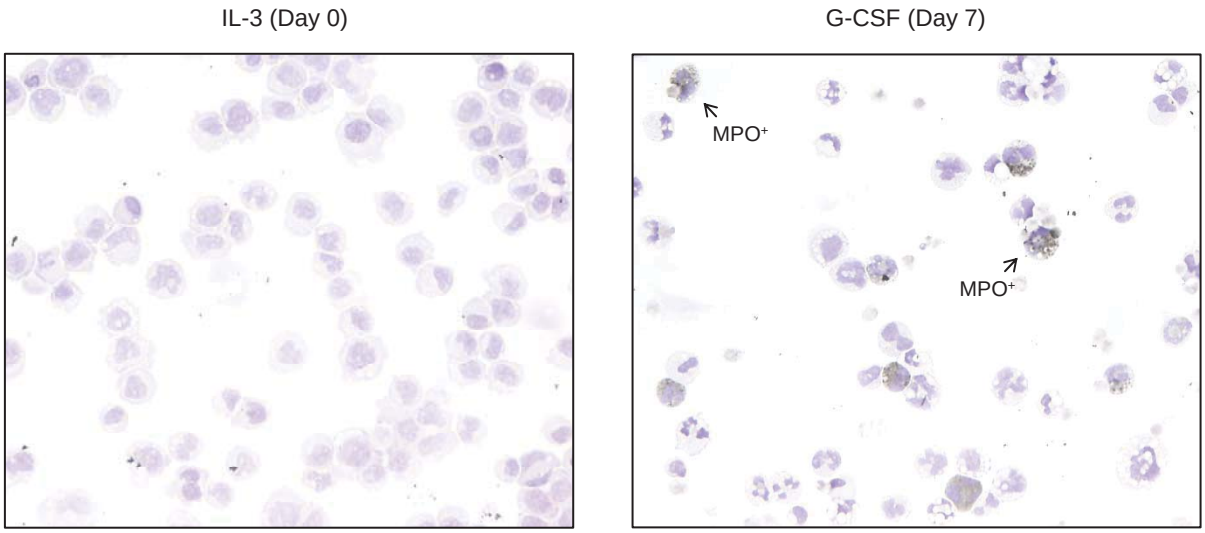

E.

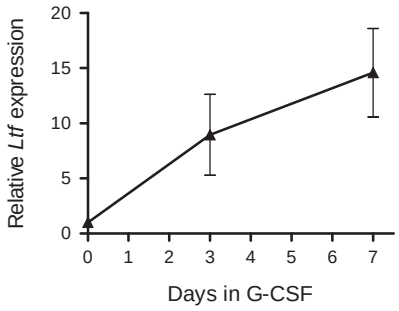

F.

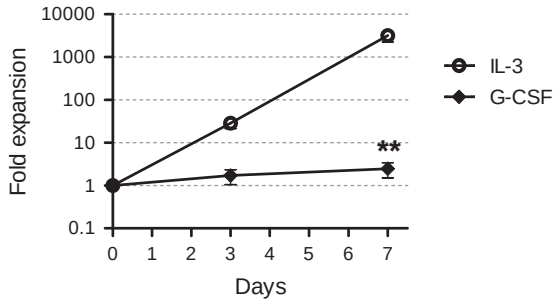

G.

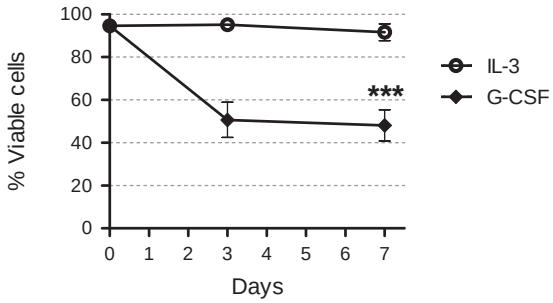

Figure 4.3 (D-F): Granulocyte differentiation of 32D cells in G-CSF. D. Representative photomicrographs showing MPO activity of 32D cells cultured in IL-3 (Day 0) or in G-CSF (Day 7). Original magnification = 200x. MPO activity was detected using the Hanker-Yates method. Examples of cells positive for MPO are indicated (MPO^+) **E.** Q-PCR detection of *Ltf* mRNA expression in 32D cells differentiated over 7 days in G-CSF. Expression was plotted relative to Day 0 (cells in IL-3). n=3. **F.** Expansion of 32D cells in IL-3 or G-CSF relative to Day 0. Live cell numbers were determined at each time-point using Trypan Blue staining and cell counts. n=3, **p<0.01. **G.** Viability of 32D cells in IL-3 or G-CSF. Percentage of live cells were determined at each time-point using Trypan Blue exclusion. n=3, ***p<0.001.

present and displayed characteristics as described in Section 4.2.1.1. More immature band cells were also visible, and could be distinguished from their mature counterparts by their thicker, ringed nuclei.

Marker staining was utilised to confirm induction of granulocyte differentiation on Day 7 (Figure 4.3B). There was a negligible change in expression of the granulocyte-associated marker Gr-1 in response to G-CSF, which is in contrast to previous studies which have reported that Gr-1 expression is strongly up-regulated during granulocyte differentiation of 32D cells (see for example Vradii, et al.[379]). Although 32D cells cultured in IL-3 were already positive for expression of the myeloid marker Mac-1, we observed a peak shift corresponding to increased expression on induction with G-CSF (mean fluorescence intensity of 27.2 and 69.5 in IL-3 and G-CSF respectively). This agrees with previous reports which have demonstrated increased Mac-1 expression on 32D cells when differentiated in G-CSF[379,380]. Antibodies to detect expression of the murine G-CSF receptor (CSF3) were not available, however Q-PCR performed on Day 0 (cells in IL-3) and Days 3 and 7 post-induction (G-CSF) revealed that *Csf3* mRNA expression increased over the course of this assay (Figure 4.3C). Increased expression of Mac-1 (a marker expressed on both granulocytes and macrophages), and of *Csf3*, is consistent with the observed morphological differentiation of 32D cells to granulocytes.

Granulocyte differentiation is also characterised by the expression of specific proteins which localise to different subsets of neutrophilic granules[381]. Myeloperoxidase (MPO) is a marker of primary neutrophilic granules, which is first detectable at the myeloblast or promyelocyte stages of granulocyte differentiation[382]. Using the Hanker-Yates method[328], 32D cells cultured in IL-3 were found to be negative for active MPO enzyme (Figure 4.3D). When cultured in G-

CSF for 7 days a proportion of 32D cells became positive for active MPO enzyme, as detected by the presence of brown/black granules. LTF is a marker of secondary neutrophilic granules, which is first detectable at the myelocyte or metamyelocyte stages of differentiation[382]. Q-PCR performed on Days 0, 3 and 7 post-induction showed that *Ltf* mRNA expression increased as 32D cells were cultured in G-CSF (Figure 4.3E). Collectively, these observations are consistent with 32D cells differentiating along the granulocyte lineage when cultured in G-CSF over 7 days. Differentiation of 32D cells was accompanied by a dramatic reduction in cell expansion compared to cells cultured in IL-3 (Figure 4.3F), and cell viability was reduced from 92% in IL-3 to 48% by Day 7 in G-CSF (Figure 4.3G).

For detection of *Klf5* expression, 32D cells were harvested on Days 1, 2, 3, 5 and 7 following addition of G-CSF, as well as on Day 0. Q-PCR analysis showed that *Klf5* mRNA expression increased during granulocytic differentiation in response to G-CSF, reaching a maximum level at Day 5 and remaining high thereafter (Figure 4.4A). A similar trend was observed for *Cebpe* (Figure 4.4B), however the fold induction of *Cebpe* expression was higher than that of *Klf5* (30-fold induction of *Cebpe* compared with 2-fold induction of *Klf5*). The observed up-regulation of *Cebpe* mRNA during G-CSF-induced differentiation of 32D cells is consistent with previously published reports[383]. *Cebpa* expression peaked early at 24 hours in G-CSF, then decreased to almost basal levels by Day 3 post-induction (Figure 4.4C), which is consistent with data published previously by Scott, et al.[384].

A.

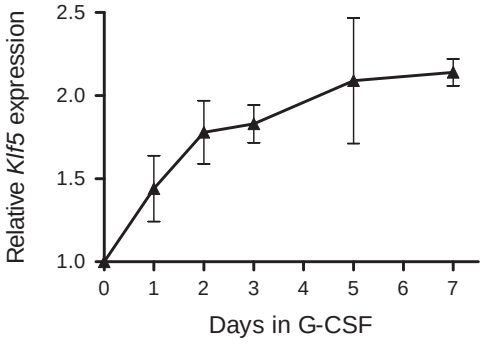

B.

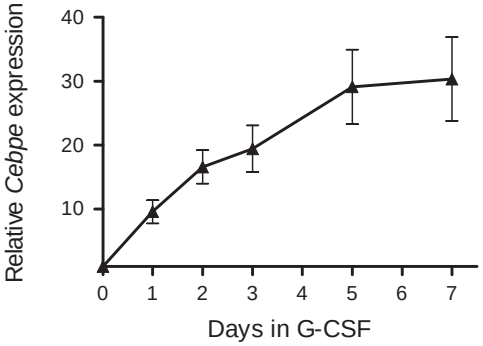

C.

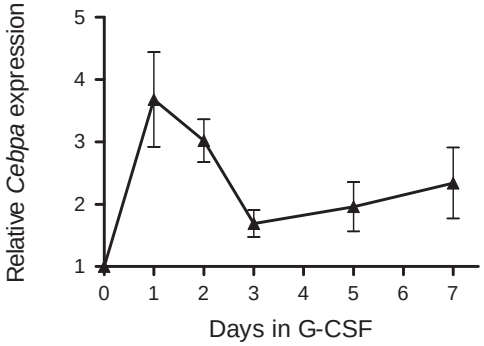

Figure 4.4: Expression of *Klf5* and *Cebp* family members during G-CSF-induced 32D cell differentiation. 32D cells were induced to differentiate over 7 days in G-CSF. Q-PCR was performed to detect: **A.** *Klf5* mRNA expression, **B.** *Cebpe* mRNA expression, and **C.** *Cebpa* mRNA expression. Expression is plotted relative to Day 0 (IL-3). n=4.

4.2.1.3 M-CSF-induced macrophage differentiation of murine bone marrow progenitors

We utilised primary murine bone marrow progenitors to assess *Klf5* mRNA expression during cytokine-induced macrophage differentiation. Bone marrow cells were freshly isolated from C57BL/6 mice treated with 5-fluorouracil to enrich for haemopoietic progenitors[385], then differentiated for 7 Days in M-CSF (100 ng/ml). Morphologically, cells treated with M-CSF differentiated almost exclusively to mature macrophages by Day 7 in culture (Figure 4.5A). Analysis of cell surface marker expression correlated with the observed morphological appearance of differentiated macrophages, with the majority of cells positive for the macrophage marker c-Fms (66%) on Day 7 in M-CSF, and relatively few cells positive for expression of the granulocyte-associated marker Gr-1 (12.3%) (Figure 4.5B). RNA was isolated from cells prior to addition of M-CSF (Day 0), and on Days 3 and 7 following addition of M-CSF. Q-PCR analysis showed a dramatic drop in *Klf5* expression, with undetectable levels remaining by Day 7 when cells had completely matured (Figure 4.5C). To confirm that *Klf5* expression did not increase at an earlier time-point in this system, Q-PCR was also performed on cells at Days 0, 1, 2 and 3 in M-CSF. This revealed an immediate decrease in *Klf5* expression by Day 1, and levels remained low thereafter (Figure 4.5D).

4.2.1.4 mRNA expression of *KLF* family members in primary haemopoietic cell populations

We utilised published microarray data to further analyse expression of *KLF5* and other *KLF* family members in haemopoietic lineages from primary murine and human tissues. Chambers, et al. performed extensive microarray analyses to identify unique genetic

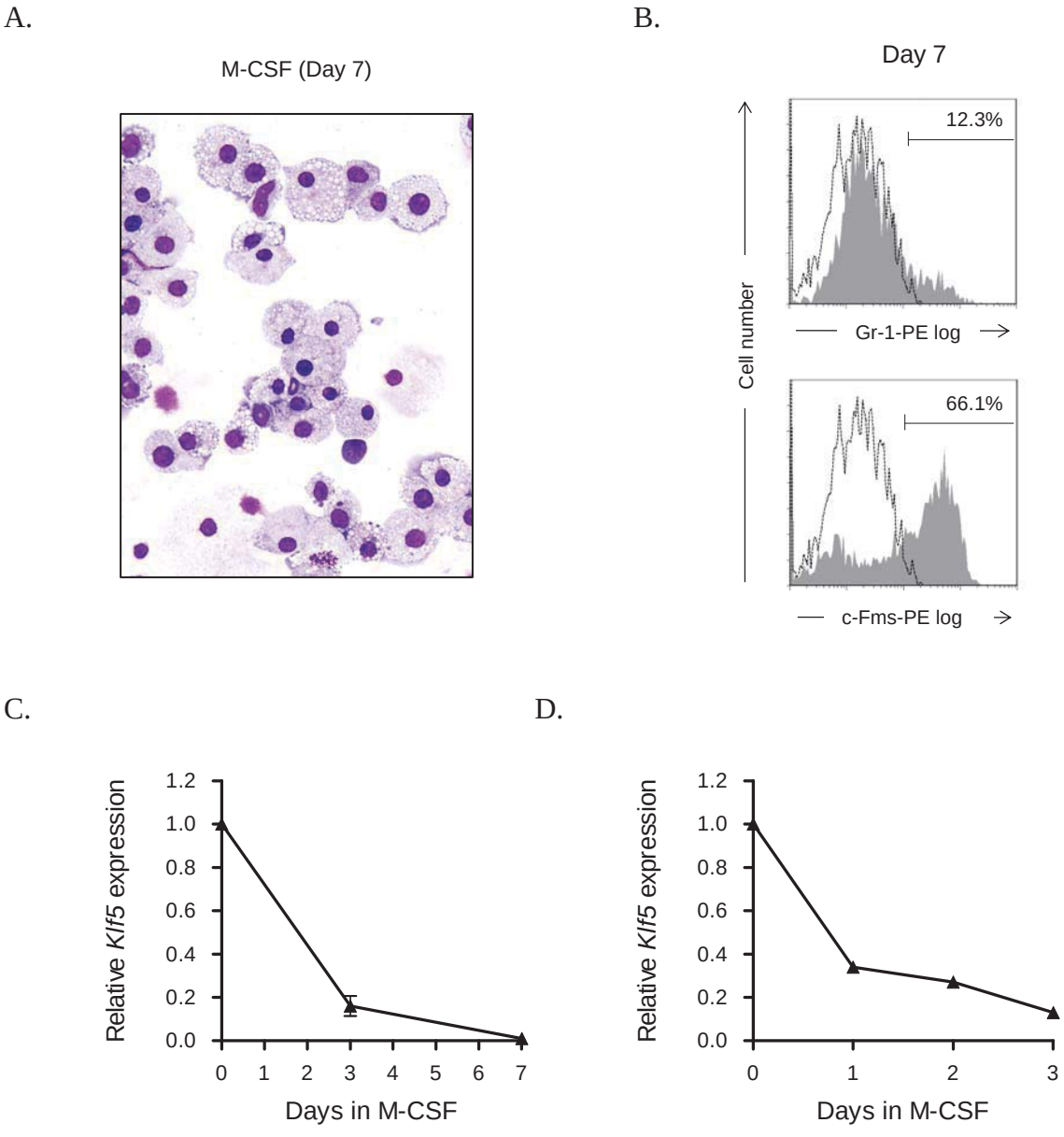

Figure 4.5: Macrophage differentiation of primary mouse bone marrow progenitors in M-CSF. A. Representative photomicrograph showing Wright-Giemsa stained cytospin preparation of mouse bone marrow progenitor cells differentiated for 7 days in M-CSF. Original magnification = 200x. **B.** Flow cytometric detection of Gr-1 and c-Fms expression on bone marrow cells in M-CSF (Day 7). Representative results from a typical experiment are shown. Empty peak = isotype control, grey peak = cell surface marker expression. **C-D.** Q-PCR was performed to detect mRNA expression levels of *Klf5* during M-CSF induced differentiation of mouse bone marrow progenitors. Expression is plotted relative to Day 0 (bone marrow harvest). Q-PCR was initially performed on Days 3 and 7 (part 'C', n=2) then performed at earlier time-points which included Days 1, 2 and 3 (part 'D', n=1).

fingerprints for mouse haemopoietic stem cells and their various myeloid and lymphoid progeny[386]. Bone marrow and peripheral blood cells were isolated from C57BL/6 mice and lineage-restricted populations obtained using a combination of surface expression markers. Purified cell populations were analysed for global gene expression differences using Affymetrix microarray chips. We extracted raw data from supplementary information provided for 15 *Klf* family members and plotted expression in monocytic, granulocytic, erythroid, and various lymphoid subpopulations relative to haemopoietic stem cells. This data is presented as a heat map in Figure 4.6A. Unsupervised hierarchical cluster analysis was performed to generate evolutionary gene trees using MultiExperiment Viewer v4.5.1.

We were also able to obtain expression data for myeloid and erythroid lineages derived from human $CD34^+$ haemopoietic progenitors. In a study by Tonks, et al., human $CD34^+$ cells from cord blood samples were cultured in IL-3, SCF and G/GM-CSF for 6 days then sorted to obtain various lineages using a combination of surface expression markers[387]. Purified cell populations were analysed for global gene expression differences using Affymetrix microarray chips. We extracted raw data for 14 *KLF* family members from supplementary information and plotted expression in monocytic, granulocytic and erythroid lineages relative to control $CD34^+$ progenitors. Data is presented as a heat map in Figure 4.6B. Unsupervised hierarchical cluster analysis was performed to generate evolutionary gene trees as described above.

The results of this expression profiling analysis were consistent with the reported expression profiles and functions of selected *KLF* family members. For example, *KLF1* (or *Erythroid Krüppel-Like Factor*) was strongly up-regulated in erythroid populations in both mouse and human data sets, consistent with studies demonstrating a role for this gene in development of

A.

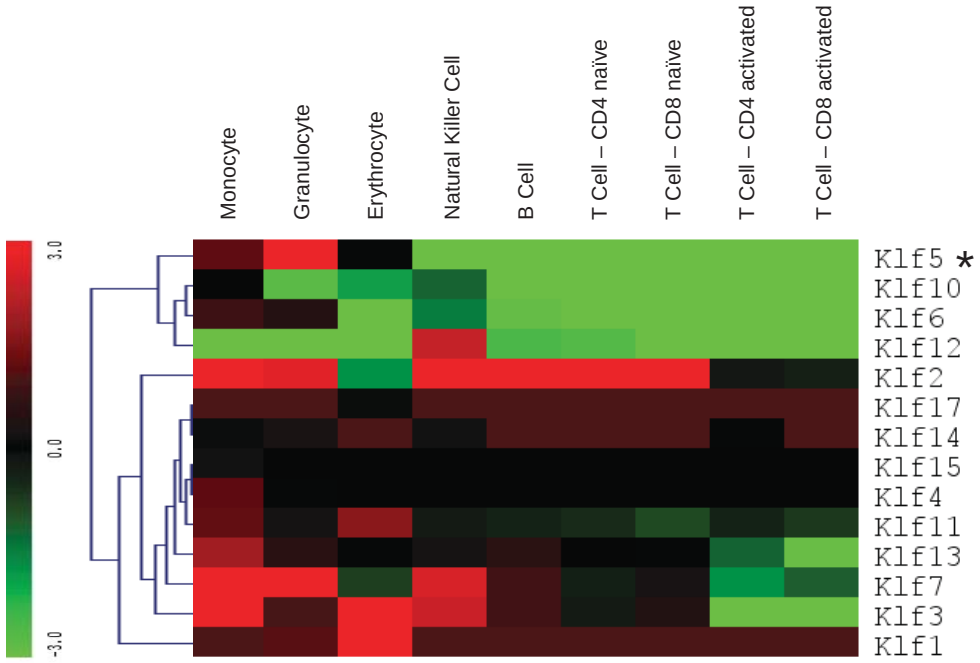

B.

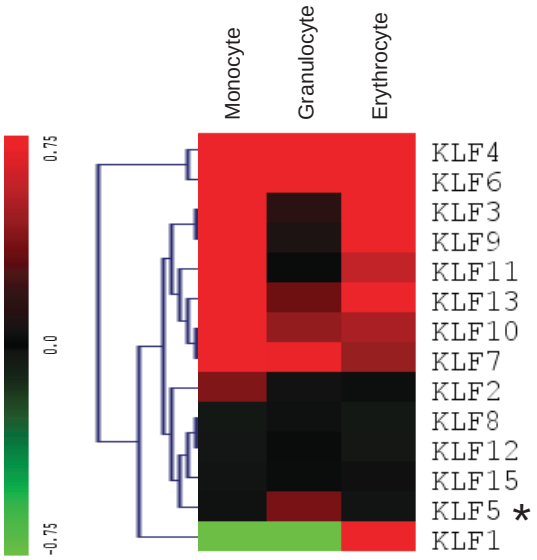

Figure 4.6: Expression of *KLF* family members in myeloid lineages (primary cells). Heat maps showing expression of *KLF5* (starred) and other family members in mouse and human haemopoietic lineages. Data was extracted from the microarray studies described below by C. Kok. Unsupervised heirarchical cluster analysis was performed to generate the evolutionary gene trees shown above (Euclidean distance metric selection and average linkage clustering). **A.** Expression of *Klf* family members in primary mouse haemopoietic lineages. Data was extracted from a study by Chambers, et al. in which mature haemopoietic cell populations and haemopoietic stem cells were freshly harvested from bone marrow or peripheral blood[386]. Gene expression for each population was analysed by microarray. Heat map colours represent fold change relative to haemopoietic stem cells as indicated by the colour scale ($\log_2$). **B.** Expression of *KLF* members in primary human haemopoietic lineages. Data was extracted from a study performed by Tonks, et al. where human $CD34^+$ cells were cultured in IL-3, SCF and G/GM-CSF for 6 days prior to isolation of mature cell populations[387]. Microarray analysis was performed to analyse gene expression levels in each mature population and in $CD34^+$ progenitor cells. Heat map colours represent fold change relative to $CD34^+$ haemopoietic progenitor cells as indicated by the colour scale ($\log_2$).

the erythroid lineage[138,139]. *Klf2* was shown to be expressed in naïve murine T-cell populations, where studies have shown that it functions in the maintenance of progenitor T-cell populations[142]. *KLF4* expression was found to be up-regulated in the monocyte lineage in both human and mouse data-sets, which is consistent with studies demonstrating that *KLF4* is an essential regulator of monocyte formation and activation[388,389].

In both the human and mouse data-sets, *KLF5* was found to be up-regulated in the granulocyte population. Interestingly, *Klf5* expression was also increased in the murine monocyte lineage, although this change was markedly less than that seen in the granulocyte compartment. There was no change in *KLF5* expression in the human monocyte lineage when compared to $CD34^+$ progenitors.

Cluster analysis of *Klf* family members in mouse haemopoietic lineages demonstrated that expression of *Klf5* most closely correlated with that of *Klf6*, *Klf10* and *Klf12*. These genes all showed decreased expression in B-cell and T-cell populations compared to haemopoietic stem cells, suggesting that down-regulation of these factors is required in development of lymphoid lineages. However, of these 4 genes, only *Klf5* was up-regulated in the granulocyte lineage. In the human data-set, *KLF5* expression clustered with *KLF8*, *KLF12* and *KLF15*. These four genes were not regulated in the monocyte or erythroid lineages, and of the four genes only *KLF5* was up-regulated in the granulocyte lineage. Of all the *KLF* family members presented in these analyses, *KLF5* was the only gene which displayed maximum up-regulation of expression in the granulocyte lineage compared to primitive populations, supporting a specific role for this *KLF* member in granulocyte development.

4.2.2 Retroviral expression of KLF5 induces macrophage differentiation, cell cycle arrest and cell death

4.2.2.1 Enforced expression in the FDB1 cell line model

To examine the effect of enforced expression of KLF5 on myeloid cell growth and differentiation, murine *Klf5* was constitutively expressed from the MIG retroviral vector[320] in FDB1 cells. FDB1 cells were transduced with the murine MIG-*Klf5* construct or the empty MIG vector as a control. Twenty-four hours after infection, GFP^+ cells were isolated using FACS and recovered overnight in growth medium containing IL-3 (500 BMU/ml). Sorted populations were seeded at $1x10^5$ cells/ml on Day 2 post-transduction in medium containing IL-3 (sorted populations were >90% positive for expression of GFP). Assays for effects on cell viability, expansion, growth arrest and differentiation were performed on Days 2 and 4 post-transduction.

FDB1 cells transduced with *Klf5* displayed significantly reduced GFP^+ cell expansion, as shown in Figure 4.7A. Analysis of total cell viability showed that this may be partly due to induction of cell death, as *Klf5*-transduced cells exhibited a 40% average reduction in viable cell number on Day 4 compared to control cells (Figure 4.7B). This result did not reach significance, however, as the effect on cell death was variable between independent assays (n=3, p=0.080). Propidium iodide staining on Day 2 post-transduction revealed a significant accumulation of cells in G0/G1 phase (82% of cells transduced with *Klf5* compared to 68% of control cells), with half as many *Klf5*-transduced cells entering the S and G2/M phases compared to control cells (Figure 4.7C). By Day 4 post-transduction, cells transduced with *Klf5* had the appearance of mature macrophages (Figure 4.7D). These were larger than control

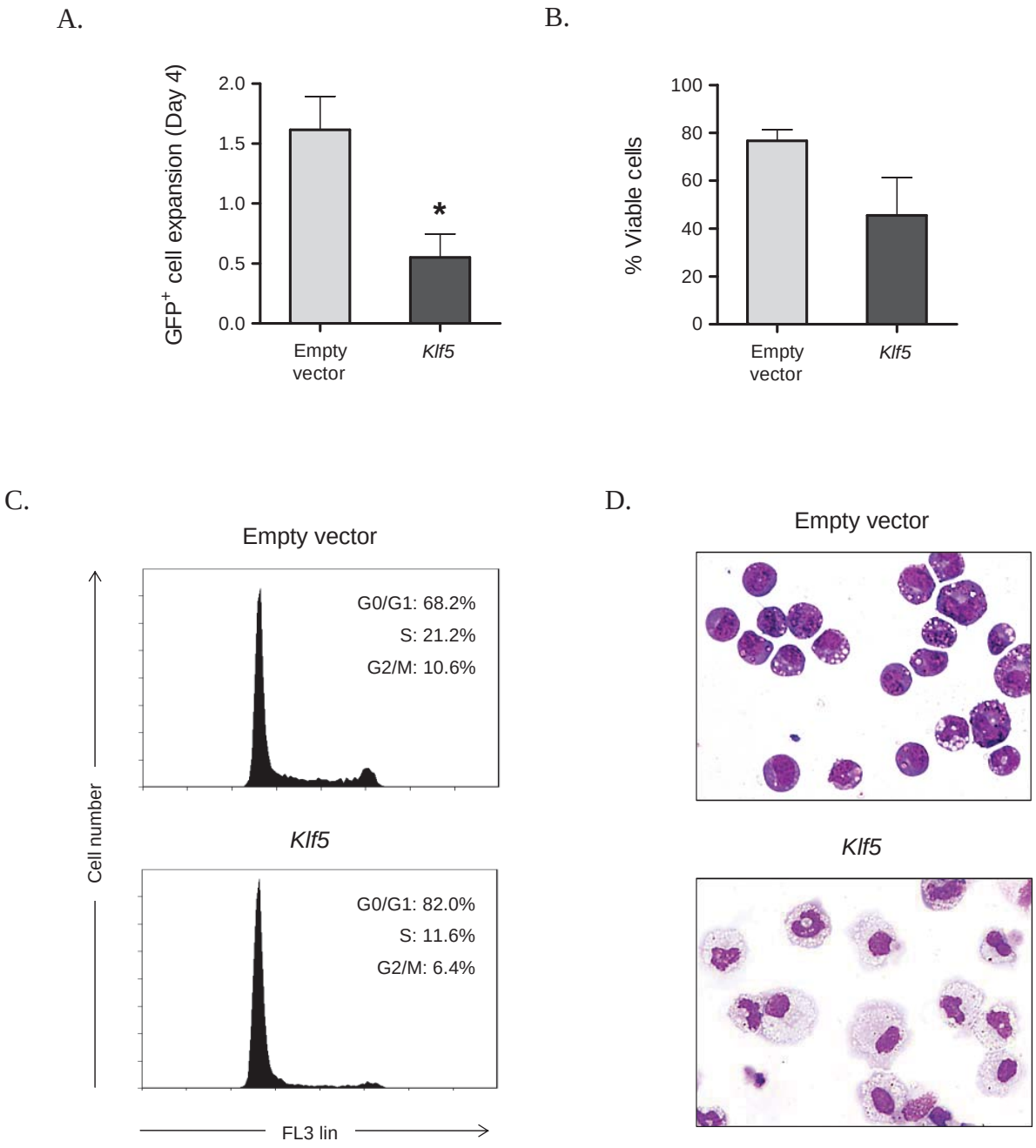

Figure 4.7 (A-D): Enforced expression of murine KLF5 in the FDB1 cell line model. A. GFP$^+$ cell expansion. The total number of live cells was determined at Day 4 by Trypan Blue staining and cell counts, and the percentage of GFP$^+$ cells determined by flow cytometry. The number of GFP$^+$ cells was hence determined and expansion calculated relative to seeding on Day 2. n=3, *p<0.05. **B.** Total cell viability was assessed by Trypan Blue staining and cell counts on Day 4 post-transduction. n=3, p=0.080. **C.** Day 2 flow cytometric assessment of cell cycle by propidium iodide staining. Representative results from a typical experiment are shown. n=3, p=0.002, 0.010 and 0.022 for G0/G1, S and G2/M phases respectively. **D.** Representative photomicrographs showing Wright-Giemsa stained cytospin preparations of FDB1 cells transduced with *Klf5* or the empty vector control in IL-3 (Day 4). Original magnification = 200x. Note that cells were >90% positive for GFP at all time-points of these assays (parts A-D).

E.

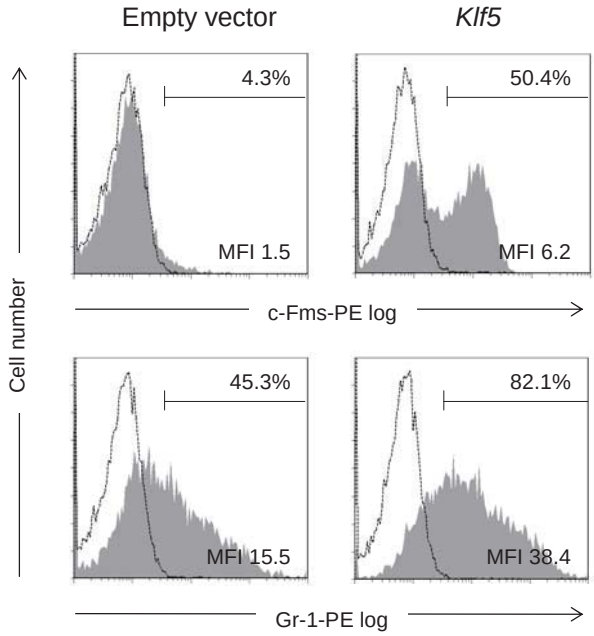

F.

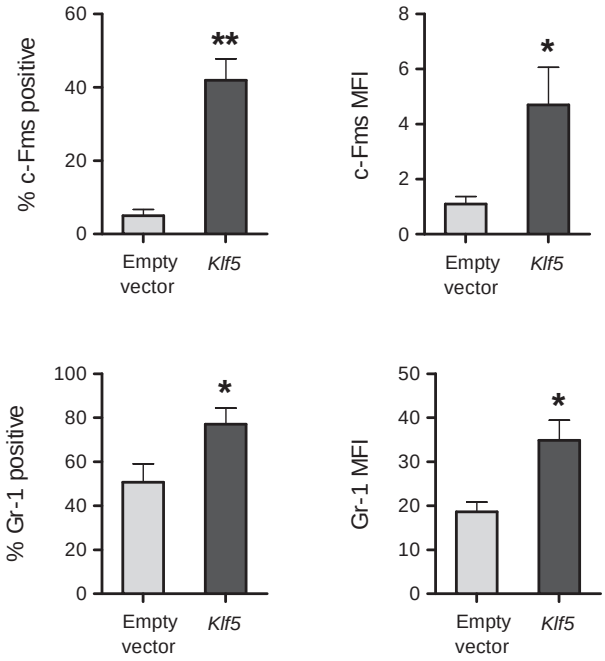

Figure 4.7 (E-F): Enforced expression of murine KLF5 in the FDB1 cell line model. E. Two-colour flow cytometric detection of c-Fms and Gr-1 expression on FDB1 cells transduced with *Klf5* or the empty vector control. Expression was detected using PE-conjugated antibodies on GFP^+ cells. Profiles show representative results from a typical experiment on Day 2 post-transduction (empty peak = isotype control, grey peak = cell surface marker expression). **F.** Average percentage expression and mean fluorescence intensity (MFI) of c-Fms and Gr-1 on FDB1 cells transduced with *Klf5* or the empty vector on Day 2 post-transduction (n=3). *p<0.05, **p<0.01

cells, and were characterised by light-staining, granular cytoplasms, small rounded nuclei, and ruffled cellular edges. Analysis of cell surface marker expression on GFP^+ cells also confirmed differentiation of *Klf5*-transduced FDB1 cells (Figure 4.7E). We observed a significant increase in the proportion of cells positive for the monocyte-specific marker c-Fms in *Klf5*-transduced populations on Day 2 post-transduction (Figure 4.7F), which is consistent with the macrophage morphology of these cells. There was also a significant increase in the level of Gr-1 expression on Day 2 post-transduction (see Figure 4.7F). Gr-1 is primarily expressed on mature granulocytes, but is also expressed transiently on a subset of monocytes during differentiation along the monocyte-macrophage lineage[390]. We have previously observed that Gr-1 is highly expressed on mature macrophages in the FDB1 cell line model (A. Brown, unpublished data), which is consistent with the macrophage morphology observed on transduction with *Klf5* (see Figure 4.7D). Collectively, these results show that KLF5 is capable of inducing macrophage differentiation and growth arrest of FDB1 cells in the presence of IL-3.

4.2.2.2 Enforced expression in primary murine bone marrow progenitors

We next wished to study the effect of enforced KLF5 expression in a primary biological system, and thus used retroviral transduction to infect murine bone marrow progenitor cells for analysis. Bone marrow cells were freshly isolated from C57BL/6 mice treated with 5-fluorouracil to enrich for haemopoietic progenitors[385]. These were cultured for 3 days in growth medium containing IL-3 (500 BMU/ml), IL-6 (10 ng/ml) and SCF (50 ng/ml), then transduced with either the murine MIG-*Klf5* construct or empty MIG vector. Forty-eight hours post-transduction cells were sorted for GFP expression, then recovered overnight. Functional assays were established from Day 3 post-transduction, with populations that contained >90% GFP^+ cells. For liquid culture experiments, all cells were seeded in a

cytokine cocktail of IL-3 (500 BMU/ml), IL-6 (10 ng/ml) and SCF (50 ng/ml). c-Kit expression and cell cycle status were assessed on Day 3, and cell expansion, viability and morphology were assessed on Days 3, 5 and 7. For colony assays, cells were seeded on Day 3 post-transduction in methylcellulose medium containing either the IL-3/IL-6/SCF cytokine cocktail (as above), or G-CSF (100 ng/ml) or M-CSF (100 ng/ml) as the sole cytokine. Colonies of ≥40 cells were scored after 7 days in culture, and individual colonies cultured in G-CSF or M-CSF were picked for morphological analysis.

As with FDB1 cells, transduction of murine haemopoietic progenitors with *Klf5* dramatically inhibited cell expansion in liquid culture (Figure 4.8A). This was again accompanied by reduced cell viability (Figure 4.8B), and an accumulation of cells in G0/G1 phase (Figure 4.8C). On Day 3 post-transduction, cells transduced with *Klf5* displayed decreased expression of c-Kit (Figure 4.8D), a marker which is highly expressed on haemopoietic stem cells and myeloid progenitors but decreases during differentiation[391]. Morphologically, the appearance of mature macrophages was detected much sooner than in cells carrying the empty vector (Figure 4.8E). Differential cell counts revealed that transduction with *Klf5* significantly increased the proportion of macrophages when compared to control cells on Days 3 and 5 post-transduction (Figure 4.8F). This was accompanied by a comparable decrease in the proportion of immature cells on these days, which is consistent with the observed reduction in c-Kit expression on Day 3 (see Figure 4.8D). We did not detect substantial differences in the proportion of granulocytes, although a small decrease (approximately 5%) was observed in cells transduced with *Klf5* on Day 5 of the assay.

Bone marrow progenitors transduced with *Klf5* or the empty vector were seeded in methylcellulose supplemented with the IL-3/IL-6/SCF cytokine cocktail, allowing formation

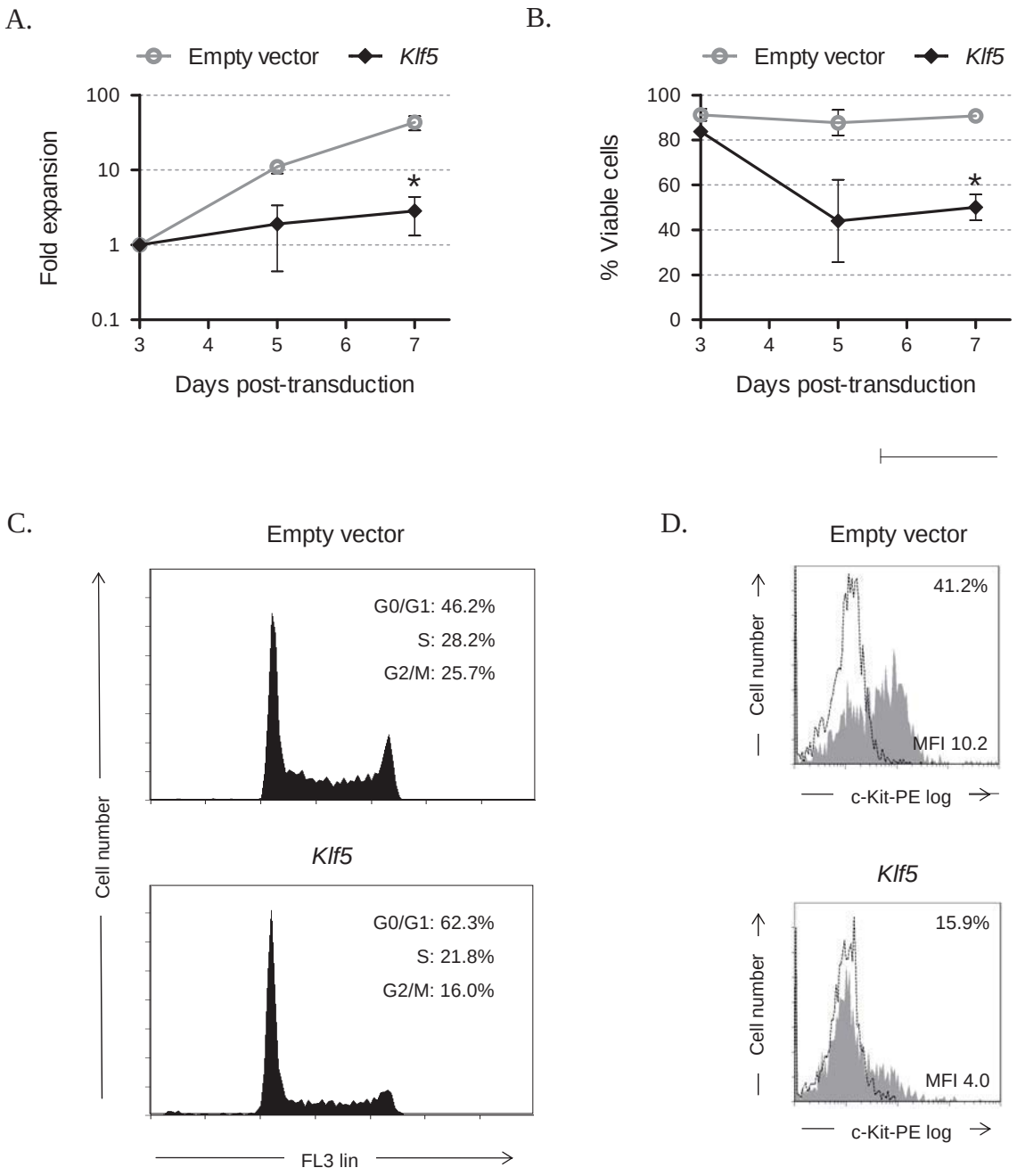

Figure 4.8 (A-D): Enforced expression of murine KLF5 in primary mouse bone marrow progenitors. Bone marrow cells transduced with *Klf5* or empty vector control were seeded in liquid culture medium containing IL-3, IL-6 and SCF (populations were >90% GFP^+ on day of seeding). **A.** The total number of live cells was determined at each time-point by Trypan Blue staining and cell counts, and cell expansion determined relative to Day 3. n=2, *$p<0.05$. **B.** Total cell viability was assessed by Trypan Blue staining and cell counts. n=2, *$p<0.05$. **C.** Day 3 flow cytometric assessment of cell cycle by propidium iodide staining. Representative results from a typical experiment are shown. n=2, p=0.045, 0.019 and 0.071 for G0/G1, S and G2/M phases respectively. **D.** Flow cytometric detection of c-Kit on GFP^+ bone marrow cells transduced with *Klf5* or the empty vector control. Expression was detected on Day 3 post-transduction using cells grown in liquid culture medium supplemented with IL-3, IL-6 and SCF. Profiles show representative results from a typical experiment (empty peak = isotype control, grey peak = cell surface marker expression).

E.

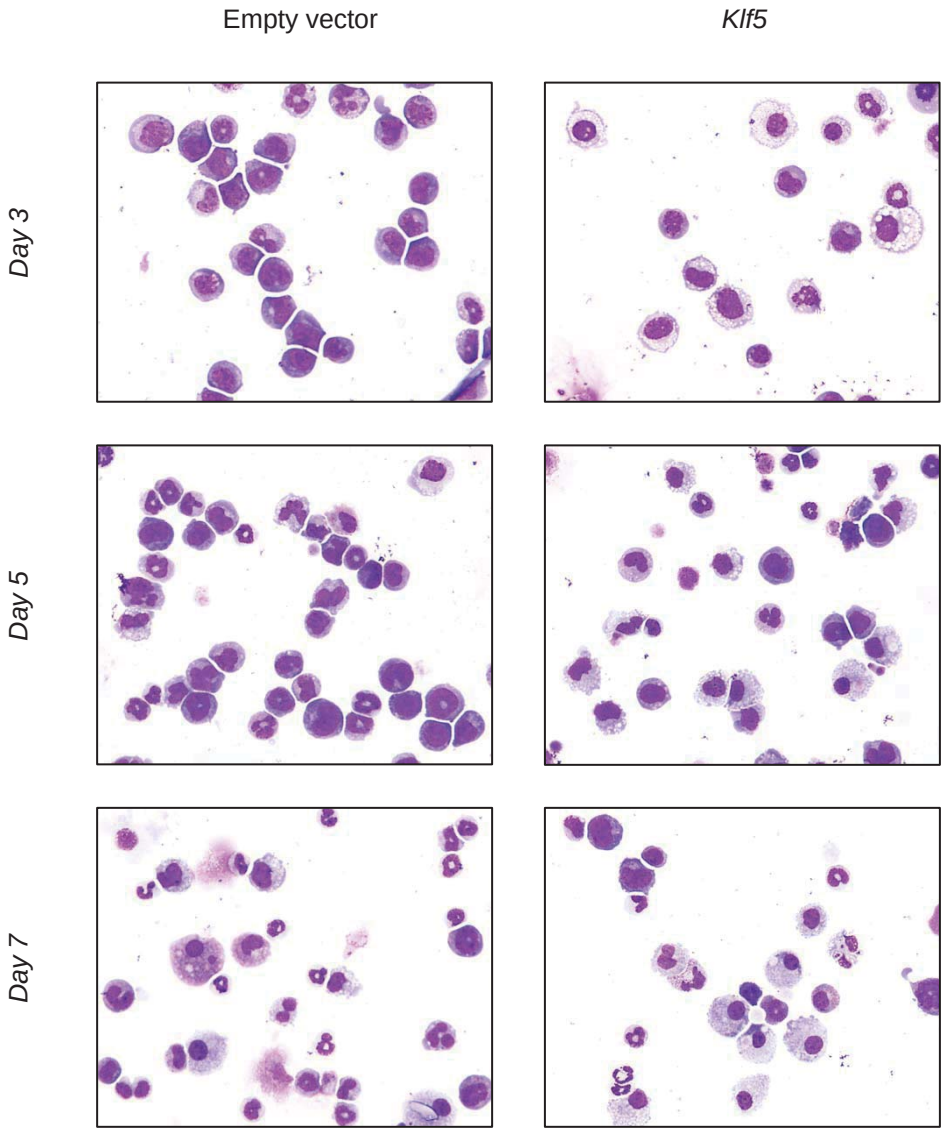

Figure 4.8 (E): Enforced expression of murine KLF5 in primary mouse bone marrow progenitors. E. Representative photomicrographs showing Wright-Giemsa stained cytospin preparations of bone marrow cells transduced with *Klf5* or the empty vector control. Cells were seeded in liquid culture medium supplemented with IL-3, IL-6 and SCF and samples taken for analysis at Days 3, 5 and 7 as indicated (populations were >90% GFP^+ on day of seeding). Original magnification = 200x.

F.

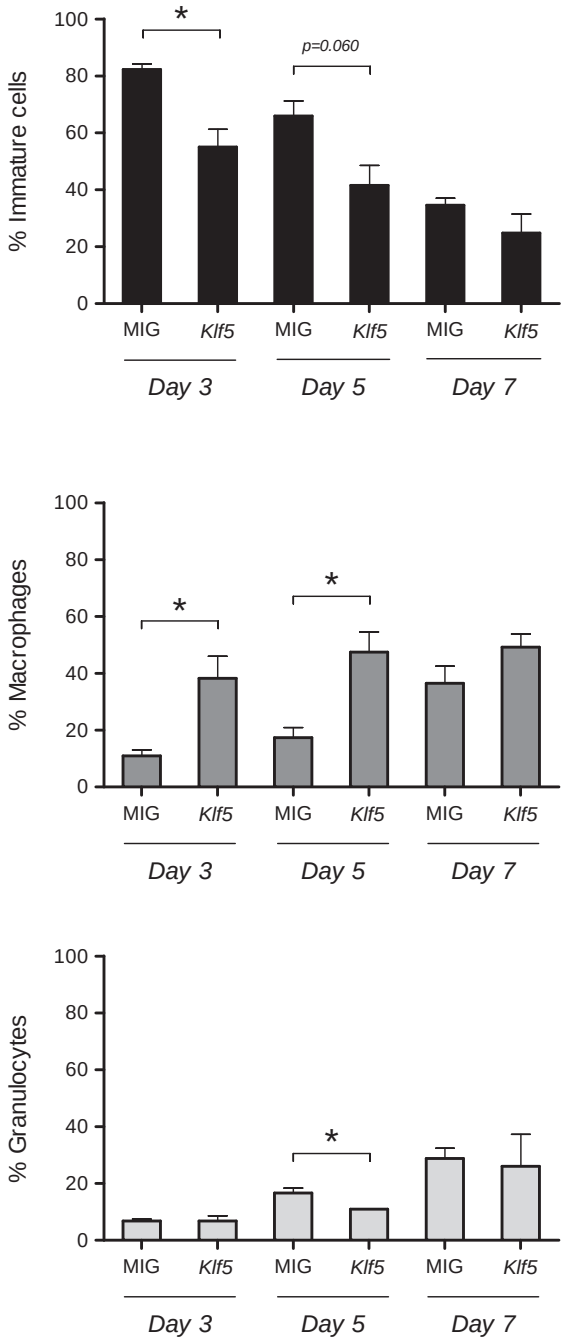

Figure 4.8 (F): Enforced expression of murine KLF5 in primary mouse bone marrow progenitors. F. Proportion of immature cells, macrophages and granulocytes in bone marrow populations transduced with *Klf5* or the empty vector control. Cells were seeded in liquid culture medium supplemented with IL-3, IL-6 and SCF, and cell counts performed using cytospin preparations taken at Days 3, 5 and 7 post-transduction (populations were >90% GFP^+ on day of seeding). * $p<0.05$, n=2.

G.

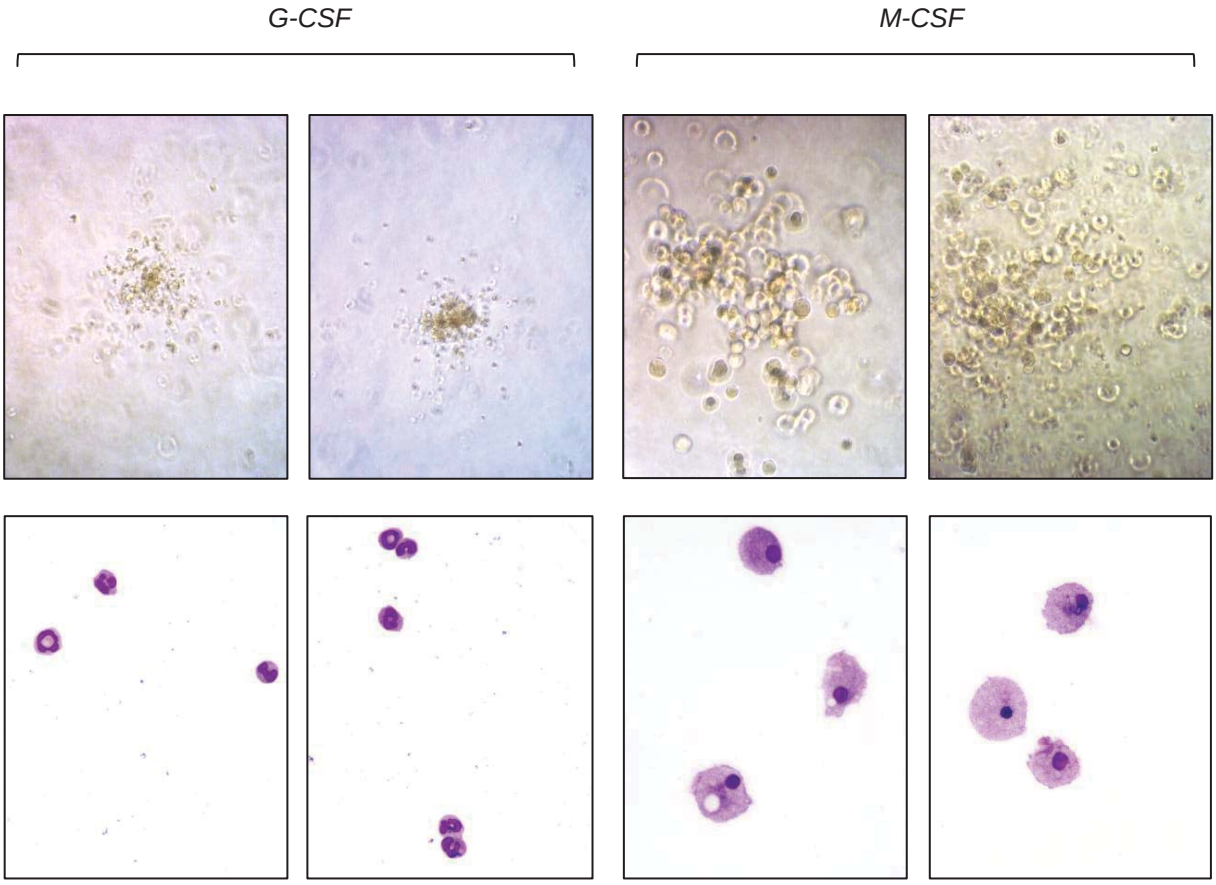

H.

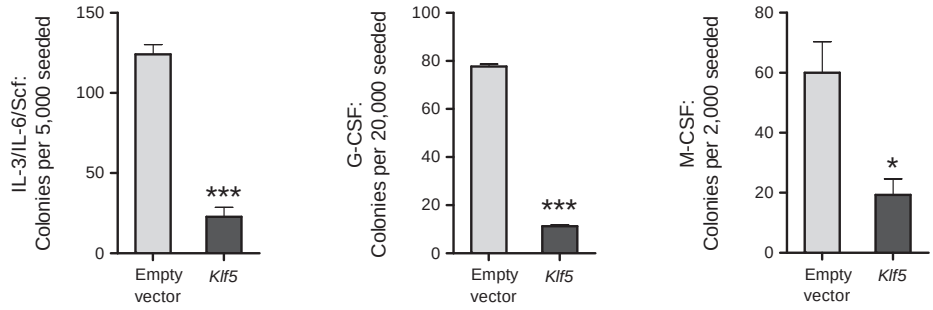

Figure 4.8 (G-H): Enforced expression of murine KLF5 in primary mouse bone marrow progenitors. G. Bone marrow cells expressing the empty vector control were seeded on Day 3 post-transduction in methylcellulose medium containing G-CSF or M-CSF alone for formation of granulocytic and monocytic colonies respectively. Two examples colonies are shown from each condition. The top panel shows colony morphology in agar (original magnification = 100x), and the bottom panel shows the morphology of cells in the colonies pictured above (original magnification = 400x). Individual colonies were harvested then centrifuged onto slides prior to Wright-Giemsa staining. **H.** Bone marrow cells transduced with *Klf5* or the empty vector control were seeded on Day 3 post-transduction in methylcellulose medium containing IL-3, IL-6 and SCF (CFU-G, CFU-M and CFU-GM), G-CSF alone (CFU-G) or M-CSF alone (CFU-M). Populations were >90% GFP^+ on day of seeding. Colonies of greater than 40 cells were counted after 7 days. n=2, *p<0.05, ***p<0.001.

of CFU-G, CFU-M and CFU-GM; or with G-CSF or M-CSF alone, which supported the exclusive formation of granulocyte or macrophage colonies respectively as shown in Figure 4.8G. *Klf5* transduction had a significant effect on the colony forming potential of murine bone marrow progenitors in all three conditions (Figure 4.8H). A 5.4-fold reduction in colony number was detected due to transduction with *Klf5* when cells were seeded in methylcellulose supplemented with the IL-3/IL-6/SCF cytokine cocktail, which is consistent with results from liquid culture experiments where transduction with *Klf5* inhibited cell expansion. As *Klf5* transduction severely reduced colony formation in this condition, we were unable to determine if there was a significant effect on lineage specification through colony typing. Interestingly, transduction with *Klf5* also decreased colony formation in both G-CSF and M-CSF (see Figure 4.8H). Collectively these results suggest that enforced expression of KLF5 acts on early myeloid progenitors to inhibit growth and survival, and promote differentiation.

4.2.3 RNAi-mediated knock-down of Klf5 induces effects consistent with reduced granulocyte differentiation

4.2.3.1 Knock-down in the 32D cell line model of G-CSF-induced granulocyte differentiation

As *Klf5* mRNA levels were found to increase during 32D cell differentiation in response to G-CSF (Section 4.2.1.2), we were interested to see if knock-down of *Klf5* in this system would suppress granulocyte differentiation. We utilised 9 independent shRNA sequences predicted to target *Klf5* in an attempt to knock-down *Klf5* expression in 32D cells by RNAi. Three *Klf5* shRNA constructs were purchased from the Open Biosystems shRNAmir library collection in the p-SHAG MAGIC 2 vector (pSM2c)[323]. shRNAmirs are designed to mimic natural

microRNA primary transcripts, enabling specific processing by endogenous RNAi pathways to produce more effective knock-down[392]. Two control shRNAs were also assessed in this vector system (one non-targeting shRNA (pSM2c-NT) and one targeting eGFP (pSM2c-GFP)). The remaining 6 shRNA constructs had been previously designed and cloned into the retroviral pMSCV-ΔLTR-H1 vector (pMΔH), which is based on the pRETRO-SUPER siRNA vector[322]. In this construct, transcription is under the control of a constitutive Histone H1 RNA polymerase III promoter which is coupled to precise termination of transcription at a run of four or more 'T' nucleotides at the end of the siRNA sequence[393]. Two control shRNAs were also assessed in this vector system (one non-targeting shRNA (pMΔH-NT), and one targeting eGFP (pMΔH-GFP)). For details of all shRNA constructs, see Chapter 2, Section 2.2.4.

32D cells were transduced with each of the shRNA constructs then cultured in medium containing puromycin for 7 days to develop stable populations. Transduction and selection of cells was undertaken in medium supplemented with IL-3. Stable populations cultured in IL-3 (500 BMU/ml) were assessed for *Klf5* mRNA expression using Q-PCR. From the 9 shRNA constructs predicted to target *Klf5*, one shRNA in the pMΔH vector (pMΔH-K1) substantially reduced *Klf5* expression compared to the relevant non-targeting control (61% knock-down, Figure 4.9A). This pMΔH-K1 population was further characterised to determine the functional effects of reduced *Klf5* expression in the 32D model of granulocyte differentiation. Expression of the remaining shRNA constructs did not substantially reduce the level of *Klf5* mRNA and were hence not characterised further.

Stable 32D cell populations transduced with pMΔH-K1 or the pMΔH-NT control construct were assayed in G-CSF (50 ng/ml) to test for cell expansion, viability and differentiation over

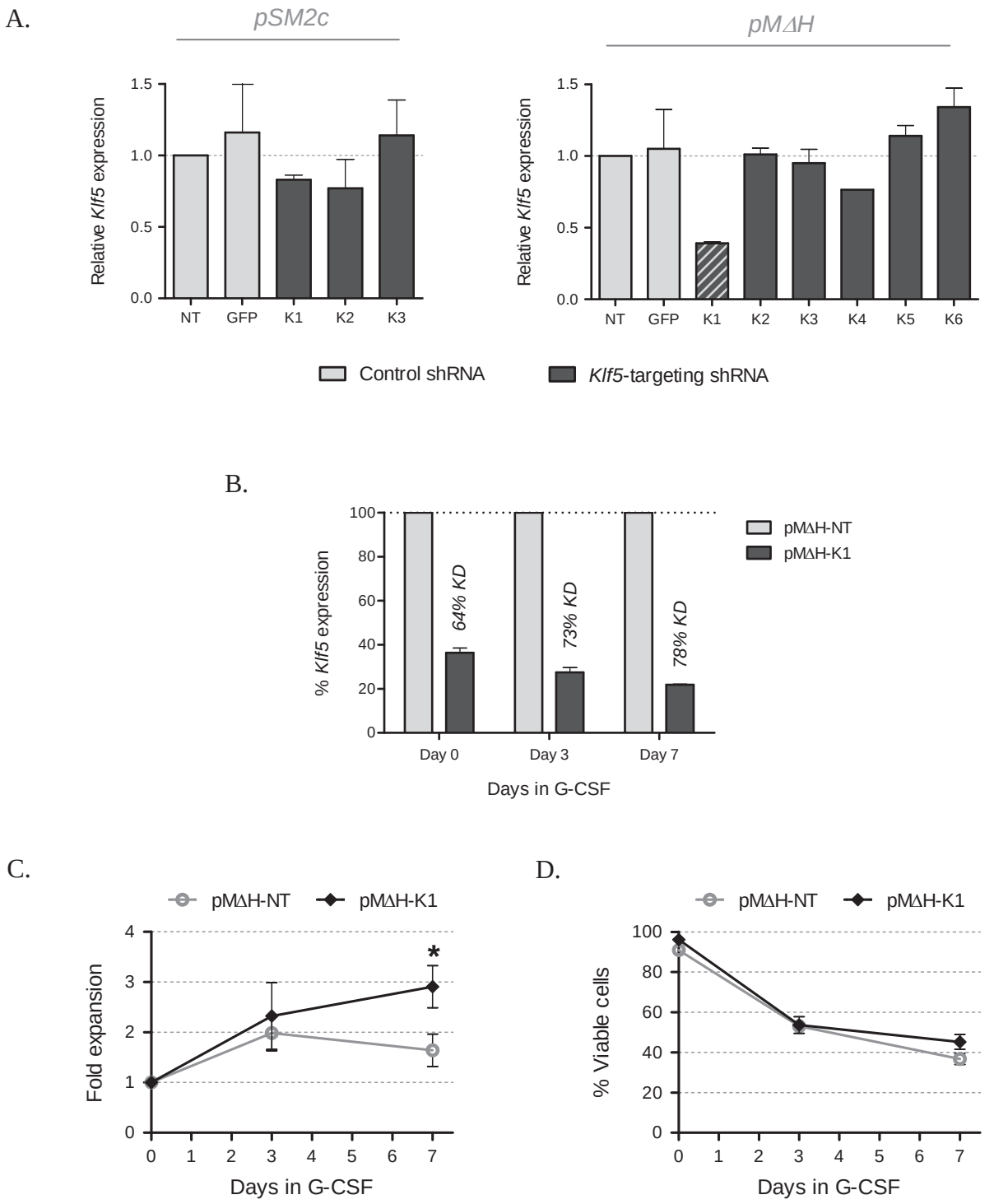

Figure 4.9 (A-D): shRNA knock-down of *Klf5* in the 32D cell line model. A. Q-PCR detection of *Klf5* mRNA levels in 32D cells expressing shRNA sequences in the pSM2c or pMΔH vector. Light grey bars indicate control shRNAs (non-targeting = NT, targeting GFP = GFP). Dark grey bars indicate shRNAs predicted to target *Klf5*. *Klf5* expression was detected in cells cultured in IL-3 and expression was plotted relative to the NT control in each case. Striped bars indicate pMΔH-K1 which showed >60% knock-down compared to the pMΔH-NT control. n=2. **B.** Q-PCR detection of *Klf5* mRNA levels in 32D cells transduced with pMΔH-K1 as a percentage of expression detected in the pMΔH-NT control. Expression was detected at Day 0 (cells in IL-3) and at Days 3 and 7 in G-CSF. The percentage knock-down at each time-point is indicated (KD). n=3. **C-D.** Cell expansion and viability of 32D cells transduced with pMΔH-K1 or the pMΔH-NT control shRNA. Cells were differentiated in G-CSF over 7 days. Viable cell counts were determined using Trypan Blue exclusion, and fold expansion determined relative to Day 0. n=3, *p<0.05.

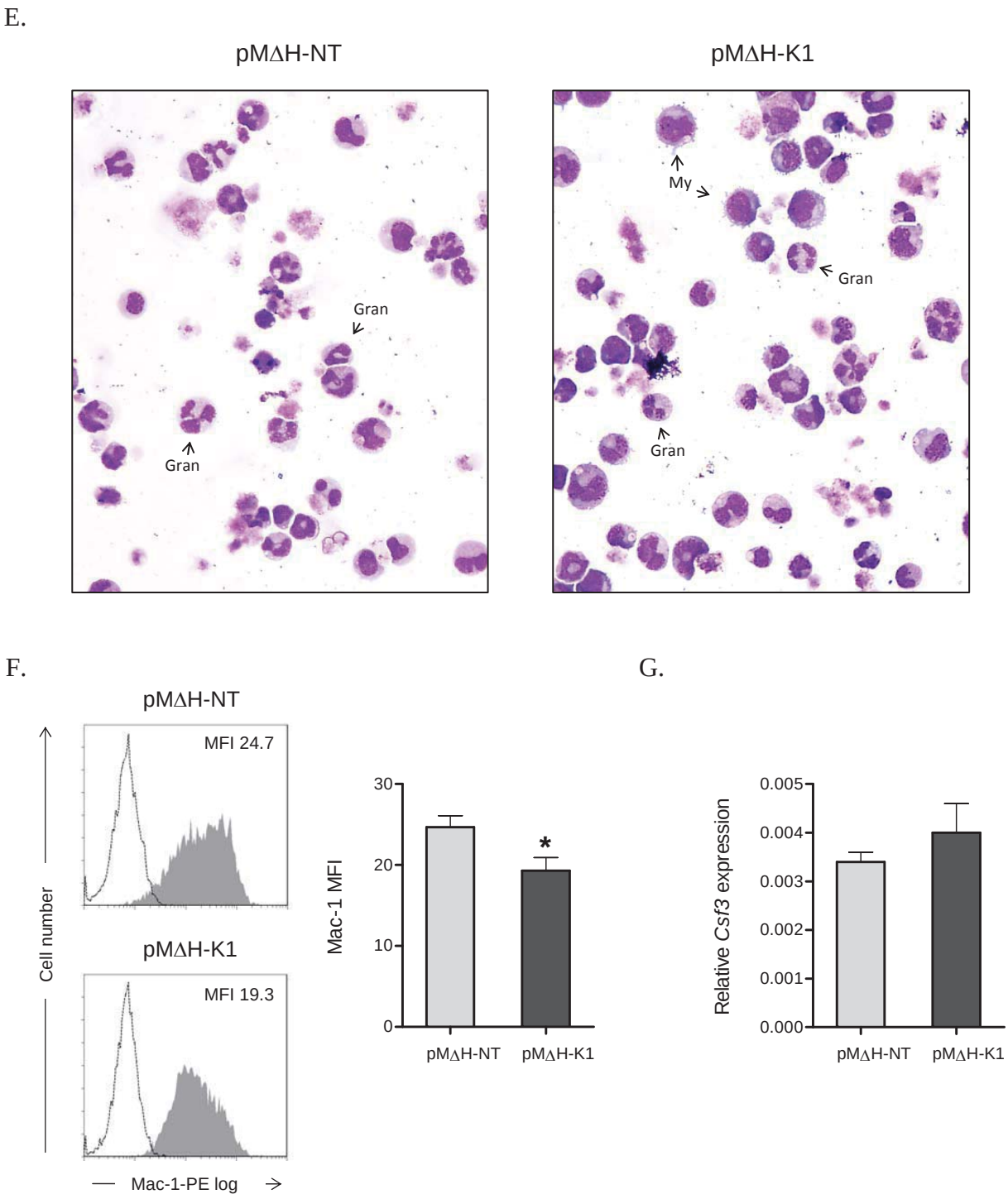

Figure 4.9 (E-G): shRNA knock-down of *Klf5* in the 32D cell line model. E. Representative photomicrographs showing Wright-Giemsa stained cytospin preparations of 32D cells expressing the non-targeting pMΔH-NT shRNA control or the *Klf5*-targeting pMΔH-K1 in G-CSF (Day 7). Original magnification = 200x. Gran = mature granuloycte, My = myelocyte. **F.** Flow cytometric detection of Mac-1 expression on 32D cells transduced with pMΔH-NT or pMΔH-K1 on Day 7 in G-CSF. Representative results from a typical experiment are shown. Empty peak = isotype control, grey peak = cell surface marker expression. Expression was detected using PE-conjugated antibodies, and the average mean fluorescence intensity (MFI) is shown. n=3, *p<0.05. **G.** mRNA expression level of *Csf3* (relative to the control *Beta-actin* gene) was assessed by Q-PCR in 32D cells transduced with pMΔH-NT or pMΔH-K1 on Day 7 in G-CSF. n=3.

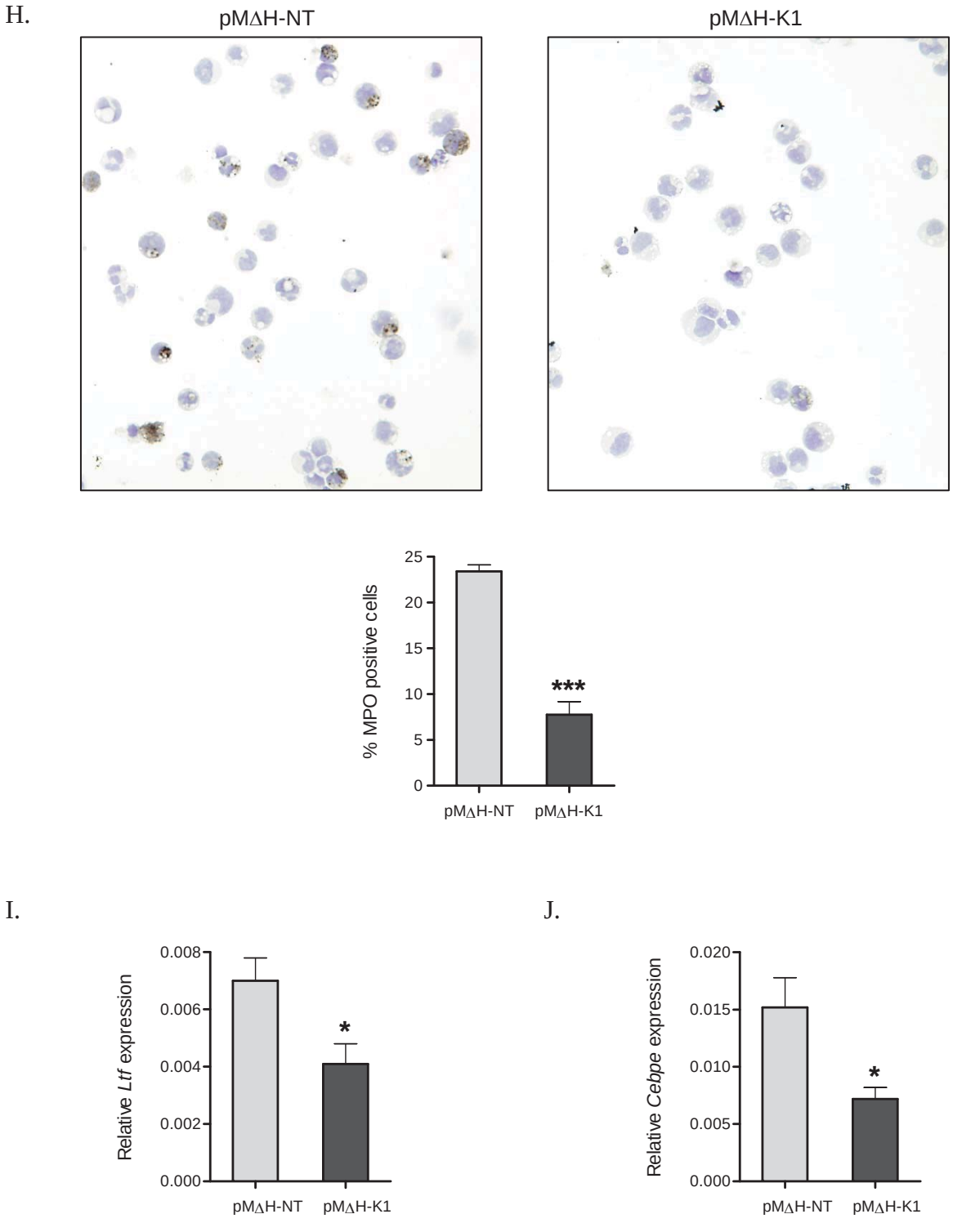

Figure 4.9 (H-J): shRNA knock-down of *Klf5* in the 32D cell line model. H. Representative photomicrographs showing MPO activity of 32D cells expressing the pMΔH-NT shRNA control or the *Klf5*-targeting pMΔH-K1 in G-CSF (Day 7). Original magnification = 200x. MPO activity was detected using the Hanker-Yates method. A total of 200 cells were counted per sample and the average percentage of cells positive for MPO is shown. n=3, ***p<0.001. **I-J.** mRNA expression levels of *Ltf* and *Cebpe* (relative to the control *Beta-actin* gene) were assessed by Q-PCR in 32D cells transduced with pMΔH-NT or pMΔH-K1 on Day 7 in G-CSF. n=3, *p<0.05.

7 days. Continued knock-down of *Klf5* expression in the pMΔH-K1 population was observed on Days 3 and 7 in G-CSF (Figure 4.9B). Functional analysis demonstrated that decreased *Klf5* expression was associated with improved expansion of pMΔH-K1 cells compared to the pMΔH-NT control population (Figure 4.9C) but did not affect cell viability (Figure 4.9D). Morphologically, pMΔH-NT control cells differentiated over 7 days in G-CSF to mature granulocytes characterised by polylobulated or ringed nuclei, as well as granulocyte intermediates (metamyelocytes and band cells) characterised by indented or 'C'-shaped nuclei (Figure 4.9E). pMΔH-K1 cells produced some mature granulocytes by Day 7 in G-CSF, however the majority of cells were granulocyte intermediates. These included metamyelocytes and band cells, and also a proportion of cells with larger and less-indented nuclei characteristic of more immature myelocytes. These observations suggest that pMΔH-K1 cells did not differentiate to the same extent as control cells.

To confirm attenuated granulocyte differentiation associated with reduced *Klf5* expression, pMΔH-K1 cells were further assessed for characteristics of granulocyte differentiation on Day 7 in G-CSF. We previously demonstrated increased expression of the differentiation markers Mac-1 (by flow cytometry) and *Csf3* (by Q-PCR) during G-CSF-induced granulocyte differentiation of the 32D cell line (see Section 4.2.1.2). Flow cytometry revealed significantly reduced expression of Mac-1 on pMΔH-K1 cells compared to the pMΔH-NT control on Day 7 in G-CSF, consistent with reduced differentiation (Figure 4.9F). mRNA expression of the murine G-CSF receptor *Csf3* was not significantly affected due to decreased *Klf5* expression (Figure 4.9G). Assays to detect markers of neutrophilic granule formation revealed that the pMΔH-K1 population had significantly fewer cells positive for MPO activity compared to the control population on Day 7 (Figure 4.9H), and *Ltf* mRNA expression was also significantly decreased as detected by Q-PCR (Figure 4.9I). Reduced *Ltf* expression is

consistent with reports demonstrating regulation of the *LTF* promoter by KLF5[201]. Finally, Q-PCR analysis also revealed significantly lower expression of the granulocytic transcription factor *Cebpe* in pMΔH-K1 cells compared to the control pMΔH-NT population (Figure 4.9J), which we and others have demonstrated increases during granulocyte differentiation of 32D cells (see Section 4.2.1.2 and Scott, et al. for example[384]). Collectively, these observations are consistent with reduced granulocyte differentiation of 32D cells in response to G-CSF associated with reduced expression of *Klf5*.

4.3 Discussion

4.3.1 Increased expression of KLF5 mRNA is predominantly associated with granulocyte differentiation

The results presented in this chapter demonstrated up-regulation of *Klf5* expression during GM-CSF-induced granulocyte-macrophage differentiation of the FDB1 cell line. Analysis of *KLF5* expression in an alternative cell line and in primary cell systems showed that increased *KLF5* expression is predominantly associated with the granulocyte lineage. Expression of *Klf5* was up-regulated during G-CSF-induced granulocyte differentiation of murine 32D cells. Conversely, *Klf5* expression was down-regulated during M-CSF-induced macrophage differentiation of mouse bone marrow progenitors. Bioinformatic analysis of published microarray data showed that *KLF5* was up-regulated to a greater extent relative to primitive haemopoietic cells in primary granulocyte populations than in monocyte or erythroid populations, and conversely demonstrated that *Klf5* expression was down-regulated in cells of lymphoid lineages. Collectively, these observations are consistent with a potential role for

KLF5 in regulation of granulocyte differentiation. It will be important to quantitate protein levels of KLF5 in these systems to confirm that this also correlates with granulocyte differentiation, as recent analyses have demonstrated that mRNA expression is not always indicative of protein expression due to parameters such as translation efficiency and protein turnover (correlation coefficients (*r*) ranging from 0.36-0.76 depending on the organism evaluated and study design)[394].

4.3.2 Enforced expression of KLF5 is sufficient to induce macrophage differentiation of FDB1 cells and primary murine bone marrow progenitors

In accordance with *KLF5* expression patterns, the functional studies presented in this chapter provide evidence supporting a role for KLF5 in myeloid differentiation. We demonstrated that retroviral expression of KLF5 was sufficient to promote macrophage differentiation of murine haemopoietic progenitor cells. In the FDB1 cell line system, transduction with *Klf5* overcame the IL-3 induced differentiation block to induce macrophage differentiation, and in primary mouse haemopoietic progenitors, enforced expression of KLF5 promoted macrophage differentiation at the expense of immature cells. KLF5-induced differentiation was accompanied by an accumulation of cells in G0/G1 phase and by cell death, both processes which are tightly linked to terminal cell maturation[395,396]. With regard to cell survival, studies have demonstrated a pro-apoptotic role for KLF5 expression in the TE2 esophageal cancer cell line[284]. From the results presented in this chapter we were not able to conclude if the reduced cell viability observed due to *Klf5* transduction in haemopoietic cells is a consequence of terminal differentiation, or whether KLF5 may also be acting to specifically induce apoptosis.

Given that *Klf5* expression is predominantly associated with granulocyte differentiation, it is interesting that we observed macrophage formation due to enforced expression of KLF5 in both FDB1 cells and primary murine bone marrow progenitors. It is possible that we were unable to detect granulocytes using these approaches as they have a shorter lifespan than macrophages[397], which could lead to selective loss of granulocytes in liquid culture. Alternatively it is possible that the observed macrophage differentiation is a consequence of inappropriate KLF5 expression. In Figures 4.2 and 4.4, we showed that *Klf5* mRNA levels increased approximately 2-fold during differentiation of both FDB1 and 32D cells, suggesting that small changes in expression of this gene may be sufficient to promote differentiation. These physiological levels are greatly exceeded through MSCV promoter-driven expression, potentially causing inappropriate activation of target-genes by KLF5. For example, as KLF family members bind to similar DNA sequences to activate target genes[195,196], it is possible that high levels of KLF5 may also be activating KLF4 target genes to direct macrophage differentiation[388]. Importantly, KLF5 has been shown to activate expression of the transcription factor *EGR1* in VSMCs[234], which in the haemopoietic system drives macrophage differentiation[398,399]. Therefore, inappropriate activation of *Egr1* by KLF5 over-expression could be another potential mechanism to account for macrophage differentiation in FDB1 cells and in murine haemopoietic progenitors.

The expression profiles of *KLF5* during granulocyte-macrophage differentiation suggest that spatial and temporal control of KLF5 expression may be important for KLF5 function. In the approach described in this chapter, KLF5 was constitutively expressed in all progenitor types rather than being restricted to a stage of committed granulocyte progenitors. Interestingly, a study performed by Sasmono, et al. suggested that macrophage differentiation acts as the 'default' pathway in myelopoiesis, and that additional signals are required to specify

granulocyte formation[314]. Thus, we could speculate that in some myeloid progenitors KLF5 induces growth arrest which then couples to this default pathway. This could be resolved by introducing KLF5 retrovirally into purified populations of granulocyte-macrophage progenitors or common myeloid progenitors. It may also be of benefit to utilise inducible over-expression experiments, which have proven to be successful in elucidating the function of transcription factors such as C/EBPα in myeloid systems[400,401]. In this way it may be possible to control timing of KLF5 induction and also the level of expression.

4.3.3 Reduced expression of Klf5 produces functional effects consistent with reduced granulocyte differentiation in the 32D cell line model

We next wished to determine if *Klf5* expression was necessary for G-CSF-induced granulocyte differentiation of 32D cells using a series of RNAi knock-down experiments. A single shRNA trigger (pMΔH-K1) consistently reduced *Klf5* mRNA expression by >60% compared to the relevant control construct when cells were cultured in IL-3 or on Days 3 and 7 in G-CSF. Reduced *Klf5* expression in this population was associated with increased cell expansion compared to the non-targeting control population in G-CSF, consistent with reduced differentiation. Correspondingly, morphological analysis revealed that cells with reduced *Klf5* mRNA expression displayed a reduced level of granulocyte differentiation, as seen by the presence of immature cells of the granulocyte series on Day 7 in G-CSF. Attenuated granulocyte differentiation due to reduced *Klf5* expression was associated with decreased expression of the myeloid marker Mac-1, the primary granule protein MPO, and the granulocyte genes *Ltf* and *Cebpe*. An independent means of reducing KLF5 function, such as independent siRNA triggers or a dominant-negative form of KLF5, will be necessary to confirm these results.

Although reduced *Klf5* expression in 32D cells resulted in functional effects which were consistent with inhibition of granulocyte differentiation, it is clear that granulocyte differentiation was not completely blocked in this system. It is possible that the 60% reduction in *Klf5* expression was not sufficient to prevent normal function in G-CSF-induced granulocyte formation. Studies assessing the role of KLF5 in ESCs have demonstrated that as little as 10-20% of normal *Klf5* mRNA expression is sufficient to maintain KLF5 function in this system[160,245]. In light of these considerations, we are constructing a transgenic mouse model where *Klf5* will be targeted for deletion specifically in the haemopoietic compartment using a Cre-Lox system. This will enable complete eradication of KLF5 expression *in vivo* for analysis of KLF5 function in a relevant biological system.

4.3.4 Evidence for a regulatory pathway involving KLF5 and members of the C/EBP family in G-CSF and GM-CSF-induced differentiation

As *KLF5* expression was up-regulated during G-CSF induced granulocyte differentiation and in primary granulocyte populations, we were interested to compare the expression profile of *KLF5* with that of the two granulocytic transcription factors *CEBPA* and *CEBPE* in our cell line models of differentiation. We demonstrated that regulation of *Klf5* mRNA expression is concordant with that of *Cebpe* during G-CSF-induced differentiation of 32D cells, and during GM-CSF-induced differentiation of FDB1 cells. Studies have demonstrated that *CEBPE* mRNA expression is induced during differentiation of primary human $CD34^+$ cells to granulocytes but not macrophages[373]. Accordingly, it has been shown that C/EBPε functions in terminal granulocyte differentiation and activation, with knock-out mouse models failing to produce mature neutrophils[375]. The highly concordant expression patterns of *Klf5* and *Cebpe*

during cytokine-induced differentiation further support a similar role for KLF5 in granulocyte differentiation.

During G-CSF-induced differentiation of 32D cells, we detected an early peak in *Cebpa* expression, which was followed by a steady increase in mRNA levels of both *Cebpe* and *Klf5*. *CEBPE* is a direct downstream target gene activated upon binding of C/EBPα[402]. *KLF5* has been previously implicated as a direct target gene of C/EBPα, as expression increased in response to enforced C/EBPα expression in human $CD34^+$ haemopoietic progenitor cells cultured in the presence of the protein synthesis inhibitor cyclohexamide[132]. Collectively, these observations suggest a regulatory cascade during G-CSF-induced differentiation whereby C/EBPα up-regulates transcription of *Cebpe* and *Klf5* which mediate terminal granulocyte differentiation. It will be necessary to show binding of C/EBPα to *KLF5* promoter sequences using ChIP assays to confirm direct regulation in granulopoiesis.

In models of granulocyte differentiation, it has been shown that G-CSF activates C/EBPα through G-CSF receptor (CSF3) signalling, and in turn C/EBPα induces expression of *CEBPE* and the primary granule gene *MPO*[402-405]. C/EBPα can also stimulate expression of *CSF3* through a positive-feedback loop[404,406]. Studies have shown that C/EBPε acts further downstream of C/EBPα by activation of the secondary granule gene *LTF*, however it does not affect expression of *MPO* or *CSF3*[375,377,407]. In 32D cells with reduced *Klf5* expression (see Section 4.2.3), we detected decreased expression of active MPO enzyme, and decreased mRNA expression of *Ltf* and *Cebpe*, but not of *Csf3*. These results, combined with our expression profiling studies (discussed above), suggest that KLF5 may act downstream of C/EBPα during granulocyte differentiation, as knock-down in 32D cells did not affect *Csf3* expression. Our analysis also suggests that KLF5 may act upstream of C/EBPε, as reduced

Klf5 expression was associated not only with decreased *Ltf* expression, but also with reduced expression of the primary granule protein MPO and of *Cebpe* itself.

Despite the up-regulation of *Klf5*, *Cebpe*, and other C/EBPα target genes (e.g. *Mmp8*, *Per2*, *Slfn2*[1]) during FDB1 differentiation, we showed that expression of *Cebpa* mRNA expression decreased during GM-CSF-induced differentiation of FDB1 cells. It is therefore possible that GM-CSF-induced differentiation of FDB1 cells occurs independently of C/EBPα, and that other proteins such as alternative members of the C/EBP family are responsible for the observed activation of C/EBPα target genes in this system. For example, there is evidence to suggest that granulopoiesis can occur independently of C/EBPα via C/EBPβ and C/EBPδ in murine cell line and animal models[408-411], and these two proteins have been shown to regulate *Klf5* expression in adipose tissue[156]. Alternatively, it is possible that C/EBPα activity in FDB1 cells may be predominantly under post-transcriptional or post-translational control in response to GM-CSF. It is well known that C/EBPα is regulated by a variety of post-translational mechanisms which alter functional activity, such as phosphorylation and sumoylation[412-414]. C/EBPα activity can also be modulated by the relative expression ratio of it's two protein isoforms, p42 and p30, which demonstrate distinct transactivational activities[37,415]. To explore these possibilities further it will be necessary to detect modified C/EBPα protein using anti-phospho-C/EBPα antibodies or anti-SUMO immunoprecipitation techniques, and also to quantitate the relative expression of C/EBPα protein isoforms during GM-CSF-induced FDB1 differentiation.

Chapter 5 – Deregulation of KLF5 in human Acute Myeloid Leukaemia.

5.1 Introduction

In AML, many transcription factors found to be important for normal haemopoiesis are affected by mutation or chromosomal translocation, resulting in enhanced growth and survival or a block in differentiation[38,416]. In particular, reduced biological activity of transcription factors with tumour suppressor function (e.g. p53, RB, C/EBPα) is an important feature in the development of AML[417]. Conventional tumour suppressor genes normally act in biological processes such as cell cycle arrest, apopotosis, or cellular differentiation[418]. The data presented in Chapter 4 is consistent with KLF5 acting as an inducer of growth arrest and myeloid differentiation, suggesting a potential role for KLF5 as a novel tumour suppressor in AML.

Tumour suppressor genes can be affected by inactivating mutations in haemopoietic malignanices, however, in the absence of mutation, the expression levels of these genes are often decreased due to deletion or other mechanisms[417]. Studies have shown that reduced mRNA expression can be a marker for identification of novel tumour suppressor genes in AML, such as *TRIB2* and *NOTCH1*[419,420]. Methylation is a frequent mechanism associated with silencing of tumour suppressor genes in AML, for example, the *SOCS1* gene was found to be hypermethylated in 60% of AML[421], and the pro-apoptotic *DAPK1* gene was reported to be hypermethylated in 47% of therapy-related AML[422]. KLF5 has been previously implicated

as a tumour suppressor in breast and prostate cancer, with studies demonstrating decreased expression due to hemi- or homozygous deletion or excessive protein degradation in disease tissue[224,295,297,300,301]. Importantly, deletion of the 13q21-22 chromosomal region containing *KLF5* has been described in various lymphoid and myeloid malignancies[305,306], and loss of hetereozygosity has also been detected for this region in AML patient samples[307,308]. CpG methylation of *KLF5* has been reported in MPN, MDS and in AML, though not thoroughly investigated[111,309]. Methyl-binding protein ChIP analysis has demonstrated methylation of *KLF5* in the AML cell lines KG-1 and U937, and in peripheral blasts from 2/9 AML patients[111]. This finding has been further corroborated by a study showing that *KLF5* was hypermethylated in 2/17 patients with secondary AML transformed from MDS[309].

We initially sought to determine if *KLF5* mRNA expression is decreased in AML samples compared to primitive haemopoietic cells from normal controls. Given that *KLF5* expression is associated with C/EBP regulatory pathways (Chapter 4, Section 4.3.4), we were also interested to see if *KLF5* expression levels correlated with any particular subtype or mutational category of AML. For these studies, we performed Q-PCR to detect *KLF5* expression in a local cohort of diagnostic bone marrow biopsies from AML patients and normal bone marrow controls, and interrogated a larger publicly-available microarray dataset for further analysis[329]. We sought to further examine CpG methylation of the *KLF5* gene as a potential mechanism for its deregulated expression in AML. Methylation of *KLF5* was examined in a panel of leukaemia cell lines and in our cohort of primary AML patient samples, and we investigated potential correlation of *KLF5* CpG methylation with specific genetic lesions or subtypes of AML. To assess whether methylation of *KLF5* functionally represses transcription, we treated leukaemia cell lines showing hypermethylation of *KLF5* with methyltransferase inhibitors to detect reactivation of expression. Leukaemia samples

were compared with normal bone marrow controls to define the genomic region of differential CpG methylation, providing some insight as to how methylation could interfere with regulation of *KLF5* expression. Finally, the tumour suppressor activity of KLF5 was investigated by retroviral expression of KLF5 in a leukaemia cell line displaying low *KLF5* expression.

5.2 Results

5.2.1 KLF5 mRNA expression is reduced in AML

5.2.1.1 Expression in a local cohort of primary AML samples and correlation with AML subtype

KLF5 mRNA expression levels were assessed in a cohort of 30 AML patients (Queen Elizabeth Hospital/IMVS cohort - details regarding collection, processing and genotyping are provided in Chapter 2, Section 2.4.1). Samples consisted of BMMNC preparations taken from patients at diagnosis (characteristics shown in Table 5.1). We included 5 bone marrow $CD34^+$ progenitor samples from healthy volunteers as normal controls. cDNA templates were prepared and replicate Q-PCR reactions were performed for each sample. *KLF5* expression levels were also examined in a range of human myeloid leukaemia cell lines (characteristics described in Table 5.2). Independent mRNA preparations were used to prepare cDNAs from each cell line (refer to Figure 5.1 for replicate numbers), and Q-PCR performed on each cDNA preparation. *KLF5* expression was determined using the average of Q-PCR results from independent cDNA templates for each cell line. AML4 was included in each Q-PCR

SAMPLE	AGE/GENDER	FAB	KARYOTYPE	*CEBPA* STATUS	*FLT3* STATUS	*NPM1* STATUS	% BLASTS	% CD34$^+$
AML 1	80/M	M1	Monosomy 7	-	-	-	83	98
AML 2	32/F	M3	t(15;17)	-	-	-	23**	1
AML 3	66/M	M8	Complex (incl. t(9;22))	-	-	-	95	97
AML 4	19/F	M4	Normal	-	*FLT3-ITD*	-	64	72
AML 5	73/M	M2	Normal	-	-	-	97	1
AML 6	70/F	M1	Complex (incl. monosomy 7, del(5))	-	-	-	60	97
AML 7	73/M	M2	Normal	-	-	4bp ins.	97	1
AML 8	65/M	M4	Complex (incl. inv(16), trisomy 8)	-	-	-	40	89
AML 9	78/M	N/A	Normal	Mut.*	-	-	24	86
AML 10	73/F	M1	Complex	-	-	-	98	100
AML 11	49/F	M2	Trisomy 14	-	-	-	45	99
AML 12	77/M	M4	Normal	-	*FLT3-ITD*	-	29	74
AML 13	63/M	M3	Trisomy 8, t(15;17)	Mut.	*FLT3-ITD*	-	40	12
AML 14	80/M	M1	Normal	-	-	-	90	94
AML 15	38/M	M1	Normal	-	*FLT3-ITD*	4bp ins.	100	<1
AML 16	51/F	M2	Monosomy 7, del(7q)	-	-	-	83	93
AML 17	71/F	M1	Del(5q)	-	*FLT3-TKD*	-	90	96
AML 18	79/M	M6	Normal	-	-	-	25	82
AML 19	37/M	M4	Inv(16)	-	*FLT3-TKD*	-	70	85
AML 20	71/F	M2	Normal	Mut.	-	-	24	83
AML 21	89/M	M5	Trisomy 5 & 8, del(5q)	-	-	4bp ins	92	<1
AML 22	83/M	M2	Trisomy 8	Mut.*	-	-	38	52
AML 23	18/M	M2	Normal	-	-	4bp ins	52	<1
AML 24	72/M	M4	Inv(16)	-	-	-	69	93
AML 25	80/M	M4	t(13;14)	Mut.*	-	-	21	18
AML 26	74/M	M3	t(15,17)	-	*FLT3-ITD*	-	76	34
AML 27	74/M	M5	Trisomy 8, t(1:17)	Mut.*	*FLT3-TKD*	4bp ins	71	<1
AML 28	69/M	N/A	Normal	Mut.	-	-	26	88
AML 29	23/M	M5	11q23 (t(10;11))	-	-	-	95	<1
AML 30	51/M	M1	Complex (incl. +11q23)	-	*FLT3-TKD*	-	91	<1

Table 5.1: Characteristics of human AML samples. AML BMMNC samples were taken at diagnosis. FAB classification, karyotype, and percentage of blasts and CD34$^+$ cells were determined at this time. Diagnostic samples were obtained from the Queen Elizabeth Hospital and the IMVS. Genomic DNA was prepared from each and assessed for *CEBPA*, *FLT3* and *NPM1* mutations. 'Mut.' in the *CEBPA* column indicates a *CEBPA* coding region mutation (Mut.* indicates the mutation is potentially a TAD2C polymorphism[423]). '4bp ins.' in the *NPM1* column indicates a 4 bp insertion in the *NPM1* gene. A dash in the *CEBPA*, *FLT3* and *NPM1* columns indicates the patient has wildtype copies of these genes. **AML2 had 63% promyelocytes. 'N/A' indicates value is unknown.

CELL LINE	LEUKAEMIA TYPE	FAB	SOURCE	AGE/ GENDER	SOURCE TISSUE	RELEVANT KARYOTYPE	RELEVANT MUTATIONS	MYELOID CHARACTERISTICS
HL-60[424]	AML	M2	AML patient at diagnosis	35/F	Peripheral blood	-	*TP53* alteration *NRAS* amplification *MYC* amplification	Monocyte and granulocyte differentiation with various reagents
K562[425]	CML	N/A	CML patient in blast crisis	53/F	Pleural effusion	t(9;22) BCR-ABL positive	*TP53* mutation	Forms recognisable granulocytic, monocytic and erythrocytic progenitors[426]
KG-1[427]	AML	M1[428]	AML patient relapsed from erythroleukaemia	59/M	Bone marrow	-	*TP53* mutation *NRAS* mutation *RB1* rearrangement	Monocyte/macrophage differentiation
MOLM-13[429]	AMML	M5	AML patient relapsed from RAEB	20/M	Peripheral blood	ins(11;9) MLL-AF9 positive	*FLT3-ITD* mutation	Monocyte differentiation
MV4;11[430]	AMML	M5	AML patient at diagnosis	10/M	Peripheral blood[430]	t(4;11) MLL-AF4 positive	*FLT3-ITD* mutation	-
THP-1[431]	AMML	M5	AML patient at relapse	1/M	Peripheral blood	t(11;9) MLL-AF9 positive	*TP53* mutation *NRAS* mutation *RB1* rearrangement	Macrophage differentiation
U937[432]	Similar to AMML	M5	Patient with generalised, diffuse histiocytic lymphoma	37/M	Pleural effusion	t(10;11) MLL-AF10 positive	*TP53* mutation	Monocyte/macrophage differentiation with various reagents

Table 5.2: Characteristics of human leukaemia cell lines. Primary references are noted for each cell line. Information pertaining to characteristics of individual cell lines was obtained from Hans G. Drexler's 'Guide to Leukemia-Lymphoma Cell Lines'[433] unless otherwise indicated. AMML = Acute myelomonocytic leukemia, RAEB = Refractory anaemia with excessive blasts.

reaction, and *KLF5* expression levels for both primary samples and cell lines were plotted relative to the AML4 reference sample.

Relative *KLF5* expression for individual samples is shown in Figure 5.1A. The majority of AML samples displayed low *KLF5* expression compared to normal $CD34^+$ controls. One notable exception was AML7, which showed 36-fold higher *KLF5* expression than the average of other AML samples, and 16-fold higher expression than the average of $CD34^+$ controls. AML7 was hence excluded from the following analyses as an outlier. Statistical analysis of *KLF5* expression (Figure 5.1B) demonstrated that average *KLF5* expression was significantly lower in AML samples than in normal $CD34^+$ controls, with a mean relative expression of 1.14 compared with 2.59. The seven leukaemia cell lines tested also showed low levels of *KLF5* expression compared to controls, with an average relative expression of 0.72.

KLF5 mRNA expression was subsequently assessed according to FAB subtype, main cytogenetic abnormality, or molecular abnormality including mutations in *CEBPA*, *FLT3* and *NPM1*. Expression was significantly reduced in FAB subtypes M1, M3 and M4 compared to normal $CD34^+$ controls (Figure 5.2A), and also in samples exhibiting *FLT3-ITD* mutations (Figure 5.2B). There were no significant differences in subgroups according to main cytogenetic abnormality, possibly due to the limited sample number in each group (Figure 5.2C).

A.

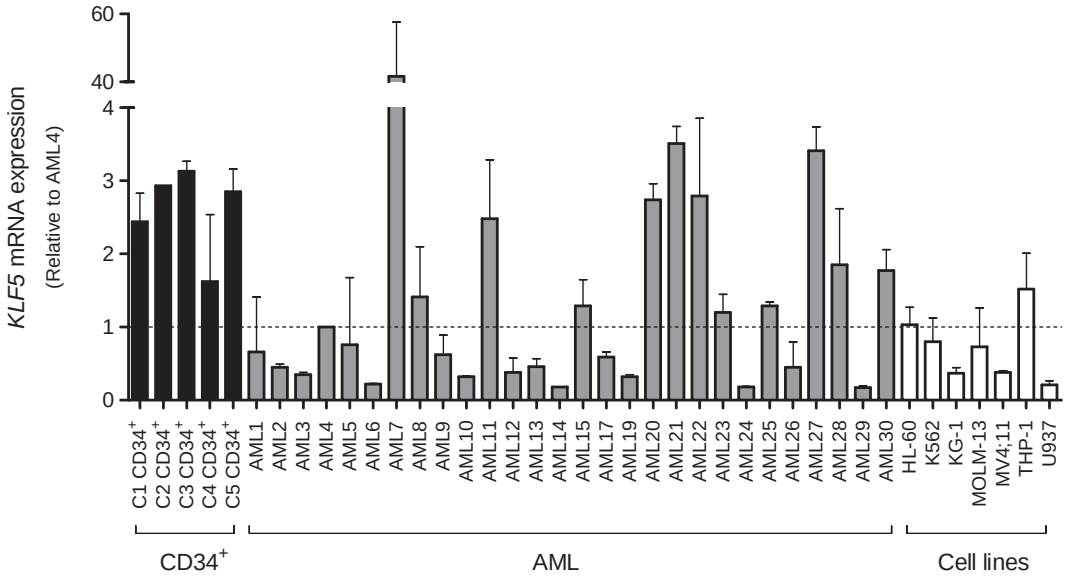

B.

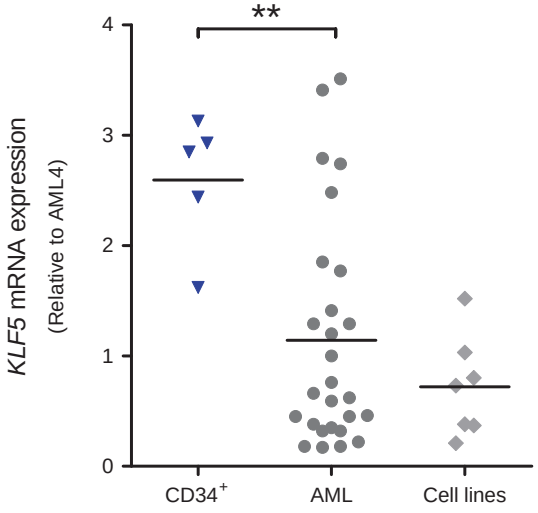

Figure 5.1: *KLF5* mRNA expression in human AML samples, normal bone marrow controls and human leukaemia cell lines as detected by Q-PCR. A. *KLF5* mRNA levels in primary human AML BMMNC samples at diagnosis (grey bars) leukaemia cell lines (white bars) and normal bone marrow CD34$^+$ controls (black bars). *KLF5* levels are shown relative to AML4 reference sample. Note that sufficient RNA was not obtained for AML16 and AML18 for Q-PCR. Control and AML samples n=2 (from one cDNA preparation), cell lines n=2 (MOLM-13), n=3 (K562, MV4;11), n=8 (HL-60, KG-1, THP-1, U937) from independent cDNA preparations. **B.** Summary of *KLF5* expression levels determined by Q-PCR for primary human AML BMMNC samples at diagnosis, leukaemia cell lines, and normal bone marrow CD34$^+$ controls (described in part 'A'). Note that AML7 from part 'A' was excluded as an outlier (determined using the ROUT method[434]). ** $p<0.01$.

A.

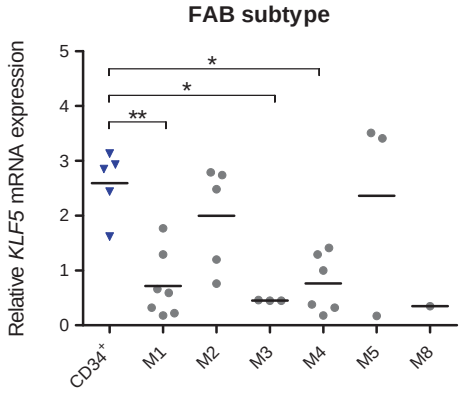

B.

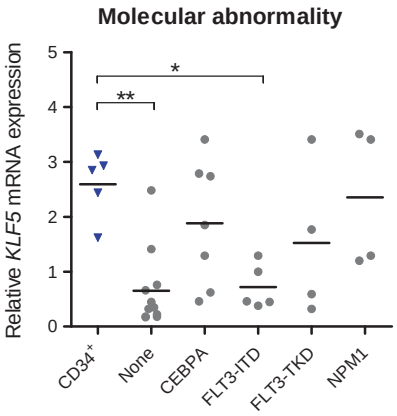

C.

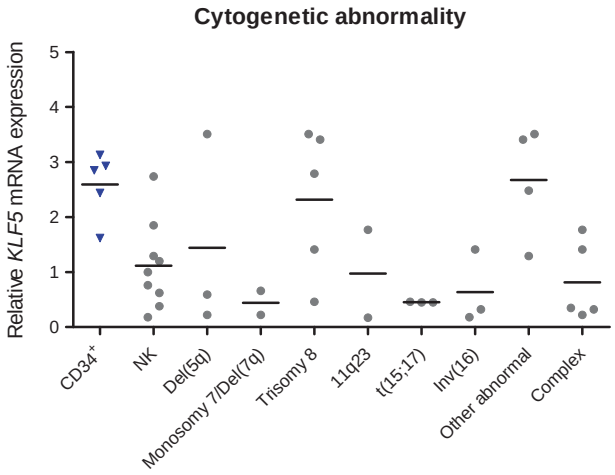

Figure 5.2: Differences in *KLF5* mRNA expression in human AML samples according to AML subtype. *KLF5* mRNA expression detected relative to reference sample AML4 by Q-PCR (see Figure 5.1). Samples were grouped according to: **A.** FAB subtype, **B.** molecular abnormality including mutations in *CEBPA*, *FLT3* and *NPM1*, and **C.** cytogenetic abnormality. Note that NK = normal karyotype, and 'None' in part 'C' indicates no mutations detected in *CEBPA*, *FLT3* or *NPM1*. Subgroups were assessed using One way ANOVA with Tukey post-test comparison (*$p<0.05$, **$p<0.01$).

5.2.1.2 Expression in an expanded cohort of primary AML samples and correlation with AML subtype

We wished to validate our analysis using a larger sample set, and in order to achieve this we accessed *KLF5* expression data for a large number of AML samples from a land-mark gene expression profiling study performed by Valk, et al.[329]. In this study, mononuclear cells (MNC) were isolated from bone marrow or peripheral blood of 285 AML patient samples and 8 healthy volunteers as controls (5 MNC and 3 $CD34^+$ samples), and gene expression analysis was performed using Affymetrix arrays. We utilised a normalised data-set for analysis of *KLF5* expression[435]. In support of our observations in Section 5.2.1.1, this analysis showed that average *KLF5* expression in AML samples was significantly lower than that of the MNC controls (log_2 RMA normalised expression of 5.6 compared to 7.0) (Figure 5.3A). *KLF5* expression in AML samples was not significantly lower than in $CD34^+$ controls, although this may be related to the small number of samples in this control group ($CD34^+$ n=3).

In Figures 5.3B-D we present the relative levels of *KLF5* mRNA in AML patient samples using the normalised Valk data-set according to FAB subtype, molecular abnormality, or main cytogenetic abnormality. Statistical analysis demonstrated significantly reduced *KLF5* expression in each subgroup examined when compared with the normal MNC control group. There were no significant differences in expression between FAB subtypes (Figure 5.3B), or between samples grouped by molecular abnormality (Figure 5.3C). There was however some variation between AML subgroups according to cytogenetic abnormality; samples exhibiting the inv(16) lesion showed significantly lower *KLF5* expression than those with trisomy 8 or a normal karyotype (Figure 5.3D). This agrees with the Q-PCR results from our local cohort of AML patients as presented in Figure 5.2C, which showed that the mean relative *KLF5*

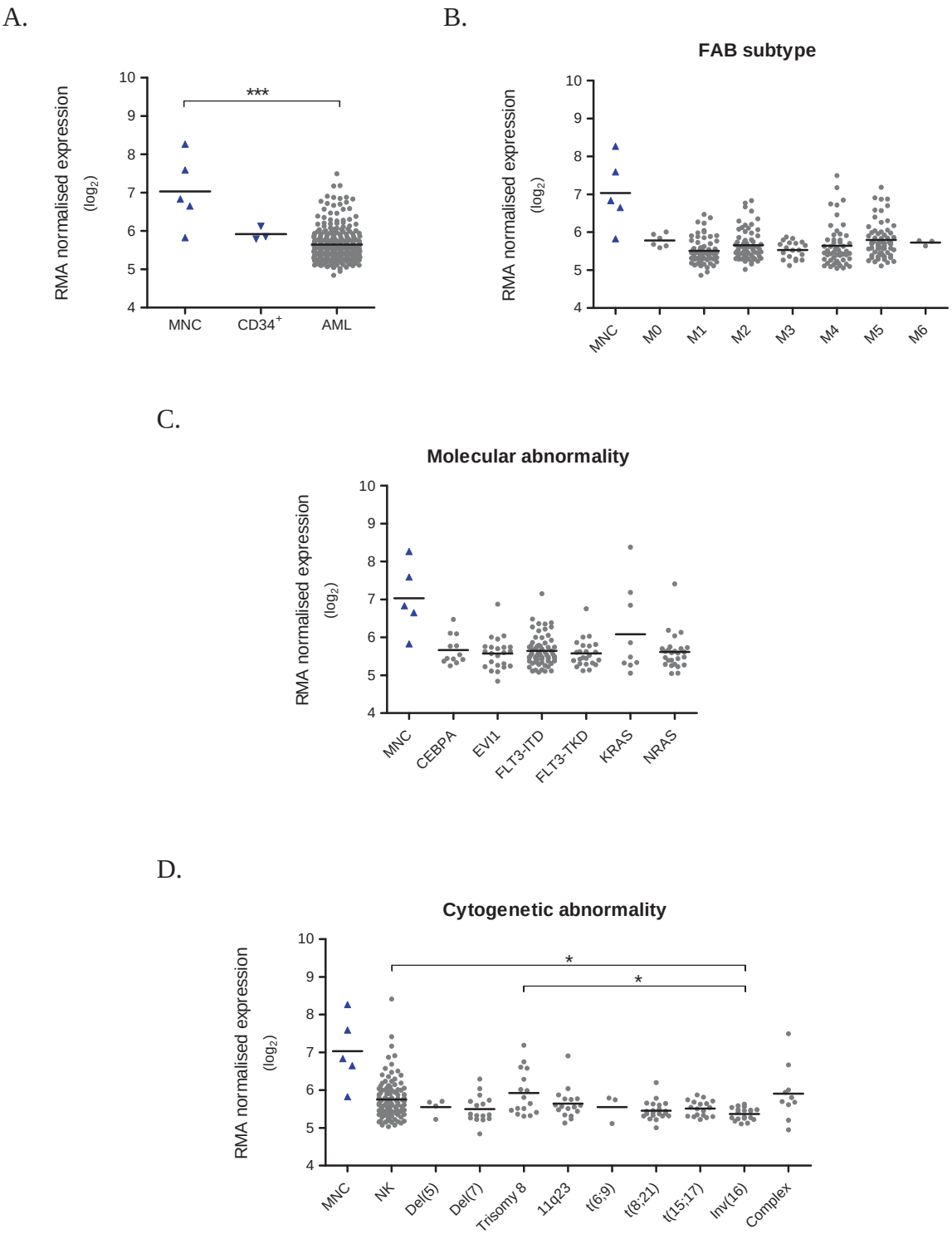

Figure 5.3: *KLF5* expression levels in the Valk cohort. A. Analysis of *KLF5* mRNA levels as detected by microarray in Valk, et al.[329]. Samples include normal controls (5 MNC and 3 $CD34^+$ samples) and AML MNC (n=274). ***p<0.001. **B-D.** Analysis of *KLF5* mRNA levels as detected by microarray using data from Valk, et al.[329] grouped by: **B.** FAB subtype, **C.** molecular abnormality (mutation in *CEBPA*, *FLT3* or *RAS*, over-expression of *EVI1*), or **D.** cytogenetic abnormality (NK=normal karyotype). All subgroups show significantly reduced *KLF5* expression compared to normal controls (blue triangles) using One way ANOVA with Tukey post-test comparison (p<0.05). *p<0.05.

expression for samples with inv(16) was lower than the mean expression for samples with trisomy 8 or a normal karyotype, although these differences did not reach significance.

5.2.2 Analysis of the KLF5 5` proximal promoter and intron 1 CpG methylation in AML

5.2.2.1 Experimental design

Methylation analysis of the *KLF5* gene was initially performed on the first 15 samples from our local AML cohort detailed in Table 5.1. The 7 leukaemia cell lines were also assessed (Table 5.2), as well as 3 normal $CD34^+$ bone marrow controls from Section 5.2.1 for which sufficient genomic DNA was available (C3-5 $CD34^+$). In addition, genomic DNA was isolated from 4 normal BMMNC samples which were included in the following analysis.

Genomic DNA was sent to the AGRF for quantitative methylation analysis using the Sequenom EpiTYPER system. The method for detection of methylation is depicted in Figure 5.4 and described briefly as follows: Genomic DNA is bisulfite-modified, converting unmethylated cytosine residues to uracil. Oligonucleotides are designed to amplify regions of converted DNA from approximately 100-500 bp in length, and PCR produces amplicons where unmethylated cytosine residues are detected as thymidine residues. These amplicons are *in vitro* transcribed and treated with Ribonuclease A for uracil-specific cleavage into small fragments. The fragments are assessed by mass spectrometry to determine differences in mass. A fragment initially containing a single unmethylated CpG residue (where the original cytosine is now detected as an adenosine residue) will be 16 Da lighter in mass than that same fragment with a methylated CpG residue (where the original cytosine is now detected as a

NOTE:
This figure is included on page 156 of the print copy of the thesis held in the University of Adelaide Library.

Figure 5.4: Overview of Sequenom EpiTYPER system for quantitative methylation analysis. A. Procedure for quantitative methylation analysis using amplification and transcription of bisulfite-converted DNA combined with MALDI-TOF mass spectrometry analysis. **B.** Interpretation of mass spectrum to quantitate percentage methylation. Figure was adapted from the Sequenom website (http://www.sequenom.com).

guanosine residue). Thus one fragment initially containing a single CpG residue can be detected by mass spectrometry as two peaks separated by 16 Da, and the ratio of these two peaks is used to calculate the percentage of DNA showing methylation at that particular CpG residue within each sample.

We analysed a region of the *KLF5* locus stretching from the proximal promoter to the end of exon 2 (Figure 5.5). This region was selected as it was predicted to contain a CpG island by two independent prediction programs (UCSC Genome Browser and Sequenom EpiDesigner program). The region analysed contains a total of 222 CpG dinucleotide residues over 4424 bp. Fifteen PCR amplicons were designed with the aid of Sequenom EpiDesigner Software to cover all but 4 of the 222 total CpG residues (see Figure 5.5). Analysis of methylation using the EpiTYPER system is limited by the size of individual cleaved fragments – methylation cannot be assessed by mass spectrometry if the fragment is too small or too large, or if there are multiple fragments of the same size within any given amplicon. From the 222 total CpG residues, we were able to quantitatively assess the methylation status of 150, which are indicated in red in Figure 5.5. CpG residues which were not informative in this analysis are indicated in green.

5.2.2.2 Identification of regions which are differentially methylated between AML samples and normal controls

The methylation status of the 150 informative CpG residues in 29 samples (AML samples, leukaemia cell lines and normal controls) is represented using a heat map in Figure 5.6 (note that CpG residues are numbered according to their total CpG number from the 222 analysed). Normal controls are shown in the top 7 rows of Figure 5.6. These displayed little CpG

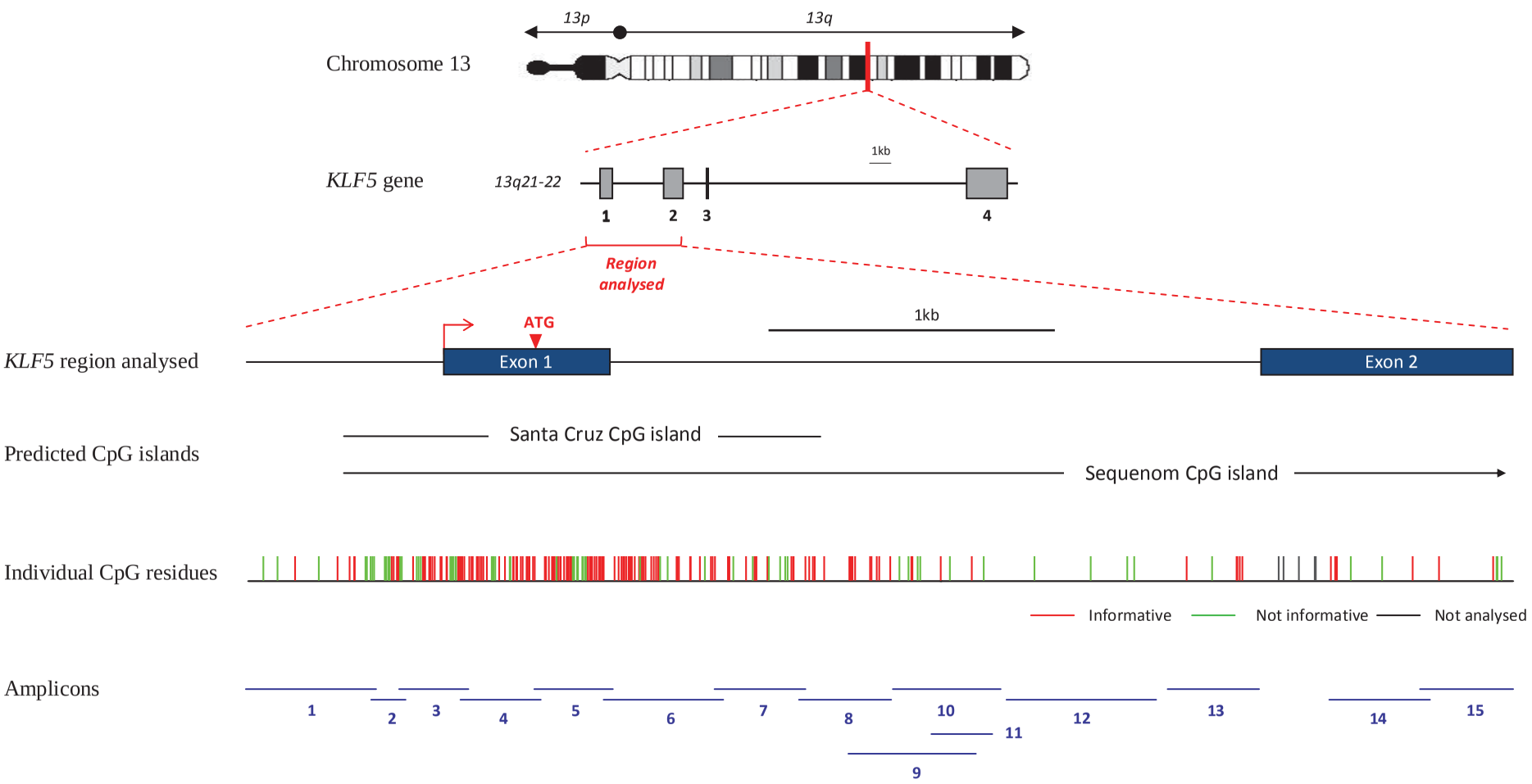

Figure 5.5: *KLF5* region analysed for methylation status. The *KLF5* gene lies on chromosome 13q21-22. Methylation analysis was performed on a region covering from the proximal promoter to the end of exon 2. CpG islands were predicted using the UCSC Genome Browser and the Sequenom EpiDesigner Program. The location of individual CpG residues within the *KLF5* region analysed is shown, and the colour scheme indicates whether CpG residues were able to be quantitatively assessed using Sequenom EpiTYPER. The location of amplicons designed to assess methylation of *KLF5* using Sequenom EpiTYPER is also depicted. Amplicons were designed with the aid of the Sequenom EpiDesigner Program (for more details see Chapter 2, Section 2.4.2.)

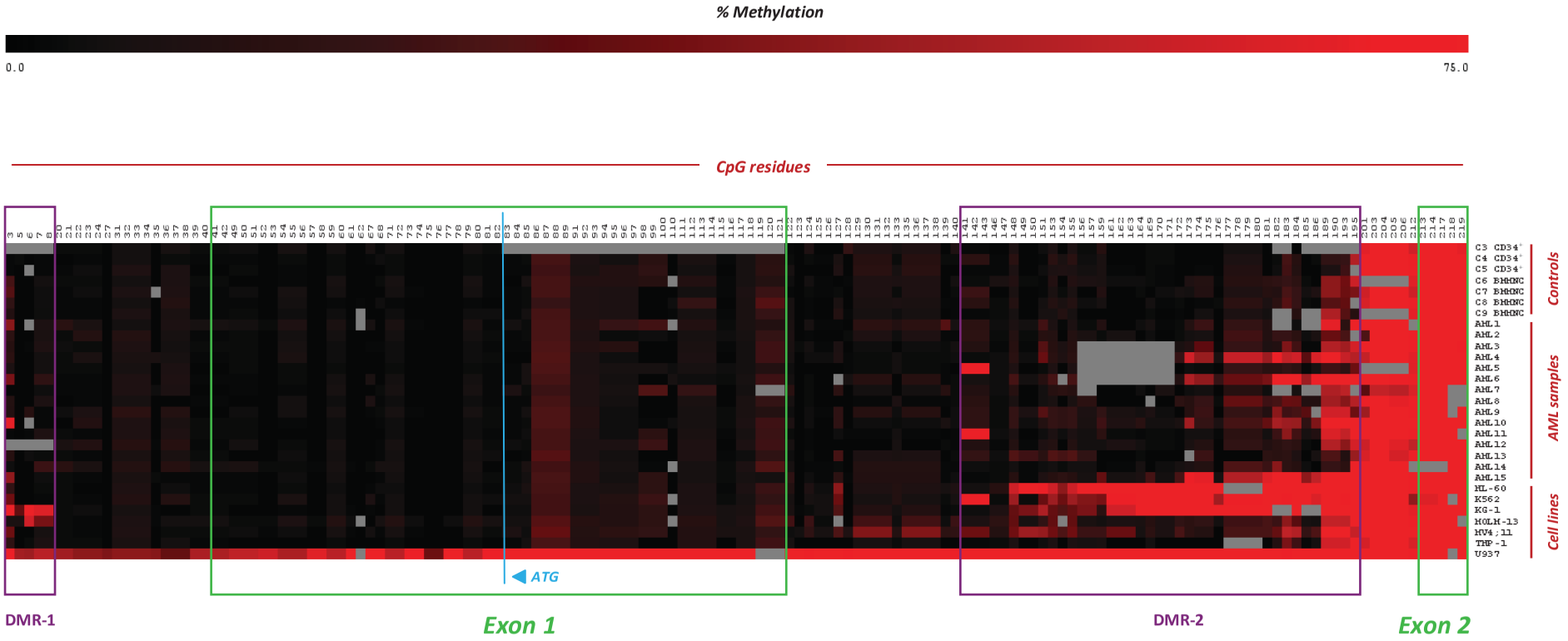

Figure 5.6: Quantitative methylation analysis of *KLF5* from the proximal promoter to the end of exon 2. Heat map showing percentage methylation at individual CpG residues for 7 normal bone marrow controls (3x $CD34^+$ and 4x BMMNC), 15 AML BMMNC samples, and 7 leukaemia cell lines. The colour scale (TOP) from black to red indicates low to high percentage methylation. A grey colour indicates the residue was not informative for this sample. CpG residues in *KLF5* exons 1 and 2 are boxed in green and the position of the ATG initiating codon is depicted with a blue line for reference. Note that where a CpG residue was covered by multiple amplicons, the average percentage methylation was calculated for that residue. Two differentially-methylated regions (DMR-1 and DMR-2) were identified visually and are outlined in purple boxes.

methylation associated with the proximal promoter, through exon 1, and into intron 1 of *KLF5*. However a higher degree of methylation was observed between CpG residues 189-195, which lie approximately midway through intron 1. In exon 2 (CpG residues 213-219) all CpG residues were highly methylated in both control and AML samples. This is not surprising, as CpG residues which are not part of CpG islands in the genome of normal tissues are usually methylated[436]. However, when compared to controls, selected primary AML and leukaemia cell line samples showed a higher degree of methylation in two distinct areas across the *KLF5* region analysed, as indicated in Figure 5.6. The first of these, termed Differentially-methylated Region 1 (DMR-1), lies at the very 5` end of the region assessed, in the *KLF5* proximal promoter. DMR-1 consists of 5 informative CpG residues numbered CpG 3-8. The second differentially-methylated region, DMR-2, lies in the first half of *KLF5* intron 1, and consists of 41 informative CpG residues numbered CpG 141-195.

We expanded our analysis to include the remaining 15 AML patient samples from our local AML cohort (details in Table 5.1), using amplicons selected to cover DMR-1 and DMR-2. Amplicon number 1 was selected for analysis of the 5 CpG residues in DMR-1, and amplicon numbers 6, 7, 8 and 9 were selected for analysis of 40/41 CpG residues (CpG 141-193) from DMR-2 (see Figure 5.5). The methylation results across DMR-1 and DMR-2 for all 30 AML samples together with leukaemia cell lines and normal controls are depicted in a heat map in Figure 5.7.

To define a smaller region representative of methylation in *KLF5* DMR-2 for further quantitative analysis we performed unsupervised hierarchical cluster analysis (Figure 5.8A). This revealed a subset of six AML patient samples which clustered independently due to high methylation specifically at three CpG residues at the 5` end of DMR-2 (CpG 141-143). These

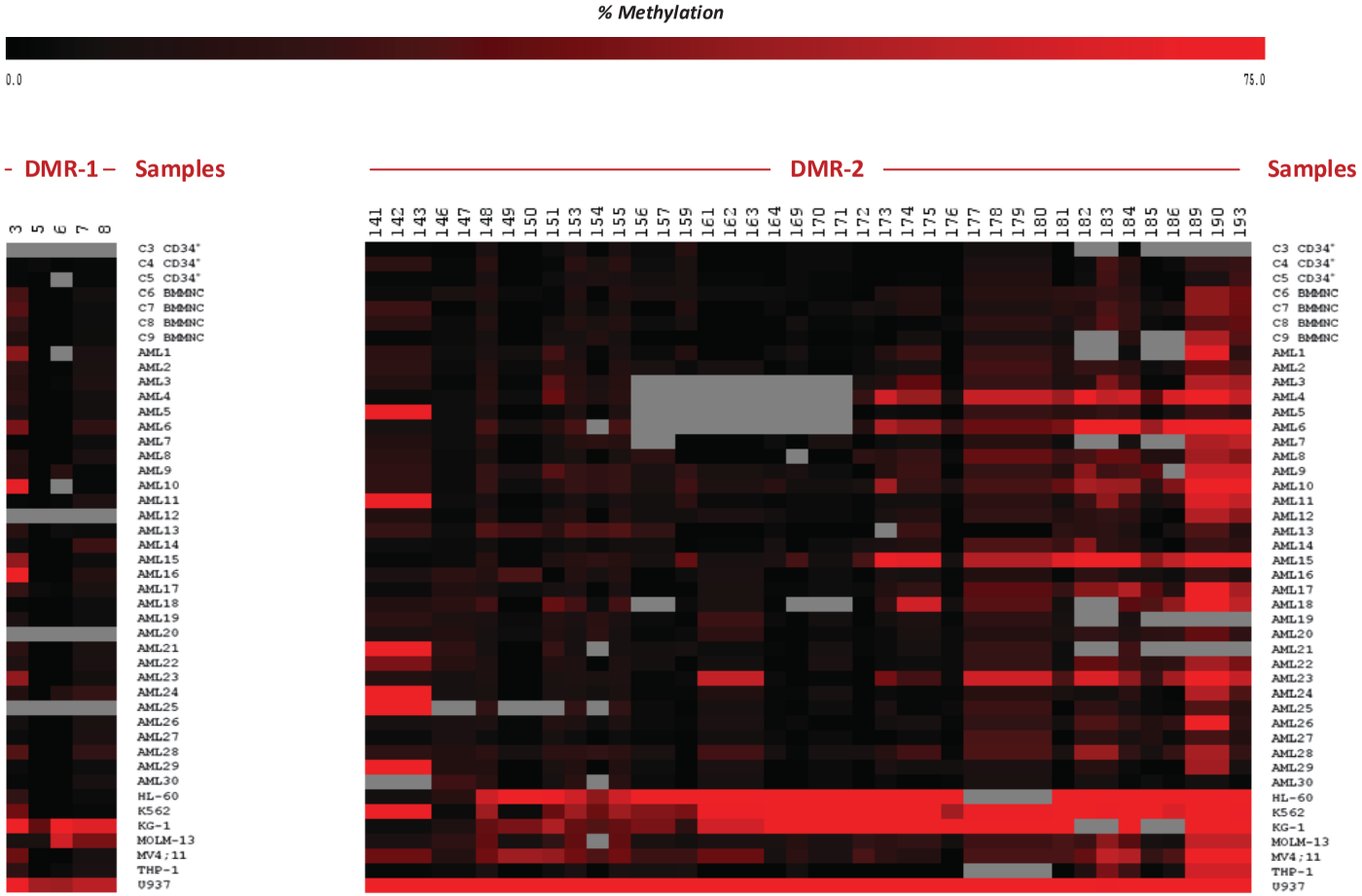

Figure 5.7: Methylation of *KLF5* in normal and leukaemic samples in DMR-1 and DMR-2. A. Heat maps depicting percentage methylation at individual CpG residues for 7 normal bone marrow controls (3x CD34$^+$ and 4x BMMNC), 30 AML BMMNC samples, and 7 leukaemia cell lines in *KLF5* differentially-methylated regions (DMR) 1 and 2. The colour scale (TOP) from black to red indicates low to high percentage methylation. A grey colour indicates the residue was not informative for this sample. For DMR-1, samples C3 CD34$^+$, AML12, AML20 and AML25 did not provide informative methylation results and were excluded from further analysis.

A.

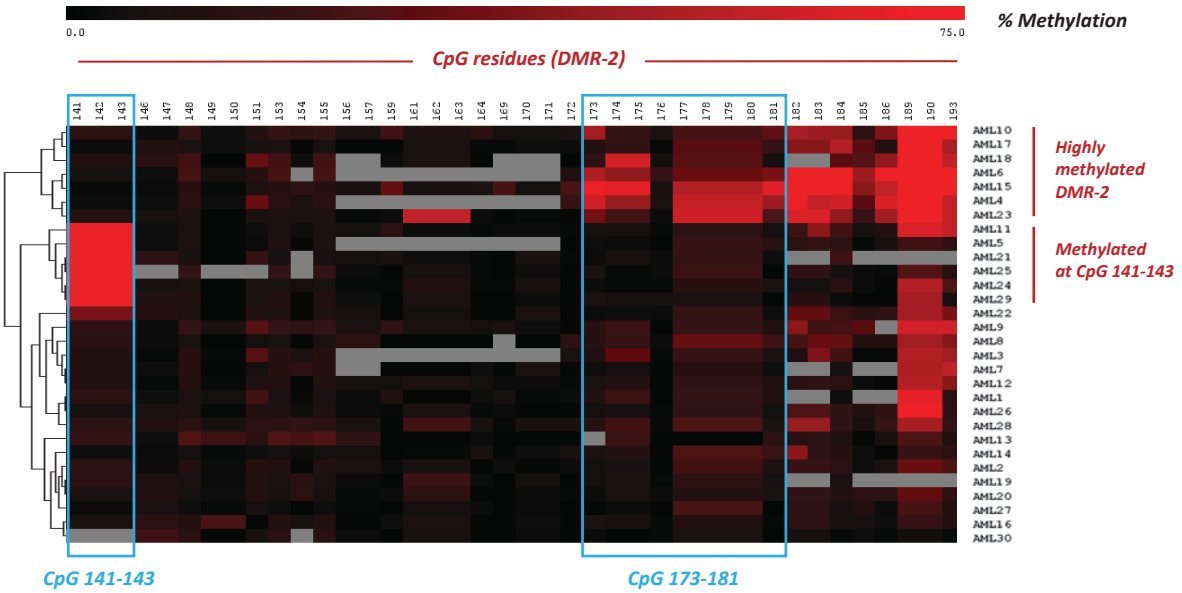

B.

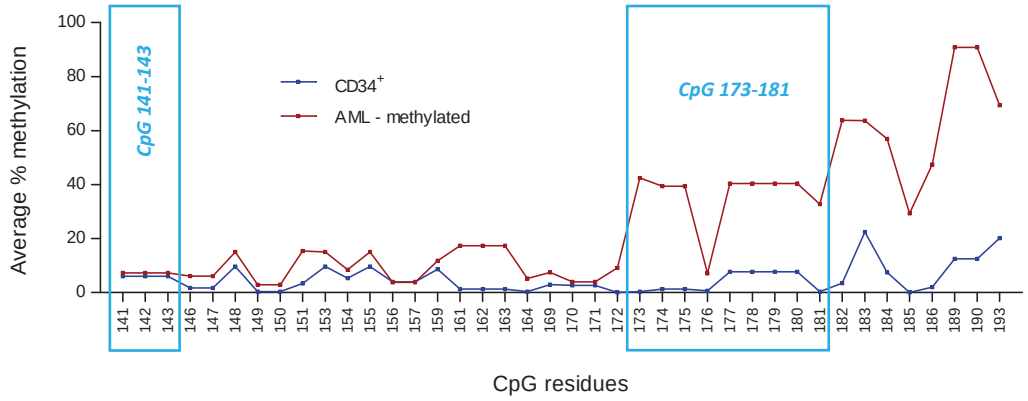

Figure 5.8 (A-B): Defining the differentially-methylated regions of *KLF5*. A. Unsupervised hierarchical clustering of AML samples (n=30) by methylation of *KLF5* CpG residues 141-193 (DMR-2). Parameters used were Euclidean distance metric selection and average linkage clustering, and the evolutionary gene tree is depicted. Heat map shows percentage methylation of individual CpG residues according to the scale shown. The AML samples with highest methylation as determined by clustering are indicated. A group of six AML samples clustered independently due to high methylation specifically at CpGs 141-143 as shown. The two regions chosen for further analysis (CpG 141-143 and CpG 173-181) are boxed in blue. Note that for CpG residues 141-143, sample AML30 did not provide informative methylation results and was excluded from further analysis. **B.** The average percentage methylation at CpG residues 141-193 for the group of highly-methylated AML samples (identified in part 'A') is shown relative to the average percentage methylation at these same residues for normal bone marrow $CD34^+$ control samples. The two regions chosen for further analysis (CpG 141-143 and CpG 173-181) are boxed in blue.

C.

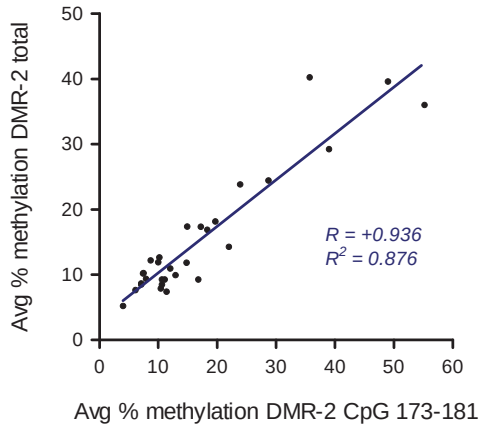

D.

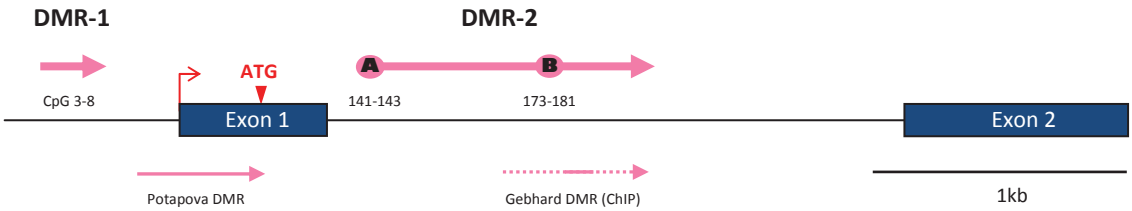

Figure 5.8 (C-D): Defining the differentially-methylated regions of *KLF5*. C. The average percentage methylation of DMR-2 CpG residues 173-181 correlates well with the average percentage methylation across the whole of DMR-2 (excluding CpG residues 141-143) as determined using linear regression analysis of methylation in AML samples (n=30). Blue line shows linear regression, R and R^2 values are indicated. **D.** The location of DMR-1 (CpG residues 3-8) and DMR-2 (CpG residues 141-193) relative to the *KLF5* genomic region assessed. The location of CpG residues 141-143 and 173-181 chosen for further analysis of DMR-2 are shown (termed DMR-2a and DMR-2b respectively). Differentially-methylated regions identified in previous studies are also indicated. Potapova, et al.[309] identified *KLF5* methylation in MDS and related disorders. Gebhard, et al.[111] identified *KLF5* methylation in leukaemia cell lines and peripheral blood from AML patients. Note that Gebhard, et al. utilised a methyl-ChIP technique to identify methylation, hence the extent of the methylated region is unclear (indicated by dotted arrow). The solid part of the arrow indicates the region used for Q-PCR in this ChIP analysis.

three CpG residues, termed DMR-2a, were hence selected for further analysis. A group of seven AML samples formed a second cluster associated with high methylation across the 3` portion of DMR-2. The average methylation in these seven methylated samples was ≥30% higher than the average methylation in normal bone marrow $CD34^+$ controls from CpG residues 173-193 (excluding CpG 176), as shown in Figure 5.8B. From this region of greatest differential methylation, we selected CpG residues 173-181 for further quantitative analysis. The average percentage methylation of these nine CpG residues, termed DMR-2b, was found to be highly representative of the average percentage methylation across the whole of DMR-2 (excluding CpG residues 141-143, DMR-2a), using results from AML samples as shown in Figure 5.8C ($R=+0.936$, $R^2=0.876$ using linear regression analysis). The nine CpG residues in DMR-2b can be assessed for methylation using a single amplicon, which will facilitate analysis of additional AML samples in the future.

The locations of DMR-1 and DMR-2 relative to the *KLF5* genomic region are depicted in Figure 5.8D. DMR-1 encompasses a 212 bp region in the proximal promoter, and DMR-2 encompasses a 1114 bp region in intron 1. The location of CpG residues selected for further analysis of methylation in DMR-2 (DMR-2a and DMR-2b) are also shown in Figure 5.8D. The location of DMR-2 (particularly DMR-2b) coincides with the region of differential methylation identified by Gebhard, et al. in AML[111]. There have been no previous reports of *KLF5* being differentially methylated in DMR-1 in AML. We did not detect any methylation in the region reported to be methylated in AML by Potapova, et al.[309].

We sought to determine if methylation of the *KLF5* proximal promoter correlated with methylation of intron 1 in AML. Using linear regression analysis, we observed that there were no significant correlations of methylation in DMR-1 with either DMR-2a or DMR-2b

(Appendix B1-2). A weak negative correlation was detected between methylation of DMR-2a and DMR-2b (Appendix B3). All further analyses were therefore performed independently on DMR-1, DMR-2a and DMR-2b.

5.2.2.3 Methylation of *KLF5* DMR-1, DMR-2a and DMR-2b in *de novo* AML

AML samples were classified as aberrantly methylated if the average percentage methylation within a particular DMR was greater than two times the standard deviation above the average methylation of BMMNC controls in the same region (Avg BMMNC + 2x STDEV). This calculation is a commonly accepted limit to define aberrant methylation (see references for example[437-439]). For DMR-1, 33% of AML samples assessed were aberrantly methylated compared to normal BMMNC controls (Figure 5.9). We were interested to determine any potential correlations of a high level of *KLF5* methylation with characteristics of AML samples at diagnosis, including FAB subtype, cytogenetic abnormality, or mutation. Interestingly, all three AML samples displaying monosomy 7/del(7q) from our cohort of 30 displayed aberrant methylation of DMR-1. Statistical analysis revealed that average DMR-1 methylation in the monosomy 7/del(7q) subgroup was significantly higher than that seen in both the BMMNC and $CD34^+$ normal controls (Figure 5.10A). It was also significantly higher than average DMR-1 methylation in a number of other cytogenetic subgroups including the normal karyotype, trisomy 8, 11q23 and t(15;17) groups (Figure 5.10A). Collectively, DMR-1 methylation was significantly greater in the monosomy 7/del(7q) subgroup than in patients negative for this abnormality (Figure 5.10B). There were no significant differences in DMR-1 methylation between different FAB subtypes and mutational categories, although there were non-significant trends observed for increased methylation in FAB M1 and in samples negative for mutations in *CEBPA, FLT3* and *NPM-1* (Figures 5.10C-D). We also assessed overall

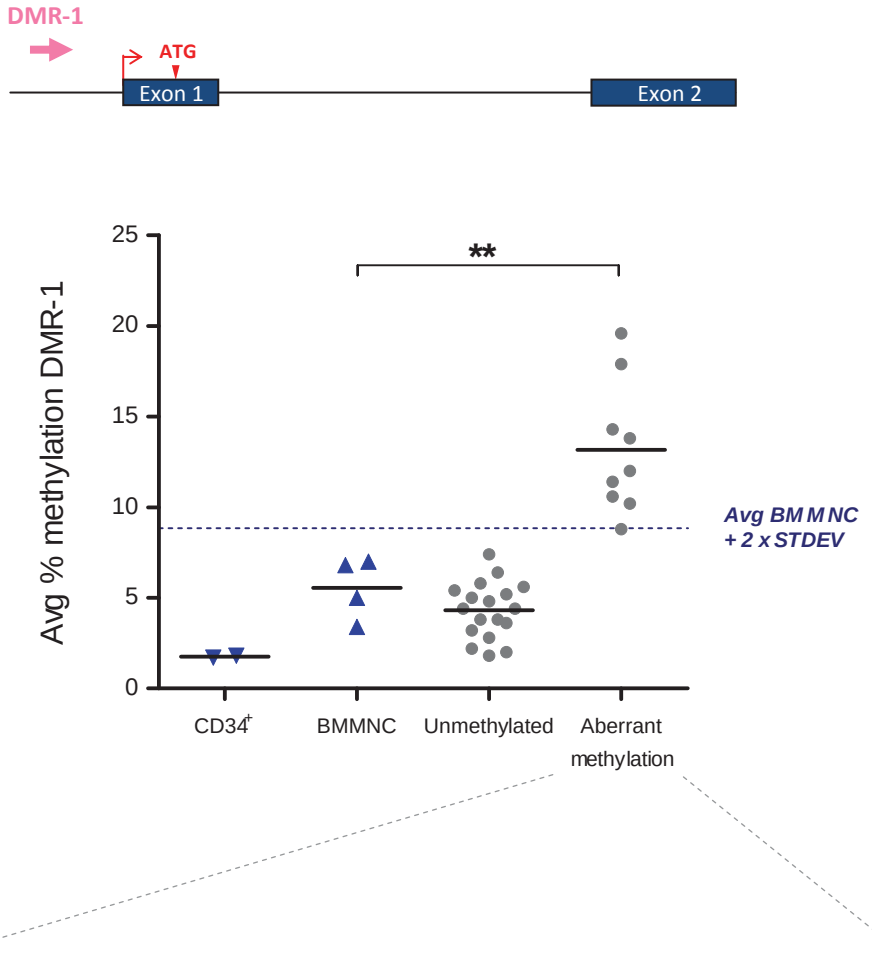

Sample	FAB	Cytogenetic abnormality	Molecular abnormality
AML1	M1	Monosomy 7	None
AML6	M1	Complex (incl. monosomy 7, del(5q))	None
AML10	M1	Complex	None
AML14	M1	Normal	None
AML15	M1	Normal	*FLT3-ITD*, *NPM1*
AML16	M2	Monosomy 7, del(7q)	None
AML23	M2	Normal	NPM1
AML24	M4	Inv(16)	None
AML28	N/A	Normal	*CEBPA*

Figure 5.9: AML samples with aberrant methylation of *KLF5* DMR-1. Average percentage methylation of DMR-1 in normal bone marrow controls (2x $CD34^+$ and 4x BMMNC) and in primary human AML BMMNC samples (n=27). The blue dotted line represents twice the standard deviation above the mean of BMMNC controls. AML samples which showed average methylation above this level were classified as aberrantly methylated (**p<0.01). The relative genomic location of DMR-1 is indicated. Characteristics of AML samples with aberrant methylation of DMR-1 are shown including FAB subtype, cytogenetic abnormality ('Normal' indicates normal karyotype), and molecular abnormality including mutations in *CEBPA*, *FLT3* or *NPM1* ('None' indicates no mutation in *CEBPA*, *FLT3* or *NPM1*). Characteristics which are over-represented in this group are indicated in purple text.

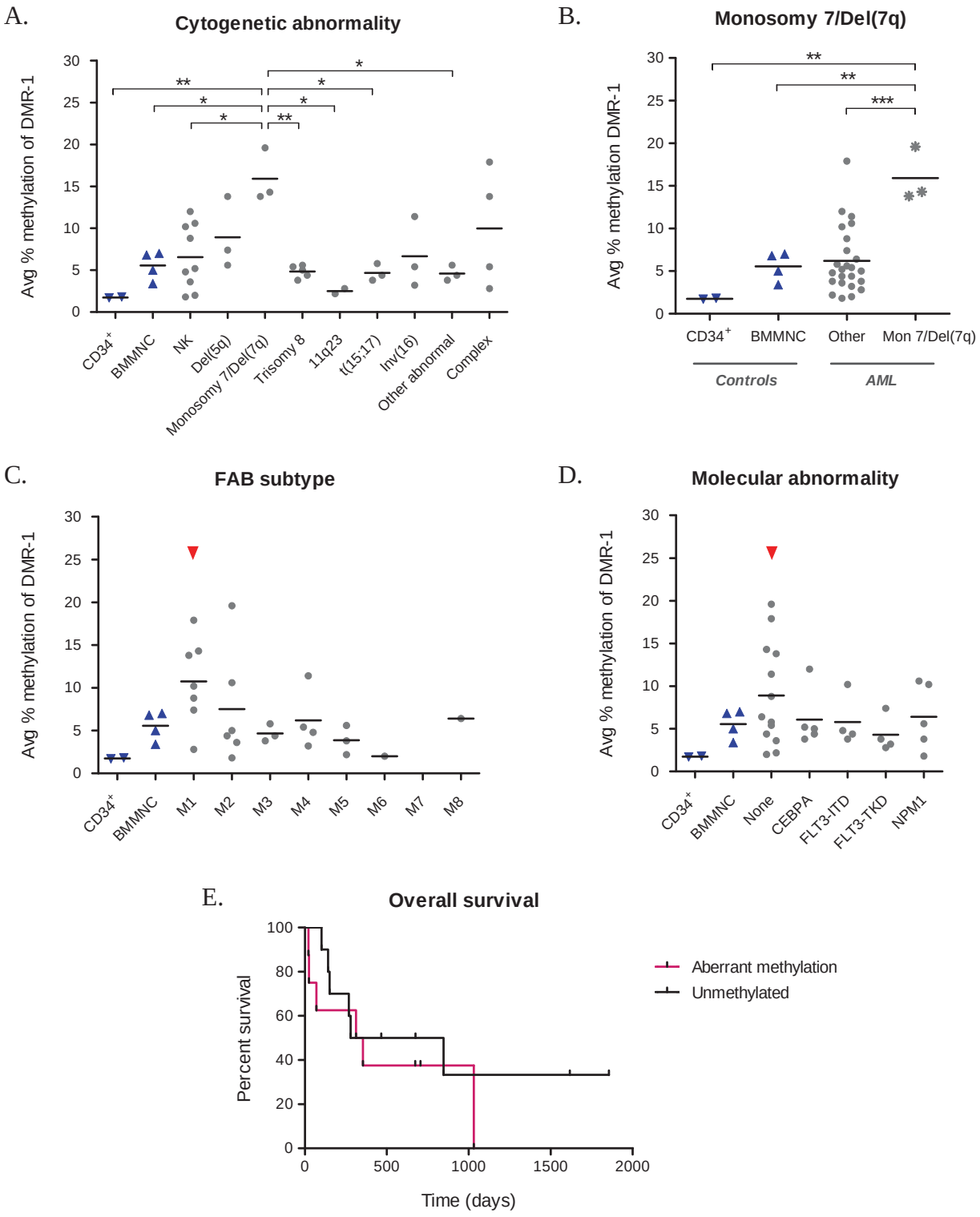

Figure 5.10: AML characteristics associated with high methylation of *KLF5* DMR-1. Average percentage methylation of *KLF5* DMR-1 in AML samples (n=27) grouped according to: **A-B.** Cytogenetic abnormality, **C.** FAB subtype, or **D. m**utation status of *CEBPA*, *FLT3* and *NPM1*. Normal bone marrow controls (2x $CD34^+$ and 4x BMMNC) are included for comparison (blue triangles). 'NK' in part 'A' indicates normal karyotype. 'None' in part 'D' indicates that these samples are negative for mutations in *CEBPA*, *FLT3* and *NPM1* but have not been screened for other point mutations common in AML. Red arrows show subgroups demonstrating trends for high methylation of DMR-1. Statistical analysis was performed using One way ANOVA with Tukey post-test comparison. *p<0.05, **p<0.01, ***p<0.001. **E.** Kaplan-Meier estimates of overall survival for patients with aberrant or normal methylation of DMR-1 (determined in Figure 5.9). Excludes FAB subtype M3 and patients who did not receive treatment. p=0.456.

survival of patients with high versus low methylation of DMR-1, excluding patients with FAB subtype M3 and those which had not received treatment. No differences in overall survival were observed, although it will be of interest to extend this analysis to a larger patient cohort (Figure 5.10E).

For DMR-2a, 24% of AML samples assessed were aberrantly methylated compared to normal BMMNC controls (Figure 5.11). Analysis of average DMR-2a methylation did not reveal a trend for increased methylation in any particular cytogenetic subgroup, although the majority of samples with high methylation of DMR-2a displayed an abnormal karyotype (Figure 5.12A). However, the difference in average DMR-2a methylation between samples presenting with a normal versus abnormal karyotype was not statistically significant ($p=0.111$) (Figure 5.12B). DMR-2a methylation did not correspond with any particular FAB subtype or mutational subgroup (Figures 5.12C-D). There were too few patients displaying hypermethylation of DMR-2a (excluding FAB M3 and untreated patients) to comment on any association with overall survival ($n=3$, Figure 5.12E).

We observed aberrant methylation of DMR-2b in 47% of AML samples (Figure 5.13). Quantitative analysis of average DMR-2b methylation revealed a trend for increased methylation in the normal karyotype group compared with normal controls and also with selected other cytogenetic subgroups (Figure 5.14A). Collectively, mean DMR-2b methylation was significantly higher in samples with normal karyotype than in those displaying abnormal cytogenetics (Figure 5.14B). There was no significant association of methylation in DMR-2b with FAB subtype or with molecular abnormality (Figure 5.14C-D). Analysis of survival revealed a trend for worse overall survival in patients displaying aberrant methylation of DMR-2b (Figure 5.14E), although this comparison did not reach significance

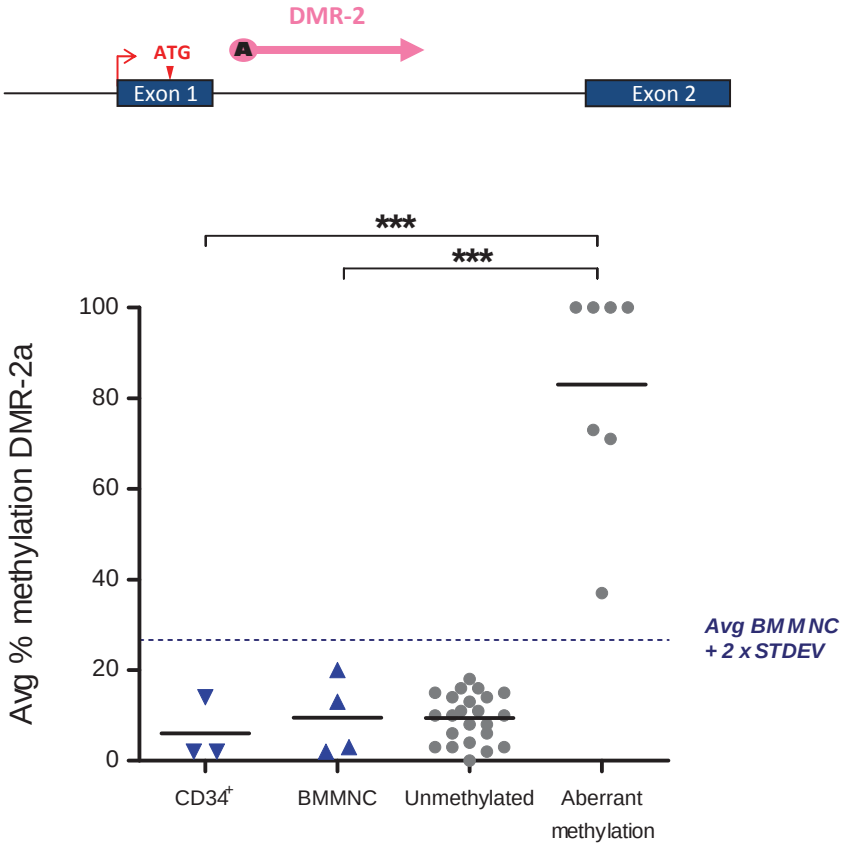

Sample	FAB	Cytogenetic abnormality	Molecular abnormality
AML5	M2	Normal	None
AML11	M2	Trisomy 14	None
AML21	M5	Trisomy 5 & 8, del(5q)	*NPM1*
AML22	M2	Trisomy 8	*CEBPA*
AML24	M4	Inv(16)	None
AML25	M4	t(13;14)	*CEBPA*
AML29	M5	t(10;11)	None

Figure 5.11: AML samples with aberrant methylation of *KLF5* DMR-2a. Average percentage methylation of DMR-2a in normal bone marrow controls (3x $CD34^+$ and 4x BMMNC) and in primary human AML BMMNC samples (n=29). The blue dotted line represents twice the standard deviation above the mean of BMMNC controls. AML samples which showed average methylation above this level were classified as aberrantly methylated (***$p<0.001$). The relative genomic location of DMR-2a is indicated. Characteristics of AML samples with aberrant methylation of DMR-2a are shown including FAB subtype, cytogenetic abnormality ('Normal' indicates normal karyotype), and molecular abnormality including mutations in *CEBPA*, *FLT3* or *NPM1* ('None' indicates no mutation in *CEBPA*, *FLT3* or *NPM1*).

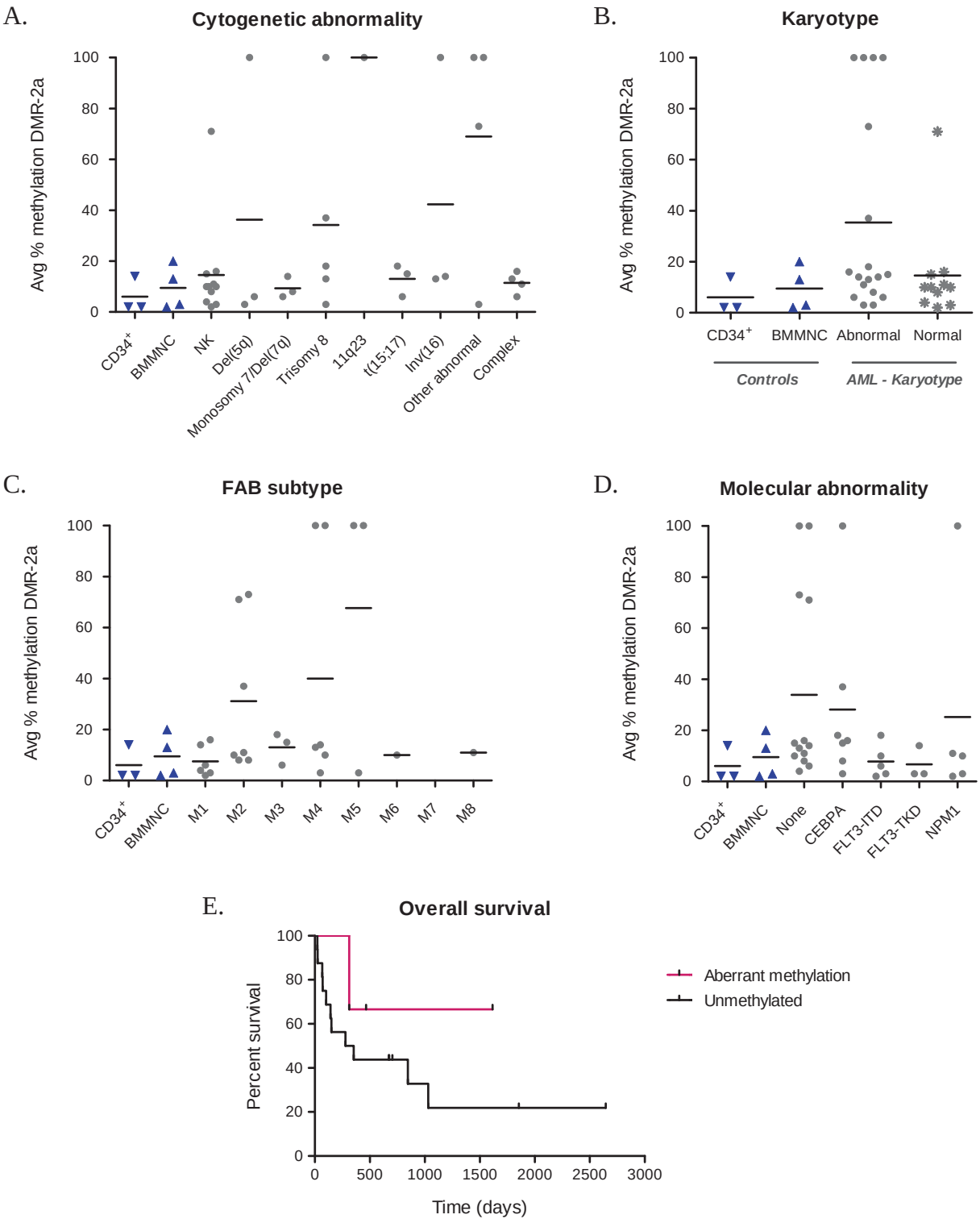

Figure 5.12: AML characteristics associated with high methylation of *KLF5* DMR-2a. Average percentage methylation of *KLF5* DMR-2a in AML samples (n=29) grouped according to: **A-B.** Cytogenetic abnormality, **C.** FAB subtype, or **D. m**utation status of *CEBPA*, *FLT3* and *NPM1*. Normal bone marrow controls (3x $CD34^+$ and 4x BMMNC) are included for comparison (blue triangles). 'NK' in part 'A' indicates normal karyotype. 'None' in part 'D' indicates that these samples are negative for mutations in *CEBPA*, *FLT3* and *NPM1* but have not been screened for other point mutations common in AML. Statistical analysis was performed using One way ANOVA with Tukey post-test comparison. **E.** Kaplan-Meier estimates of overall survival for patients with aberrant or normal methylation of DMR-2a (determined in Figure 5.11). Excludes FAB subtype M3 and patients who did not receive treatment. p=0.283.

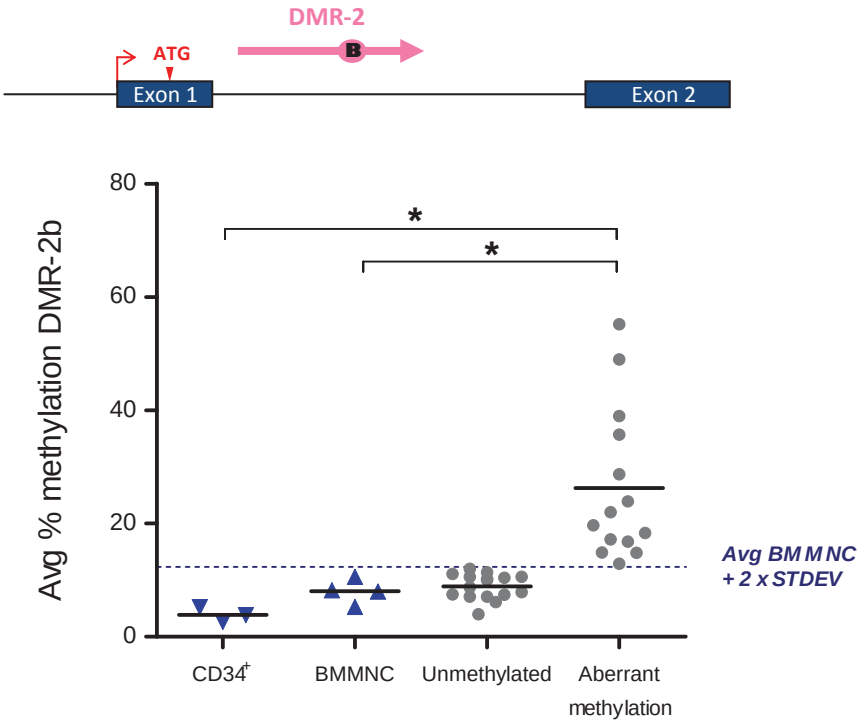

Sample	FAB	Cytogenetic abnormality	Molecular abnormality
AML1	M1	Monosomy 7	None
AML2	M3	t(15;17)	None
AML3	M8	Complex (incl. t(9;22))	None
AML4	M4	Normal	*FLT3-ITD*
AML6	M1	Complex (incl. monosomy 7, del(5q))	None
AML8	M4	Complex (incl. inv(16), trisomy 8)	None
AML9	N/A	Normal	*CEBPA*
AML10	M1	Complex	None
AML14	M1	Normal	None
AML15	M1	Normal	*FLT3-ITD*, *NPM1*
AML17	M1	Del(5q)	*FLT3-TKD*
AML18	M6	Normal	None
AML23	M2	Normal	*NPM1*
AML28	N/A	Normal	*CEBPA*

Figure 5.13: AML samples with aberrant methylation of *KLF5* DMR-2b. Average percentage methylation of DMR-2b in normal bone marrow controls (3x $CD34^+$ and 4x BMMNC) and in primary human AML BMMNC samples (n=30). The blue dotted line represents twice the standard deviation above the mean of BMMNC controls. AML samples which showed average methylation above this level were classified as aberrantly methylated (*$p<0.05$). The relative genomic location of DMR-2b is indicated. Characteristics of AML samples with aberrant methylation of DMR-2b are shown including FAB subtype, cytogenetic abnormality ('Normal' indicates normal karyotype), and molecular abnormality including mutations in *CEBPA*, *FLT3* or *NPM1* ('None' indicates no mutation in *CEBPA*, *FLT3* or *NPM1*). Characteristics which are over-represented in this group are indicated in purple text.

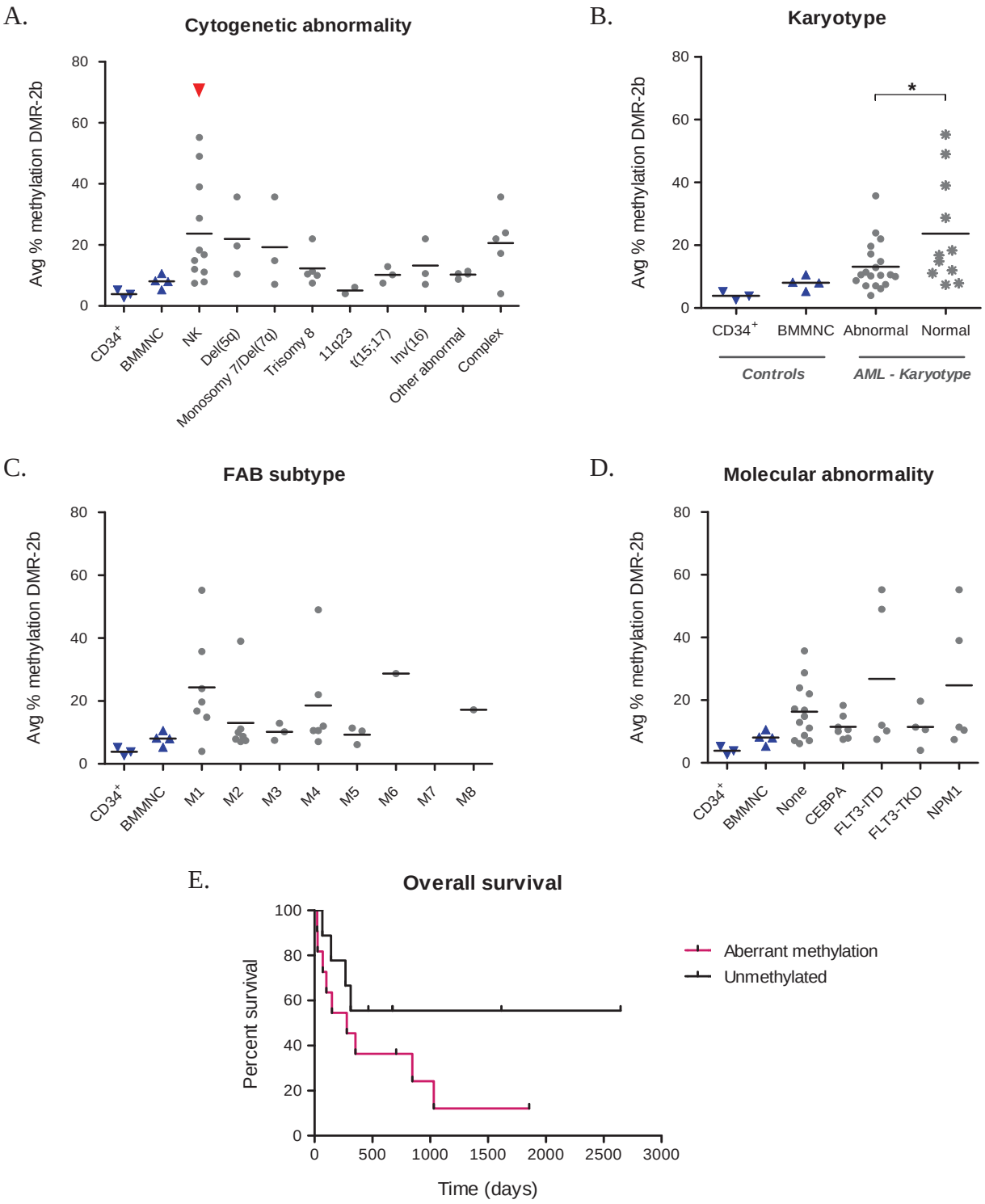

Figure 5.14: AML characteristics associated with high methylation of *KLF5* DMR-2b. Average percentage methylation of *KLF5* DMR-2b in AML samples (n=30) grouped according to: **A-B.** Cytogenetic abnormality, **C.** FAB subtype, or **D. m**utation status of *CEBPA*, *FLT3* and *NPM1*. Normal bone marrow controls (3x $CD34^+$ and 4x BMMNC) are included for comparison (blue triangles). 'NK' in part 'A' indicates normal karyotype. 'None' in part 'D' indicates that these samples are negative for mutations in *CEBPA*, *FLT3* and *NPM1* but have not been screened for other point mutations common in AML. Red arrows show subgroups demonstrating trends for high methylation of DMR-2b. Statistical analysis was performed using One way ANOVA with Tukey post-test comparison. *p<0.05. **E.** Kaplan-Meier estimates of overall survival for patients with aberrant or normal methylation of DMR-2a (determined in Figure 5.13). Excludes FAB subtype M3 and patients who did not receive treatment. p=0.257.

(p=0.257). It will be necessary to further investigate comparisons of *KLF5* methylation in each of the DMRs with AML characteristics and overall survival due to the limited number of AML samples in the current analysis.

5.2.2.4 Correlation of *KLF5* methylation with relative mRNA expression

We next sought to determine whether methylation of *KLF5* in any of the DMRs correlated with relative *KLF5* expression as detected by Q-PCR in Section 5.2.1.1. Linear regression analysis and Fisher's exact test did not detect a significant correlation of aberrant methylation in any DMR with reduced *KLF5* mRNA expression (Appendix C). We did, however, observe a non-significant trend for decreased average *KLF5* expression in AML samples with aberrant methylation of DMR-1 or DMR-2b compared with unmethylated samples (Figure 5.15). This trend was not observed for DMR-2a. Aberrant methylation of either DMR-1 or DMR-2b was not detected in any samples displaying a high level of *KLF5* mRNA expression (relative expression level of >2.0), which is consistent with hypermethylation of these two regions acting to repress *KLF5* transcription. Note that AML7 was excluded from these analyses as an outlier, as it displayed abnormally high levels of *KLF5* expression (see Section 5.2.1.1). However, consistent with this observation, we observed little methylation of AML7 in DMR-1 or DMR-2 (see Figure 5.7). Analysis of additional samples may improve the significance of the correlation between hypermethylation of DMR-1/DMR-2b and reduced mRNA expression.

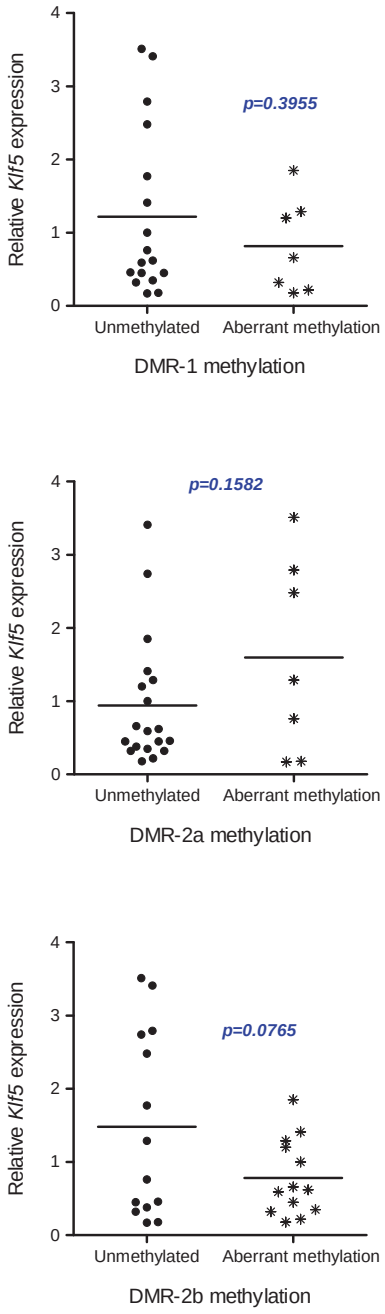

Figure 5.15: Correlation of relative *KLF5* mRNA expression with average methylation of *KLF5* DMR-1, DMR-2a and DMR-2b. *KLF5* mRNA expression as detected by Q-PCR (relative to AML4 – see Figure 5.1) in AML samples according to methylation status of DMR-1, DMR-2a or DMR-2b. Aberrantly methylated samples were determined in Figures 5.9, 5.11 and 5.13 for DMR-1, DMR-2a and DMR-2b respectively. Note that AML7 was excluded as an outlier (see Figure 5.1).

5.2.2.5 Treatment with demethylating agents activates *KLF5* transcription

We selected four leukaemia cell lines for functional analysis of *KLF5* methylation including THP-1, HL-60, KG-1 and U937 cells (characteristics shown in Table 5.2). These cell lines exhibited a range of *KLF5* expression levels, as shown in Figure 5.16A, and of *KLF5* methylation in DMR-1 and DMR-2, shown in Figure 5.16B. The cell lines were treated with methyltransferase inhibitors (4 μM 5-azacytidine or 5 μM 5-aza-2-deoxycytidine) for 48 hours to induce global DNA demethylation. RNA was isolated from treated and untreated cells at this time-point, and Q-PCR performed to quantitate *KLF5* expression. For each cell line, *KLF5* expression was determined relative to untreated cells.

U937 cells, which displayed the lowest *KLF5* expression and highest methylation, showed a 3.0-fold reactivation of *KLF5* expression on treatment with 5-azacytidine and a 7.8-fold reactivation on treatment with 5-aza-2-deoxycytidine (Figure 5.16C). THP-1 cells, which conversely displayed the highest *KLF5* expression and lowest methylation, did not show reactivation of *KLF5* expression on treatment with 5-azacytidine. We did however observe a modest induction of *KLF5* expression in THP-1 cells treated with 5-aza-2-deoxycytidine (2.6-fold). We observed a greater induction of *KLF5* expression in KG-1 cells than in HL-60 cells on treatment with the demethylating agents. This was particularly evident on treatment with 5-aza-2-deoxycytidine, where KG-1 cells showed a similar level of reactivation to U937 cells (7.4 and 7.8-fold respectively), while HL-60 cells showed less reactivation than THP-1 cells (2.2 and 2.6-fold respectively). Taken together with the observation that HL-60 cells displayed higher methylation than KG-1 cells in DMR-2, and less methylation in DMR-1, this suggests that methylation at DMR-1 may be involved in functional repression of *KLF5* transcription.

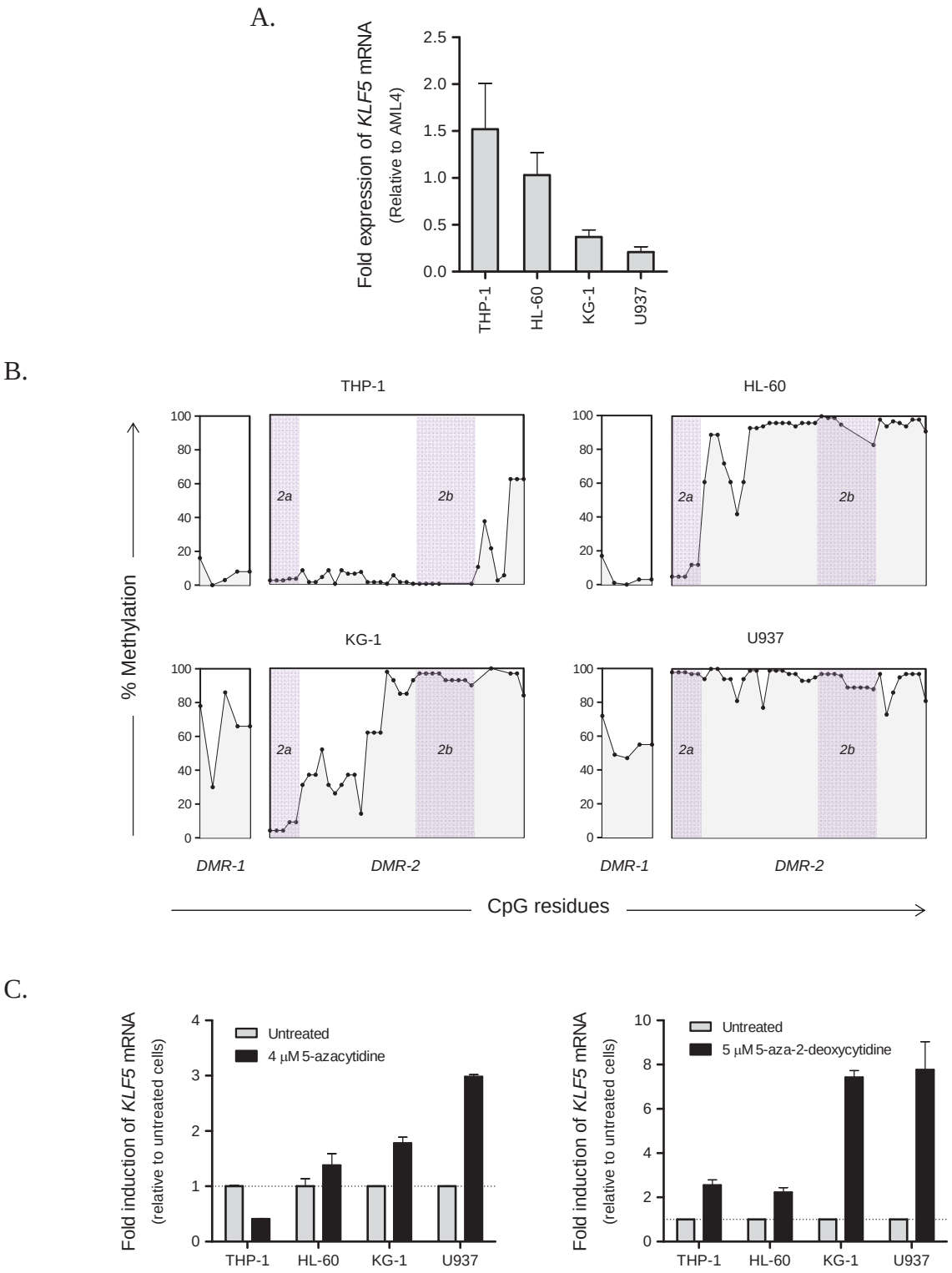

Figure 5.16: Reactivation of *KLF5* mRNA expression on treatment with demethylating agents. A. *KLF5* mRNA expression of selected human leukaemia cell lines relative to AML4 (see Figure 5.1, n=8). **B.** Percentage methylation of CpG residues in *KLF5* DMR-1 and DMR-2 in selected human leukaemia cell lines (determined in Section 5.2.2.2). DMR-1 = 5 CpG residues, DMR-2 = 40 CpG residues. The location of residues used for analysis of DMR-2a and DMR-2b are shown in purple. **C.** Induction of *KLF5* expression in selected human leukaemia cell lines in response to treatment with 5-azacytidine (n=3) or 5-aza-2-deoxycytidine (n=3). Cells were treated for 48 hours with the demethylating agents at the concentrations indicated, and *KLF5* expression was determined by Q-PCR and plotted relevant to expression in untreated cells.

5.2.2.6 Potential significance of differentially-methylated regions for the transcriptional regulation of *KLF5*

We were interested to investigate how methylation of DMR-1 and DMR-2 could potentially affect *KLF5* transcription. Figure 5.17 shows features of the *KLF5* genomic region analysed and alignment with the differentially-methylated regions identified in this study. The degree of interspecies conservation across the *KLF5* region analysed is also depicted (44 vertebrate species, UCSC Genome Browser). There are two regions of highly-conserved homology in intron 1 of *KLF5*, termed Homology regions 1 and 2 (HR-1 and HR-2). Figure 5.17 also shows known transcription factor binding sites, as well as interspecies conserved binding sites predicted using the UCSC Genome Browser.

DMR-1 lies in the proximal promoter of *KLF5* (-529 to -318 bp from initiation of transcription). It encompasses a relatively highly conserved region of DNA which includes a known CEBPβ/δ binding site[156]. This binding site also corresponds with the consensus sequence for binding of C/EBPα, which is consistent with observations suggesting that C/EBPα may be an upstream activator of *KLF5* expression in haemopoiesis (discussed in Chapter 4, Section 4.3.4). Hence it is conceivable that *KLF5* expression may be deregulated due to methylation across this C/EBP binding site in AML.

DMR-2 lies in the 5` portion of intron 1 (+744 to +1855 bp from initiation of transcription). CpG residues 141-143 in DMR-2 (DMR-2a, +744 to +755 bp from initiation of transcription) are specifically methylated in a subset of AML samples as shown in Figure 5.8A. These do not lie in a region of high interspecies conserved homology (Appendix D1). Using a transcription factor binding site prediction program from the Technical University of

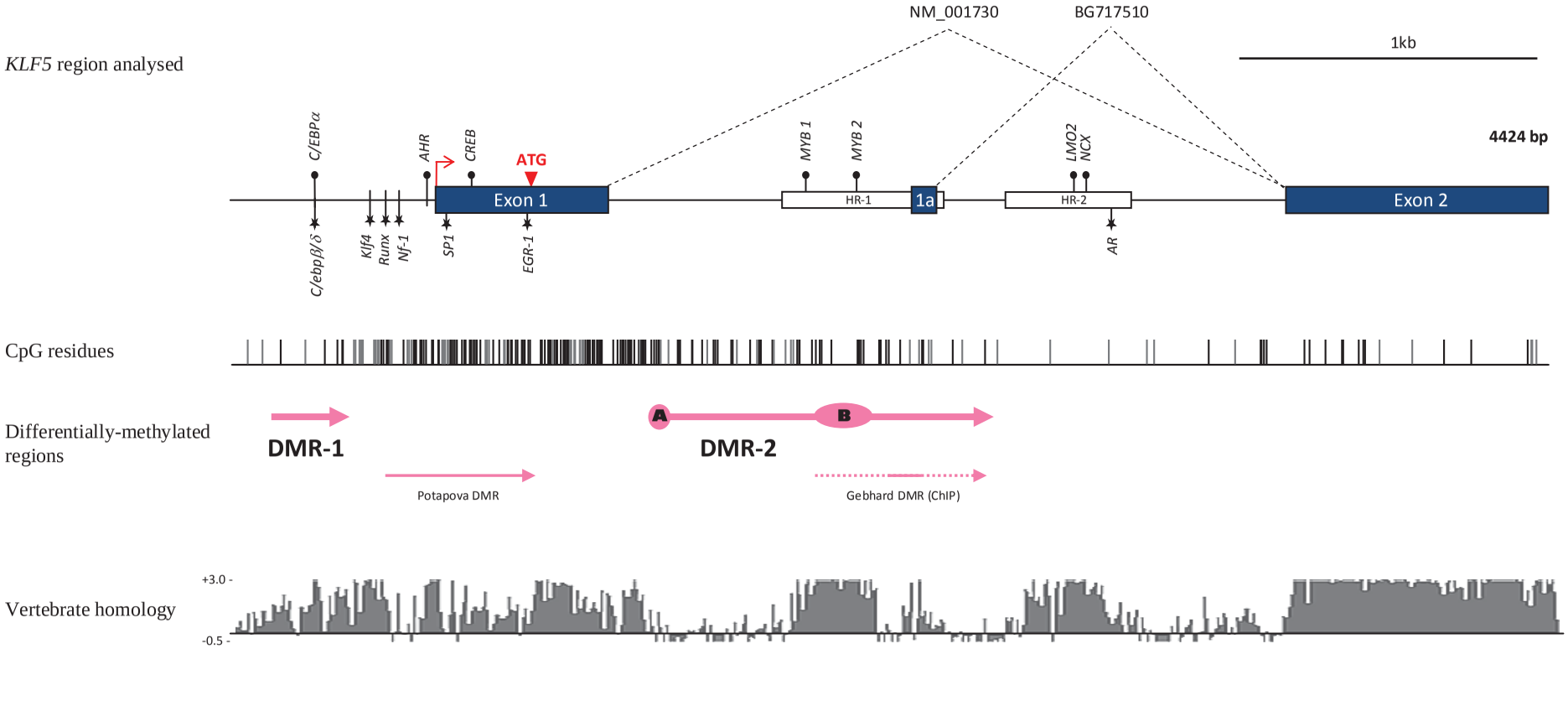

Figure 5.17: Methylation and potential mechanisms for deregulation of *KLF5* expression in AML. Detailed representation of the *KLF5* genomic region analysed by Sequenom EpiTYPER. Exons are shown in blue, intronic regions of highly conserved homology in vertebrates are depicted as white boxes (HR-1 and HR-2 = Homology Regions #1 and #2). Known transcription factor binding sites are indicated with stars, predicted transcription factor binding sites (UCSC Genome Browser) are indicated with circles. Note that lower case transcription factor names indicate that regulation by these transcription factors has been shown in rat or mouse and remains to be validated for the human promoter. Dotted lines represent splice variants, including the common *KLF5* transcript (NM_001730) and the EST containing alternative exon 1a (BG717510). Individual CpG residues are indicated. Differentially-methylated regions are shown with pink arrows. DMR-1 and DMR-2 were identified in the current study, and the relative location of selected residues for analysis of DMR-2 is shown (DMR-2a = CpG 141-143 and DMR-2b = CpG 173-181). The relative conservation amongst 44 vertebrate species across the *KLF5* region analysed is also shown (UCSC Genome Browser). Highly homologous sequences between species are given positive scores, indicating that they have evolved more slowly than would have been predicted. Divergent sequences are given a negative score, as they have evolved more quickly. For a detailed explanation of the homology scoring system see UCSC Genome Browser, Vertebrate Multiz Alignment and Conservation feature.

Catalonia[440,441], we found predicted binding sites for human ENKTF1, E2F1, p53, PAX5 and FOXP3 in the DNA sequence encompassing CpG residues 141-143 (+5 nucleotide residues upstream of CpG 141, and +5 nucleotide residues downstream of CpG 143) (Appendix D2). However there have been no reports of *KLF5* transcriptional regulation by these proteins to date.

Interestingly, the 3` half of DMR-2 encompasses the first of the two highly conserved regions in intron 1 of *KLF5* (HR-1) (see Figure 5.17). This high degree of homology suggests an evolutionarily conserved regulatory function for this DNA sequence in control of *KLF5* expression. Using the UCSC Genome Browser, we identified two predicted MYB binding sites within DMR-2, raising the possibility that the oncogenic MYB protein may have a role in regulating *KLF5* expression, and that this may be altered by methylation in AML. The CpG residues in DMR-2b (CpG 173-181, +1284 to +1446 bp from initiation of transcription) encompass the second predicted MYB binding site, and CpG residues 177-179 lie within this predicted binding sequence.

Further investigation of this region using the UCSC Genome Browser identified a previously undescribed alternative exon within *KLF5* intron 1, which also lies in the highly conserved HR-1 and within DMR-2b (see Figure 5.17). We identified an EST (accession number BG717510) cloned from a testis cDNA library (NIH_MGC_97) which contains the alternative exon (termed exon 1a) spliced to exon 2 of *KLF5*. Sequencing of the clone revealed that the cDNA sequence begins at this alternative exon 1a rather than the previously annotated exon 1 (Figure 5.18A), suggesting an alternative transcription start site for *KLF5*. As exon 1a lies adjacent to the predicted MYB binding sites, this led us to speculate that these

binding sites form part of an alternative promoter region for initiation of transcription at exon 1a.

To verify that this variant isoform of *KLF5* is expressed, oligonucleotide primers were designed to specifically detect splicing from exon 1a to exon 2 (BG717510 primer set) using reverse-transcription PCR. The primer set used for Q-PCR analysis of *KLF5* expression, which detects both the BG717510 and the primary NM_001730 *KLF5* transcripts (splicing from exon 2 to exon 3), was also utilised as a control. The location of these oligonucleotide primers relative to each transcript is depicted in Figure 5.18A. mRNA was isolated and cDNA produced from a range of templates including a non-haemopoietic, non-tumorous cell line (HEK-293T - fibroblast), a non-haemopoietic, cancerous cell line (MCF7 – breast cancer), seven human leukaemia cell lines with varying degrees of *KLF5* expression and methylation (HL-60, K562, KG-1, MOLM-13, MV4;11, THP-1 and U937), and a primary normal human BMMNC control sample (C8 BMMNC).

PCR using the BG717510 primer set on the cDNA templates listed above produced a product at approximately 300 bp in the MCF7 breast cancer cell line, and in the HL-60 and K562 leukaemia cell lines, which is consistent with the expected product size of 298 bp (Figure 5.18B). These products were excised and isolated from the agarose gel and sequenced to verify amplification of the correct product. Sequencing confirmed splicing of exon 1a to exon 2 as detected in the initial EST clone BG717510 (Figure 5.18C). The complete BG717510 EST clone consists of exons 1a, 2, 3 and 4 of *KLF5*. Translation of this EST from the ATG start codon in exon 2 would produce a truncated KLF5 protein lacking the N-terminal 91 amino acids (Figures 5.18D-E). This truncated protein would still retain the KLF5 nuclear export signal, and the transactivation and DNA-binding domains.

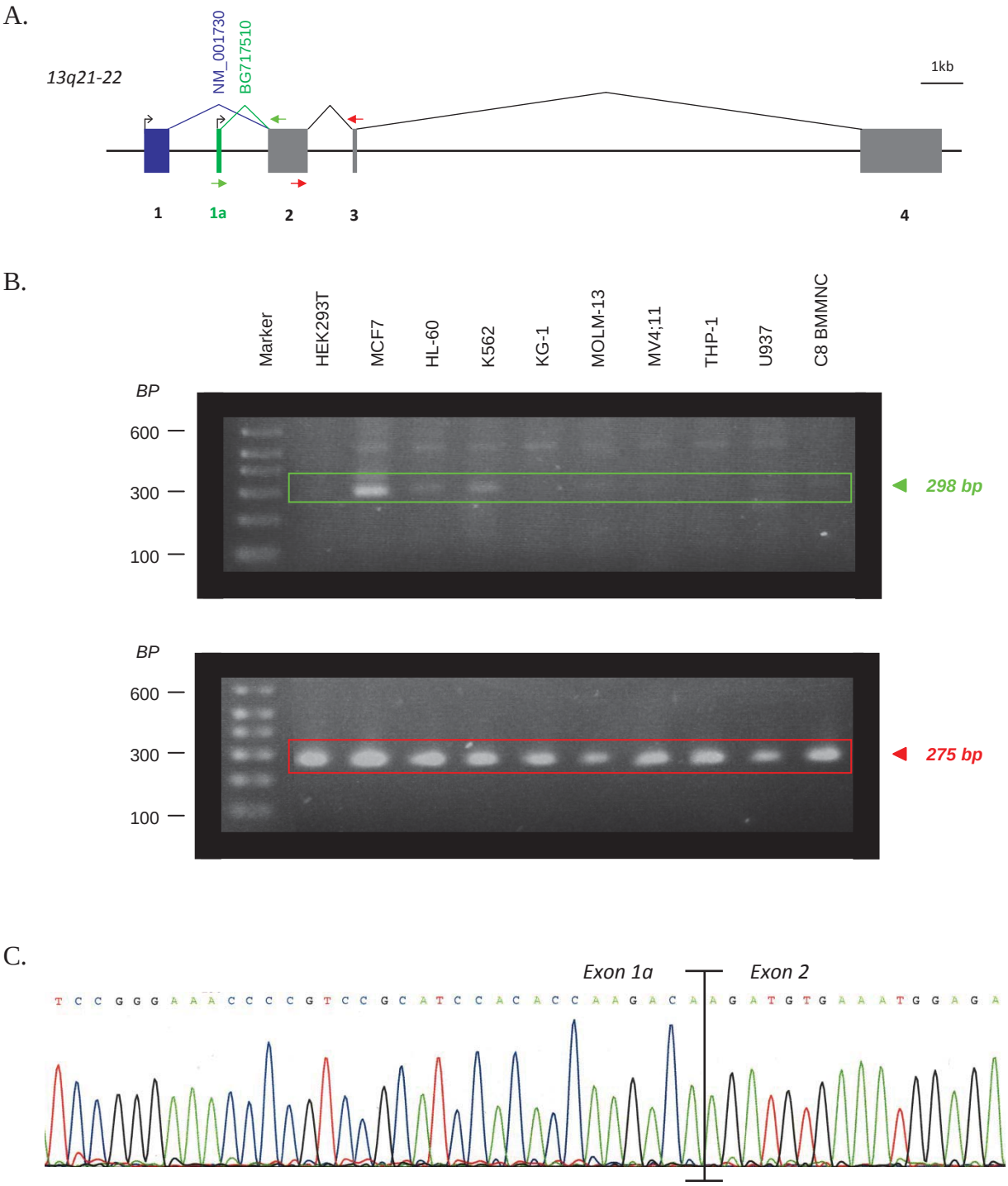

Figure 5.18 (A-C): *KLF5* EST BG717510. A. Structure of transcripts for *KLF5* NM_001730 and BG717510. Transcription for NM_001730 begins at exon 1 (blue) and is spliced to exon 2. Transcription for BG717510 is predicted to begin at exon 1a (green) and is spliced to exon 2. The location of oligonucleotide primers for specific detection of the BG717510 transcript are depicted with green arrows, and the control oligonucleotide primers which detect both transcripts are depicted with red arrows. **B.** Top panel: PCR was performed on cDNA from a range of cell types using primers to specifically detect the BG717510 *KLF5* transcript. The green box indicates the expected product size for this PCR (298 bp). Bottom panel: PCR was performed on the same cDNA using control primers which detect both BG717510 and NM_001730 *KLF5* transcripts. The expected product size for this PCR is 275 bp (boxed in red). **C.** Chromatogram sequence of the PCR product from primers used to detect the *KLF5* BG717510 transcript. The chromatogram shows 50 bp of the 298 bp product, and the boundary between exon 1a and exon 2.

D.

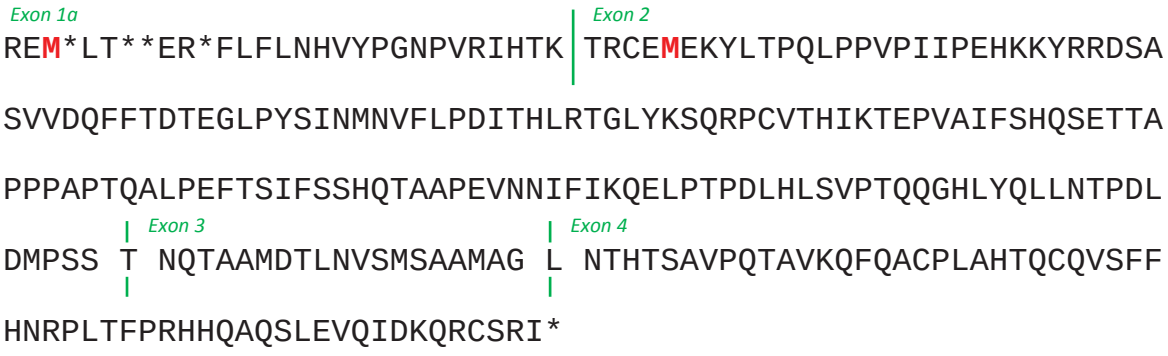

E.

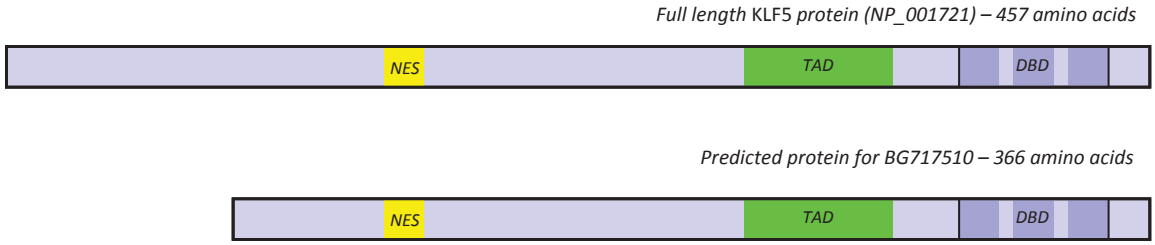

Figure 5.18 (D-E): *KLF5* EST BG717510. D. In-frame translation of EST BG717510. Potential initiating methionines are shown in red, stop codons are shown with *. Initiation at the first methionine would result in an untranslated *KLF5* mRNA; initiation at the second methionine would produce a protein containing most of exon 2, and all of exons 3 and 4. **E.** Full length KLF5 protein (NP_001721) and predicted protein resulting from translation of BG717510 at the second initiating methionine. NES = nuclear export signal, TAD = transactivation domain, DBD = zinc-finger DNA-binding domain.

5.2.3 Enforced expression of KLF5 in the U937 leukaemia cell line enhances differentiation

5.2.3.1 KLF5 induces expression of the myeloid marker CD11B in U937 leukaemia cells

Of the four leukaemia cell lines assessed in Section 5.2.2.5, the U937 cell line displayed the lowest relative level of *KLF5* mRNA expression and highest methylation of the *KLF5* proximal promoter and intron 1 (see Figures 5.16A-B). In order to assess the potential tumour suppressor activity of KLF5, we expressed KLF5 in the U937 cell line and analysed functional effects on growth, survival and differentiation. For these experiments, human *KLF5* was constitutively expressed from the MIG retroviral vector. Cells were retrovirally transduced with the empty MIG vector or MIG-*KLF5*, and sorted for GFP expression 48 hours later. Purified GFP^+ populations were allowed to recover overnight then seeded in assays for functional assessment (Day 3 post-transduction). Note that the percentage of cells positive for GFP in each population was ≥85% at all time points of the assay.

Growth and viability were assessed by determining GFP^+ cell number and total cell viability over 2 weeks following transduction. Transduction with *KLF5* did not affect expansion (Figure 5.19A) or viability (Figure 5.19B) of U937 cells when compared to cells transduced with the empty vector control. Stable populations were further assessed for effects on differentiation using morphological analysis and staining for expression of the cell surface markers CD11B and CD14. Two-colour flow cytometry demonstrated that transduction with *KLF5* significantly increased the MFI of CD11B expression on GFP^+ cells compared with controls (Figures 5.19C-D). There was no effect on expression of the monocytic marker

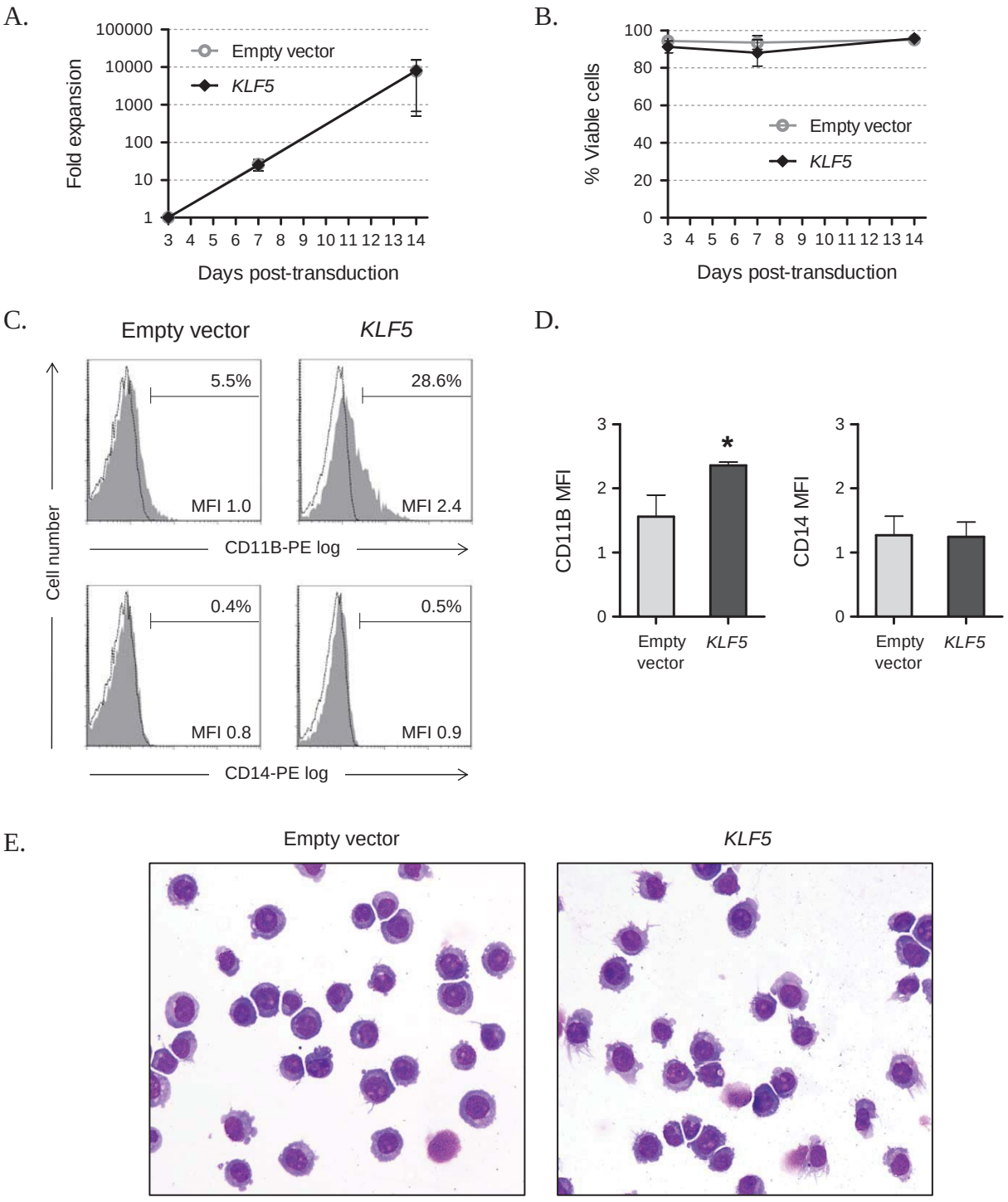

Figure 5.19: Enforced expression of KLF5 in the U937 leukaemia cell line model. A. GFP$^+$ cell expansion. The total number of live cells was determined at each time-point by Trypan Blue staining and cell counts, and the percentage of GFP$^+$ cells determined by flow cytometry. The number of GFP$^+$ cells was hence determined and expansion calculated relative to seeding on Day 3. n=2. **B.** Total cell viability was assessed by Trypan Blue staining and cell counts at each time-point. n=2. **C.** Two-colour flow cytometric detection of CD11B and CD14 expression on U937 cells transduced with *KLF5* or the empty vector control. Expression was detected using PE-conjugated antibodies on GFP$^+$ cells. Profiles show representative results from a typical experiment on Day 21 post-transduction (stable cell populations). Empty peak = isotype control, grey peak = cell surface marker expression. **D.** Average MFI of CD11B and CD14 on U937 cells transduced with *KLF5* or the empty vector on Day 21 post-transduction (n=3). *p<0.05. **E.** Representative photomicrographs showing Wright-Giemsa stained cytospin preparations of U937 cells transduced with *KLF5* or the empty vector control (Day 21). Original magnification = 200x. Note that cells were ≥85% GFP$^+$ at all time-points of these assays.

CD14 due to transduction with *KLF5*. We did not observe gross changes in morphology of U937 cells transduced with *KLF5*, although these cells displayed increased formation of cytoplasmic protrusions compared to control cells (Figure 5.19E).

5.2.3.2 KLF5 enhances the response of the U937 cell line to differentiation-inducing agents

Stable U937 cell populations transduced with *KLF5* or the empty vector control (from Section 5.2.3.1) were treated with chemical inducers of myeloid differentiation to determine if enforced expression of KLF5 cooperates to enhance differentiation in these conditions. U937 is a myelomonocytic leukaemia cell line (see Table 5.2) which undergoes monocyte-macrophage differentiation in response to a number of reagents including PMA, Vitamin D_3 and Interferon-gamma[442-444]. In response to ATRA, U937 cells exhibit some characteristics of granulocyte differentiation, such as increased CD11B expression but not CD14, and lobulated nuclei[445,446], however studies have also shown up-regulation of several genes related to a more monocyte-macrophage phenotype in this system[447-452]. U937 cells transduced with *KLF5* or the empty MIG vector were treated with 0.3 μM ATRA or 5 nM PMA to determine if enforced expression of KLF5 enhanced granulocyte and/or monocyte differentiation in these conditions. Populations were seeded at $1x10^5$ cells/ml and assayed over 5 days for effects on cell viability, expansion, and differentiation. Note that the percentage of cells positive for GFP in each population was ≥85% at all time points of these assays.

Transduction with *KLF5* did not affect expansion of GFP^+ cells (Figure 5.20A) or total cell viability (Figure 5.20B) of U937 cells cultured in ATRA when compared to empty vector-transduced control cells. Two-colour flow cytometry was utilised to detect expression of the

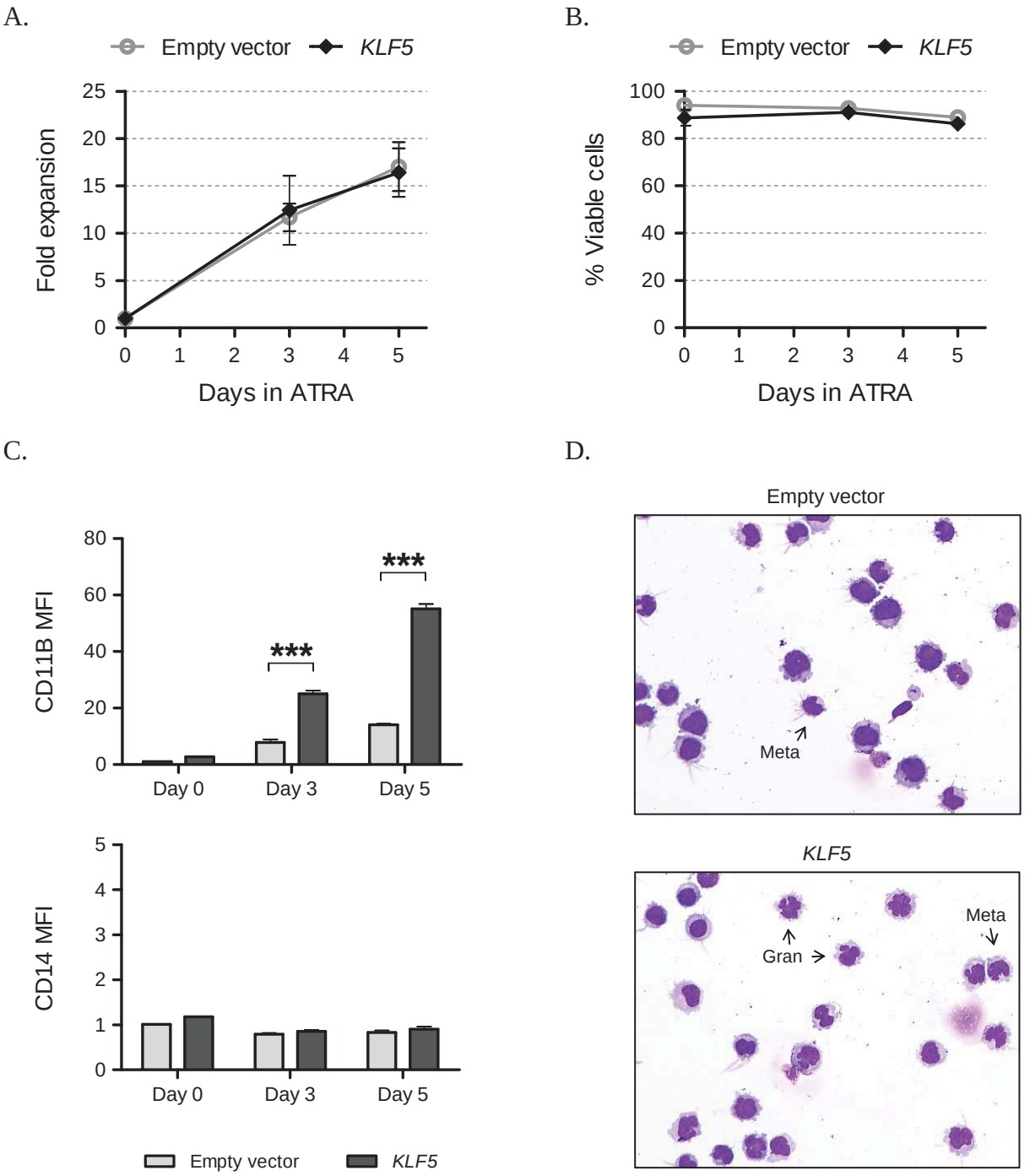

Figure 5.20: ATRA treatment of *KLF5*-transduced U937 cells. A. GFP$^+$ cell expansion in ATRA. The total number of live cells was determined at each time-point by Trypan Blue staining and cell counts, and the percentage of GFP$^+$ cells determined by flow cytometry. The number of GFP$^+$ cells was hence determined and expansion calculated relative to seeding on Day 0. n=3. **B.** Total cell viability was assessed by Trypan Blue staining and cell counts at each time-point following ATRA treatment. n=3. **C.** Two-colour flow cytometric detection of CD11B and CD14 expression on ATRA-treated U937 cells transduced with *KLF5* or the empty vector control. Expression was detected using PE-conjugated antibodies on GFP$^+$ cells. Figures show average MFI on Days 0, 3 and 5 post-treatment (n=3). ***p<0.001. **D.** Representative photomicrographs showing Wright-Giemsa stained cytospin preparations of U937 cells transduced with *KLF5* or the empty vector control at Day 5 post-ATRA treatment. Meta = metamyelocytes, Gran = segmented or lobulated mature granulocyte. Original magnification = 200x. Note that cells were ≥85% GFP$^+$ at all time-points of these assays.

myeloid marker CD11B and the monocytic marker CD14 on GFP^+ U937 cells transduced with *KLF5* or the empty vector control (Figure 5.20C). The MFI of CD11B expression on control cells increased over 5 days of ATRA treatment, consistent with myeloid differentiation, however this increase was significantly greater in cells transduced with *KLF5* indicating enhanced differentiation. No changes in CD14 expression were observed in either control cells or *KLF5*-transduced cells, which is consistent with the development of a granulocytic phenotype in response to ATRA treatment rather than a monocytic phenotype. Morphologically, control cells developed cytoplasmic protrusions by Day 5 of ATRA treatment, and a proportion of cells exhibited indented nuclei which are characteristic of metamyelocytes (Figure 5.20D). *KLF5*-transduced cells treated with ATRA for 5 days also differentiated to metamyelocytes, however a proportion of cells displayed lobulated or segmented nuclei which are characteristic of more mature cells of the granulocyte series. These observations are consistent with enhanced granulocyte differentiation of U937 cells in ATRA due to transduction with *KLF5*.

When cultured in PMA, *KLF5*-transduced cells exhibited reduced GFP^+ cell expansion compared to cells carrying the empty vector (Figure 5.21A). The reduced expansion was not a consequence of decreased cell viability (Figure 5.21B). Flow cytometric analysis demonstrated that expression of both the myeloid marker CD11B and the monocytic marker CD14 increased on PMA treatment of control cells (Figure 5.21C). However this increase was significantly higher in cells transduced with *KLF5* compared to cells carrying the empty vector on Day 5 of treatment. Morphologically, control U937 cells showed evidence of macrophage differentiation when treated with PMA, with mature macrophages observed on Day 5 of treatment characterised by a large cytoplasm-to-nucleus volume ratio, light-staining granular cytoplasms, small rounded nuclei, and ruffled cellular edges (Figure 5.21D). No

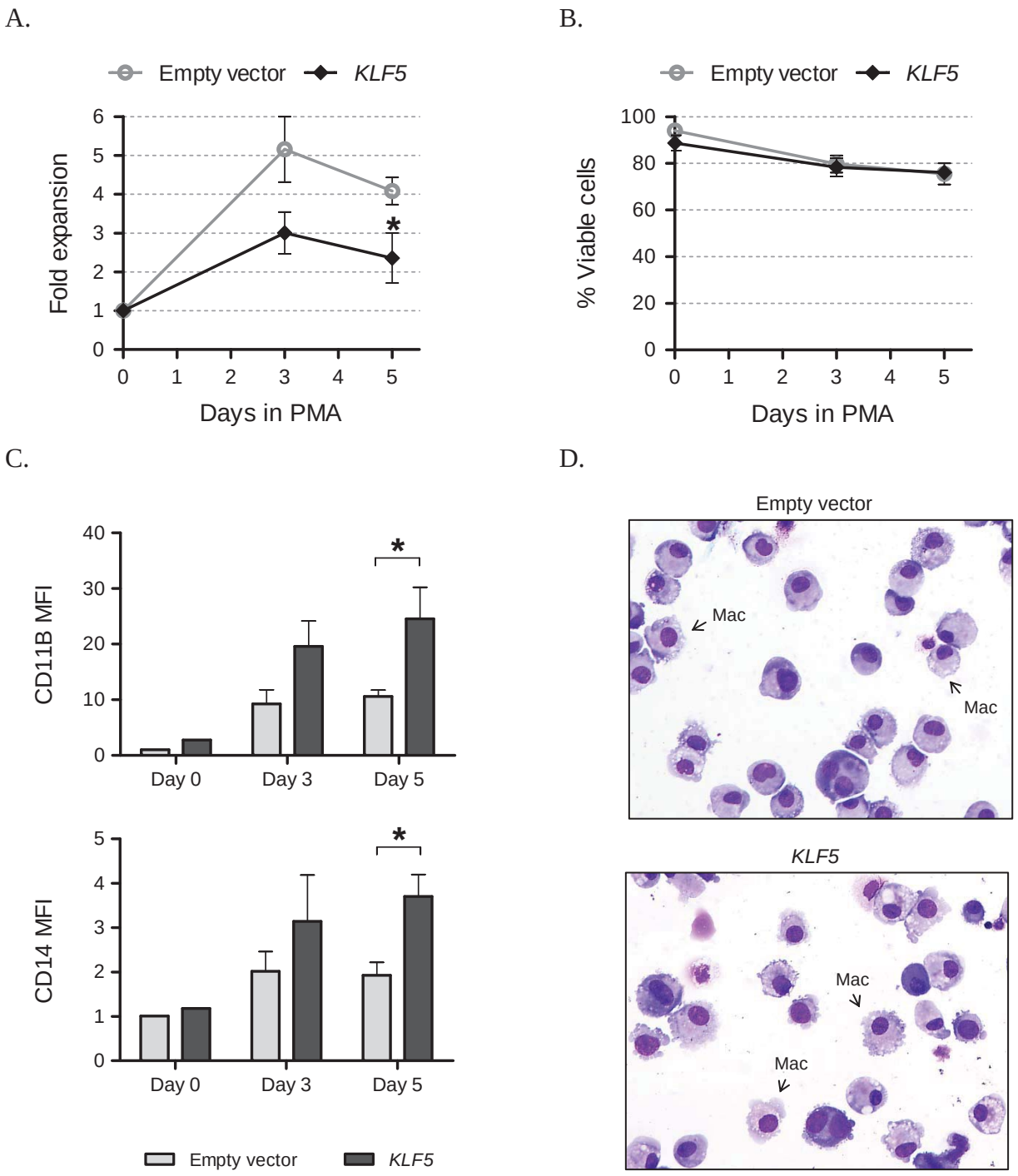

Figure 5.21: PMA treatment of *KLF5*-transduced U937 cells. A. GFP$^+$ cell expansion in PMA. The total number of live cells was determined at each time-point by Trypan Blue staining and cell counts, and the percentage of GFP$^+$ cells determined by flow cytometry. The number of GFP$^+$ cells was hence determined and expansion calculated relative to seeding on Day 0. n=3. **B.** Total cell viability was assessed by Trypan Blue staining and cell counts at each time-point following PMA treatment. n=3. **C.** Two-colour flow cytometric detection of CD11B and CD14 expression on PMA-treated U937 cells transduced with *KLF5* or the empty vector control. Expression was detected using PE-conjugated antibodies on GFP$^+$ cells. Figures show average MFI on Days 0, 3 and 5 post-treatment (n=3). *p<0.05. **D.** Representative photomicrographs showing Wright-Giemsa stained cytospin preparations of U937 cells transduced with *KLF5* or the empty vector control at Day 5 post-PMA treatment. Mac = macrophages. Original magnification = 200x. Note that cells were ≥85% GFP$^+$ at all time-points of these assays.

additional effects were observed on cellular morphology due to transduction with *KLF5*. These observations are consistent with enhanced macrophage differentiation of U937 cells in PMA due to transduction with *KLF5*.

5.3 Discussion

5.3.1 Reduced KLF5 expression potentially contributes to the disease pathogenesis of AML

The results presented in this chapter demonstrate that *KLF5* mRNA expression is decreased in human AML BMMNC compared to normal controls; Q-PCR analysis of our local AML cohort showed that expression levels of *KLF5* were reduced by 2.3-fold on average in AML BMMNC samples when compared with control bone marrow $CD34^+$ cells. *KLF5* expression levels were also decreased in human leukaemia cell lines by an average of 3.6-fold compared to $CD34^+$ control samples. The findings for leukaemia cell lines are comparable to those reported by Chen, et al. for both breast and prostate cancer cell lines (3.7-fold and 3.8-fold reduction of *KLF5* expression compared to relevant controls assessed by Q-PCR)[295,301]. We validated our Q-PCR results using bioinformatic analysis of a larger, publicly-available microarray data-set, which demonstrated that *KLF5* expression was significantly reduced in human AML MNC samples compared to normal MNC controls. As *KLF5* expression increases during myeloid differentiation (see Chapter 4, Section 4.2.1), it is possible that decreased expression in AML may be a consequence of blocked differentiation in this disease. However, our evidence that average *KLF5* expression is reduced in comparison to that in primitive $CD34^+$ haemopoietic progenitor cells is consistent with deregulation of *KLF5* being a pathological feature of AML development. This is further supported by the observation that

KLF5 mRNA expression is reduced specifically in leukaemic stem cells compared to haemopoietic stem cells (mean RMA normalised expression of 27 and 128 respectively, $p<0.0001$. C. Kok, unpublished analysis of microarray data from Majeti, et al.[453]). It will be of benefit to determine whether KLF5 expression is also reduced at the protein level in leukaemic samples, as mRNA and protein expression are not always correlated (as discussed in Section 4.3.1). As *KLF5* is a differentiation-associated gene in the myeloid system (Chapter 4), reduced *KLF5* expression may act as a Class II abnormality by contributing to the differentiation block which is central to the AML disease process.

5.3.2 Deregulation of KLF5 expression by common genetic lesions in AML.

Our bioinformatics analysis revealed that *KLF5* expression was significantly reduced in all AML subtypes assessed when compared to normal MNC controls (see Figure 5.3). Q-PCR analysis correspondingly revealed significantly reduced *KLF5* expression in selected subgroups relative to bone marrow $CD34^+$ control cells (see Figure 5.2). In particular, *KLF5* expression was significantly lower in the FAB subtypes M1, M3 and M4. M1 represents a minimally-differentiated AML subtype and comprises approximately 15% of adult AML. It is not specifically associated with a common cytogenetic abnormality, although point mutations in *RUNX1* and *CEBPA* have been shown to occur at a high frequency in this subtype[454,455]. Reduced *KLF5* expression in this subtype may provide a novel insight into the biology of AML M1. The pre-granulocytic M3 subtype comprises a distinct phenotypic form of AML, APL, which is characterised by the t(15;17) translocation. The oncogenic PML-RARα fusion protein produced by the t(15;17) translocation can inhibit myeloid differentiation by repressing the expression of proteins necessary for granulocyte differentiation, such as p21, C/EBPβ and PU.1[456,457]. The observation that *KLF5* expression is significantly reduced in the

M3 subtype of AML suggests that it may also act downstream of, or be repressed by, the PML-RARα fusion protein, contributing to the block in granulocyte differentiation characteristic to APL.

KLF5 expression was also significantly reduced in the monocytic M4 FAB subtype of AML. The inv(16) chromosomal abnormality is frequently detected in the M4 subtype[458,459], and accordingly half of the patients in our M4 subgroup displayed the inv(16) lesion (3/6). Our bioinformatic analysis of the Valk data-set demonstrated that mean *KLF5* expression in the inv(16) subgroup was not only significantly lower than that seen in normal MNC controls, but it was also significantly reduced compared to other subtypes of AML (including the trisomy 8 and normal karyotype subgroups). These observations suggest that *KLF5* may be repressed in AML down-stream of the CBFβ-MYH11 fusion protein produced by the inv(16) abnormality. The CBFβ-MYH11 fusion protein contributes to leukaemogenesis by interfering with activation of RUNX1 (AML1) target genes[460], which is consistent with the observation that transcription of the rat *Klf5* gene can be directly activated by RUNX proteins[209].

Our Q-PCR expression analysis also demonstrated that *KLF5* expression was significantly reduced in AML samples positive for the *FLT3-ITD* mutation (see Figure 5.2). The *FLT3* gene encodes a receptor tyrosine kinase which is activated upon binding of the FLT ligand and induces down-stream signalling pathways which modulate cell proliferation, growth, and differentiation in normal haemopoiesis[461]. Internal tandem duplication (ITD) of a section of the FLT3 receptor within the juxtamembrane domain occurs in approximately 25% of AML, and results in constitutive activation of signalling pathways which contribute to ligand-independent cellular proliferation[461]. Aberrant signalling from the FLT3-ITD receptor can down-regulate expression of tumour suppressor genes such as *GADD45A*[326]. Our results

suggest that *KLF5* expression may also be reduced downstream of the FLT3-ITD activated receptor. It is possible that this may occur through abnormal activation of pathways such as the MEK/ERK, AKT and STAT pathways, which have been shown to regulate expression of KLF5 in other tissues (see Chapter 1, Section 1.3.7.2).

In Chapter 4, Section 4.3.4, we discussed evidence for *KLF5* being a target of activation by C/EBPα, which is commonly mutated or hypermethylated in AML[462]. Our analyses demonstrated that reduced *KLF5* expression was not selectively associated with the *CEBPA* mutational subgroup, and we were not able to detect significantly reduced expression in the *CEBPA* subgroup relative to bone marrow $CD34^+$ controls using Q-PCR (see Figures 5.2-5.3). These observations suggest that while mutation of *CEBPA* may contribute to reduced *KLF5* expression in selected AML samples, there are most likely additional mechanisms which contribute to down-regulation of *KLF5* mRNA levels in AML.

5.3.3 DNA methylation of KLF5 as a potential mechanism for down-regulation in AML

CpG methylation was subsequently investigated as a potential mechanism for the observed reduction of *KLF5* mRNA expression in AML. We identified two discrete regions of the *KLF5* gene locus which were aberrantly methylated in a subset of AML patient samples and leukaemia cell lines compared to normal BMMNC and $CD34^+$ controls. These were termed Differentially-methylated regions (DMR) 1 (in the *KLF5* 5` proximal promoter) and DMR-2 (in *KLF5* intron 1). The location of DMR-2 is consistent with the region previously found to be methylated in AML by Gebhard, et al.[111], and accordingly we confirmed that this region is hypermethylated in U937 and KG-1 cells, but not in THP-1 cells (see Figure 5.7). We did not

observe any hypermethylation in our AML samples within the region identified by Potapova, et al. [309], however this may be due to the fact that Potapova assessed secondary AML patients transformed from MDS, whereas in the current study we have assessed *de novo* AML samples. In our cohort of AML samples, *KLF5* was found to be specifically methylated in two independent regions of DMR-2, which were subsequently named DMR-2a and DMR-2b. The incidence of aberrant methylation of *KLF5* in AML was 33% in DMR-1, and 24% and 47% in DMR-2a and DMR-2b respectively. Aberrant methylation was not strongly correlated with reduced *KLF5* expression in any of the DMRs, however, we determined in Section 5.2.2.6 that the Q-PCR primers used to measure *KLF5* mRNA levels in this study can detect expression of multiple isoforms of *KLF5*. Hence, it will now be necessary to quantitate expression of these different isoforms to determine any specific correlation with methylation status at each DMR. The observation that overall *KLF5* mRNA levels were relatively low even in samples which did not display aberrant methylation also suggests that multiple mechanisms may account for down-regulation of *KLF5* expression in AML, as discussed in Section 5.3.2. Demethylation treatment of leukaemia cell lines displaying aberrant methylation of *KLF5* induced *KLF5* mRNA expression, which is consistent with methylation acting to functionally repress *KLF5* transcription.

5.3.4 Aberrant methylation of KLF5 is associated with selected cytogenetic subgroups in AML

In the present study, we observed significant association of *KLF5* methylation (DMR-1) with monosomy 7/del(7q) in patients with *de novo* AML. Deletion of part or all of chromosome 7 is a common cytogenetic feature in both *de novo* and therapy-related MDS and AML[463,464]. Several genes on the long arm of chromosome 7 have been proposed as putative tumour

suppressors, however the mechanisms by which monosomy 7/del(7q) contributes to myeloid malignancy remain unclear. It has been suggested that monosomy 7 may act as a Class I aberration, as bone marrow cells from MDS patients with monosomy 7 demonstrate abnormal activation of STAT1 and STAT5 signalling pathways[465]. Studies have demonstrated a strong association of monosomy 7/del(7q) in therapy-related MDS/AML with inactivating point mutations or chromosomal translocations involving *RUNX1*[466], and with hypermethylation of the tumour suppressor gene *CDKN2B* (*p15*)[38]. Our results are consistent with aberrant methylation of *KLF5* acting as a Class II mutation which cooperates with the Class I-acting monosomy 7/del(7q) in the pathogenesis of AML. However it will be necessary to expand the patient cohort size to further confirm the significance of this association, and additional studies will be required to determine the mechanisms by which these two abnormalities may cooperate in the development of myeloid leukaemia.

Aberrant methylation of the 3` portion of DMR-2 (DMR-2b) was significantly associated with normal karyotype AML samples. Up to half of all newly-diagnosed AML patients do not have karyotypic abnormalities detectable by Fluorescence *in-situ* hybridisation (FISH) techniques[2,106,107]. Studies have demonstrated that these patients can exhibit recurring mutations in individual genes (e.g. *FLT3*, *NPM1*), aberrant expression of molecular markers (e.g. *MN1*, *ERG*), small copy number changes not detectable by FISH (both duplications and deletions), and copy-neutral LOH[467,468]. Although global methylation is not associated with karyotype in AML[469], Griffiths, et al. demonstrated significantly higher methylation of tumour suppressor genes such as *CEBPA*, *CTNNA1*, *ER1*, and *FHIT* in normal karyotype AML compared to those patients displaying karyotypic abnormalities[470]. Our results suggest that deregulation of *KLF5* expression by methylation in DMR-2b (intron 1) may also contribute to the pathogenesis of AML in patients with normal karyotype.

5.3.5 Mechanisms for transcriptional deregulation of KLF5 expression in AML

The observation that the *KLF5* gene is differentially methylated across distinct regions in AML may provide insights into mechanisms leading to deregulation of expression. DMR-1 lies in the proximal promoter of *KLF5* and encompasses a highly-conserved C/EBP binding site (see Oishi, et al.[156] and Figure 5.17). This raises the possibility that methylation of DMR-1 may prevent activation of *KLF5* expression by C/EBPα, or other members of the C/EBP family, facilitating the differentiation block characteristic of this disease. It will be necessary to demonstrate direct regulation of *KLF5* by C/EBPα using ChIP analysis and reporter assays. Interestingly, demethylation of leukaemia cell lines displaying highly methylated DMR-1 resulted in the greatest reactivation of *KLF5* expression, suggesting that methylation of this region may be particularly important in repression of *KLF5* transcription.

The second differentially-methylated region, DMR-2, lies within intron 1 of the *KLF5* gene. DMR-2b encompasses two interspecies-conserved predicted MYB transcription factor binding sites. MYB is a proto-oncogene highly expressed or amplified in AML[471-473], and studies have demonstrated that enforced expression of MYB can transform haemopoietic cells[474,475]. The transcriptional regulation of target genes by MYB is complex, depending on the relative expression of different isoforms, various coregulator interactions, MYB protein modifications, and methylation of target binding sequences[476-479]. Most MYB target genes exhibit groups of at least two MYB binding sites[476], which is consistent with the configuration observed in intron 1 of *KLF5*. Although precise mechanisms of target gene activation by MYB remain elusive, it is conceivable that methylation of *KLF5* intron 1 could alter binding

affinities of different isoforms of MYB or coregulators at these two binding sites to influence *KLF5* expression in AML. It will be necessary to demonstrate direct binding of MYB to intron 1 of *KLF5* using ChIP. The effect of MYB on transcription of *KLF5* may be investigated through MYB over-expression or knock-down and subsequent examination of *KLF5* mRNA expression.

An alternative possibility is raised by the identification of a putative alternative initiating exon adjacent to the predicted MYB binding sites in *KLF5* intron 1. The *KLF5* EST BG717510 contains this alternative exon (exon 1a) spliced to exon 2 of *KLF5*. Accordingly, we utilised reverse-transcription PCR to demonstrate that exon 1a is transcribed in selected leukaemia cell lines and spliced to exon 2. Although the BG717510 EST was constructed using a CAP-trapper cDNA synthesis protocol for enrichment of full-length cDNAs at the 5` end[480], it will be necessary to perform Rapid amplification of 5` cDNA ends (5` RACE) to validate that exon 1a represents a true alternative transcription start site for *KLF5*. It is possible that MYB or other factors may be acting to regulate transcription of this alternative isoform of *KLF5*. Translation of this isoform is predicted to produce a N-terminal-truncated KLF5 protein which lacks the first 99 amino acids (from a total of 457). The function of the KLF5 N-terminus has not yet been fully elucidated. Chen, et al. demonstrated that the N-terminal 19 amino acids were necessary for ubiquitin-independent degradation of KLF5[227], however it is conceivable that loss of this N-terminal region could also interfere with other functional aspects of the KLF5 protein such as target gene specificity. Alternatively, it is possible that N-terminal truncation of the KLF5 protein may not significantly affect normal activity, and that the function of these alternative start sites is instead to drive different tissue-specific expression patterns. *GATA1* is an example of a gene where tissue-specific expression is achieved through the use of alternative promoter regions which control transcription initiation

from alternative upstream exons. The first exon in each case is non-coding, however the different regulatory elements recruit specific transcriptional regulators which allow expression of *GATA1* in the testis or in the erythrocyte/megakaryocyte lineages at appropriate stages of development[481]. It will now be of interest to investigate regulation of the alternative *KLF5* isoform by MYB or other transcription factors in normal haemopoiesis and in leukaemogenesis, and to determine how the biological function of the protein produced from the BG717510 isoform may differ from the primary KLF5 protein.

5.3.6 Tumour suppressor function of KLF5 in human leukaemia cells

Finally, we assessed potential tumour suppressor activity of KLF5 using retroviral transduction of the U937 leukaemia cell line, which displayed a high degree of *KLF5* methylation and correspondingly low *KLF5* gene expression. Expression of KLF5 in U937 cells induced expression of the myeloid marker CD11B. *KLF5*-transduced cells also showed increased cytoplasmic protrusions, which were similar to those seen in ATRA-treated control U937 cells. These observations are consistent with induction of granulocyte differentiation in this cell line. However, there were no corresponding effects observed on cell expansion or viability due to transduction with *KLF5*. It is possible that expression of KLF5 alone was not sufficient to completely overcome the leukaemic differentiation block, and that activation or repression of additional genes may be necessary for cooperative reversal of the leukaemic phenotype. Alternatively, it is likely that KLF5 is targeted at the protein level for rapid degradation in U937 cells. It may be possible to construct a stabilised form of KLF5 to use in these studies, by introducing mutations which are known to enhance KLF5 protein stability (e.g. mutations which prevent interaction with ubiquitin ligases, and deletion of the N-terminal region to prevent ubiquitin-independent degradation – see Chapter 1, Section 1.3.4).

Transduction with *KLF5* enhanced differentiation of U937 cells towards the granulocyte lineage in ATRA, and towards the macrophage lineage in PMA, suggesting that activation of KLF5 facilitates differentiation of leukaemia cells in response to differentiation-inducing agents (discussed further in Chapter 6, Section 6.2.8). These data are consistent with KLF5 having tumour suppressor function, and suggest that reactivation of KLF5 may be of particular relevance in the treatment of AML, especially in the development of combination therapies.

Chapter 6 – Discussion

The overarching aim of this thesis was to identify and characterise genes important for regulation of haemopoietic growth and differentiation with potential roles as myeloid oncogenes or tumour suppressors. In Chapter 3 of this thesis, an expression cloning approach was undertaken to identify putative oncogenes contributing to the development of AML. This Chapter describes optimisation of methods for construction of high-quality retroviral cDNA libraries, and the production and screening of such a library from a murine myeloid leukaemia cell line (M1). These methods will be applicable to future research utilising retroviral expression cloning to identify oncogenes in AML.

Chapters 4 and 5 of this thesis focus on characterisation of a novel myeloid transcription factor acting as a potential transcriptional regulator of granulocyte-macrophage differentiation[1]. Transcription factors play a vital role in the maintenance of the haemopoietic system, and disrupted function can contribute to the pathogenesis of AML (see Chapter 1, Section 1.1.2). In particular, the differentiation block which is a hallmark of AML can often be attributed to decreased or altered function of transcription factors with roles in normal haemopoietic differentiation. A major aim in the field is therefore to identify and characterise the functions of these differentiation-associated transcription factors in haemopoiesis, which will lead to a greater understanding of how their deregulation contributes to human disease. We wished to determine the role of KLF5 as an inducer of myeloid differentiation, and to examine its potential function as a tumour suppressor gene which is deregulated in the pathogenesis of AML. The key findings from this study are discussed below.

6.1 KLF5 expression and function in normal myelopoiesis

6.1.1 Expression of KLF5 during myeloid differentiation

In Chapter 4 of this thesis, we provide evidence demonstrating that KLF5 acts as a novel regulator in the myeloid lineage. Results presented in Section 4.2.1 demonstrated that *Klf5* mRNA expression increased during granulocyte-macrophage differentiation of the FDB1 myeloid cell line, consistent with microarray results published by Brown, et al.[1]. *Klf5* expression also increased during G-CSF-induced granulocyte differentiation of the 32D murine myeloid cell line, and analysis of published microarray studies confirmed that expression was higher in primary granulocyte populations than in human cord blood $CD34^+$ progenitors or in murine bone marrow haemopoietic stem cells[386,387]. Conversely, *Klf5* expression decreased during M-CSF-induced macrophage differentiation of primary murine bone marrow progenitors. This granulocyte-associated expression pattern implies a potential role for KLF5 in differentiation of this lineage. In addition, the time-course of *Klf5* mRNA expression in FDB1 cells undergoing granulocyte-macrophage differentiation and in 32D cells undergoing granulocyte differentiation closely mirrored that of the granulocytic transcription factor *Cebpe*, suggesting a similar functional role for these two genes and a potential common mechanism of transcriptional regulation (discussed further in Section 6.2.3).

6.1.2 KLF5 function

In Section 4.2.3, siRNA knock-down experiments demonstrated that decreased *Klf5* expression was associated with reduced granulocyte differentiation of the murine 32D

myeloid cell line in response to G-CSF, consistent with a predicted role in the granulocyte lineage based on expression studies. Reduced *Klf5* expression was associated with decreased levels of the neutrophil granule markers MPO (active enzyme) and *Ltf* (mRNA), suggesting that KLF5 may function early during granulocyte differentiation at the myeloblast or promyelocyte stages, prior to the first appearance of these markers. Although the time-course expression profile of *Klf5* was similar to that of *Cebpe* during granulocyte-macrophage (FDB1) or granulocyte-only (32D) differentiation (see Section 6.1.1), suggesting a common mechanism of regulation, knock-down of *Klf5* was associated with reduced *Cebpe* expression in the 32D cell line, which is consistent with KLF5 acting upstream of *Cebpe* to regulate granulocyte differentiation.

Consistent with results from *Klf5* knock-down experiments, results presented in Section 4.2.2 demonstrated that enforced expression of *Klf5* from a retroviral promoter was sufficient to induce differentiation of the murine myeloid cell line FDB1 and of primary murine bone marrow progenitors. This was accompanied by cell cycle arrest and reduced cell viability. Although our expression studies and knock-down experiments support a role for *Klf5* in granulocyte differentiation, enforced expression of *Klf5* induced macrophage differentiation of FDB1 cells and murine bone marrow progenitors. This may reflect an experimental limitation associated with enforced expression (discussed in Section 4.3.2), or alternatively it could imply a role for KLF5 in development of the macrophage lineage. There is increasing evidence to suggest that key myeloid transcriptional regulators such as PU.1 and C/EBPα can regulate both granulocyte and macrophage differentiation in different contexts. PU.1 is commonly accepted as a critical regulator of macrophage differentiation, however studies have also demonstrated a role for this transcription factor in development of the granulocyte lineage[482]. The concentration of PU.1 is an important factor in determining which lineage is

produced; Laslo, et al. demonstrated that low levels of PU.1 protein activate a mixed pattern of macrophage and neutrophil specific genes, whereas higher levels of PU.1 activate additional transcriptional programs involving repression of granulocyte regulators which ultimately leads to macrophage specification[483]. For C/EBPα, targeted gene disruption in mouse models has established an essential role in normal granulocyte development[484]. However, an independent study by Wang and colleagues demonstrated that exogenous expression of physiologically relevant levels of C/EBPα in primary murine bone marrow progenitors can promote macrophage formation[401]. It is particularly interesting that *in vivo* ablation of the late-acting granulocytic transcription factor *Cebpe*, whose expression mirrors that of *Klf5* during myeloid differentiation (see Section 4.2.1), also demonstrated a functional role for this gene in differentiation of macrophages[485]. Our expression analyses showed that although the highest level of *KLF5* expression was detected in the granulocyte compartment of primary haemopoietic populations, it was also up-regulated to a lesser extent in murine macrophages (see Figure 4.6). This further supports a potential role for KLF5 in development of the macrophage lineage, and suggests that like PU.1, the relative concentration of KLF5 may be an important factor in determining whether granulocytes or macrophages are produced.

To better establish the role of KLF5 in granulocyte-macrophage lineage specification requires targeted disruption of the gene in the haemopoietic system *in vivo*. Although murine models for *in vivo* deletion of *Klf5* have been reported in literature, these have not been utilised for analysis of the haemopoietic system. *Klf5*$^{-/-}$ mice are embryonic lethal prior to the onset of definitive haemopoiesis[157,160]. Heterozygous *Klf5*$^{+/-}$ mice have a number of defects in adipogenesis, cardiovascular remodelling, and intestinal development[156,157], however there have been no reports of gross defects in the haemopoietic system of these animals. The

creation of a Cre-Lox mouse model for conditional deletion of *Klf5* has been undertaken by our laboratory. Mice carrying floxed *Klf5* alleles have been generated and will now be crossed with a transgenic strain which produces Cre recombinase from the haemopoietic *Vav* promoter[486]. This system will enable a detailed *in vivo* analysis of the effect of *Klf5* deletion on haemopoiesis, and will further elucidate any specific roles KLF5 may have in granulocyte versus macrophage lineage determination.

6.1.3 KLF family members in the haemopoietic system

The findings described above are consistent with KLF5 acting as a novel haemopoietic transcriptional regulator, adding to the growing number of KLF family members with roles in the haemopoietic system[175]. In the erythroid system, *in vivo* mouse models have demonstrated essential functional roles for two KLF family members, KLF1 and KLF13. Mice homozygous for the null allele of *Klf1*, or *Erythroid Krüppel-like factor*, develop a fatal anemia due to insufficient haemoglobin production[138,139], whereas mice with homozygous disruption of *Klf13* display a decreased number of circulating erythrocytes with an increased proportion of immature erythroid cells in the liver[184]. In the lymphoid lineage, gene targeting experiments in mice have demonstrated a role for KLF2 in maintaining the quiescent state of progenitor T-cell populations[142], and a role for KLF13 in T-cell survival[187].

Relatively few studies have assessed the role of KLF family members in the myeloid lineage. Although *KLF1* was originally believed to be an erythroid-specific gene, it has been demonstrated that KLF1 can regulate transcription of *IL12B* during monocyte activation[487]. *Klf3* knock-out mice develop a chronic myeloproliferative disorder due to increased proliferative capacity of myeloid cells, suggesting a role for KLF3 in modulating the

proliferative and/or survival capacity of myeloid progenitor cells[488]. The most detailed studies with regard to KLF family members in myelopoiesis have been undertaken with KLF4. Feinberg, et al. demonstrated an essential role for KLF4 in monocyte formation[388]. Enforced expression of KLF4 in murine common myeloid progenitors (CMP) induced formation of predominantly macrophage colonies in semi-solid medium, whereas ablation of KLF4 in CMPs induced development of granulocyte colonies at the expense of macrophage colonies. KLF4 and KLF5 display similar tissue distribution patterns, and numerous studies have shown that they often act in a complementary manner[150]. For example, KLF4 is highly expressed in mature cells of intestinal villi where it acts to negatively regulate cell growth, whereas KLF5 expression is specific to proliferating crypt cells where it functions to enhance cell proliferation. In the myeloid system, KLF4 expression is specific to the monocyte lineage where it is a direct target of the monocytic transcription factor PU.1[388]. In contrast, our studies show that *Klf5* is expressed predominantly in the granulocyte lineage, and Cammenga, et al. identified *Klf5* as a target which is activated by C/EBPα in human $CD34^+$ haemopoietic progenitor cells[132]. As PU.1 and C/EBPα have complementary functions in determination of granulocyte versus monocyte lineage[489,490], it is interesting to speculate that KLF4 and KLF5 may also have opposing or antagonistic roles in the myeloid system, possibly acting as key downstream mediators of PU.1 and C/EBPα.

Our studies have focused on defining the role of KLF5 in the granulocyte and/or macrophage lineages, however there is evidence to suggest that KLF5 may also function in other haemopoietic cell types. Zhang, et al. demonstrated that *KLF5* mRNA expression increases during erythroid differentiation of the K562 CML blast crisis cell line, where it binds to and activates transcription of the haemoglobin *HBG1* gene[237]. Our observation that *Klf5* expression is reduced in mature T-cell populations relative to murine haemopoietic stem cells

(see Figure 4.6) concurs with a previous study which reported that precursor T-cells have high levels of *KLF5* mRNA and that expression decreases on maturation[204]. It was demonstrated that KLF5 can activate the T-cell receptor *TCR Dβ1* gene which is necessary for the development of T-cells[204].

Taken together, these studies suggest that the KLF family of transcription factors may act at many points in the haemopoietic system, with various members such as KLF5 controlling distinct aspects of haemopoietic growth and differentiation.

6.2 Deregulation of KLF5 in AML

6.2.1 KLF5 mRNA expression in AML

In Chapter 5 of this thesis, we demonstrated a potential role for KLF5 as a tumour suppressor gene in AML. The classical model of tumour suppression involves inactivation of both alleles of a tumour suppressor gene, a concept known as Knudson's 'two-hit' hypothesis[491]. However there is increasing evidence that haploinsufficiency of tumour suppressor genes is sometimes sufficient to contribute to tumourigenesis, and studies have shown that gene dosage reduction by mechanisms other than mutation or allele loss (e.g. DNA methylation, protein degradation) can also be important factors in the development of cancer[492].

The results presented in Section 5.2.1 demonstrated that *KLF5* mRNA expression is reduced in AML samples relative to normal controls, suggesting that decreased dosage may be contributing to the pathogenesis of this disease. We showed by Q-PCR that mean *KLF5* expression was significantly lower in AML blasts than in bone marrow $CD34^+$ control

samples, and this was consistent with our bioinformatics analysis of a larger published microarray data-set (Valk, et al.[329]) which demonstrated significantly reduced *KLF5* expression compared to normal MNCs. The observation that *KLF5* mRNA expression is reduced in AML blasts relative to primitive bone marrow $CD34^+$ cells, and also in leukaemic stem cells compared to normal haemopoietic stem cells, suggests that reduced *KLF5* expression is not a consequence of blocked differentiation, but rather that it is functionally contributing to the pathogenesis of AML (discussed in Section 5.3.1).

Analysis of the Valk gene expression profiling study demonstrated that *KLF5* expression was significantly reduced in all AML subtypes and mutational categories relative to MNC controls (see Figure 5.3). Our Q-PCR analysis demonstrated that mean *KLF5* expression was also significantly reduced in selected subtypes relative to the more primitive CD34+ control bone marrow populations (see Figure 5.2). This included the minimally-differentiated M1 subtype of AML, and also the pre-granulocytic M3 and monocytic M4 subtypes. FAB M3 is almost exclusively associated with the t(15;17) translocation which produces the oncogenic fusion protein PML-RARα[493], and FAB M4 is commonly associated with aberrations of chromosome 16, including inv(16) which produces the CBFβ-MYH11 fusion protein[458,459]. Targeting oncogenic fusion proteins has proven successful in developing efficient therapeutic strategies in the treatment of AML, for example, the use of ATRA for specific targeting of the PML-RARα protein[43]. However, the elucidation of down-stream biological effectors of these proteins which may contribute to altered growth and differentiation could potentially suggest novel approaches for the development of improved targeted therapies for these AML subtypes, particularly for those patients who do not respond to conventional chemotherapy or who relapse following initial response to ATRA therapy[494]. Q-PCR also showed that *KLF5* expression was significantly reduced in AML samples displaying *FLT3-ITD* mutations,

suggesting that it may act as a Class II lesion contributing to the differentiation block in AML through cooperation with the Class I *FLT3-ITD* lesion. As the application of FLT3 inhibitors has shown limited success in clinical trials to date[495], it is possible that approaches aimed at reactivation of KLF5 in *FLT3-ITD*-positive samples may synergise to improve the efficacy of these inhibitors in treatment of this AML subtype.

6.2.2 Methylation of KLF5 in AML

Hypermethylation of CpG dinucleotides is a common mechanism for silencing of tumour suppressor genes in AML (discussed in Section 5.1). In Section 5.2.2, we demonstrated that the *KLF5* promoter and intron 1 are hypermethylated in selected leukaemia cell lines and in bone marrow MNC samples from a subset of AML patients compared to normal bone marrow controls (MNC and $CD34^+$ cells). Treatment of leukaemia cell lines exhibiting methylation of *KLF5* with methyltransferase inhibitors induced *KLF5* expression, consistent with DNA methylation being a significant factor in reduced *KLF5* expression (see Figure 5.16). Deregulation by hypermethylation has been demonstrated for selected members of the *KLF* family in human disease. *KLF4* in particular is hypermethylated in gastric cancer, colon cancer and in T-cell leukaemia[496-498]. Hypermethylation of *KLF6* may partly contribute to repression in hepatocellular carcinoma[499,500], and *KLF11* is reportedly down-regulated by methylation in various haematological disorders, particularly in MDS[309]. The observation that the *KLF5* gene is hypermethylated in AML in the proximal promoter and in intron 1 provides additional evidence that KLF members may act as tumour suppressors in a variety of malignancies, where they are commonly down-regulated by hypermethylation.

6.2.3 Transcriptional deregulation of KLF5 by methylation of the 5` proximal promoter in AML and potential relevance to CEBPA activity

We identified two distinct regions of CpG methylation at the *KLF5* locus in AML. One third of AML patient samples displayed hypermethylation of the first of these regions, which lies in the 5` proximal promoter of *KLF5*. This region encompasses a C/EBP binding site which is known to bind CEBPβ/δ[156], and also corresponds with the consensus binding sequence for C/EBPα (see Figure 5.17). This observation is consistent with previous studies which have demonstrated that C/EBPα is an upstream activator of *KLF5* transcription in human $CD34^+$ cells[132]. Our expression studies in Section 4.2.1 are also consistent with C/EBPα activating *Klf5* transcription during GM-CSF and G-CSF-induced differentiation of the FDB1 and 32D myeloid cell lines respectively, as the time-course of *Klf5* expression closely correlated with that of the known C/EBPα target gene *Cebpe* in both of these model systems. During G-CSF-induced granulocyte differentiation of the 32D cell line, *Cebpa* mRNA expression peaked early and was followed by a steady increase in the levels of *Klf5* and *Cebpe*, suggesting that expression of both may be coordinated by C/EBPα (see Figures 4.2 and 4.4). Interestingly, the greatest increase of *KLF5* expression upon treatment with methyltransferase inhibitors occurred in cell lines that showed high methylation of the *KLF5* 5` proximal promoter across the C/EBP binding site (see Figure 5.16). These findings are consistent with *KLF5* mRNA expression being repressed in AML due to methylation of the proximal promoter associated with reduced C/EBPα binding.

Although selected AML samples showed relatively high CpG methylation of the *KLF5* proximal promoter, there were clearly samples which did not exhibit increased methylation of this region yet still displayed relatively low levels of *KLF5* expression. This suggests that

down-regulation of *KLF5* mRNA expression in AML may occur through additional mechanisms. It is possible that deregulation of C/EBPα upstream of *KLF5* may also contribute to decreased *KLF5* expression in AML. Approximately 10% of AML cases have mutations in the *CEBPA* gene, which functional studies have suggested generate dominant-negative C/EBPα isforms[37]. *CEBPA* expression can be reduced in AML through hypermethylation of the promoter region[68,75,501-504]. Global studies of CpG methylation and gene expression in AML have shown that samples with mutated or hypermethylated *CEBPA* are associated with distinct expression profiles, which includes down-regulation of tumour suppressor genes such as *CTNNA1*[108,505]. Accordingly, we found significantly reduced *KLF5* expression in AML samples exhibiting *CEBPA* mutations compared to normal MNC controls (see Figure 5.3). Patients demonstrating hypermethylation of the *CEBPA* locus also displayed reduced *KLF5* expression (Figure 6.1). Thus it is likely that deregulation of C/EBPα by several mechanisms may affect *KLF5* expression in AML.

6.2.4 Transcriptional deregulation of KLF5 by methylation of intron 1 in AML

For almost half of the AML patient samples assessed we demonstrated hypermethylation of *KLF5* within intron 1 of the gene locus. This region is highly conserved amongst vertebrate species and encompasses a putative alternative promoter region regulating initiation of transcription of *KLF5* from an alternative exon (exon 1a) (see Figure 5.17). Translation of this alternative isoform of KLF5 would produce either an untranslated transcript, or an N-terminal-truncated form of the KLF5 protein (discussed in Section 5.3.5). Although alternative exon usage has been implicated by sequencing of a number of EST clones which map to the *KLF5* locus, evidence supporting formation of alternative *KLF5* isoforms is not

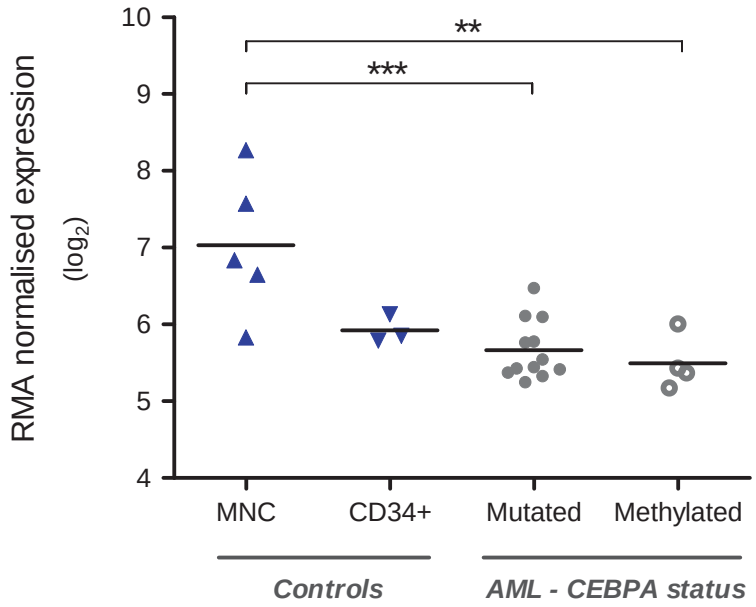

Figure 6.1: *KLF5* expression levels in AML samples with mutated or hypermethylated *CEBPA*. Analysis of *KLF5* mRNA levels as detected by microarray in Valk, et al.[329]. Samples include normal controls (5 MNC and 3 $CD34^+$ samples) and AML MNC for patients with mutated *CEBPA* (n=12) or hypermethylated *CEBPA* (n=4). ***p<0.001, **p<0.01 (assessed using One way ANOVA with Tukey post-test comparison).

conclusive. The primary *KLF5* cDNA is 3350 bp in length, and a smaller 1.5 kb transcript has been detected by northern blotting in the testis[201]. Lower molecular weight species have been detected by western blotting with various KLF5 antibodies in breast and colorectal epithelial cell lines, although it is not known whether these are the result of alternatively spliced transcripts or protein cleavage/degradation[201,224,229]. Our results presented in Section 5.2.2.6 provide the first evidence of an alternative mRNA isoform of *KLF5* associated with transcription and splicing of an alternative exon. It will be important to examine expression of this alternative isoform in normal and malignant tissues, and to determine the functional significance and regulation of this isoform in normal haemopoiesis and in AML. The identification of two highly conserved putative MYB binding sites directly upstream of exon 1a raises the possibility that the alternative isoform of *KLF5* may be regulated by the oncogenic MYB protein (discussed in Section 5.3.5). Collectively these studies will help define the relevance of *KLF5* intron 1 hypermethylation in AML.

It is well established that aberrant methylation of alternative start sites can contribute to the pathogenesis of human disease by altering the normal expression ratio of variant isoforms. For example, the growth inhibitor *ING1* is transcribed from three different initiating exons, which can generate four alternative transcript variants with the use of alternative splicing. Two of these isoforms, p24 and p33, show varying degrees of expression in head and neck carcinomas, which correlates with hypermethylation at their distinct initiating exons[506]. The tumour suppressor *CDKN2A* (*p16*) can also be transcribed from alternative initiating exons, the shorter of which is not translated into protein. In a number of non-small cell lung carcinoma cell lines, hypermethylation of the upstream promoter region was detected, leading to enhanced transcription of the shorter isoform initiating from alternative exon 1b, and consequently reduced protein expression[507]. Interestingly, one member of the *KLF* family also

displays alternative splicing in human disease; alternative splicing of *KLF6* results in the production of at least 4 isoforms, one of which acts as a dominant-negative, oncogenic form (KLF6-SV1) which is over-expressed in a number of different cancers[508]. Thus it is plausible that deregulation of *KLF5* isoforms produced by alternative transcription initiation start sites may also contribute to altered KLF5 function in disease.

6.2.5 Biological relevance of KLF5 methylation studies in AML

In Section 5.2.2.3, we demonstrated that methylation of the *KLF5* proximal promoter was significantly higher in patients with monosomy 7 or del(7q) than in patients negative for these abnormalities. Previous studies have demonstrated that methylation of specific genes may cooperate with common mutations in AML, for example, there is evidence to suggest that methylation of WNT inhibitor genes is associated with Class II mutations in transcription factors such as *CEBPA*[509]. Alvarez, et al. demonstrated that patients who have a *FLT3* mutation together with methylation of the cell cycle gene *DCB1* have a significantly shorter overall survival than patients with only one of these abnormalities[510]. It will now be interesting to examine the mechanisms by which methylation of *KLF5* may cooperate with the monosomy 7 or del(7q) abnormalities in the pathogenesis of leukaemia (discussed in Section 5.3.4).

The identification of molecular abnormalities in AML, including epigenetic changes such as DNA hypermethylation, is particularly important in normal karyotype AML, which displays considerable heterogeneity in clinical outcome[511]. We identified *KLF5* as a gene which displayed significantly higher CpG methylation of intron 1 in normal karyotype AML than in samples with abnormal cytogenetics. Thus KLF5 may be one of a number of tumour

suppressor genes which are silenced by hypermethylation in normal karyotype AML (discussed in Section 5.3.4). Identification of samples with aberrant CpG methylation of these tumour suppressor genes may aid in selection of patients with normal karyotype AML who could benefit from treatment with demethylating agents in combination with standard AML chemotherapeutics.

6.2.6 Prognostic relevance of methylation studies in AML

Genome-wide DNA methylation analyses utilising microarray-based methods[512] have demonstrated that distinct CpG methylation patterns can identify patient groups which correlate highly with prognosis[68,513]. This approach was used to identify sets of patients who were not otherwise linked by a common abnormality, highlighting how methylation analysis may aid in disease classification and prediction of outcome. The effect of CpG methylation on prognosis is gene dependent[469]. For example, hypermethylation of the *ESR1* or *HOXA5* genes is indicative of a good prognosis[514,515], whereas hypermethylation of genes such as *CDH1*, *WIF1* and *SFRP2/5* genes is associated with a poor outcome[516-518]. Our analysis of *KLF5* methylation revealed a trend for decreased overall survival in patients displaying hypermethylation of *KLF5* intron 1 (see Fig 5.14). It will now be of interest to extend our methylation analysis of *KLF5* to a larger cohort of AML patients to determine if methylation of the *KLF5* proximal promoter or intron 1 may be a significant independent predictor of prognosis.

6.2.7 Other potential mechanisms for KLF5 deregulation in AML

Although we have identified methylation of *KLF5* as a mechanism potentially associated with reduced mRNA levels in AML, it is likely that *KLF5* mRNA expression is also decreased by other mechanisms in this disease. Transcriptional repression by upstream oncogenic pathways, or reduced activation due to mutation or silencing of C/EBPα, may represent additional mechanisms for reduced *KLF5* expression in AML, as discussed in Sections 6.2.1 and 6.2.3. A single A>G polymorphism (rs3812852) has been reported to be associated with reduced *KLF5* expression in schizophrenia, and it will be important to establish whether this is also prevalent in AML[203]. Over-expression of targeting microRNAs is another mechanism recently shown to reduce tumour suppressor expression in AML, for example, the oncogenic microRNA-155 is over-expressed in selected subgroups of AML where it acts to degrade candidate tumour suppressor mRNAs such as *SPI1*[519-522]. MicroRNAs 143, 145 and 448 have been shown to regulate *KLF5* activity through RNA degradation[214,215]. Studies have shown that microRNAs 143 and 145 are commonly down-regulated in solid tumours such as colorectal cancer, which is consistent with *KLF5* acting as a highly expressed oncogene in these tissues[523,524]. Expression of these microRNAs is also reduced in B-cell leukaemia[525]. However, Volinia, et al. demonstrated that microRNA-143 is highly expressed in Acute Myelomonocytic Leukaemia (AMML)[524], consistent with microRNA-143 acting as an oncogene which acts to degrade *KLF5* mRNA in AML.

It is possible that *KLF5* mRNA may also be reduced due to deletion, as small heterozygous chromosomal deletions on chromosome 13 have been reported for myeloid disorders such as MPD, MDS and also in some cases of AML[305]. These deletions span from 13q12/q14 to 13q21/q22, which encompasses all or part of the *KLF5* gene on chromosome 13q21-q22. The

human *FLT3* gene (commonly activated by mutation or over-expression in AML[461,526]) also maps to chromosome 13q12-q13[527]. Heterozygous deletion of the *FLT3* genomic region may reflect loss of the remaining allele of this gene. However, a single AML patient in the study described above demonstrated heterozygous deletion spanning from 13q14-q22, which encompasses the *KLF5* gene but does not affect the *FLT3* locus[305]. This raises the possibility that the pathogenesis of AML associated with deletions of 13q may be attributed to loss of *KLF5* rather than a *FLT3* gene aberration. It will now be of interest to determine if patients with heterozygous 13q deletion encompassing the *KLF5* genomic region display inactivation of the remaining *KLF5* allele through hypermethylation or mutation.

6.2.8 Targeting KLF5 for activation in AML

The results presented in Section 5.2.3 demonstrate that expression of KLF5 in a leukaemia cell line with low basal levels of *KLF5* expression can induce changes associated with myeloid differentiation. This finding suggests that targeting *KLF5* for reactivation may be of potential benefit as a therapeutic approach in selected cases of AML. As *KLF5* is hypermethylated in the proximal promoter and intron 1 in a subset of AML samples, and expression is induced in leukaemia cell lines treated with demethylating agents, the use of epigenetic modifiers may prove beneficial in treatment for these patients. Clinical trials utilising epigenetic modifiers such as DNA methyltransferase inhibitors (e.g. 5-azacytidine) and HDAC inhibitors (e.g. SAHA – Vorinostat) have already demonstrated a beneficial response in patients with MDS or AML, particularly when used in combination[528-532]. As larger studies are performed with these agents it may be possible to link response to methylation of particular genes, including *KLF5*.

It may also be of benefit to consider alternative methods to activate *KLF5* expression in AML samples which do not demonstrate hypermethylation of this gene. The observation that enforced KLF5 expression enhanced differentiation of a human leukaemia cell line in response to ATRA and PMA suggests that targeting KLF5 may be a viable strategy in combinatorial therapy for AML (see Figures 5.21-22). For example, although the use of ATRA has significantly improved survival rates in AML patients harbouring the t(15;17) translocation (APL), the success of this for treatment of other subtypes has remained limited[533]. There is evidence to suggest that the limited effect of ATRA on non-APL leukaemia cells is due to a deficiency in components of the retinoic acid signalling pathway; for example, *RARβ2* is commonly silenced by hypermethylation in AML[534], and expression of *RARα* is often decreased via methylation-independent mechanisms[535]. Chen, et al. demonstrated that KLF5 can activate expression of a number of genes associated with the retinoic acid signalling pathway (e.g. *RAIG1*, *MN1*, *TGM2*)[251], and hence it is conceivable that KLF5 expression may synergise with ATRA by increasing the expression of components necessary for efficient ATRA-induced differentiation of non-APL leukaemia cells. Alternatively, it has been demonstrated that the KLF5 protein directly interacts with RARα to synergistically influence transcription of down-stream target genes in VSMCs[157,264,266]. Thus, reactivation of *KLF5* may improve ATRA-induced differentiation of leukaemic blasts in non-APL subtypes.

KLF5 expression can be activated by a number of signalling pathways depending on cell type including the MEK/ERK, p38 MAPK and STAT3 pathways (see Section 1.3.7.2). Interestingly, a study performed by Bialkowska, et al. identified 6 small molecule activators of *KLF5* transcription[294]. These included PMA, a known inducer of leukaemia cell differentiation, and interestingly Piceatannol, an inhibitor of the non-receptor tyrosine kinases

SYK and LCK[294]. Hahn and colleagues recently identified SYK as an important modulator of myeloid cell proliferation, and demonstrated that it was highly expressed and constitutively activated in the majority of AML samples assessed[536]. Inhibition of SYK by siRNA or the application of SYK inhibitors decreased proliferation and cell viability and induced differentiation in a range of myeloid leukaemia cell lines and also in primary AML blasts. Chemical inhibition of SYK also reduced tumourigenicity in a xenograft model of human AML. The SYK inhibitors R406 and R788 are currently being utilised in Phase I clinical trials for rheumatoid arthritis, lymphoma, and Chronic Lymphocytic Leukaemia (CLL)[537,538]. It will be interesting to evaluate the efficacy of these inhibitors in AML clinical trials, and to determine whether activation of KLF5 downstream of these chemicals plays a role in their differentiation-inducing effect on AML cells.

6.3 Summary and concluding remarks

In summary, we have demonstrated that the transcription factor KLF5 acts as a novel inducer of myeloid differentiation. *KLF5* mRNA expression is reduced in primary human AML, consistent with tumour suppressor function in the myeloid lineage. Methylation of *KLF5* partly contributes to this repression, however it is likely that alternative mechanisms also contribute to aberrant regulation in AML. Finally, we demonstrated that expression of KLF5 may be of potential benefit in treatment of this disease. The findings presented in this thesis contribute to a more complete understanding of the transcriptional control of normal haemopoiesis, and how this may be deregulated to facilitate the development of AML. Future work including the use of tissue-specific targeted *Klf5* ablation in murine models will further elucidate the role of KLF5 in normal haemopoiesis, and the role that it plays in specification of granulocyte versus monocyte lineage determination. It will be of interest to determine if

ablation of *Klf5* in these models contributes to AML development, either as a single genetic aberration or in cooperation with known Class I mutations such as the *FLT3-ITD* activated receptor. Our studies evaluating *KLF5* expression and methylation in primary human AML suggest that further investigation into how KLF5 may be deregulated in the pathogenesis of AML is warranted. It will be necessary to expand cohort size to determine any correlation of these factors with outcome. Determining the regulation and functional significance of alternative KLF5 isoforms will be of particular interest in the future given the importance of alternative isoforms of other genes in normal haemopoiesis and in AML. Evaluation of KLF5 expression in clinical trials of epigenetic agents and chemical activators of KLF5 expression (e.g. SYK inhibitors) will provide insights into the role of KLF5 as a tumour suppressor in AML. Ultimately, a comprehensive knowledge of the function of KLF5 in AML may aid in the development of more efficient targeted therapies for this disease.

Appendices

Appendix A: Details for selected clones from the four fractions of the M1 cDNA library 220

Appendix B: Correlation of methylation in *KLF5* DMR-1, DMR-2a and DMR-2b .. 222

Appendix C: Correlation of relative KLF5 mRNA expression with methylation of *KLF5* DMR-1, DMR-2a and DMR-2b using linear regression and Fisher's exact test 223

Appendix D: Features of *KLF5* DMR-2a 224

Fraction 1

Clone #	Approxmiate insert size (kb)	Accession	Clone description	Full-length?
1	N/A	N/A	Uncut vector	N/A
2	0.85	AK005904	RIKEN cDNA 1700012G05	5`-truncated
3	0.25	AK151118	RIKEN clone I830025I02 hypothetical protein	5`- and 3`-truncated
4	N/A	N/A	Multiple inserts	N/A
5	0.55	BC012957	Ash2 (absent, small or homeotic)-like (Drosophila)	5`-truncated
6	0.4	NM_025624	Proteasome maturation protein	5`-truncated
7	0.6	BC035296	Pleckstrin homology, Sec7 and coiled-coil domains 3	5`- and 3`-truncated
8	0.8	NM_02060	Ribosomal protein S14	yes
9	0.4	AK154073	Peptidylprolyl isomerase B	5`-truncated
10	0.8	NM_010887	NADH dehydrogenase (ubiquinone) Fe-S protein 4	yes
11	0.7	AK019597	Similar to 3-oxo-5-alpha-steroid-4-dehydrogenase 1	5`-truncated
12	0.5	AK088070	Ribosomal protein, large, P1	5`-truncated

Fraction 2

Clone #	Approxmiate insert size (kb)	Accession	Clone description	Full-length?
1	1.9	BC088985	Heat shock protein 90 kDa alpha (cystolic)	5`-truncated
2	N/A	N/A	No sequence data obtained	N/A
3	2.7	NM_146157, NM_001039200, AK077496	Multiple cDNA aligments, hypothetical protein	5`-truncated
4	2.5	NM_007639	CD1d1 antigen	yes
5	1.9	NM_025840	Basic leucine zipper and W2 domains 2	3`-truncated
6	2.5	AK142813	Ras GTPase-activating-like protein IQGAP2 homolog (homo sapiens)	5`-truncated
7	1.8	AK146301	Cellular nucleic acid binding protein	yes
8	3.0	NM_019650	Golgi SNAP receptor complex member 2	yes
9	2.4	NM_175751	Zinc finger protein 608	5`-truncated
10	2.2	NM_001042501	RIKEN cDNA 5830415L20 gene LOC68152	yes
11	1.9	NM_145445	Eukaryotic translation initiation factor 2B, subunit 2 (beta, 39KD)	yes
12	3.0	NM_001033468	G protein-coupled receptor 114	yes

Details for selected clones from the four fractions of the M1 cDNA library (Fractions 1 and 2). Approximate insert size was estimated using agarose gel electrophoresis. Completeness of the clone (‘full-length’) was evaluated relative to the 5` and 3` ends given for each accession number shown. This data is summarised in Chapter 3, Table 3.1. N/A = not applicable.

Fraction 3

Clone #	Approxmiate insert size (kb)	Accession	Clone description	Full-length?
1	4.5	NM_181278	RIKEN cDNA B230219D22 gene, hypothetical protein	yes
2	N/A	N/A	Culture didn't grow	N/A
3	3.5	AC113029	Chromosome 5 genomic sequence clone RP23-206J17	N/A
4	3.4	AK035515	RIKEN cDNA clone 9530058P10, hypothetical protein	yes
5	3.8	NM_027421	Integrator complex subunit 2	5`-truncated
6	3.2	NM_133847	Transmembrane 9 superfamily protein member 4	yes
7	3.7	BC067029	Isoleucine-tRNA synthetase	yes
8	4.0	AK163981	V-crk sarcoma virus C10 oncogene homolog (avian)-like	yes
9	0.15	AY030275	RNA binding protein	5`- and 3`-truncated
10	1.0	NM_021303	Nucleolar complex associated 2 homolog	5`-truncated
11	3.0	BC008995	Threonyl-tRNA synthetase-like 1	yes
12	4.5	AK154170	PRP39 pre-mRNA processing factor 39 homolog (yeast)	yes

Fraction 4

Clone #	Approxmiate insert size (kb)	Accession	Clone description	Full-length?
1	0.4	BC108333	SET domain containing (lysine methyl-transferase) 8	5`-truncated
2	N/A	N/A	Linearised vector (mutation in SFI1A site)	N/A
3	>5	NM_175258	Rap guanine nucleotide excange factor (GEF) 6	5`-truncated
4	>5	NM_026009	Adipocyte-specific protein 4 homolog	yes
5	N/A	N/A	Uncut vector	N/A
6	0.6	BC081449	Ribosomal protein S14	yes
7	1.1	BC054768	Ubiquitin-like 1 (sentrin) activating enzyme E13	5`-truncated
8	0.3	AK144134	SCY1-like 1	5`-truncated
9	0.2	NM_023133	Ribosomal protein S19	5`-truncated
10	0.45	BC081463	Finkel-Biskis-Reilly murine sarcoma virus (FBR-MuSV) ubiquitously expressed (fox derived)	5`-truncated
11	2.1	NM_024229	Phosphate cytidylyltransferase 2	yes
12	0.8	N/A	Original vector (with eGFP stuffer)	N/A

Details for selected clones from the four fractions of the M1 cDNA library (Fractions 3 and 4). Approximate insert size was estimated using agarose gel electrophoresis. Completeness of the clone (‘full-length’) was evaluated relative to the 5` and 3` ends given for each accession number shown. This data is summarised in Chapter 3, Table 3.1. N/A = not applicable

Appendix B.

1.

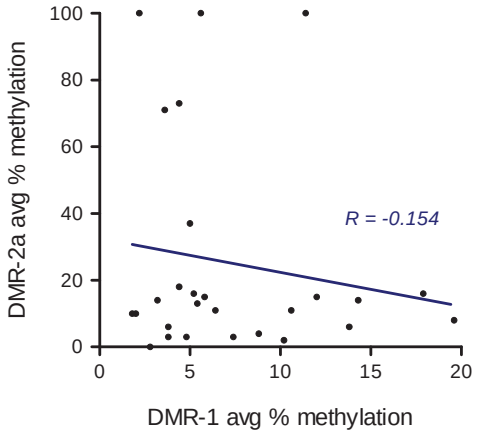

2.

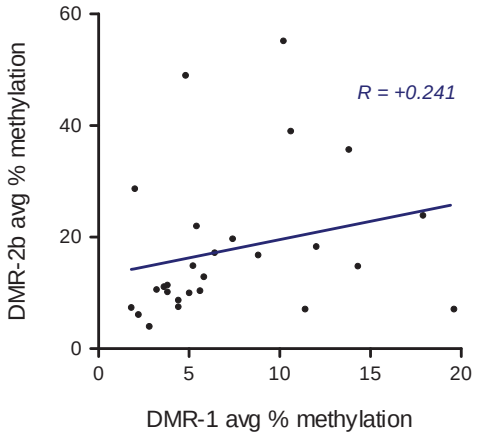

3.

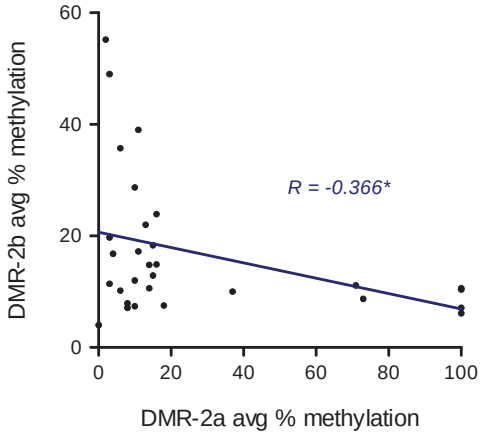

Correlation of methylation in *KLF5* DMR-1, DMR-2a and DMR2b. Average percentage methylation of **1.** DMR-2a plotted relative to DMR-1 (n=27), **2.** DMR-2b plotted relative to DMR-1 (n=27), and **3.** DMR-2b plotted relative to DMR-2a (n=29) in AML samples described in Chapter 5, Section 5.2.2.2. The blue line represents linear regression with R values indicated, *p<0.05

Appendix C.

	Linear regression			*Fisher*
	R value	**R^2 value**	**P value**	**P value**
DMR-1	-0.255	0.065	0.230	0.629
DMR-2a	+0.161	0.026	0.432	0.293
DMR-2b	-0.135	0.018	0.502	0.077
Multiple	0.291	0.085	0.632	N/A

Correlation of relative *KLF5* mRNA expression with methylation of *KLF5* DMR-1, DMR-2a and DMR-2b using linear regression and Fisher's exact test. Statistics for the correlation of relative *KLF5* mRNA expression (Q-PCR) with methylation of DMR-1, DMR-2a or DMR-2b using linear regression analysis and Fisher's exact test. Multiple linear regression analysis was also performed to determine the combined influence of methylation at DMR-1 and both regions of DMR-2 on relative *KLF5* mRNA expression. For Fisher's exact test, the high methylation groups consist of samples classified as aberrantly methylated in Chapter 5, Figures 5.9, 5.11 and 5.13 for DMR-1, DMR-2a and DMR-2b respectively. Note that AML7 was excluded as an outlier (see Chapter 5, Figure 5.1). Samples were defined as having high *KLF5* expression if the relative expression was >1.5.

Appendix D.

1. DNA homology of region containing CpG residues 141-143 (DMR-2a)

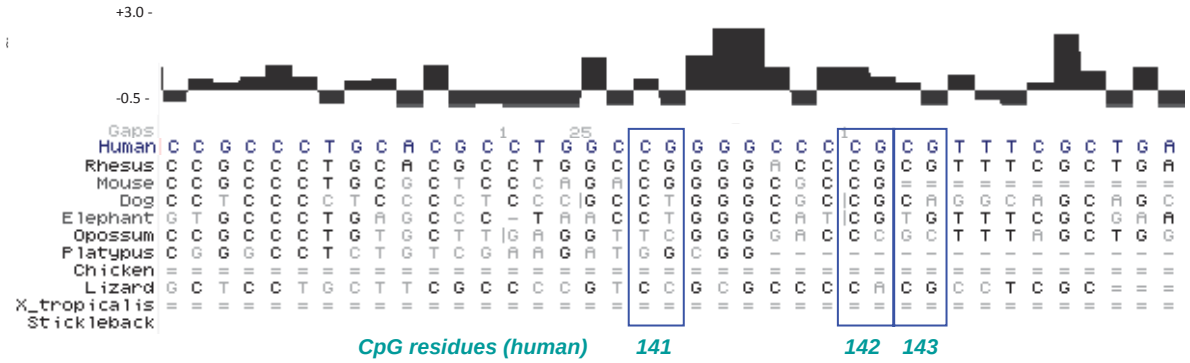

2. Predicted transcription factor binding sites in DMR-2a

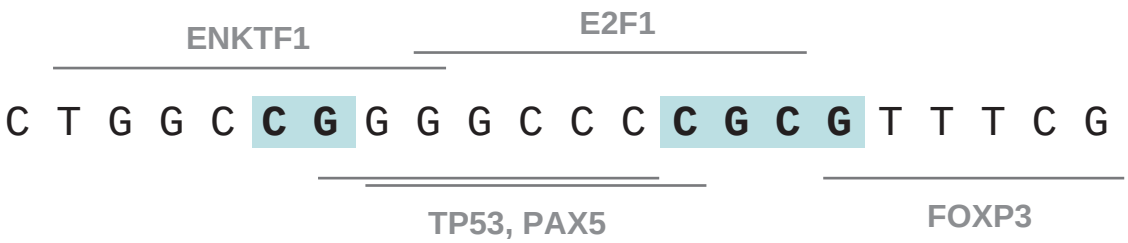

Features of *KLF5* DMR-2a. 1. Homology of DNA region containing *KLF5* CpG 141-143 (DMR-2a) amongst selected vertebrate species (UCSC Genome Browser). Histogram shows relative conservation amongst 44 vertebrate species. Highly homologous sequences between species are given positive scores, indicating that they have evolved more slowly than would have been predicted. Divergent sequences are given a negative score, as they have evolved more quickly. For a detailed explanation of the homology scoring system see UCSC Genome Browser, Vertebrate Multiz Alignment and Conservation feature. Alignment for 11 vertebrate species is shown below the histogram. Human CpG residues 141-143 are boxed in blue. Note that a horizontal dash shows nucleotides missing in this alignment, and a vertical dash shows the position of extra nucleotides in this alignment. **2.** Predicted transcription factor binding sites (human) for the DNA sequence containing CpG residues 141-143 (boxed in blue). Transcription factor binding sites were predicted using the Technical University of Catalonia ALGGEN-PROMO web-based program[440,441].

References

1. Brown, A.L., *et al.* Genetic regulators of myelopoiesis and leukemic signaling identified by gene profiling and linear modeling. *J Leukoc Biol* **80**, 433-447 (2006).
2. Giles, F.J., *et al.* Acute myeloid leukemia. *Hematology Am Soc Hematol Educ Program*, 73-110 (2002).
3. Baldus, C.D., Mrozek, K., Marcucci, G. & Bloomfield, C.D. Clinical outcome of de novo acute myeloid leukaemia patients with normal cytogenetics is affected by molecular genetic alterations: a concise review. *Br J Haematol* **137**, 387-400 (2007).
4. Wheatley, K., *et al.* A simple, robust, validated and highly predictive index for the determination of risk-directed therapy in acute myeloid leukaemia derived from the MRC AML 10 trial. United Kingdom Medical Research Council's Adult and Childhood Leukaemia Working Parties. *Br J Haematol* **107**, 69-79 (1999).
5. Slovak, M.L., *et al.* Karyotypic analysis predicts outcome of preremission and postremission therapy in adult acute myeloid leukemia: a Southwest Oncology Group/Eastern Cooperative Oncology Group Study. *Blood* **96**, 4075-4083 (2000).
6. Byrd, J.C., *et al.* Pretreatment cytogenetic abnormalities are predictive of induction success, cumulative incidence of relapse, and overall survival in adult patients with de novo acute myeloid leukemia: results from Cancer and Leukemia Group B (CALGB 8461). *Blood* **100**, 4325-4336 (2002).
7. Hoang, T. The origin of hematopoietic cell type diversity. *Oncogene* **23**, 7188-7198 (2004).
8. Wilson, A. & Trumpp, A. Bone-marrow haematopoietic-stem-cell niches. *Nat Rev Immunol* **6**, 93-106 (2006).
9. Rothenberg, E.V. Cell lineage regulators in B and T cell development. *Nat Immunol* **8**, 441-444 (2007).
10. Laiosa, C.V., Stadtfeld, M. & Graf, T. Determinants of lymphoid-myeloid lineage diversification. *Annu Rev Immunol* **24**, 705-738 (2006).
11. Takahama, Y. Journey through the thymus: stromal guides for T-cell development and selection. *Nat Rev Immunol* **6**, 127-135 (2006).
12. Cumano, A. & Godin, I. Ontogeny of the hematopoietic system. *Annu Rev Immunol* **25**, 745-785 (2007).
13. Nagasawa, T. Microenvironmental niches in the bone marrow required for B-cell development. *Nat Rev Immunol* **6**, 107-116 (2006).
14. Iwasaki, H. & Akashi, K. Myeloid lineage commitment from the hematopoietic stem cell. *Immunity* **26**, 726-740 (2007).
15. Lessard, J., Faubert, A. & Sauvageau, G. Genetic programs regulating HSC specification, maintenance and expansion. *Oncogene* **23**, 7199-7209 (2004).
16. Miyamoto, T. & Akashi, K. Lineage promiscuous expression of transcription factors in normal hematopoiesis. *Int J Hematol* **81**, 361-367 (2005).
17. Malhotra, S. & Kincade, P.W. Wnt-related molecules and signaling pathway equilibrium in hematopoiesis. *Cell Stem Cell* **4**, 27-36 (2009).
18. Bhatia, M., *et al.* Bone morphogenetic proteins regulate the developmental program of human hematopoietic stem cells. *J Exp Med* **189**, 1139-1148 (1999).
19. Robb, L. Cytokine receptors and hematopoietic differentiation. *Oncogene* **26**, 6715-6723 (2007).
20. Metcalf, D. Hematopoietic cytokines. *Blood* **111**, 485-491 (2008).

21. Perkins, A. Erythroid Kruppel like factor: from fishing expedition to gourmet meal. *Int J Biochem Cell Biol* **31**, 1175-1192 (1999).
22. Lekstrom-Himes, J.A. The role of C/EBP(epsilon) in the terminal stages of granulocyte differentiation. *Stem Cells* **19**, 125-133 (2001).
23. Cobaleda, C., Schebesta, A., Delogu, A. & Busslinger, M. Pax5: the guardian of B cell identity and function. *Nat Immunol* **8**, 463-470 (2007).
24. Gilliland, D.G. Hematologic malignancies. *Curr Opin Hematol* **8**, 189-191 (2001).
25. Renneville, A., *et al.* Cooperating gene mutations in acute myeloid leukemia: a review of the literature. *Leukemia* **22**, 915-931 (2008).
26. Stirewalt, D.L. & Meshinchi, S. Receptor tyrosine kinase alterations in AML - biology and therapy. *Cancer Treat Res* **145**, 85-108 (2010).
27. Scholl, C., Gilliland, D.G. & Frohling, S. Deregulation of signaling pathways in acute myeloid leukemia. *Semin Oncol* **35**, 336-345 (2008).
28. Fenaux, P., *et al.* P53 gene mutations in acute myeloid leukemia with 17p monosomy. *Blood* **78**, 1652-1657 (1991).
29. Slingerland, J.M., Minden, M.D. & Benchimol, S. Mutation of the p53 gene in human acute myelogenous leukemia. *Blood* **77**, 1500-1507 (1991).
30. Sauerbrey, A., Stammler, G., Zintl, F. & Volm, M. Expression of the retinoblastoma tumor suppressor gene (RB-1) in acute leukemia. *Leuk Lymphoma* **28**, 275-283 (1998).
31. Ahuja, H.G., Jat, P.S., Foti, A., Bar-Eli, M. & Cline, M.J. Abnormalities of the retinoblastoma gene in the pathogenesis of acute leukemia. *Blood* **78**, 3259-3268 (1991).
32. Bradbury, D.A. & Russell, N.H. Comparative quantitative expression of bcl-2 by normal and leukaemic myeloid cells. *Br J Haematol* **91**, 374-379 (1995).
33. Bradbury, D.A., Zhu, Y.M. & Russell, N.H. Bcl-2 expression in acute myeloblastic leukaemia: relationship with autonomous growth and CD34 antigen expression. *Leuk Lymphoma* **24**, 221-228 (1997).
34. Porwit-MacDonald, A., *et al.* Bcl-2 protein expression in normal human bone marrow precursors and in acute myelogenous leukemia. *Leukemia* **9**, 1191-1198 (1995).
35. Andreeff, M., *et al.* Expression of Bcl-2-related genes in normal and AML progenitors: changes induced by chemotherapy and retinoic acid. *Leukemia* **13**, 1881-1892 (1999).
36. Mueller, B.U., *et al.* Heterozygous PU.1 mutations are associated with acute myeloid leukemia. *Blood* **100**, 998-1007 (2002).
37. Pabst, T., *et al.* Dominant-negative mutations of CEBPA, encoding CCAAT/enhancer binding protein-alpha (C/EBPalpha), in acute myeloid leukemia. *Nat Genet* **27**, 263-270 (2001).
38. Licht, J.D. & Sternberg, D.W. The molecular pathology of acute myeloid leukemia. *Hematology Am Soc Hematol Educ Program*, 137-142 (2005).
39. Eklund, E.A. The role of HOX genes in malignant myeloid disease. *Curr Opin Hematol* **14**, 85-89 (2007).
40. Eklund, E.A. The role of HOX genes in myeloid leukemogenesis. *Curr Opin Hematol* **13**, 67-73 (2006).
41. Argiropoulos, B. & Humphries, R.K. Hox genes in hematopoiesis and leukemogenesis. *Oncogene* **26**, 6766-6776 (2007).
42. Perkins, A., Kongsuwan, K., Visvader, J., Adams, J.M. & Cory, S. Homeobox gene expression plus autocrine growth factor production elicits myeloid leukemia. *Proc Natl Acad Sci U S A* **87**, 8398-8402 (1990).

43. Deininger, M.W. & Druker, B.J. Specific targeted therapy of chronic myelogenous leukemia with imatinib. *Pharmacol Rev* **55**, 401-423 (2003).
44. Castaigne, S., *et al.* Effectiveness and pharmacokinetics of low-dose all-trans retinoic acid (25 mg/m2) in acute promyelocytic leukemia. *Blood* **82**, 3560-3563 (1993).
45. Million, R.P., Aster, J., Gilliland, D.G. & Van Etten, R.A. The Tel-Abl (ETV6-Abl) tyrosine kinase, product of complex (9;12) translocations in human leukemia, induces distinct myeloproliferative disease in mice. *Blood* **99**, 4568-4577 (2002).
46. Kelly, L.M., *et al.* FLT3 internal tandem duplication mutations associated with human acute myeloid leukemias induce myeloproliferative disease in a murine bone marrow transplant model. *Blood* **99**, 310-318 (2002).
47. Quintas-Cardama, A. & Cortes, J. Molecular biology of bcr-abl1-positive chronic myeloid leukemia. *Blood* **113**, 1619-1630 (2009).
48. Morgan, K.J. & Gilliland, D.G. A role for JAK2 mutations in myeloproliferative diseases. *Annu Rev Med* **59**, 213-222 (2008).
49. Okuda, T., *et al.* Expression of a knocked-in AML1-ETO leukemia gene inhibits the establishment of normal definitive hematopoiesis and directly generates dysplastic hematopoietic progenitors. *Blood* **91**, 3134-3143 (1998).
50. Castilla, L.H., *et al.* The fusion gene Cbfb-MYH11 blocks myeloid differentiation and predisposes mice to acute myelomonocytic leukaemia. *Nat Genet* **23**, 144-146 (1999).
51. Kim, H.G., *et al.* FLT3-ITD cooperates with inv(16) to promote progression to acute myeloid leukemia. *Blood* **111**, 1567-1574 (2008).
52. Ahuja, H.G., Popplewell, L., Tcheurekdjian, L. & Slovak, M.L. NUP98 gene rearrangements and the clonal evolution of chronic myelogenous leukemia. *Genes Chromosomes Cancer* **30**, 410-415 (2001).
53. Ding, Y., Harada, Y., Imagawa, J., Kimura, A. & Harada, H. AML1/RUNX1 point mutation possibly promotes leukemic transformation in myeloproliferative neoplasms. *Blood* **114**, 5201-5205 (2009).
54. Harada, Y. & Harada, H. Molecular pathways mediating MDS/AML with focus on AML1/RUNX1 point mutations. *J Cell Physiol* **220**, 16-20 (2009).
55. Dohner, K. & Dohner, H. Molecular characterization of acute myeloid leukemia. *Haematologica* **93**, 976-982 (2008).
56. Ishikawa, Y., *et al.* Comprehensive analysis of cooperative gene mutations between class I and class II in de novo acute myeloid leukemia. *Eur J Haematol* **83**, 90-98 (2009).
57. Owen, C., Barnett, M. & Fitzgibbon, J. Familial myelodysplasia and acute myeloid leukaemia--a review. *Br J Haematol* **140**, 123-132 (2008).
58. Galm, O., Herman, J.G. & Baylin, S.B. The fundamental role of epigenetics in hematopoietic malignancies. *Blood Rev* **20**, 1-13 (2006).
59. Chen, J., Odenike, O. & Rowley, J.D. Leukaemogenesis: more than mutant genes. *Nat Rev Cancer* **10**, 23-36 (2010).
60. Imhof, A. Epigenetic regulators and histone modification. *Brief Funct Genomic Proteomic* **5**, 222-227 (2006).
61. Vaissiere, T., Sawan, C. & Herceg, Z. Epigenetic interplay between histone modifications and DNA methylation in gene silencing. *Mutat Res* **659**, 40-48 (2008).
62. Watt, F. & Molloy, P.L. Cytosine methylation prevents binding to DNA of a HeLa cell transcription factor required for optimal expression of the adenovirus major late promoter. *Genes Dev* **2**, 1136-1143 (1988).
63. Kanduri, C., *et al.* Functional association of CTCF with the insulator upstream of the H19 gene is parent of origin-specific and methylation-sensitive. *Curr Biol* **10**, 853-856 (2000).

64. Jones, P.L., *et al.* Methylated DNA and MeCP2 recruit histone deacetylase to repress transcription. *Nat Genet* **19**, 187-191 (1998).
65. Nan, X., *et al.* Transcriptional repression by the methyl-CpG-binding protein MeCP2 involves a histone deacetylase complex. *Nature* **393**, 386-389 (1998).
66. Esteller, M. CpG island hypermethylation and tumor suppressor genes: a booming present, a brighter future. *Oncogene* **21**, 5427-5440 (2002).
67. Yamashita, K., Dai, T., Dai, Y., Yamamoto, F. & Perucho, M. Genetics supersedes epigenetics in colon cancer phenotype. *Cancer Cell* **4**, 121-131 (2003).
68. Figueroa, M.E., *et al.* DNA methylation signatures identify biologically distinct subtypes in acute myeloid leukemia. *Cancer Cell* **17**, 13-27 (2010).
69. Herman, J.G., *et al.* Distinct patterns of inactivation of p15INK4B and p16INK4A characterize the major types of hematological malignancies. *Cancer Res* **57**, 837-841 (1997).
70. Galm, O., *et al.* Clinical implications of aberrant DNA methylation patterns in acute myelogenous leukemia. *Ann Hematol* **84 Suppl 1**, 39-46 (2005).
71. Toyota, M., *et al.* Methylation profiling in acute myeloid leukemia. *Blood* **97**, 2823-2829 (2001).
72. Melki, J.R., Vincent, P.C. & Clark, S.J. Concurrent DNA hypermethylation of multiple genes in acute myeloid leukemia. *Cancer Res* **59**, 3730-3740 (1999).
73. Ekmekci, C.G., Gutierrez, M.I., Siraj, A.K., Ozbek, U. & Bhatia, K. Aberrant methylation of multiple tumor suppressor genes in acute myeloid leukemia. *Am J Hematol* **77**, 233-240 (2004).
74. Rethmeier, A., *et al.* Promoter hypermethylation of the retinoic acid receptor beta2 gene is frequent in acute myeloid leukaemia and associated with the presence of CBFbeta-MYH11 fusion transcripts. *Br J Haematol* **133**, 276-283 (2006).
75. Figueroa, M.E., *et al.* Genome-wide epigenetic analysis delineates a biologically distinct immature acute leukemia with myeloid/T-lymphoid features. *Blood* **113**, 2795-2804 (2009).
76. Quesnel, B., *et al.* Methylation of the p15(INK4b) gene in myelodysplastic syndromes is frequent and acquired during disease progression. *Blood* **91**, 2985-2990 (1998).
77. Jiang, Y., *et al.* Aberrant DNA methylation is a dominant mechanism in MDS progression to AML. *Blood* **113**, 1315-1325 (2009).
78. Mizuno, S., *et al.* Expression of DNA methyltransferases DNMT1, 3A, and 3B in normal hematopoiesis and in acute and chronic myelogenous leukemia. *Blood* **97**, 1172-1179 (2001).
79. Ley, T.J., *et al.* DNMT3A Mutations in Acute Myeloid Leukemia. *N Engl J Med* (2010).
80. Figueroa, M.E., *et al.* Leukemic IDH1 and IDH2 Mutations Result in a Hypermethylation Phenotype, Disrupt TET2 Function, and Impair Hematopoietic Differentiation. *Cancer Cell* **18**, 553-567 (2010).
81. Liu, S., *et al.* Interplay of RUNX1/MTG8 and DNA methyltransferase 1 in acute myeloid leukemia. *Cancer Res* **65**, 1277-1284 (2005).
82. Di Croce, L., *et al.* Methyltransferase recruitment and DNA hypermethylation of target promoters by an oncogenic transcription factor. *Science* **295**, 1079-1082 (2002).
83. Strahl, B.D. & Allis, C.D. The language of covalent histone modifications. *Nature* **403**, 41-45 (2000).
84. Kouzarides, T. Chromatin modifications and their function. *Cell* **128**, 693-705 (2007).
85. Li, H., *et al.* Molecular basis for site-specific read-out of histone H3K4me3 by the BPTF PHD finger of NURF. *Nature* **442**, 91-95 (2006).

86. Wysocka, J., *et al.* A PHD finger of NURF couples histone H3 lysine 4 trimethylation with chromatin remodelling. *Nature* **442**, 86-90 (2006).
87. Shogren-Knaak, M., *et al.* Histone H4-K16 acetylation controls chromatin structure and protein interactions. *Science* **311**, 844-847 (2006).
88. Ferreira, H., Flaus, A. & Owen-Hughes, T. Histone modifications influence the action of Snf2 family remodelling enzymes by different mechanisms. *J Mol Biol* **374**, 563-579 (2007).
89. Jackson, J.P., Lindroth, A.M., Cao, X. & Jacobsen, S.E. Control of CpNpG DNA methylation by the KRYPTONITE histone H3 methyltransferase. *Nature* **416**, 556-560 (2002).
90. Fuks, F., Hurd, P.J., Deplus, R. & Kouzarides, T. The DNA methyltransferases associate with HP1 and the SUV39H1 histone methyltransferase. *Nucleic Acids Res* **31**, 2305-2312 (2003).
91. Honda, S. & Selker, E.U. Direct interaction between DNA methyltransferase DIM-2 and HP1 is required for DNA methylation in Neurospora crassa. *Mol Cell Biol* **28**, 6044-6055 (2008).
92. Jenuwein, T. & Allis, C.D. Translating the histone code. *Science* **293**, 1074-1080 (2001).
93. Mizzen, C.A. & Allis, C.D. Linking histone acetylation to transcriptional regulation. *Cell Mol Life Sci* **54**, 6-20 (1998).
94. Choi, J.K. & Howe, L.J. Histone acetylation: truth of consequences? *Biochem Cell Biol* **87**, 139-150 (2009).
95. Cheung, P. & Lau, P. Epigenetic regulation by histone methylation and histone variants. *Mol Endocrinol* **19**, 563-573 (2005).
96. Grignani, F., *et al.* Fusion proteins of the retinoic acid receptor-alpha recruit histone deacetylase in promyelocytic leukaemia. *Nature* **391**, 815-818 (1998).
97. Wang, J., Hoshino, T., Redner, R.L., Kajigaya, S. & Liu, J.M. ETO, fusion partner in t(8;21) acute myeloid leukemia, represses transcription by interaction with the human N-CoR/mSin3/HDAC1 complex. *Proc Natl Acad Sci U S A* **95**, 10860-10865 (1998).
98. Amann, J.M., *et al.* ETO, a target of t(8;21) in acute leukemia, makes distinct contacts with multiple histone deacetylases and binds mSin3A through its oligomerization domain. *Mol Cell Biol* **21**, 6470-6483 (2001).
99. Krivtsov, A.V. & Armstrong, S.A. MLL translocations, histone modifications and leukaemia stem-cell development. *Nat Rev Cancer* **7**, 823-833 (2007).
100. Dou, Y. & Hess, J.L. Mechanisms of transcriptional regulation by MLL and its disruption in acute leukemia. *Int J Hematol* **87**, 10-18 (2008).
101. van Haaften, G., *et al.* Somatic mutations of the histone H3K27 demethylase gene UTX in human cancer. *Nat Genet* **41**, 521-523 (2009).
102. Makishima, H., *et al.* Novel homo- and hemizygous mutations in EZH2 in myeloid malignancies. *Leukemia* **24**, 1799-1804 (2010).
103. Boultwood, J., *et al.* Frequent mutation of the polycomb-associated gene ASXL1 in the myelodysplastic syndromes and in acute myeloid leukemia. *Leukemia* **24**, 1062-1065 (2010).
104. Beck, S., Faradji, F., Brock, H. & Peronnet, F. Maintenance of Hox gene expression patterns. *Adv Exp Med Biol* **689**, 41-62 (2010).
105. Fuks, F. DNA methylation and histone modifications: teaming up to silence genes. *Curr Opin Genet Dev* **15**, 490-495 (2005).
106. Look, A.T. Oncogenic transcription factors in the human acute leukemias. *Science* **278**, 1059-1064 (1997).

107. Grimwade, D., *et al.* The importance of diagnostic cytogenetics on outcome in AML: analysis of 1,612 patients entered into the MRC AML 10 trial. The Medical Research Council Adult and Children's Leukaemia Working Parties. *Blood* **92**, 2322-2333 (1998).
108. Wouters, B.J., *et al.* Distinct gene expression profiles of acute myeloid/T-lymphoid leukemia with silenced CEBPA and mutations in NOTCH1. *Blood* **110**, 3706-3714 (2007).
109. Gale, R.E., *et al.* Relationship between FLT3 mutation status, biologic characteristics, and response to targeted therapy in acute promyelocytic leukemia. *Blood* **106**, 3768-3776 (2005).
110. Guidez, F., *et al.* RARalpha-PLZF overcomes PLZF-mediated repression of CRABPI, contributing to retinoid resistance in t(11;17) acute promyelocytic leukemia. *Proc Natl Acad Sci U S A* **104**, 18694-18699 (2007).
111. Gebhard, C., *et al.* Genome-wide profiling of CpG methylation identifies novel targets of aberrant hypermethylation in myeloid leukemia. *Cancer Res* **66**, 6118-6128 (2006).
112. Khulan, B., *et al.* Comparative isoschizomer profiling of cytosine methylation: the HELP assay. *Genome Res* **16**, 1046-1055 (2006).
113. Walter, M.J., *et al.* Acquired copy number alterations in adult acute myeloid leukemia genomes. *Proc Natl Acad Sci U S A* **106**, 12950-12955 (2009).
114. Bullinger, L., *et al.* Identification of acquired copy number alterations and uniparental disomies in cytogenetically normal acute myeloid leukemia using high-resolution single-nucleotide polymorphism analysis. *Leukemia* **24**, 438-449 (2010).
115. Grand, F.H., *et al.* Frequent CBL mutations associated with 11q acquired uniparental disomy in myeloproliferative neoplasms. *Blood* **113**, 6182-6192 (2009).
116. Makishima, H., *et al.* Mutations of e3 ubiquitin ligase cbl family members constitute a novel common pathogenic lesion in myeloid malignancies. *J Clin Oncol* **27**, 6109-6116 (2009).
117. Delhommeau, F., *et al.* Mutation in TET2 in myeloid cancers. *N Engl J Med* **360**, 2289-2301 (2009).
118. Mardis, E.R., *et al.* Recurring mutations found by sequencing an acute myeloid leukemia genome. *N Engl J Med* **361**, 1058-1066 (2009).
119. Pardanani, A., *et al.* IDH1 and IDH2 mutation analysis in chronic- and blast-phase myeloproliferative neoplasms. *Leukemia* **24**, 1146-1151 (2010).
120. Tefferi, A., *et al.* IDH1 and IDH2 mutation studies in 1473 patients with chronic-, fibrotic- or blast-phase essential thrombocythemia, polycythemia vera or myelofibrosis. *Leukemia* **24**, 1302-1309 (2010).
121. Meyerson, M., Gabriel, S. & Getz, G. Advances in understanding cancer genomes through second-generation sequencing. *Nat Rev Genet* **11**, 685-696 (2010).
122. Mushinski, J.F., Potter, M., Bauer, S.R. & Reddy, E.P. DNA rearrangement and altered RNA expression of the c-myb oncogene in mouse plasmacytoid lymphosarcomas. *Science* **220**, 795-798 (1983).
123. Kabrun, N., Bumstead, N., Hayman, M.J. & Enrietto, P.J. Characterization of a novel promoter insertion in the c-rel locus. *Mol Cell Biol* **10**, 4788-4794 (1990).
124. Akagi, K., Suzuki, T., Stephens, R.M., Jenkins, N.A. & Copeland, N.G. RTCGD: retroviral tagged cancer gene database. *Nucleic Acids Res* **32**, D523-527 (2004).
125. Starr, R., *et al.* A family of cytokine-inducible inhibitors of signalling. *Nature* **387**, 917-921 (1997).
126. Watanabe-Okochi, N., *et al.* Possible involvement of RasGRP4 in leukemogenesis. *Int J Hematol* **89**, 470-481 (2009).

127. Mourtada-Maarabouni, M., *et al.* Functional expression cloning reveals proapoptotic role for protein phosphatase 4. *Cell Death Differ* **10**, 1016-1024 (2003).
128. McCormack, M.P. & Gonda, T.J. Novel murine myeloid cell lines that exhibit a differentiation switch in response to IL-3 or GM-CSF, or to different constitutively active mutants of the GM-CSF receptor beta subunit. *Blood* **95**, 120-127 (2000).
129. Brown, A.L., Peters, M., D'Andrea, R.J. & Gonda, T.J. Constitutive mutants of the GM-CSF receptor reveal multiple pathways leading to myeloid cell survival, proliferation, and granulocyte-macrophage differentiation. *Blood* **103**, 507-516 (2004).
130. Perugini, M., *et al.* Alternative modes of GM-CSF receptor activation revealed using activated mutants of the common beta-subunit. *Blood* **115**, 3346-3353 (2010).
131. Koschmieder, S., Rosenbauer, F., Steidl, U., Owens, B.M. & Tenen, D.G. Role of transcription factors C/EBPalpha and PU.1 in normal hematopoiesis and leukemia. *Int J Hematol* **81**, 368-377 (2005).
132. Cammenga, J., *et al.* Induction of C/EBPalpha activity alters gene expression and differentiation of human CD34+ cells. *Blood* **101**, 2206-2214 (2003).
133. Pearson, R., Fleetwood, J., Eaton, S., Crossley, M. & Bao, S. Kruppel-like transcription factors: a functional family. *Int J Biochem Cell Biol* **40**, 1996-2001 (2008).
134. McConnell, B.B. & Yang, V.W. Mammalian Kruppel-like factors in health and diseases. *Physiol Rev* **90**, 1337-1381 (2010).
135. Miller, I.J. & Bieker, J.J. A novel, erythroid cell-specific murine transcription factor that binds to the CACCC element and is related to the Kruppel family of nuclear proteins. *Mol Cell Biol* **13**, 2776-2786 (1993).
136. Wieschaus, E., Nusslein-Volhard, C. & Kluding, H. Kruppel, a gene whose activity is required early in the zygotic genome for normal embryonic segmentation. *Dev Biol* **104**, 172-186 (1984).
137. Frontelo, P., *et al.* Novel role for EKLF in megakaryocyte lineage commitment. *Blood* **110**, 3871-3880 (2007).
138. Nuez, B., Michalovich, D., Bygrave, A., Ploemacher, R. & Grosveld, F. Defective haematopoiesis in fetal liver resulting from inactivation of the EKLF gene. *Nature* **375**, 316-318 (1995).
139. Perkins, A.C., Sharpe, A.H. & Orkin, S.H. Lethal beta-thalassaemia in mice lacking the erythroid CACCC-transcription factor EKLF. *Nature* **375**, 318-322 (1995).
140. Basu, P., *et al.* KLF2 is essential for primitive erythropoiesis and regulates the human and murine embryonic beta-like globin genes in vivo. *Blood* **106**, 2566-2571 (2005).
141. Carlson, C.M., *et al.* Kruppel-like factor 2 regulates thymocyte and T-cell migration. *Nature* **442**, 299-302 (2006).
142. Kuo, C.T., Veselits, M.L. & Leiden, J.M. LKLF: A transcriptional regulator of single-positive T cell quiescence and survival. *Science* **277**, 1986-1990 (1997).
143. Kuo, C.T., *et al.* The LKLF transcription factor is required for normal tunica media formation and blood vessel stabilization during murine embryogenesis. *Genes Dev* **11**, 2996-3006 (1997).
144. Lee, J.S., *et al.* Klf2 is an essential regulator of vascular hemodynamic forces in vivo. *Dev Cell* **11**, 845-857 (2006).
145. Nakagawa, M., *et al.* Generation of induced pluripotent stem cells without Myc from mouse and human fibroblasts. *Nat Biotechnol* **26**, 101-106 (2008).
146. Wani, M.A., Wert, S.E. & Lingrel, J.B. Lung Kruppel-like factor, a zinc finger transcription factor, is essential for normal lung development. *J Biol Chem* **274**, 21180-21185 (1999).

147. Wu, J., Srinivasan, S.V., Neumann, J.C. & Lingrel, J.B. The KLF2 transcription factor does not affect the formation of preadipocytes but inhibits their differentiation into adipocytes. *Biochemistry* **44**, 11098-11105 (2005).
148. Crossley, M., *et al.* Isolation and characterization of the cDNA encoding BKLF/TEF-2, a major CACCC-box-binding protein in erythroid cells and selected other cells. *Mol Cell Biol* **16**, 1695-1705 (1996).
149. Sue, N., *et al.* Targeted disruption of the basic Kruppel-like factor gene (Klf3) reveals a role in adipogenesis. *Mol Cell Biol* **28**, 3967-3978 (2008).
150. Ghaleb, A.M., *et al.* Kruppel-like factors 4 and 5: the yin and yang regulators of cellular proliferation. *Cell Res* **15**, 92-96 (2005).
151. Katz, J.P., *et al.* The zinc-finger transcription factor Klf4 is required for terminal differentiation of goblet cells in the colon. *Development* **129**, 2619-2628 (2002).
152. McConnell, B.B., Ghaleb, A.M., Nandan, M.O. & Yang, V.W. The diverse functions of Kruppel-like factors 4 and 5 in epithelial biology and pathobiology. *Bioessays* **29**, 549-557 (2007).
153. Segre, J.A., Bauer, C. & Fuchs, E. Klf4 is a transcription factor required for establishing the barrier function of the skin. *Nat Genet* **22**, 356-360 (1999).
154. Takahashi, K. & Yamanaka, S. Induction of pluripotent stem cells from mouse embryonic and adult fibroblast cultures by defined factors. *Cell* **126**, 663-676 (2006).
155. Takahashi, K., *et al.* Induction of pluripotent stem cells from adult human fibroblasts by defined factors. *Cell* **131**, 861-872 (2007).
156. Oishi, Y., *et al.* Kruppel-like transcription factor KLF5 is a key regulator of adipocyte differentiation. *Cell Metab* **1**, 27-39 (2005).
157. Shindo, T., *et al.* Kruppel-like zinc-finger transcription factor KLF5/BTEB2 is a target for angiotensin II signaling and an essential regulator of cardiovascular remodeling. *Nat Med* **8**, 856-863 (2002).
158. Takeda, N., *et al.* Cardiac fibroblasts are essential for the adaptive response of the murine heart to pressure overload. *J Clin Invest* **120**, 254-265 (2010).
159. Wan, H., *et al.* Kruppel-like factor 5 is required for perinatal lung morphogenesis and function. *Development* **135**, 2563-2572 (2008).
160. Ema, M., *et al.* Kruppel-like factor 5 is essential for blastocyst development and the normal self-renewal of mouse ESCs. *Cell Stem Cell* **3**, 555-567 (2008).
161. Lin, S.C., Wani, M.A., Whitsett, J.A. & Wells, J.M. Klf5 regulates lineage formation in the pre-implantation mouse embryo. *Development* **137**, 3953-3963 (2010).
162. Parisi, S., *et al.* Direct targets of Klf5 transcription factor contribute to the maintenance of mouse embryonic stem cell undifferentiated state. *BMC Biol* **8**, 128 (2010).
163. Bourillot, P.Y. & Savatier, P. Kruppel-like transcription factors and control of pluripotency. *BMC Biol* **8**, 125 (2010).
164. Matsumoto, N., *et al.* Developmental regulation of yolk sac hematopoiesis by Kruppel-like factor 6. *Blood* **107**, 1357-1365 (2006).
165. Li, D., *et al.* Kruppel-like factor-6 promotes preadipocyte differentiation through histone deacetylase 3-dependent repression of DLK1. *J Biol Chem* **280**, 26941-26952 (2005).
166. Botella, L.M., *et al.* Transcriptional activation of endoglin and transforming growth factor-beta signaling components by cooperative interaction between Sp1 and KLF6: their potential role in the response to vascular injury. *Blood* **100**, 4001-4010 (2002).
167. Das, A., *et al.* Disruption of an SP2/KLF6 repression complex by SHP is required for farnesoid X receptor-induced endothelial cell migration. *J Biol Chem* **281**, 39105-39113 (2006).

168. Laub, F., *et al.* Transcription factor KLF7 is important for neuronal morphogenesis in selected regions of the nervous system. *Mol Cell Biol* **25**, 5699-5711 (2005).
169. Kanazawa, A., *et al.* Single nucleotide polymorphisms in the gene encoding Kruppel-like factor 7 are associated with type 2 diabetes. *Diabetologia* **48**, 1315-1322 (2005).
170. van Vliet, J., Turner, J. & Crossley, M. Human Kruppel-like factor 8: a CACCC-box binding protein that associates with CtBP and represses transcription. *Nucleic Acids Res* **28**, 1955-1962 (2000).
171. Martin, K.M., Metcalfe, J.C. & Kemp, P.R. Expression of Klf9 and Klf13 in mouse development. *Mech Dev* **103**, 149-151 (2001).
172. Morita, M., *et al.* Functional analysis of basic transcription element binding protein by gene targeting technology. *Mol Cell Biol* **23**, 2489-2500 (2003).
173. Simmen, F.A., *et al.* Dysregulation of intestinal crypt cell proliferation and villus cell migration in mice lacking Kruppel-like factor 9. *Am J Physiol Gastrointest Liver Physiol* **292**, G1757-1769 (2007).
174. Simmen, R.C., *et al.* Subfertility, uterine hypoplasia, and partial progesterone resistance in mice lacking the Kruppel-like factor 9/basic transcription element-binding protein-1 (Bteb1) gene. *J Biol Chem* **279**, 29286-29294 (2004).
175. Cao, Z., Sun, X., Icli, B., Wara, A.K. & Feinberg, M.W. Role of Kruppel-like factors in leukocyte development, function, and disease. *Blood* (2010).
176. Hawse, J.R., *et al.* TIEG-null mice display an osteopenic gender-specific phenotype. *Bone* **42**, 1025-1031 (2008).
177. Rajamannan, N.M., *et al.* TGFbeta inducible early gene-1 (TIEG1) and cardiac hypertrophy: Discovery and characterization of a novel signaling pathway. *J Cell Biochem* **100**, 315-325 (2007).
178. Subramaniam, M., *et al.* TIEG1 null mouse-derived osteoblasts are defective in mineralization and in support of osteoclast differentiation in vitro. *Mol Cell Biol* **25**, 1191-1199 (2005).
179. Bensamoun, S.F., *et al.* Age-dependent changes in the mechanical properties of tail tendons in TGF-beta inducible early gene-1 knockout mice. *J Appl Physiol* **101**, 1419-1424 (2006).
180. Cook, T., Gebelein, B., Mesa, K., Mladek, A. & Urrutia, R. Molecular cloning and characterization of TIEG2 reveals a new subfamily of transforming growth factor-beta-inducible Sp1-like zinc finger-encoding genes involved in the regulation of cell growth. *J Biol Chem* **273**, 25929-25936 (1998).
181. Song, C.Z., Gavriilidis, G., Asano, H. & Stamatoyannopoulos, G. Functional study of transcription factor KLF11 by targeted gene inactivation. *Blood Cells Mol Dis* **34**, 53-59 (2005).
182. Imhof, A., *et al.* Transcriptional regulation of the AP-2alpha promoter by BTEB-1 and AP-2rep, a novel wt-1/egr-related zinc finger repressor. *Mol Cell Biol* **19**, 194-204 (1999).
183. Suda, S., Rai, T., Sohara, E., Sasaki, S. & Uchida, S. Postnatal expression of KLF12 in the inner medullary collecting ducts of kidney and its trans-activation of UT-A1 urea transporter promoter. *Biochem Biophys Res Commun* **344**, 246-252 (2006).
184. Gordon, A.R., *et al.* Splenomegaly and modified erythropoiesis in KLF13-/- mice. *J Biol Chem* **283**, 11897-11904 (2008).
185. Outram, S.V., *et al.* KLF13 influences multiple stages of both B and T cell development. *Cell Cycle* **7**, 2047-2055 (2008).
186. Lavallee, G., *et al.* The Kruppel-like transcription factor KLF13 is a novel regulator of heart development. *EMBO J* **25**, 5201-5213 (2006).

187. Zhou, M., *et al.* Kruppel-like transcription factor 13 regulates T lymphocyte survival in vivo. *J Immunol* **178**, 5496-5504 (2007).
188. Scohy, S., *et al.* Identification of KLF13 and KLF14 (SP6), novel members of the SP/XKLF transcription factor family. *Genomics* **70**, 93-101 (2000).
189. Fisch, S., *et al.* Kruppel-like factor 15 is a regulator of cardiomyocyte hypertrophy. *Proc Natl Acad Sci U S A* **104**, 7074-7079 (2007).
190. Gray, S., *et al.* Regulation of gluconeogenesis by Kruppel-like factor 15. *Cell Metab* **5**, 305-312 (2007).
191. Wang, B., *et al.* The Kruppel-like factor KLF15 inhibits connective tissue growth factor (CTGF) expression in cardiac fibroblasts. *J Mol Cell Cardiol* **45**, 193-197 (2008).
192. D'Souza, U.M., Lammers, C.H., Hwang, C.K., Yajima, S. & Mouradian, M.M. Developmental expression of the zinc finger transcription factor DRRF (dopamine receptor regulating factor). *Mech Dev* **110**, 197-201 (2002).
193. van Vliet, J., *et al.* Human KLF17 is a new member of the Sp/KLF family of transcription factors. *Genomics* **87**, 474-482 (2006).
194. Yan, W., Burns, K.H., Ma, L. & Matzuk, M.M. Identification of Zfp393, a germ cell-specific gene encoding a novel zinc finger protein. *Mech Dev* **118**, 233-239 (2002).
195. Kaczynski, J., Cook, T. & Urrutia, R. Sp1- and Kruppel-like transcription factors. *Genome Biol* **4**, 206 (2003).
196. Bieker, J.J. Kruppel-like factors: three fingers in many pies. *J Biol Chem* **276**, 34355-34358 (2001).
197. Sogawa, K., *et al.* cDNA cloning and transcriptional properties of a novel GC box-binding protein, BTEB2. *Nucleic Acids Res* **21**, 1527-1532 (1993).
198. Conkright, M.D., Wani, M.A., Anderson, K.P. & Lingrel, J.B. A gene encoding an intestinal-enriched member of the Kruppel-like factor family expressed in intestinal epithelial cells. *Nucleic Acids Res* **27**, 1263-1270 (1999).
199. Dong, J.T. & Chen, C. Essential role of KLF5 transcription factor in cell proliferation and differentiation and its implications for human diseases. *Cell Mol Life Sci* **66**, 2691-2706 (2009).
200. Moore, D.L., *et al.* KLF family members regulate intrinsic axon regeneration ability. *Science* **326**, 298-301 (2009).
201. Shi, H., Zhang, Z., Wang, X., Liu, S. & Teng, C.T. Isolation and characterization of a gene encoding human Kruppel-like factor 5 (IKLF): binding to the CAAT/GT box of the mouse lactoferrin gene promoter. *Nucleic Acids Res* **27**, 4807-4815 (1999).
202. Watanabe, N., *et al.* BTEB2, a Kruppel-like transcription factor, regulates expression of the SMemb/Nonmuscle myosin heavy chain B (SMemb/NMHC-B) gene. *Circ Res* **85**, 182-191 (1999).
203. Yanagi, M., *et al.* Expression of Kruppel-like factor 5 gene in human brain and association of the gene with the susceptibility to schizophrenia. *Schizophr Res* **100**, 291-301 (2008).
204. Yang, X.O., Doty, R.T., Hicks, J.S. & Willerford, D.M. Regulation of T-cell receptor D beta 1 promoter by KLF5 through reiterated GC-rich motifs. *Blood* **101**, 4492-4499 (2003).
205. Kawai-Kowase, K., Kurabayashi, M., Hoshino, Y., Ohyama, Y. & Nagai, R. Transcriptional activation of the zinc finger transcription factor BTEB2 gene by Egr-1 through mitogen-activated protein kinase pathways in vascular smooth muscle cells. *Circ Res* **85**, 787-795 (1999).
206. Chen, C., *et al.* Regulation of KLF5 involves the Sp1 transcription factor in human epithelial cells. *Gene* **330**, 133-142 (2004).

207. Yatsula, B., *et al.* Identification of binding sites of EVI1 in mammalian cells. *J Biol Chem* **280**, 30712-30722 (2005).
208. Parisi, S., *et al.* Klf5 is involved in self-renewal of mouse embryonic stem cells. *J Cell Sci* **121**, 2629-2634 (2008).
209. Mori, D., Okuro, N., Fujii-Kuriyama, Y. & Sogawa, K. Gene structure and promoter analysis of the rat BTEB2 gene. *Gene* **304**, 163-170 (2003).
210. Tetreault, M.P., *et al.* Esophageal squamous cell dysplasia and delayed differentiation with deletion of kruppel-like factor 4 in murine esophagus. *Gastroenterology* **139**, 171-181 e179 (2010).
211. Dang, D.T., Zhao, W., Mahatan, C.S., Geiman, D.E. & Yang, V.W. Opposing effects of Kruppel-like factor 4 (gut-enriched Kruppel-like factor) and Kruppel-like factor 5 (intestinal-enriched Kruppel-like factor) on the promoter of the Kruppel-like factor 4 gene. *Nucleic Acids Res* **30**, 2736-2741 (2002).
212. Oishi, Y., *et al.* Regulatory polymorphism in transcription factor KLF5 at the MEF2 element alters the response to angiotensin II and is associated with human hypertension. *FASEB J*.
213. Frigo, D.E., *et al.* Induction of Kruppel-like factor 5 expression by androgens results in increased CXCR4-dependent migration of prostate cancer cells in vitro. *Mol Endocrinol* (2009).
214. Cheng, Y., *et al.* MicroRNA-145, a novel smooth muscle cell phenotypic marker and modulator, controls vascular neointimal lesion formation. *Circ Res* **105**, 158-166 (2009).
215. Trakooljul, N., Hicks, J.A. & Liu, H.C. Identification of target genes and pathways associated with chicken microRNA miR-143. *Anim Genet*.
216. Kinoshita, M., *et al.* Regulation of adipocyte differentiation by activation of serotonin (5-HT) receptors 5-HT2AR and 5-HT2CR and involvement of microRNA-448-mediated repression of KLF5. *Mol Endocrinol* **24**, 1978-1987 (2010).
217. Du, J.X., Bialkowska, A.B., McConnell, B.B. & Yang, V.W. SUMOylation regulates nuclear localization of Kruppel-like factor 5. *J Biol Chem* **283**, 31991-32002 (2008).
218. Zhang, Z. & Teng, C.T. Phosphorylation of Kruppel-like factor 5 (KLF5/IKLF) at the CBP interaction region enhances its transactivation function. *Nucleic Acids Res* **31**, 2196-2208 (2003).
219. Liu, Y., Wen, J.K., Dong, L.H., Zheng, B. & Han, M. Kruppel-like factor (KLF) 5 mediates cyclin D1 expression and cell proliferation via interaction with c-Jun in Ang II-induced VSMCs. *Acta Pharmacol Sin* **31**, 10-18 (2009).
220. He, M., Han, M., Zheng, B., Shu, Y.N. & Wen, J.K. Angiotensin II stimulates KLF5 phosphorylation and its interaction with c-Jun leading to suppression of p21 expression in vascular smooth muscle cells. *J Biochem* **146**, 683-691 (2009).
221. Guo, P., *et al.* Pro-proliferative factor KLF5 becomes anti-proliferative in epithelial homeostasis upon signaling-mediated modification. *J Biol Chem* **284**, 6071-6078 (2009).
222. Guo, P., Zhao, K.W., Dong, X.Y., Sun, X. & Dong, J.T. Acetylation of KLF5 alters the assembly of P15 transcription factors in TGFbeta-mediated induction in epithelial cells. *J Biol Chem* (2009).
223. Oishi, Y., *et al.* SUMOylation of Kruppel-like transcription factor 5 acts as a molecular switch in transcriptional programs of lipid metabolism involving PPAR-delta. *Nat Med* **14**, 656-666 (2008).
224. Chen, C., *et al.* Ubiquitin-proteasome degradation of KLF5 transcription factor in cancer and untransformed epithelial cells. *Oncogene* **24**, 3319-3327 (2005).

225. Liu, N., *et al.* The Fbw7/human CDC4 tumor suppressor targets proproliferative factor KLF5 for ubiquitination and degradation through multiple phosphodegron motifs. *J Biol Chem* **285**, 18858-18867 (2010).
226. Chen, C. Regulation of Krupple-like factor 5 by targeted protein degradation. *Methods Mol Biol* **647**, 267-277 (2010).
227. Chen, C., Zhou, Z., Guo, P. & Dong, J.T. Proteasomal degradation of the KLF5 transcription factor through a ubiquitin-independent pathway. *FEBS Lett* **581**, 1124-1130 (2007).
228. Meyer, S.E., *et al.* Kruppel-like factor 5 is not required for K-RasG12D lung tumorigenesis, but represses ABCG2 expression and is associated with better disease-specific survival. *Am J Pathol* **177**, 1503-1513 (2010).
229. Bateman, N.W., Tan, D., Pestell, R.G., Black, J.D. & Black, A.R. Intestinal tumor progression is associated with altered function of KLF5. *J Biol Chem* **279**, 12093-12101 (2004).
230. Nandan, M.O., Chanchevalap, S., Dalton, W.B. & Yang, V.W. Kruppel-like factor 5 promotes mitosis by activating the cyclin B1/Cdc2 complex during oncogenic Ras-mediated transformation. *FEBS Lett* **579**, 4757-4762 (2005).
231. Martinez-Ceballos, E., Chambon, P. & Gudas, L.J. Differences in gene expression between wild type and Hoxa1 knockout embryonic stem cells after retinoic acid treatment or leukemia inhibitory factor (LIF) removal. *J Biol Chem* **280**, 16484-16498 (2005).
232. Shao, J., Yang, V.W. & Sheng, H. Prostaglandin E2 and Kruppel-like transcription factors synergistically induce the expression of decay-accelerating factor in intestinal epithelial cells. *Immunology* **125**, 397-407 (2008).
233. Yang, Y., Goldstein, B.G., Nakagawa, H. & Katz, J.P. Kruppel-like factor 5 activates MEK/ERK signaling via EGFR in primary squamous epithelial cells. *FASEB J* **21**, 543-550 (2007).
234. Nagai, R., Kowase, K. & Kurabayashi, M. Transcriptional regulation of smooth muscle phenotypic modulation. *Ann N Y Acad Sci* **902**, 214-222; discussion 222-213 (2000).
235. Liu, R., Zheng, H.Q., Zhou, Z., Dong, J.T. & Chen, C. KLF5 promotes breast cell survival partially through FGF-BP-pERK-mediated MKP-1 protein phosphorylation and stabilization. *J Biol Chem* (2009).
236. Zheng, H.Q., *et al.* Kruppel-like factor 5 promotes breast cell proliferation partially through upregulating the transcription of fibroblast growth factor binding protein 1. *Oncogene* **28**, 3702-3713 (2009).
237. Zhang, P., *et al.* A functional screen for Kruppel-like factors that regulate the human gamma-globin gene through the CACCC promoter element. *Blood Cells Mol Dis* **35**, 227-235 (2005).
238. Yang, Y., Tetreault, M.P., Yermolina, Y.A., Goldstein, B.G. & Katz, J.P. Kruppel-like factor 5 controls keratinocyte migration via the integrin-linked kinase. *J Biol Chem* **283**, 18812-18820 (2008).
239. Piccinni, S.A., *et al.* Kruppel-like factors regulate the Lama1 gene encoding the laminin alpha1 chain. *J Biol Chem* **279**, 9103-9114 (2004).
240. Wong, W.K., Chen, K. & Shih, J.C. Regulation of human monoamine oxidase B gene by Sp1 and Sp3. *Mol Pharmacol* **59**, 852-859 (2001).
241. Sun, S.G., *et al.* miR-146a and Kruppel-like factor 4 form a feedback loop to participate in vascular smooth muscle cell proliferation. *EMBO Rep* (2010).
242. Shinoda, Y., *et al.* Kruppel-like factor 5 causes cartilage degradation through transactivation of matrix metalloproteinase 9. *J Biol Chem* **283**, 24682-24689 (2008).

243. Guo, P., *et al.* Opposing effects of KLF5 on the transcription of MYC in epithelial proliferation in the context of transforming growth factor beta. *J Biol Chem* **284**, 28243-28252 (2009).
244. Nagai, R., *et al.* Phenotypic modulation of vascular smooth muscle cells: dissection of transcriptional regulatory mechanisms. *Ann N Y Acad Sci* **947**, 56-66; discussion 66-57 (2001).
245. Jiang, J., *et al.* A core Klf circuitry regulates self-renewal of embryonic stem cells. *Nat Cell Biol* **10**, 353-360 (2008).
246. Aizawa, K., *et al.* Regulation of platelet-derived growth factor-A chain by Kruppel-like factor 5: new pathway of cooperative activation with nuclear factor-kappaB. *J Biol Chem* **279**, 70-76 (2004).
247. Usui, S., *et al.* Blood lipid mediator sphingosine 1-phosphate potently stimulates platelet-derived growth factor-A and -B chain expression through S1P1-Gi-Ras-MAPK-dependent induction of Kruppel-like factor 5. *J Biol Chem* **279**, 12300-12311 (2004).
248. Zhao, Y., *et al.* Kruppel-like factor 5 modulates p53-independent apoptosis through Pim1 survival kinase in cancer cells. *Oncogene* **27**, 1-8 (2008).
249. Adam, P.J., Regan, C.P., Hautmann, M.B. & Owens, G.K. Positive- and negative-acting Kruppel-like transcription factors bind a transforming growth factor beta control element required for expression of the smooth muscle cell differentiation marker SM22alpha in vivo. *J Biol Chem* **275**, 37798-37806 (2000).
250. Zhu, N., *et al.* KLF5 Interacts with p53 in regulating survivin expression in acute lymphoblastic leukemia. *J Biol Chem* **281**, 14711-14718 (2006).
251. Chen, C., *et al.* KLF5 promotes cell proliferation and tumorigenesis through gene regulation and the TSU-Pr1 human bladder cancer cell line. *Int J Cancer* **118**, 1346-1355 (2006).
252. Bourillot, P.Y., *et al.* Novel STAT3 target genes exert distinct roles in the inhibition of mesoderm and endoderm differentiation in cooperation with Nanog. *Stem Cells* **27**, 1760-1771 (2009).
253. Sur, I., Unden, A.B. & Toftgard, R. Human Kruppel-like factor5/KLF5: synergy with NF-kappaB/Rel factors and expression in human skin and hair follicles. *Eur J Cell Biol* **81**, 323-334 (2002).
254. Matsumura, T., *et al.* The deacetylase HDAC1 negatively regulates the cardiovascular transcription factor Kruppel-like factor 5 through direct interaction. *J Biol Chem* **280**, 12123-12129 (2005).
255. Munemasa, Y., *et al.* Promoter region-specific histone incorporation by the novel histone chaperone ANP32B and DNA-binding factor KLF5. *Mol Cell Biol* **28**, 1171-1181 (2008).
256. Kojima, S., *et al.* Transcriptional activation domain of human BTEB2, a GC box-binding factor. *J Biochem* **121**, 389-396 (1997).
257. Miyamoto, S., *et al.* Positive and negative regulation of the cardiovascular transcription factor KLF5 by p300 and the oncogenic regulator SET through interaction and acetylation on the DNA-binding domain. *Mol Cell Biol* **23**, 8528-8541 (2003).
258. Du, J.X., Yun, C.C., Bialkowska, A. & Yang, V.W. Protein inhibitor of activated STAT1 interacts with and up-regulates activities of the pro-proliferative transcription factor Kruppel-like factor 5. *J Biol Chem* **282**, 4782-4793 (2007).
259. Lee, M.Y., *et al.* KLF5 enhances SREBP-1 action in androgen-dependent induction of fatty acid synthase in prostate cancer cells. *Biochem J* **417**, 313-322 (2009).

260. McConnell, B.B., *et al.* Haploinsufficiency of Kruppel-like factor 5 rescues the tumor-initiating effect of the Apc(Min) mutation in the intestine. *Cancer Res* **69**, 4125-4133 (2009).
261. Guo, P., *et al.* Estrogen-induced interaction between KLF5 and estrogen receptor (ER) suppresses the function of ER in ER-positive breast cancer cells. *Int J Cancer* **126**, 81-89.
262. Mori, A., *et al.* Up-regulation of Kruppel-like factor 5 in pancreatic cancer is promoted by interleukin-1beta signaling and hypoxia-inducible factor-1alpha. *Mol Cancer Res* **7**, 1390-1398 (2009).
263. Suzuki, T., *et al.* Functional interaction between the transcription factor Kruppel-like factor 5 and poly(ADP-ribose) polymerase-1 in cardiovascular apoptosis. *J Biol Chem* **282**, 9895-9901 (2007).
264. Kada, N., *et al.* Acyclic retinoid inhibits functional interaction of transcription factors Kruppel-like factor 5 and retinoic acid receptor-alpha. *FEBS Lett* **582**, 1755-1760 (2008).
265. Chen, Z., Couble, M.L., Mouterfi, N., Magloire, H. & Bleicher, F. Spatial and temporal expression of KLF4 and KLF5 during murine tooth development. *Arch Oral Biol* **54**, 403-411 (2009).
266. Fujiu, K., *et al.* Synthetic retinoid Am80 suppresses smooth muscle phenotypic modulation and in-stent neointima formation by inhibiting KLF5. *Circ Res* **97**, 1132-1141 (2005).
267. Kruse, J.J., te Poele, J.A., Russell, N.S., Boersma, L.J. & Stewart, F.A. Microarray analysis to identify molecular mechanisms of radiation-induced microvascular damage in normal tissues. *Int J Radiat Oncol Biol Phys* **58**, 420-426 (2004).
268. McConnell, B.B., Klapproth, J.M., Sasaki, M., Nandan, M.O. & Yang, V.W. Kruppel-like factor 5 mediates transmissible murine colonic hyperplasia caused by Citrobacter rodentium infection. *Gastroenterology* **134**, 1007-1016 (2008).
269. Chanchevalap, S., *et al.* Kruppel-like factor 5 is an important mediator for lipopolysaccharide-induced proinflammatory response in intestinal epithelial cells. *Nucleic Acids Res* **34**, 1216-1223 (2006).
270. Goldstein, B.G., *et al.* Overexpression of Kruppel-like factor 5 in esophageal epithelia in vivo leads to increased proliferation in basal but not suprabasal cells. *Am J Physiol Gastrointest Liver Physiol* **292**, G1784-1792 (2007).
271. Giefing, M., *et al.* Chromosomal gains and losses indicate oncogene and tumor suppressor gene candidates in salivary gland tumors. *Neoplasma* **55**, 55-60 (2008).
272. Chanchevalap, S., Nandan, M.O., Merlin, D. & Yang, V.W. All-trans retinoic acid inhibits proliferation of intestinal epithelial cells by inhibiting expression of the gene encoding Kruppel-like factor 5. *FEBS Lett* **578**, 99-105 (2004).
273. Sun, R., Chen, X. & Yang, V.W. Intestinal-enriched Kruppel-like factor (Kruppel-like factor 5) is a positive regulator of cellular proliferation. *J Biol Chem* **276**, 6897-6900 (2001).
274. Suzuki, T., *et al.* Kruppel-like factor 5 shows proliferation-specific roles in vascular remodeling, direct stimulation of cell growth, and inhibition of apoptosis. *J Biol Chem* **284**, 9549-9557 (2009).
275. McConnell, B.B., *et al.* Kruppel-Like Factor 5 Protects Against Dextran Sulfate Sodium-Induced Colonic Injury by Promoting Epithelial Repair in Mice. *Gastroenterology* (2010).
276. Gao, D., Niu, X., Ning, N. & Hao, G. Regulation of angiotensin II-Induced Kruppel-like factor 5 expression in vascular smooth muscle cells. *Biol Pharm Bull* **29**, 2004-2008 (2006).

277. Nandan, M.O., *et al.* Kruppel-like factor 5 mediates the transforming activity of oncogenic H-Ras. *Oncogene* **23**, 3404-3413 (2004).
278. Zhang, H., *et al.* Lysophosphatidic acid facilitates proliferation of colon cancer cells via induction of Kruppel-like factor 5. *J Biol Chem* **282**, 15541-15549 (2007).
279. Ziemer, L.T., Pennica, D. & Levine, A.J. Identification of a mouse homolog of the human BTEB2 transcription factor as a beta-catenin-independent Wnt-1-responsive gene. *Mol Cell Biol* **21**, 562-574 (2001).
280. Zhang, X.H., Zheng, B., Han, M., Miao, S.B. & Wen, J.K. Synthetic retinoid Am80 inhibits interaction of KLF5 with RAR alpha through inducing KLF5 dephosphorylation mediated by the PI3K/Akt signaling in vascular smooth muscle cells. *FEBS Lett* **583**, 1231-1236 (2009).
281. Moore-Scott, B.A., Opoka, R., Lin, S.C., Kordich, J.J. & Wells, J.M. Identification of molecular markers that are expressed in discrete anterior-posterior domains of the endoderm from the gastrula stage to mid-gestation. *Dev Dyn* **236**, 1997-2003 (2007).
282. Bafford, R., Sui, X.X., Wang, G. & Conte, M. Angiotensin II and tumor necrosis factor-alpha upregulate survivin and Kruppel-like factor 5 in smooth muscle cells: Potential relevance to vein graft hyperplasia. *Surgery* **140**, 289-296 (2006).
283. Cullingford, T.E., *et al.* Differential regulation of Kruppel-like factor family transcription factor expression in neonatal rat cardiac myocytes: effects of endothelin-1, oxidative stress and cytokines. *Biochim Biophys Acta* **1783**, 1229-1236 (2008).
284. Yang, Y., Goldstein, B.G., Chao, H.H. & Katz, J.P. KLF4 and KLF5 regulate proliferation, apoptosis and invasion in esophageal cancer cells. *Cancer Biol Ther* **4**, 1216-1221 (2005).
285. Sur, I., Rozell, B., Jaks, V., Bergstrom, A. & Toftgard, R. Epidermal and craniofacial defects in mice overexpressing Klf5 in the basal layer of the epidermis. *J Cell Sci* **119**, 3593-3601 (2006).
286. Nandan, M.O., *et al.* Kruppel-like factor 5 mediates cellular transformation during oncogenic KRAS-induced intestinal tumorigenesis. *Gastroenterology* **134**, 120-130 (2008).
287. Lin, S., *et al.* The absence of LPA2 attenuates tumor formation in an experimental model of colitis-associated cancer. *Gastroenterology* **136**, 1711-1720 (2009).
288. Nandan, M.O., *et al.* Kruppel-like factor 5 is a crucial mediator of intestinal tumorigenesis in mice harboring combined ApcMin and KRASV12 mutations. *Mol Cancer* **9**, 63 (2010).
289. Dardousis, K., *et al.* Identification of differentially expressed genes involved in the formation of multicellular tumor spheroids by HT-29 colon carcinoma cells. *Mol Ther* **15**, 94-102 (2007).
290. Tong, D., *et al.* Expression of KLF5 is a prognostic factor for disease-free survival and overall survival in patients with breast cancer. *Clin Cancer Res* **12**, 2442-2448 (2006).
291. Huang, D., *et al.* Isolation and identification of cancer stem-like cells in esophageal carcinoma cell lines. *Stem Cells Dev* **18**, 465-473 (2009).
292. Gyorffy, B. & Schafer, R. Biomarkers Downstream of RAS: A Search for Robust Transcriptional Targets. *Curr Cancer Drug Targets* (2010).
293. Lin, S., Lee, S.J., Shim, H., Chun, J. & Yun, C.C. The absence of LPA receptor 2 reduces the tumorigenesis by ApcMin mutation in the intestine. *Am J Physiol Gastrointest Liver Physiol* **299**, G1128-1138 (2010).
294. Bialkowska, A.B., Du, Y., Fu, H. & Yang, V.W. Identification of novel small-molecule compounds that inhibit the proproliferative Kruppel-like factor 5 in colorectal cancer cells by high-throughput screening. *Mol Cancer Ther* **8**, 563-570 (2009).

295. Chen, C., Bhalala, H.V., Vessella, R.L. & Dong, J.T. KLF5 is frequently deleted and down-regulated but rarely mutated in prostate cancer. *Prostate* **55**, 81-88 (2003).
296. Dong, J.T., Chen, C., Stultz, B.G., Isaacs, J.T. & Frierson, H.F., Jr. Deletion at 13q21 is associated with aggressive prostate cancers. *Cancer Res* **60**, 3880-3883 (2000).
297. Chen, C., *et al.* Human Kruppel-like factor 5 is a target of the E3 ubiquitin ligase WWP1 for proteolysis in epithelial cells. *J Biol Chem* **280**, 41553-41561 (2005).
298. Tsai, H.T., *et al.* Increased cytoplasmic localization of KLF5 in prostate cancer (abstract). In: Proceedings of the 42nd annual Meeting of the American Society for Clinical Oncology Part I; 2006 June 2-6; Atlanta. Georgia (GA). *J Clin Oncol* **24**, Abstract #14652 (2006).
299. Duhagon, M.A., Hurt, E.M., Sotelo-Silveira, J.R., Zhang, X. & Farrar, W.L. Genomic profiling of tumor initiating prostatospheres. *BMC Genomics* **11**, 324 (2010).
300. Kainu, T., *et al.* Somatic deletions in hereditary breast cancers implicate 13q21 as a putative novel breast cancer susceptibility locus. *Proc Natl Acad Sci U S A* **97**, 9603-9608 (2000).
301. Chen, C., Bhalala, H.V., Qiao, H. & Dong, J.T. A possible tumor suppressor role of the KLF5 transcription factor in human breast cancer. *Oncogene* **21**, 6567-6572 (2002).
302. Zhou, W., Zeng, X. & Liu, T. Aberrations of Chromosome 13q in Gastrointestinal Stromal Tumors: Analysis of 91 Cases by Fluorescence In Situ Hybridization (FISH). *Diagn Mol Pathol* **18**, 72-80 (2009).
303. Fang, W., *et al.* Transcriptional patterns, biomarkers and pathways characterizing nasopharyngeal carcinoma of Southern China. *J Transl Med* **6**, 32 (2008).
304. Kwak, M.K., *et al.* Expression of Kruppel-like factor 5 in human gastric carcinomas. *J Cancer Res Clin Oncol* **134**, 163-167 (2008).
305. La Starza, R., *et al.* Molecular delineation of 13q deletion boundaries in 20 patients with myeloid malignancies. *Blood* **91**, 231-237 (1998).
306. Knuutila, S., *et al.* DNA copy number losses in human neoplasms. *Am J Pathol* **155**, 683-694 (1999).
307. Gorletta, T.A., *et al.* Frequent loss of heterozygosity without loss of genetic material in acute myeloid leukemia with a normal karyotype. *Genes Chromosomes Cancer* **44**, 334-337 (2005).
308. Barresi, V., *et al.* Broad copy neutral-loss of heterozygosity regions and rare recurring copy number abnormalities in normal karyotype-acute myeloid leukemia genomes. *Genes Chromosomes Cancer* **49**, 1014-1023 (2010).
309. Potapova, A., *et al.* Epigenetic inactivation of tumour suppressor gene KLF11 in myelodysplastic syndromes*. *Eur J Haematol* (2009).
310. Hanahan, D., Jessee, J. & Bloom, F.R. Plasmid transformation of Escherichia coli and other bacteria. *Methods Enzymol* **204**, 63-113 (1991).
311. Sambrook, J., Maniatis, T. & Fritsch, E.F. *Molecular cloning: a laboratory manual.*, (Cold Spring Harbour Press, Cold Spring Harbour, 1989).
312. Fritsch, E.F., Sambrook, J. & Maniatis, T. *Molecular cloning: A laboratory manual.*, (Cold Spring Harbour Press, Cold Spring Harbour, 1982).
313. Muller, P.Y., Janovjak, H., Miserez, A.R. & Dobbie, Z. Processing of gene expression data generated by quantitative real-time RT-PCR. *Biotechniques* **32**, 1372-1374, 1376, 1378-1379 (2002).
314. Sasmono, R.T., *et al.* Mouse neutrophilic granulocytes express mRNA encoding the macrophage colony-stimulating factor receptor (CSF-1R) as well as many other macrophage-specific transcripts and can transdifferentiate into macrophages in vitro in response to CSF-1. *J Leukoc Biol* **82**, 111-123 (2007).

315. Logel, J., Dill, D. & Leonard, S. Synthesis of cRNA probes from PCR-generated DNA. *Biotechniques* **13**, 604-610 (1992).
316. Rozen, S. & Skaletsky, H. Primer3 on the WWW for general users and for biologist programmers. *Methods Mol Biol* **132**, 365-386 (2000).
317. Wang, X. & Seed, B. A PCR primer bank for quantitative gene expression analysis. *Nucleic Acids Res* **31**, e154 (2003).
318. Spandidos, A., *et al.* A comprehensive collection of experimentally validated primers for Polymerase Chain Reaction quantitation of murine transcript abundance. *BMC Genomics* **9**, 633 (2008).
319. Spandidos, A., Wang, X., Wang, H. & Seed, B. PrimerBank: a resource of human and mouse PCR primer pairs for gene expression detection and quantification. *Nucleic Acids Res* **38**, D792-799 (2010).
320. Hawley, R.G., Lieu, F.H., Fong, A.Z. & Hawley, T.S. Versatile retroviral vectors for potential use in gene therapy. *Gene Ther* **1**, 136-138 (1994).
321. Sayers, E.W., *et al.* Database resources of the National Center for Biotechnology Information. *Nucleic Acids Res* **37**, D5-15 (2009).
322. Brummelkamp, T.R., Bernards, R. & Agami, R. Stable suppression of tumorigenicity by virus-mediated RNA interference. *Cancer Cell* **2**, 243-247 (2002).
323. Paddison, P.J., *et al.* Cloning of short hairpin RNAs for gene knockdown in mammalian cells. *Nat Methods* **1**, 163-167 (2004).
324. Leirdal, M. & Sioud, M. Gene silencing in mammalian cells by preformed small RNA duplexes. *Biochem Biophys Res Commun* **295**, 744-748 (2002).
325. Levenkova, N., Gu, Q. & Rux, J.J. Gene specific siRNA selector. *Bioinformatics* **20**, 430-432 (2004).
326. Perugini, M., *et al.* Repression of Gadd45alpha by activated FLT3 and GM-CSF receptor mutants contributes to growth, survival and blocked differentiation. *Leukemia* **23**, 729-738 (2009).
327. Persons, D.A., Mehaffey, M.G., Kaleko, M., Nienhuis, A.W. & Vanin, E.F. An improved method for generating retroviral producer clones for vectors lacking a selectable marker gene. *Blood Cells Mol Dis* **24**, 167-182 (1998).
328. Hanker, J.S., Yates, P.E., Metz, C.B. & Rustioni, A. A new specific, sensitive and non-carcinogenic reagent for the demonstration of horseradish peroxidase. *Histochem J* **9**, 789-792 (1977).
329. Valk, P.J., *et al.* Prognostically useful gene-expression profiles in acute myeloid leukemia. *N Engl J Med* **350**, 1617-1628 (2004).
330. Ehrich, M., *et al.* Quantitative high-throughput analysis of DNA methylation patterns by base-specific cleavage and mass spectrometry. *Proc Natl Acad Sci U S A* **102**, 15785-15790 (2005).
331. Coolen, M.W., Statham, A.L., Gardiner-Garden, M. & Clark, S.J. Genomic profiling of CpG methylation and allelic specificity using quantitative high-throughput mass spectrometry: critical evaluation and improvements. *Nucleic Acids Res* **35**, e119 (2007).
332. Saeed, A.I., *et al.* TM4: a free, open-source system for microarray data management and analysis. *Biotechniques* **34**, 374-378 (2003).
333. Kent, W.J., *et al.* The human genome browser at UCSC. *Genome Res* **12**, 996-1006 (2002).
334. Rhead, B., *et al.* The UCSC Genome Browser database: update 2010. *Nucleic Acids Res* **38**, D613-619 (2010).

335. Rayner, J.R. & Gonda, T.J. A simple and efficient procedure for generating stable expression libraries by cDNA cloning in a retroviral vector. *Mol Cell Biol* **14**, 880-887 (1994).
336. Wong, B.Y., Chen, H., Chung, S.W. & Wong, P.M. High-efficiency identification of genes by functional analysis from a retroviral cDNA expression library. *J Virol* **68**, 5523-5531 (1994).
337. Whitehead, I., Kirk, H. & Kay, R. Expression cloning of oncogenes by retroviral transfer of cDNA libraries. *Mol Cell Biol* **15**, 704-710 (1995).
338. Kitamura, T., *et al.* Efficient screening of retroviral cDNA expression libraries. *Proc Natl Acad Sci U S A* **92**, 9146-9150 (1995).
339. Pear, W.S., Nolan, G.P., Scott, M.L. & Baltimore, D. Production of high-titer helper-free retroviruses by transient transfection. *Proc Natl Acad Sci U S A* **90**, 8392-8396 (1993).
340. Morita, S., Kojima, T. & Kitamura, T. Plat-E: an efficient and stable system for transient packaging of retroviruses. *Gene Ther* **7**, 1063-1066 (2000).
341. Kitamura, T., *et al.* Retrovirus-mediated gene transfer and expression cloning: powerful tools in functional genomics. *Exp Hematol* **31**, 1007-1014 (2003).
342. Kawashima, T., *et al.* MgcRacGAP is involved in the control of growth and differentiation of hematopoietic cells. *Blood* **96**, 2116-2124 (2000).
343. Mourtada-Maarabouni, M., Kirkham, L., Farzaneh, F. & Williams, G.T. Regulation of apoptosis by fau revealed by functional expression cloning and antisense expression. *Oncogene* **23**, 9419-9426 (2004).
344. Harbers, M. The current status of cDNA cloning. *Genomics* **91**, 232-242 (2008).
345. Perez, O.D., *et al.* Activation of the PKB/AKT pathway by ICAM-2. *Immunity* **16**, 51-65 (2002).
346. Fletcher, B.S., Dragstedt, C., Notterpek, L. & Nolan, G.P. Functional cloning of SPIN-2, a nuclear anti-apoptotic protein with roles in cell cycle progression. *Leukemia* **16**, 1507-1518 (2002).
347. Ichikawa, Y. Differentiation of a cell line of myeloid leukemia. *J Cell Physiol* **74**, 223-234 (1969).
348. Gearing, D.P., *et al.* Molecular cloning and expression of cDNA encoding a murine myeloid leukaemia inhibitory factor (LIF). *EMBO J* **6**, 3995-4002 (1987).
349. Shabo, Y., *et al.* The myeloid blood cell differentiation-inducing protein MGI-2A is interleukin-6. *Blood* **72**, 2070-2073 (1988).
350. Bruce, A.G., Hoggatt, I.H. & Rose, T.M. Oncostatin M is a differentiation factor for myeloid leukemia cells. *J Immunol* **149**, 1271-1275 (1992).
351. Hayashi, M., Fibach, E. & Sachs, L. Control of normal differentiation of myeloid leukemic cells. V. Normal differentiation in aneuploid leukemic cells and the chromosome banding pattern of D+ and D minus clones. *Int J Cancer* **14**, 40-48 (1974).
352. Adler, A.A.c. SMART(TM) cDNA Library Construction Kit. in *Clontechniques*, Vol. October 12-13 (Clontech, Palo Alto, CA, USA, 1998).
353. Zhu, Y.Y., Machleder, E.M., Chenchik, A., Li, R. & Siebert, P.D. Reverse transcriptase template switching: a SMART approach for full-length cDNA library construction. *Biotechniques* **30**, 892-897 (2001).
354. Draper, M.P., August, P.R., Connolly, T., Packard, B. & Call, K.M. Efficient cloning of full-length cDNAs based on cDNA size fractionation. *Genomics* **79**, 603-607 (2002).
355. Altschul, S.F., Gish, W., Miller, W., Myers, E.W. & Lipman, D.J. Basic local alignment search tool. *J Mol Biol* **215**, 403-410 (1990).

356. Dexter, T.M., Garland, J., Scott, D., Scolnick, E. & Metcalf, D. Growth of factor-dependent hemopoietic precursor cell lines. *J Exp Med* **152**, 1036-1047 (1980).
357. D'Andrea, R., *et al.* A mutation of the common receptor subunit for interleukin-3 (IL-3), granulocyte-macrophage colony-stimulating factor, and IL-5 that leads to ligand independence and tumorigenicity. *Blood* **83**, 2802-2808 (1994).
358. Gustincich, S., *et al.* The complexity of the mammalian transcriptome. *J Physiol* **575**, 321-332 (2006).
359. Ying, S.Y. *Generation of cDNA Libraries: Methods and Protocols.*, (Humana Press, 2003).
360. Carninci, P., *et al.* Normalization and subtraction of cap-trapper-selected cDNAs to prepare full-length cDNA libraries for rapid discovery of new genes. *Genome Res* **10**, 1617-1630 (2000).
361. Maruyama, K. & Sugano, S. Oligo-capping: a simple method to replace the cap structure of eukaryotic mRNAs with oligoribonucleotides. *Gene* **138**, 171-174 (1994).
362. Zhulidov, P.A., *et al.* Simple cDNA normalization using kamchatka crab duplex-specific nuclease. *Nucleic Acids Res* **32**, e37 (2004).
363. Passioura, T., Shen, S., Symonds, G. & Dolnikov, A. A retroviral library genetic screen identifies IRF-2 as an inhibitor of N-ras-induced growth suppression in leukemic cells. *Oncogene* **24**, 7327-7336 (2005).
364. Scholl, C., *et al.* Synthetic lethal interaction between oncogenic KRAS dependency and STK33 suppression in human cancer cells. *Cell* **137**, 821-834 (2009).
365. Koh, E.Y., Chen, T. & Daley, G.Q. Genetic complementation of cytokine signaling identifies central role of kinases in hematopoietic cell proliferation. *Oncogene* **23**, 1214-1220 (2004).
366. Reuther, G.W., Lambert, Q.T., Caligiuri, M.A. & Der, C.J. Identification and characterization of an activating TrkA deletion mutation in acute myeloid leukemia. *Mol Cell Biol* **20**, 8655-8666 (2000).
367. Reuther, G.W., *et al.* RasGRP4 is a novel Ras activator isolated from acute myeloid leukemia. *J Biol Chem* **277**, 30508-30514 (2002).
368. Rosenbauer, F. & Tenen, D.G. Transcription factors in myeloid development: balancing differentiation with transformation. *Nat Rev Immunol* **7**, 105-117 (2007).
369. Tenen, D.G., Hromas, R., Licht, J.D. & Zhang, D.E. Transcription factors, normal myeloid development, and leukemia. *Blood* **90**, 489-519 (1997).
370. Tsujimura, H., Nagamura-Inoue, T., Tamura, T. & Ozato, K. IFN consensus sequence binding protein/IFN regulatory factor-8 guides bone marrow progenitor cells toward the macrophage lineage. *J Immunol* **169**, 1261-1269 (2002).
371. Tamura, T., Nagamura-Inoue, T., Shmeltzer, Z., Kuwata, T. & Ozato, K. ICSBP directs bipotential myeloid progenitor cells to differentiate into mature macrophages. *Immunity* **13**, 155-165 (2000).
372. Holtschke, T., *et al.* Immunodeficiency and chronic myelogenous leukemia-like syndrome in mice with a targeted mutation of the ICSBP gene. *Cell* **87**, 307-317 (1996).
373. Yamanaka, R., *et al.* CCAAT/enhancer binding protein epsilon is preferentially up-regulated during granulocytic differentiation and its functional versatility is determined by alternative use of promoters and differential splicing. *Proc Natl Acad Sci U S A* **94**, 6462-6467 (1997).
374. Halene, S., *et al.* C/EBPepsilon directs granulocytic-vs-monocytic lineage determination and confers chemotactic function via Hlx. *Exp Hematol* (2009).

375. Yamanaka, R., *et al.* Impaired granulopoiesis, myelodysplasia, and early lethality in CCAAT/enhancer binding protein epsilon-deficient mice. *Proc Natl Acad Sci U S A* **94**, 13187-13192 (1997).
376. Khanna-Gupta, A., Zibello, T., Simkevich, C., Rosmarin, A.G. & Berliner, N. Sp1 and C/EBP are necessary to activate the lactoferrin gene promoter during myeloid differentiation. *Blood* **95**, 3734-3741 (2000).
377. Verbeek, W., *et al.* Myeloid transcription factor C/EBPepsilon is involved in the positive regulation of lactoferrin gene expression in neutrophils. *Blood* **94**, 3141-3150 (1999).
378. Valtieri, M., *et al.* Cytokine-dependent granulocytic differentiation. Regulation of proliferative and differentiative responses in a murine progenitor cell line. *J Immunol* **138**, 3829-3835 (1987).
379. Vradii, D., *et al.* Point mutation in AML1 disrupts subnuclear targeting, prevents myeloid differentiation, and effects a transformation-like phenotype. *Proc Natl Acad Sci U S A* **102**, 7174-7179 (2005).
380. Kim, J., Ogata, Y. & Feldman, R.A. Fes tyrosine kinase promotes survival and terminal granulocyte differentiation of factor-dependent myeloid progenitors (32D) and activates lineage-specific transcription factors. *J Biol Chem* **278**, 14978-14984 (2003).
381. Borregaard, N. & Cowland, J.B. Granules of the human neutrophilic polymorphonuclear leukocyte. *Blood* **89**, 3503-3521 (1997).
382. Borregaard, N., Sehested, M., Nielsen, B.S., Sengelov, H. & Kjeldsen, L. Biosynthesis of granule proteins in normal human bone marrow cells. Gelatinase is a marker of terminal neutrophil differentiation. *Blood* **85**, 812-817 (1995).
383. Nakajima, H. & Ihle, J.N. Granulocyte colony-stimulating factor regulates myeloid differentiation through CCAAT/enhancer-binding protein epsilon. *Blood* **98**, 897-905 (2001).
384. Scott, L.M., Civin, C.I., Rorth, P. & Friedman, A.D. A novel temporal expression pattern of three C/EBP family members in differentiating myelomonocytic cells. *Blood* **80**, 1725-1735 (1992).
385. Ogawa, M., Shih, J.P. & Katayama, N. Enrichment for primitive hemopoietic progenitors of marrow cells from 5-fluorouracil-treated mice and normal mice. *Blood Cells* **20**, 7-11; discussion 11-13 (1994).
386. Chambers, S.M., *et al.* Hematopoietic fingerprints: an expression database of stem cells and their progeny. *Cell Stem Cell* **1**, 578-591 (2007).
387. Tonks, A., *et al.* Transcriptional dysregulation mediated by RUNX1-RUNX1T1 in normal human progenitor cells and in acute myeloid leukaemia. *Leukemia* **21**, 2495-2505 (2007).
388. Feinberg, M.W., *et al.* The Kruppel-like factor KLF4 is a critical regulator of monocyte differentiation. *EMBO J* **26**, 4138-4148 (2007).
389. Alder, J.K., *et al.* Kruppel-like factor 4 is essential for inflammatory monocyte differentiation in vivo. *J Immunol* **180**, 5645-5652 (2008).
390. Hestdal, K., *et al.* Characterization and regulation of RB6-8C5 antigen expression on murine bone marrow cells. *J Immunol* **147**, 22-28 (1991).
391. Escribano, L., Ocqueteau, M., Almeida, J., Orfao, A. & San Miguel, J.F. Expression of the c-kit (CD117) molecule in normal and malignant hematopoiesis. *Leuk Lymphoma* **30**, 459-466 (1998).
392. Chang, K., Elledge, S.J. & Hannon, G.J. Lessons from Nature: microRNA-based shRNA libraries. *Nat Methods* **3**, 707-714 (2006).

393. Yu, J.Y., DeRuiter, S.L. & Turner, D.L. RNA interference by expression of short-interfering RNAs and hairpin RNAs in mammalian cells. *Proc Natl Acad Sci U S A* **99**, 6047-6052 (2002).
394. Maier, T., Guell, M. & Serrano, L. Correlation of mRNA and protein in complex biological samples. *FEBS Lett* **583**, 3966-3973 (2009).
395. Furukawa, Y. Cell cycle control during hematopoietic cell differentiation. *Hum Cell* **10**, 159-164 (1997).
396. McKenna, S.L. & Cotter, T.G. Functional aspects of apoptosis in hematopoiesis and consequences of failure. *Adv Cancer Res* **71**, 121-164 (1997).
397. Dale, D.C., Boxer, L. & Liles, W.C. The phagocytes: neutrophils and monocytes. *Blood* **112**, 935-945 (2008).
398. Krishnaraju, K., Nguyen, H.Q., Liebermann, D.A. & Hoffman, B. The zinc finger transcription factor Egr-1 potentiates macrophage differentiation of hematopoietic cells. *Mol Cell Biol* **15**, 5499-5507 (1995).
399. Krishnaraju, K., Hoffman, B. & Liebermann, D.A. The zinc finger transcription factor Egr-1 activates macrophage differentiation in M1 myeloblastic leukemia cells. *Blood* **92**, 1957-1966 (1998).
400. Radomska, H.S., *et al.* CCAAT/enhancer binding protein alpha is a regulatory switch sufficient for induction of granulocytic development from bipotential myeloid progenitors. *Mol Cell Biol* **18**, 4301-4314 (1998).
401. Wang, D., D'Costa, J., Civin, C.I. & Friedman, A.D. C/EBPalpha directs monocytic commitment of primary myeloid progenitors. *Blood* **108**, 1223-1229 (2006).
402. Friedman, A.D. Runx1, c-Myb, and C/EBPalpha couple differentiation to proliferation or growth arrest during hematopoiesis. *J Cell Biochem* **86**, 624-629 (2002).
403. Iida, S., Watanabe-Fukunaga, R., Nagata, S. & Fukunaga, R. Essential role of C/EBPalpha in G-CSF-induced transcriptional activation and chromatin modification of myeloid-specific genes. *Genes Cells* **13**, 313-327 (2008).
404. Wang, X., Scott, E., Sawyers, C.L. & Friedman, A.D. C/EBPalpha bypasses granulocyte colony-stimulating factor signals to rapidly induce PU.1 gene expression, stimulate granulocytic differentiation, and limit proliferation in 32D cl3 myeloblasts. *Blood* **94**, 560-571 (1999).
405. Wang, W., Wang, X., Ward, A.C., Touw, I.P. & Friedman, A.D. C/EBPalpha and G-CSF receptor signals cooperate to induce the myeloperoxidase and neutrophil elastase genes. *Leukemia* **15**, 779-786 (2001).
406. Smith, L.T., Hohaus, S., Gonzalez, D.A., Dziennis, S.E. & Tenen, D.G. PU.1 (Spi-1) and C/EBP alpha regulate the granulocyte colony-stimulating factor receptor promoter in myeloid cells. *Blood* **88**, 1234-1247 (1996).
407. Khanna-Gupta, A., Zibello, T., Sun, H., Lekstrom-Himes, J. & Berliner, N. C/EBP epsilon mediates myeloid differentiation and is regulated by the CCAAT displacement protein (CDP/cut). *Proc Natl Acad Sci U S A* **98**, 8000-8005 (2001).
408. Zhang, P., *et al.* Induction of granulocytic differentiation by 2 pathways. *Blood* **99**, 4406-4412 (2002).
409. Zhang, P., *et al.* Upregulation of interleukin 6 and granulocyte colony-stimulating factor receptors by transcription factor CCAAT enhancer binding protein alpha (C/EBP alpha) is critical for granulopoiesis. *J Exp Med* **188**, 1173-1184 (1998).
410. Hirai, H., *et al.* C/EBPbeta is required for 'emergency' granulopoiesis. *Nat Immunol* **7**, 732-739 (2006).
411. Jones, L.C., *et al.* Expression of C/EBPbeta from the C/ebpalpha gene locus is sufficient for normal hematopoiesis in vivo. *Blood* **99**, 2032-2036 (2002).

412. Behre, G., *et al.* Ras signaling enhances the activity of C/EBP alpha to induce granulocytic differentiation by phosphorylation of serine 248. *J Biol Chem* **277**, 26293-26299 (2002).
413. Ross, S.E., *et al.* Phosphorylation of C/EBPalpha inhibits granulopoiesis. *Mol Cell Biol* **24**, 675-686 (2004).
414. Khanna-Gupta, A. Sumoylation and the function of CCAAT enhancer binding protein alpha (C/EBP alpha). *Blood Cells Mol Dis* **41**, 77-81 (2008).
415. Gombart, A.F., *et al.* Mutations in the gene encoding the transcription factor CCAAT/enhancer binding protein alpha in myelodysplastic syndromes and acute myeloid leukemias. *Blood* **99**, 1332-1340 (2002).
416. Pabst, T. & Mueller, B.U. Transcriptional dysregulation during myeloid transformation in AML. *Oncogene* **26**, 6829-6837 (2007).
417. Krug, U., Ganser, A. & Koeffler, H.P. Tumor suppressor genes in normal and malignant hematopoiesis. *Oncogene* **21**, 3475-3495 (2002).
418. Sherr, C.J. Principles of tumor suppression. *Cell* **116**, 235-246 (2004).
419. Gilby, D.C., *et al.* Tribbles-1 and -2 are tumour suppressors, down-regulated in human acute myeloid leukaemia. *Immunol Lett* **130**, 115-124 (2010).
420. Chen, P.M., *et al.* Down-regulation of Notch-1 expression decreases PU.1-mediated myeloid differentiation signaling in acute myeloid leukemia. *Int J Oncol* **32**, 1335-1341 (2008).
421. Chen, C.Y., *et al.* SOCS1 methylation in patients with newly diagnosed acute myeloid leukemia. *Genes Chromosomes Cancer* **37**, 300-305 (2003).
422. Voso, M.T., *et al.* Aberrant methylation of DAP-kinase in therapy-related acute myeloid leukemia and myelodysplastic syndromes. *Blood* **103**, 698-700 (2004).
423. Wouters, B.J., Louwers, I., Valk, P.J., Lowenberg, B. & Delwel, R. A recurrent in-frame insertion in a CEBPA transactivation domain is a polymorphism rather than a mutation that does not affect gene expression profiling-based clustering of AML. *Blood* **109**, 389-390 (2007).
424. Collins, S.J., Gallo, R.C. & Gallagher, R.E. Continuous growth and differentiation of human myeloid leukaemic cells in suspension culture. *Nature* **270**, 347-349 (1977).
425. Lozzio, C.B. & Lozzio, B.B. Human chronic myelogenous leukemia cell-line with positive Philadelphia chromosome. *Blood* **45**, 321-334 (1975).
426. Rizzo, M.G., *et al.* Wt-p53 action in human leukaemia cell lines corresponding to different stages of differentiation. *Br J Cancer* **77**, 1429-1438 (1998).
427. Koeffler, H.P. & Golde, D.W. Acute myelogenous leukemia: a human cell line responsive to colony-stimulating activity. *Science* **200**, 1153-1154 (1978).
428. Lozzio, B.B., Lozzio, C.B., Bamberger, E.G. & Feliu, A.S. A multipotential leukemia cell line (K-562) of human origin. *Proc Soc Exp Biol Med* **166**, 546-550 (1981).
429. Matsuo, Y., *et al.* Two acute monocytic leukemia (AML-M5a) cell lines (MOLM-13 and MOLM-14) with interclonal phenotypic heterogeneity showing MLL-AF9 fusion resulting from an occult chromosome insertion, ins(11;9)(q23;p22p23). *Leukemia* **11**, 1469-1477 (1997).
430. Lange, B., *et al.* Growth factor requirements of childhood acute leukemia: establishment of GM-CSF-dependent cell lines. *Blood* **70**, 192-199 (1987).
431. Tsuchiya, S., *et al.* Establishment and characterization of a human acute monocytic leukemia cell line (THP-1). *Int J Cancer* **26**, 171-176 (1980).
432. Sundstrom, C. & Nilsson, K. Establishment and characterization of a human histiocytic lymphoma cell line (U-937). *Int J Cancer* **17**, 565-577 (1976).
433. Drexler, H.G. (ed.) *Guide to leukemia-lymphoma cell lines*, (2005).

434. Motulsky, H.J. & Brown, R.E. Detecting outliers when fitting data with nonlinear regression - a new method based on robust nonlinear regression and the false discovery rate. *BMC Bioinformatics* **7**, 123 (2006).
435. Kok, C.H., Brown, A.L., Ekert, P.G. & D'Andrea, R.J. Gene expression analysis reveals HOX gene upregulation in trisomy 8 AML. *Leukemia* **24**, 1239-1243 (2010).
436. Bird, A.P. CpG-rich islands and the function of DNA methylation. *Nature* **321**, 209-213 (1986).
437. Muggerud, A.A., *et al.* Frequent aberrant DNA methylation of ABCB1, FOXC1, PPP2R2B and PTEN in ductal carcinoma in situ and early invasive breast cancer. *Breast Cancer Res* **12**, R3 (2010).
438. Dejeux, E., *et al.* DNA methylation profiling in doxorubicin treated primary locally advanced breast tumours identifies novel genes associated with survival and treatment response. *Mol Cancer* **9**, 68 (2010).
439. Caldwell, G.M., *et al.* Wnt signalling in adenomas of familial adenomatous polyposis patients. *Br J Cancer* (2010).
440. Messeguer, X., *et al.* PROMO: detection of known transcription regulatory elements using species-tailored searches. *Bioinformatics* **18**, 333-334 (2002).
441. Farre, D., *et al.* Identification of patterns in biological sequences at the ALGGEN server: PROMO and MALGEN. *Nucleic Acids Res* **31**, 3651-3653 (2003).
442. Liu, M.Y. & Wu, M.C. Induction of human monocyte cell line U937 differentiation and CSF-1 production by phorbol ester. *Exp Hematol* **20**, 974-979 (1992).
443. Olsson, I., Gullberg, U., Ivhed, I. & Nilsson, K. Induction of differentiation of the human histiocytic lymphoma cell line U-937 by 1 alpha,25-dihydroxycholecalciferol. *Cancer Res* **43**, 5862-5867 (1983).
444. Ralph, P., *et al.* Lymphokine inducing "terminal differentiation" of the human monoblast leukemia line U937: a role for gamma interferon. *Blood* **62**, 1169-1175 (1983).
445. Nakajima, H., *et al.* All-trans and 9-cis retinoic acid enhance 1,25-dihydroxyvitamin D3-induced monocytic differentiation of U937 cells. *Leuk Res* **20**, 665-676 (1996).
446. Jiang, Y.J., *et al.* Cyclooxygenase expression is elevated in retinoic acid-differentiated U937 cells. *Biochim Biophys Acta* **1633**, 51-60 (2003).
447. Taipale, J., Matikainen, S., Hurme, M. & Keski-Oja, J. Induction of transforming growth factor beta 1 and its receptor expression during myeloid leukemia cell differentiation. *Cell Growth Differ* **5**, 1309-1319 (1994).
448. Matikainen, S., Ronni, T., Hurme, M., Pine, R. & Julkunen, I. Retinoic acid activates interferon regulatory factor-1 gene expression in myeloid cells. *Blood* **88**, 114-123 (1996).
449. Weber, C., *et al.* Retinoic acid inhibits basal and interferon-gamma-induced expression of intercellular adhesion molecule 1 in monocytic cells. *J Leukoc Biol* **57**, 401-406 (1995).
450. Defacque, H., Commes, T., Contet, V., Sevilla, C. & Marti, J. Differentiation of U937 myelomonocytic cell line by all-trans retinoic acid and 1,25-dihydroxyvitamin D3: synergistic effects on tissue transglutaminase. *Leukemia* **9**, 1762-1767 (1995).
451. Koyama, T., Hirosawa, S., Kawamata, N., Tohda, S. & Aoki, N. All-trans retinoic acid upregulates thrombomodulin and downregulates tissue-factor expression in acute promyelocytic leukemia cells: distinct expression of thrombomodulin and tissue factor in human leukemic cells. *Blood* **84**, 3001-3009 (1994).
452. Tanaka, K., *et al.* Increased expression of AML1 during retinoic-acid-induced differentiation of U937 cells. *Biochem Biophys Res Commun* **211**, 1023-1030 (1995).

453. Majeti, R., *et al.* Dysregulated gene expression networks in human acute myelogenous leukemia stem cells. *Proc Natl Acad Sci U S A* **106**, 3396-3401 (2009).
454. Tang, J.L., *et al.* AML1/RUNX1 mutations in 470 adult patients with de novo acute myeloid leukemia: prognostic implication and interaction with other gene alterations. *Blood* **114**, 5352-5361 (2009).
455. Leroy, H., *et al.* CEBPA point mutations in hematological malignancies. *Leukemia* **19**, 329-334 (2005).
456. Casini, T. & Pelicci, P.G. A function of p21 during promyelocytic leukemia cell differentiation independent of CDK inhibition and cell cycle arrest. *Oncogene* **18**, 3235-3243 (1999).
457. Mueller, B.U., *et al.* ATRA resolves the differentiation block in t(15;17) acute myeloid leukemia by restoring PU.1 expression. *Blood* **107**, 3330-3338 (2006).
458. Betts, D.R., *et al.* Abnormalities of chromosome 16q in myeloid malignancy: 14 new cases and a review of the literature. *Leukemia* **6**, 1250-1256 (1992).
459. Hogge, D.E., Misawa, S., Parsa, N.Z., Pollak, A. & Testa, J.R. Abnormalities of chromosome 16 in association with acute myelomonocytic leukemia and dysplastic bone marrow eosinophils. *J Clin Oncol* **2**, 550-557 (1984).
460. Shigesada, K., van de Sluis, B. & Liu, P.P. Mechanism of leukemogenesis by the inv(16) chimeric gene CBFB/PEBP2B-MHY11. *Oncogene* **23**, 4297-4307 (2004).
461. Meshinchi, S. & Appelbaum, F.R. Structural and functional alterations of FLT3 in acute myeloid leukemia. *Clin Cancer Res* **15**, 4263-4269 (2009).
462. Pabst, T. & Mueller, B.U. Complexity of CEBPA dysregulation in human acute myeloid leukemia. *Clin Cancer Res* **15**, 5303-5307 (2009).
463. Johnson, E. & Cotter, F.E. Monosomy 7 and 7q--associated with myeloid malignancy. *Blood Rev* **11**, 46-55 (1997).
464. Godley, L.A. & Larson, R.A. Therapy-related myeloid leukemia. *Semin Oncol* **35**, 418-429 (2008).
465. Sloand, E.M., *et al.* Granulocyte colony-stimulating factor preferentially stimulates proliferation of monosomy 7 cells bearing the isoform IV receptor. *Proc Natl Acad Sci U S A* **103**, 14483-14488 (2006).
466. Pedersen-Bjergaard, J., Christiansen, D.H., Desta, F. & Andersen, M.K. Alternative genetic pathways and cooperating genetic abnormalities in the pathogenesis of therapy-related myelodysplasia and acute myeloid leukemia. *Leukemia* **20**, 1943-1949 (2006).
467. Gregory, T.K., *et al.* Molecular prognostic markers for adult acute myeloid leukemia with normal cytogenetics. *J Hematol Oncol* **2**, 23 (2009).
468. Akagi, T., *et al.* Frequent genomic abnormalities in acute myeloid leukemia/myelodysplastic syndrome with normal karyotype. *Haematologica* **94**, 213-223 (2009).
469. Deneberg, S., *et al.* Gene-specific and global methylation patterns predict outcome in patients with acute myeloid leukemia. *Leukemia* **24**, 932-941 (2010).
470. Griffiths, E.A., *et al.* Epigenetic differences in cytogenetically normal versus abnormal acute myeloid leukemia. *Epigenetics* **5**(2010).
471. Tesch, H., Furbass, R., Stasiecki, P. & Diehl, V. Constitutive expression of multiple cellular oncogenes in acute myeloid leukemia cells. *Leukemia and Lymphoma* **1**, 35-41 (1989).
472. Mavilio, F., *et al.* Expression of cellular oncogenes in primary cells from human acute leukemias. *Proc Natl Acad Sci U S A* **83**, 4394-4398 (1986).

473. Pelicci, P.G., Lanfrancone, L., Brathwaite, M.D., Wolman, S.R. & Dalla-Favera, R. Amplification of the c-myb oncogene in a case of human acute myelogenous leukemia. *Science* **224**, 1117-1121 (1984).
474. Ferrao, P., Macmillan, E.M., Ashman, L.K. & Gonda, T.J. Enforced expression of full length c-Myb leads to density-dependent transformation of murine haemopoietic cells. *Oncogene* **11**, 1631-1638 (1995).
475. Fu, S.L. & Lipsick, J.S. Constitutive expression of full-length c-Myb transforms avian cells characteristic of both the monocytic and granulocytic lineages. *Cell Growth Differ* **8**, 35-45 (1997).
476. Ramsay, R.G. & Gonda, T.J. MYB function in normal and cancer cells. *Nat Rev Cancer* **8**, 523-534 (2008).
477. Miglarese, M.R., Richardson, A.F., Aziz, N. & Bender, T.P. Differential regulation of c-Myb-induced transcription activation by a phosphorylation site in the negative regulatory domain. *J Biol Chem* **271**, 22697-22705 (1996).
478. Klempnauer, K.H. Methylation-sensitive DNA binding by v-myb and c-myb proteins. *Oncogene* **8**, 111-115 (1993).
479. O'Rourke, J.P. & Ness, S.A. Alternative RNA splicing produces multiple forms of c-Myb with unique transcriptional activities. *Mol Cell Biol* **28**, 2091-2101 (2008).
480. Carninci, P., *et al.* High-efficiency full-length cDNA cloning by biotinylated CAP trapper. *Genomics* **37**, 327-336 (1996).
481. Kobayashi, M. & Yamamoto, M. Regulation of GATA1 gene expression. *J Biochem* **142**, 1-10 (2007).
482. Lloberas, J., Soler, C. & Celada, A. The key role of PU.1/SPI-1 in B cells, myeloid cells and macrophages. *Immunol Today* **20**, 184-189 (1999).
483. Laslo, P., *et al.* Multilineage transcriptional priming and determination of alternate hematopoietic cell fates. *Cell* **126**, 755-766 (2006).
484. Zhang, D.E., *et al.* Absence of granulocyte colony-stimulating factor signaling and neutrophil development in CCAAT enhancer binding protein alpha-deficient mice. *Proc Natl Acad Sci U S A* **94**, 569-574 (1997).
485. Tavor, S., *et al.* Macrophage functional maturation and cytokine production are impaired in C/EBP epsilon-deficient mice. *Blood* **99**, 1794-1801 (2002).
486. Georgiades, P., *et al.* VavCre transgenic mice: a tool for mutagenesis in hematopoietic and endothelial lineages. *Genesis* **34**, 251-256 (2002).
487. Luo, Q., *et al.* Activation and repression of interleukin-12 p40 transcription by erythroid Kruppel-like factor in macrophages. *J Biol Chem* **279**, 18451-18456 (2004).
488. Perkins, A.C., Yang, H., Crossley, P.M., Fujiwara, S.H. & Orkin, S.H. Deficiency of the CACC-element binding protein, BKLF, leads to a progressive myeloproliferative disease and impaired expression of SHP-1 (abstract). In: Proceedings of the 12th ASH Annual Meeting and Exposition; 1997 December 5-9. *Blood (ASH Annual Meeting Abstracts)* **90 (Suppl. 1)**, 575 (1997).
489. Dahl, R., *et al.* Regulation of macrophage and neutrophil cell fates by the PU.1:C/EBPalpha ratio and granulocyte colony-stimulating factor. *Nat Immunol* **4**, 1029-1036 (2003).
490. Reddy, V.A., *et al.* Granulocyte inducer C/EBPalpha inactivates the myeloid master regulator PU.1: possible role in lineage commitment decisions. *Blood* **100**, 483-490 (2002).
491. Knudson, A.G., Jr. Mutation and cancer: statistical study of retinoblastoma. *Proc Natl Acad Sci U S A* **68**, 820-823 (1971).
492. Santarosa, M. & Ashworth, A. Haploinsufficiency for tumour suppressor genes: when you don't need to go all the way. *Biochim Biophys Acta* **1654**, 105-122 (2004).

493. Diverio, D., Riccioni, R., Mandelli, F. & Lo Coco, F. The PML/RAR alpha fusion gene in the diagnosis and monitoring of acute promyelocytic leukemia. *Haematologica* **80**, 155-160 (1995).
494. Lo-Coco, F., Ammatuna, E., Montesinos, P. & Sanz, M.A. Acute promyelocytic leukemia: recent advances in diagnosis and management. *Semin Oncol* **35**, 401-409 (2008).
495. Wiernik, P.H. FLT3 Inhibitors for the Treatment of Acute Myeloid Leukemia. *Clin Adv Hematol Oncol* **8**, 429-444 (2010).
496. Wei, D., *et al.* Drastic down-regulation of Kruppel-like factor 4 expression is critical in human gastric cancer development and progression. *Cancer Res* **65**, 2746-2754 (2005).
497. Zhao, W., *et al.* Identification of Kruppel-like factor 4 as a potential tumor suppressor gene in colorectal cancer. *Oncogene* **23**, 395-402 (2004).
498. Yasunaga, J., *et al.* Identification of aberrantly methylated genes in association with adult T-cell leukemia. *Cancer Res* **64**, 6002-6009 (2004).
499. Song, J., *et al.* Genetic and epigenetic alterations of the KLF6 gene in hepatocellular carcinoma. *J Gastroenterol Hepatol* **21**, 1286-1289 (2006).
500. Hirasawa, Y., *et al.* Methylation status of genes upregulated by demethylating agent 5-aza-2'-deoxycytidine in hepatocellular carcinoma. *Oncology* **71**, 77-85 (2006).
501. Chim, C.S., Wong, A.S. & Kwong, Y.L. Infrequent hypermethylation of CEBPA promotor in acute myeloid leukaemia. *Br J Haematol* **119**, 988-990 (2002).
502. Hackanson, B., *et al.* Epigenetic modification of CCAAT/enhancer binding protein alpha expression in acute myeloid leukemia. *Cancer Res* **68**, 3142-3151 (2008).
503. Jost, E., *et al.* Aberrant DNA methylation of the transcription factor C/EBPalpha in acute myelogenous leukemia. *Leuk Res* **33**, 443-449 (2009).
504. Lu, Y., Chen, W., Stein, A., Weiss, L.M. & Huang, Q. C/EBPA gene mutation and C/EBPA promoter hypermethylation in acute myeloid leukemia with normal cytogenetics. *Am J Hematol* **85**, 426-430 (2010).
505. Dufour, A., *et al.* Acute myeloid leukemia with biallelic CEBPA gene mutations and normal karyotype represents a distinct genetic entity associated with a favorable clinical outcome. *J Clin Oncol* **28**, 570-577 (2010).
506. San, A.S., *et al.* Methylation analysis and mRNA expression status of ING1 splicing variants in head and neck carcinomas. *Journal of Hard Tissue Biology* **14**, 296-297 (2005).
507. Shapiro, G.I., *et al.* Multiple mechanisms of p16INK4A inactivation in non-small cell lung cancer cell lines. *Cancer Res* **55**, 6200-6209 (1995).
508. DiFeo, A., Martignetti, J.A. & Narla, G. The role of KLF6 and its splice variants in cancer therapy. *Drug Resist Updat* **12**, 1-7 (2009).
509. Hou, H.A., *et al.* Aberrant methylation of WNT pathway inhibitors and its cooperation with other genetic alterations with distinct characteristics in acute myeloid leukemia (abstract). In: 14th Congress of the European Hematology Association; 2009 June 4-7; Berlin, Germany. *Haematologica* **94**, 220, Abstract #0539 (2009).
510. Alvarez, S., *et al.* DNA methylation profiles and their relationship with cytogenetic status in adult acute myeloid leukemia. *PLoS One* **5**, e12197 (2010).
511. Nimer, S.D. Is it important to decipher the heterogeneity of "normal karyotype AML"? *Best Pract Res Clin Haematol* **21**, 43-52 (2008).
512. Hatada, I. Emerging technologies for genome-wide DNA methylation profiling in cancer. *Crit Rev Oncog* **12**, 205-223 (2006).
513. Bullinger, L., *et al.* Quantitative DNA methylation predicts survival in adult acute myeloid leukemia. *Blood* **115**, 636-642 (2010).

514. Li, Q., *et al.* Estrogen receptor methylation is associated with improved survival in adult acute myeloid leukemia. *Clin Cancer Res* **5**, 1077-1084 (1999).
515. Kim, S.Y., *et al.* Level of HOXA5 hypermethylation in acute myeloid leukemia is associated with short-term outcome. *Korean J Lab Med* **30**, 469-473 (2010).
516. Shimamoto, T., Ohyashiki, J.H. & Ohyashiki, K. Methylation of p15(INK4b) and E-cadherin genes is independently correlated with poor prognosis in acute myeloid leukemia. *Leuk Res* **29**, 653-659 (2005).
517. Chim, C.S., Chan, W.W., Pang, A. & Kwong, Y.L. Preferential methylation of Wnt inhibitory factor-1 in acute promyelocytic leukemia: an independent poor prognostic factor. *Leukemia* **20**, 907-909 (2006).
518. Griffiths, E.A., *et al.* Acute myeloid leukemia is characterized by Wnt pathway inhibitor promoter hypermethylation. *Leuk Lymphoma* **51**, 1711-1719 (2010).
519. O'Connell, R.M., *et al.* Sustained expression of microRNA-155 in hematopoietic stem cells causes a myeloproliferative disorder. *J Exp Med* **205**, 585-594 (2008).
520. Garzon, R., *et al.* Distinctive microRNA signature of acute myeloid leukemia bearing cytoplasmic mutated nucleophosmin. *Proc Natl Acad Sci U S A* **105**, 3945-3950 (2008).
521. Garzon, R., *et al.* MicroRNA signatures associated with cytogenetics and prognosis in acute myeloid leukemia. *Blood* **111**, 3183-3189 (2008).
522. Jongen-Lavrencic, M., Sun, S.M., Dijkstra, M.K., Valk, P.J. & Lowenberg, B. MicroRNA expression profiling in relation to the genetic heterogeneity of acute myeloid leukemia. *Blood* **111**, 5078-5085 (2008).
523. Akao, Y., *et al.* Role of anti-oncomirs miR-143 and -145 in human colorectal tumors. *Cancer Gene Ther* **17**, 398-408 (2010).
524. Volinia, S., *et al.* Reprogramming of miRNA networks in cancer and leukemia. *Genome Res* **20**, 589-599 (2010).
525. Akao, Y., Nakagawa, Y., Kitade, Y., Kinoshita, T. & Naoe, T. Downregulation of microRNAs-143 and -145 in B-cell malignancies. *Cancer Sci* **98**, 1914-1920 (2007).
526. Parcells, B.W., Ikeda, A.K., Simms-Waldrip, T., Moore, T.B. & Sakamoto, K.M. FMS-like tyrosine kinase 3 in normal hematopoiesis and acute myeloid leukemia. *Stem Cells* **24**, 1174-1184 (2006).
527. Carow, C.E., *et al.* Localization of the human stem cell tyrosine kinase-1 gene (FLT3) to 13q12-->q13. *Cytogenet Cell Genet* **70**, 255-257 (1995).
528. Chen, J., Odenike, O. & Rowley, J.D. Leukaemogenesis: more than mutant genes. *Nat Rev Cancer* **10**, 23-36.
529. Silverman, L.R., *et al.* Further analysis of trials with azacitidine in patients with myelodysplastic syndrome: studies 8421, 8921, and 9221 by the Cancer and Leukemia Group B. *J Clin Oncol* **24**, 3895-3903 (2006).
530. Sudan, N., *et al.* Treatment of acute myelogenous leukemia with outpatient azacitidine. *Cancer* **107**, 1839-1843 (2006).
531. Silverman, L.R., *et al.* A phase I trial of the epigenetic modulators Vorinostat, in combination with Azacitidine (azaC) in patients with the Myelodysplastic Syndrome (MDS) and Acute Myeloid Leukemia (AML): A study of the New York Cancer Consortium (abstract). In: Proceedings of the 50th ASH Annual Meeting and Exposition; 2008 December 6-9; San Fransisco. California (CA). *Blood (ASH Annual Meeting Abstracts)* **112**, Abstract #3656 (2008).
532. Bishton, M., Kenealy, M., Johnstone, R., Rasheed, W. & Prince, H.M. Epigenetic targets in hematological malignancies: combination therapies with HDACis and demethylating agents. *Expert Rev Anticancer Ther* **7**, 1439-1449 (2007).

533. Petrie, K., Zelent, A. & Waxman, S. Differentiation therapy of acute myeloid leukemia: past, present and future. *Curr Opin Hematol* **16**, 84-91 (2009).
534. Fazi, F., *et al.* Heterochromatic gene repression of the retinoic acid pathway in acute myeloid leukemia. *Blood* **109**, 4432-4440 (2007).
535. Glasow, A., *et al.* DNA methylation-independent loss of RARA gene expression in acute myeloid leukemia. *Blood* **111**, 2374-2377 (2008).
536. Hahn, C.K., *et al.* Proteomic and genetic approaches identify Syk as an AML target. *Cancer Cell* **16**, 281-294 (2009).
537. Weinblatt, M.E., *et al.* Treatment of rheumatoid arthritis with a Syk kinase inhibitor: a twelve-week, randomized, placebo-controlled trial. *Arthritis Rheum* **58**, 3309-3318 (2008).
538. Friedberg, J.W., *et al.* Inhibition of Syk with fostamatinib disodium has significant clinical activity in non-Hodgkin lymphoma and chronic lymphocytic leukemia. *Blood* **115**, 2578-2585 (2010).